The petrology and geochemistry of ophiolites from the Khawr Fakkan region. Northern Oman range, United Arab Emirates

A. H. Al-Khamees

The Petrology and Geochemistry of Ophiolites from the Khawr Fakkan Region. Northern Oman Range, United Arab Emirates

A.H. Al-Khamees
B.Sc. Texas, M.Sc. Kuwait
(Graduate Society)

A thesis submitted for the degree of Master of Science in the University of Durham.

June 1980

ABSTRACT

The field relationships, petrography, geochemistry and phase chemistry of the peridotite-gabbro-basalt sequence of the Khawr Fakkan - Wadi Shi - Wadi Madha area suggest that the various components are genetically related. They result from partial melting of the upper mantle, followed by fractional crystallisation of the basic magma generated by this process. The rocks comprise a typical ophiolite sequence and are similar to assemblages from other Alpine-type ultramafic complexes.

The area studied may be broadly subdivided into two major zones. In the west the rocks are principally tectonised ultramafics, while to the east of these a series of cumulate gabbros, with dolerite dykes particularly prevelant in the east, passes upwards into basaltic lavas.

The tectonised ultramafics are separated from the gabbroic and basaltic rocks by an easterly-dipping thrust-fault zone, which strikes approximately north-south.

The rock types exposed in the area to the west of the major thrust fault are harzburgites, dunites and wehrlites. They are all, to some extent, serpentinised. The harzburgites have an intensely tectonised fabric, and consist of an assemblage of highly refractory chemistry. The dunites also show a strong tectonic fabric and total

absence of cumulus textures. Textural evidence shows that most of the wehrlites are strongly deformed. A set of criteria to distinguish the refractory residua of partial melting from the cumulates are developed from analytical data and textural evidence.

The rock types exposed to the east of the major thrust fault are gabbro cumulates. The cumulus types recognised include olivine pyroxenites, olivine gabbros, norites and hypersthene gabbros, gabbros and anorthosites and leucocratic gabbros. Where transected by faults gabbro mylonites are developed. Cumulus textures include heteradcumulates, adcumulates and mesocumulates.

The basaltic rocks occur both as intrusive dolerite dykes and as lava flows. The basalts are invariably altered, with ferromagnesian minerals being represented by amphibole in the most part. They are also silicified.

Variation in major and trace elements reveal that the crustal members of the ophiolite suite (gabbros and basaltic rocks) are tholeiitic. The parent magma being a low-Ti and low-K tholeiitic type. Whole-rock analyses and mineral chemistry are used in an attempt to estimate the nature and composition of the partial-melt magma from which both the cumulate gabbros and basaltic rocks have evolved.

A variety of methods have been used, and compared, in an attempt to estimate the equilibration temperatures and pressures of the ultramafic rocks and cumulate gabbros.

The application of several geothermometers gave values for dunite of 872 to 1075°C, for harzburgites of 1099 to 1167°C, for a wehrlite of 1104°C, and for the rare rock-type plagioclase peridotite, a somewhat higher value of 1263°C. Temperatures recorded for olivine pyroxenite cumulates range from 879 to 974°C, and for gabbros and norites from 839 to 999°C. Lower temperatures of 909 to 989°C using an orthopyroxene-clinopyroxene geothermometer, as compared to 1099 to 1167°C, for the harzburgites may reflect the late, lower temperature, crystallisation of clinopyroxene from trapped liquid.

In all cases pressures were less than 7 Kb and correspond to a maximum depth of about 22 Km in the oceanic setting.

ACKNOWLEDGEMENTS

I would like to thank Kuwait University for the award of a Research Studentship and the opportunity to visit the field area and the authorities of the Khawr Fakkan Region and Mr. Ali-Alhamood, President of Public Works at Dubai, for providing the accommodation during my stay in Khawr Fakkan.

I also wish to thank Professors G.M. Brown and M.H.P. Bott for the use of facilities in the Department of Geological Sciences, Durham University.

I am very grateful to my supervisors, Professor G.M. Brown and Dr. D.M. Hirst for various discussions, advice, interest and encouragement during the course of this research. In particular I would like to thank Dr. D.M. Hirst for his critical advice, interest and encouragement which have contributed much to my research. I would especially like to acknowledge many valuable discussions on the subject, and also his assistance in the construction of the manuscript. In addition, I am indebted to Professor G.M. Brown for his valuable comments while reading the finalised chapters of this thesis.

I would like to thank Dr. J.G. Holland and Mr. R.G. Hardy for supervision in X-ray Fluorescence analysis.

In addition, I am indebted to Dr. R.H. Pinsent for

the theory course of the electron microprobe and Dr. A. Peckett for his instruction and assistance, in the use of the electron microprobe.

I would like to extend my thanks to the technical staff of the Department, especially to Mr. G. Randall and Mr. L. McGregor for preparing probe slides and thin sections respectively; Mr. G. Dresser for help in the production of various photographic plates and Mr. R. Lambert for instruction in wet chemical analysis.

Many members of the Department, both past and present, have contributed much through active assistance and discussion. Amongst them, I would especially like to thank Dr. B.Beddoe-Stephens, Dr. D. Egin, Dr. C.H. Emeleus and Mr. R. Phillips.

Less directly, help was received through discussions from fellow research students, namely Mr. I. Williamson, Miss A.H. Hoey, Mr. R.M. Forster, Mr. R. Dogan and Mr. R.H. Hunter.

Finally, I would like to thank Mrs. C.L. Mines for typing the manuscript so expertly and efficiently.

CONTENTS

LIST OF FIGURE CAPTIONS

* = Figure located in the attached map pocket.

LIST OF TABLES

LIST OF PLATES

CHAPTER 1: Introduction

1.1. Scope of Work

The aim of the present work is a study of the ophiolites in part of the Northern Oman Range lying within the United Arab Emirates. The study investigates the characteristics of the various ophiolitic rocks, based on their petrography, mineralogy and geochemistry. Owing to the extensive size of the ophiolite belt, which outcrops over an area of more than 5000 square miles, a sequence in the Khawr Fakkan - Wadi Madha - Wadi Shi region (70 km^2) has been chosen for a detailed study.

1.2. Regional Geology

The Khawr Fakkan area forms a small part of the Oman Mountains, and although the rocks exposed near Khawr Fakkan are entirely igneous, it is worth considering the area in the context of the general regional geology. The main features of the geology of the Oman Mountains are shown in Fig. 1.1 and the structural succession shown in Fig. 1.2. The following account serves to summarise the regional geology and illustrates also the historical development of ideas relating to the evolution of the area.

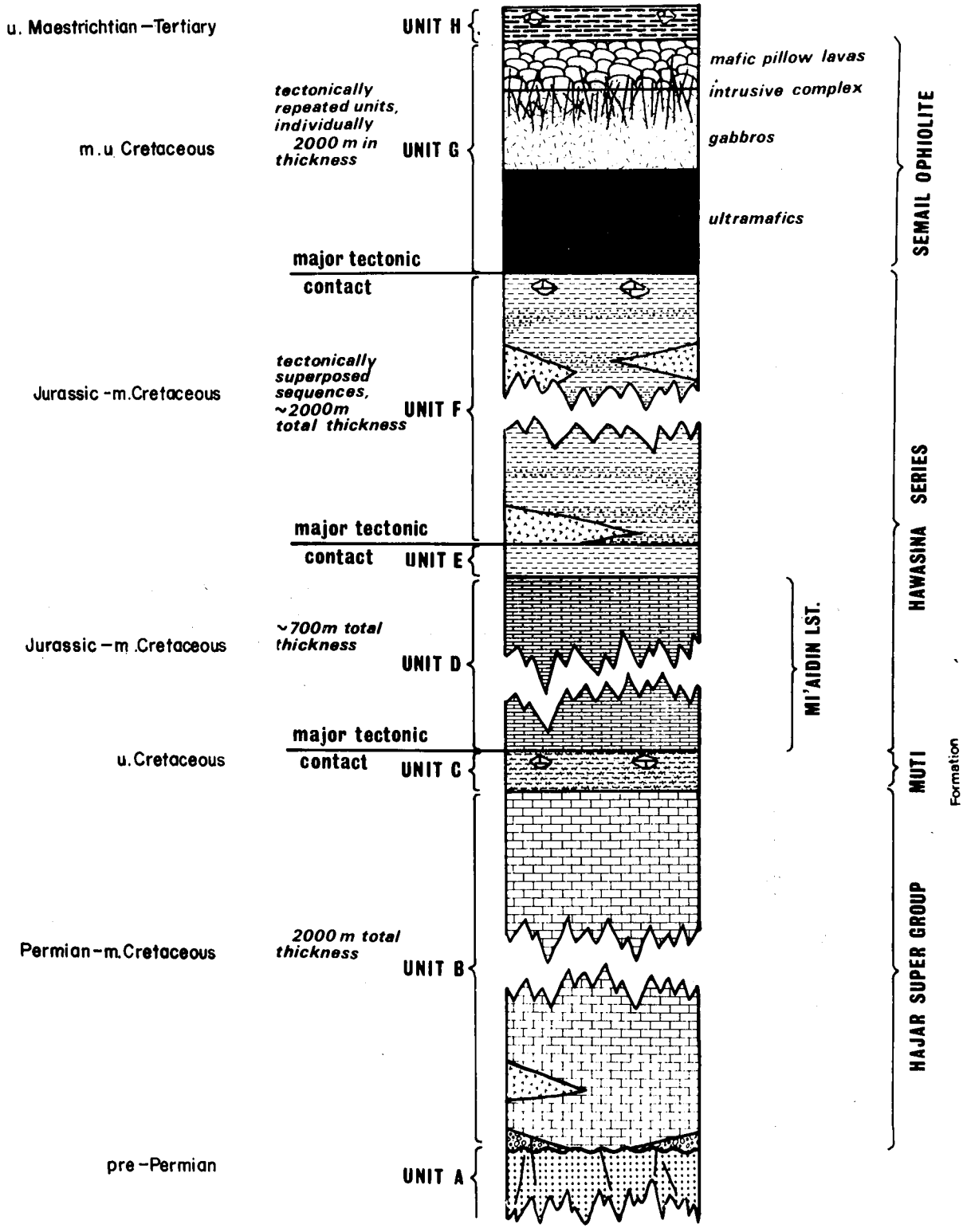

Figure 1·2 Schematic stratigraphic and tectonic sequence characteristic of Oman mountains. (Welland and Mitchell, 1977)

The earliest recorded visit of a geological nature was by Blanford (1872), who collected a few Triassic fossils from the northernmost point of the Ruus Al Jibal. In the winter of 1904-1905, Pilgrim (1908) undertook a survey in the same region and crossed the Oman Range from Dibba to Ras Al Khaimah. This was probably the earliest reconnaissance of the geology of the Oman Mountains. Pilgrim was the first to study the igneous rocks of Oman, in the vicinity of Muscat in Wadi Semail, and at Dibba in the Northern Oman Range. He used the term "Basic igneous series of Oman", but later renamed these rocks "The Semail intrusive series". He considered that the igneous rocks had a limited distribution compared with that of the common limestones. He ascribed an upper Cretaceous age to the Semail igneous rocks.

Lees (1928) outlined the geology and tectonics of Oman, including the Trucial States (United Arab Emirates). This study formed an important foundation for subsequent work. Among the rock formations of the Oman mountain belt, Lees described the Hawasina series and the Semail Igneous Series, suggesting that the former constitutes a great thrust sheet, or nappes, overlain by the nappe of the Semail igneous rocks, and that the movement is from the east. He also mentioned that dykes of very coarse grained gabbros, 6 to 12 feet in thickness, are common

in the igneous series.

A paper dealing with the general geology of a limited area of the northern part of the Oman Range was published by Hudson, Brown and Chatton (1954A). They described the highly complex Jabal Qamar Zone, situated immediately to the south of the Dibba fault line. The authors discovered that this complex area consisted of three tectonic zones: (a) an outer (western) belt of vertical Jurassic-Lower Cretaceous limestones with some chert, part of the vertical limb of a thrust-fold, overridden from the east by (b) a thrust-sheet of Permian-Triassic limestone massifs covered by a Jurassic-Lower Cretaceous succession of radiolarian cherts, epidote-schists and serpentinite, overridden also from the east by (c) the western margin of the Semail thrust-sheet.

Hudson, McGugan and Morton (1954b) described the results of reconnaissance surveys in the Jabel Haqab region which lies on the western front of the Oman Mountains and east of Ras al Khaimah. The outcropping strata of Jabal Haqab consists of limestone and radiolarian chert of Jurassic and Lower Cretaceous age, with a facies expressing the sedimentation in the Arabian Gulf embayment of Southern Tethys and extending southwards between, and overlapping onto, the Arabio-Ethiopian and Indian Massifs.

Hudson and Chatton (1959) described the stratigraphy of the Musandam Limestones, which are located in the extreme north of the Oman Range. These outcrops have a total thickness of about 3,400 metres and are considered to be the backbone of the Northern Oman Range. These authors divided the Musandam Limestones into three main stratigraphical successions: (1) upper brown beds of argillaceous limestones, (2) middle calcite-mudstones and (3) lower, grey-green or purple marls.

Morton (1959) published a comprehensive account of the geology of Oman as a whole. He discussed Lees' views on the tectonics of the region, and considered the Hawasina and Semail Formations to be autochthonous. Morton regarded the "chaotic structure" as being due to tectonics associated with large-scale extrusion of an Upper Cretaceous igneous series.

Hudson (1960) published valuable information on the stratigraphy of the deepest exposed part of the Ruus Al Jibal. These rocks comprise the Hajar super-group, a partly fossiliferous dolomite-limestone succession of over 200 metres thickness. He subdivided them into several formations which are as follows: At the base, a few metres of sandstones are found below the Permian dolomites. A thrust cuts out a possible older section.

Southwest of the unit, however, are more than 100 metres of thick-bedded limestones containing algal stromatolites. These are thought to underly the basal part exposed in the above section. The sandstones are succeeded by the main mass of the Permo-Triassic sediments which are characterized by dolomites and limestones. Above lies a Triassic section characterized by sandstone, marl, and shale laminae (the Muti Formation).

Tschopp (1967) attempted to synthesise all the geological data obtained from exploration wells, and from geological and geophysical fieldwork. His conclusions were as follows: During the Cambrian, clastic and carbonates were deposited in two sedimentary cycles in the Oman Mountains region. Simultaneously, a thick sequence of salt and other evaporites was being formed to the west in the area now occupied by the desert plains. Continental sedimentation occurred in the Cambro-Ordovician, changing upwards to shallow marine deposition. During the Campanian, a geosyncline was formed in the area and flysch-type sediments were deposited. Ultrabasic rocks (the ophiolites) were extruded, probably along tension faults in the Gulf of Oman, and were accumulated in the geosyncline. As a result of the filling of the geosyncline, a compressional tectonic phase elevated the region of the Oman Mountains. Thereafter, a succession

of Tertiary marine transgressions followed in the Palaeocene, Oligocene and Miocene.

Greenwood and Loney (1968) considered the geology and mineral resources of the Northern Oman Range, between latitudes $24^{o}45'$ and $25^{o}37'$ N. Although their work is mainly concerned with the potentiality of the region for mineral resources, they presented a geologic map (1:250,000), based on aerial photographs, showing the principal litho-ligic units. These authors regarded the Semail igneous rocks of the Northern Oman Range as a suite produced by several successive phases of ophiolitic magmatism. These included rocks of plutonic aspects and related serpentin-ites together with hypabyssal and extrusive representatives. The latter occur interlayered with the Hawasina series. The same authors considered the Semail, and at least a part of the Hawasina Series, as allochthonous. Their development history is thought to have involved the intrusion of Semail rocks into a core of geosynclinal sediments (Hawasina) and subsequent tectonic translation of the whole assemblage south-westwards with a concomitant thrusting of Hawasina rocks and metamorphism of geosyn-clinal flysch. Their account is the first to consider the igneous suite in terms of the ophiolite assemblage.

Reinhardt (1969) considered the genesis and emplace-ment of ophiolites in the Oman mountains geosyncline. He

presented petrological studies on the igneous rocks based on an E-W traverse crossing the central Oman Range. Reinhardt discussed a new model for the emplacement of the ophiolites in which he incorporated concepts developed by consideration of modern oceanic ridges. He considered the ultrabasic rocks and related serpentinites as part of the upper mantle which has been thrust over the Hawasina series. He arranged the igneous formations found in Wadi Semail in Muscat, from top to base in the following manner: (1) Volcanic, extrusive rocks, (2) subvolcanic feeder dykes, (3) hypabyssal gabbroic rocks, (4) gabbros, (5) transition zone between gabbros and peridotites, and (6) ultramafic rocks.

Wilson (1969) published a detailed study on the Eugeosynclinal sedimentation, gravity tectonics and ophiolite emplacement of the Oman Range. This study was based on the data obtained from the surveys carried out by the Shell Oil Company geologists in 1962-1966. From structural evidence and the extrapolation of the established sequence of events in the Oman Mountains, Wilson concluded that a tensional structural environment governed the evolution of the Late Cretaceous orogeny. He considered that regional tensional relief was accompanied by crustal separation and flood extrusion of an ultrabasic magma which cooled slowly under great hydrostatic pressure

along the axis of the trough in which the Hawasina sediments were deposited. Wilson considered the nappe to be autochthonous, formed by small-scale gravity slumping from the NE-lying landmass. His interpretation is very similar to that of Tschopp (1967).

Allemann and Peters (1972) presented new data on the Mesozoic sediments of the Ruus al Jibal area, and attempted a reconstruction of the structural history of the Oman Mountains, based on stratigraphic and petrographic data. These authors arrived at the following conclusions based on their structural studies:

1. The oldest rocks of the Ruus al Jibal area (the Hajar Super-Group and Muti Formation) represent a para-autochthonous sedimentary sheet lying on the eastern margin of the Arabian platform.
2. The Hawasina Complex is composed of strongly imbricated sheets of a deep-water, radiolarite-shale-turbidite-volcanic series embodying numerous shallow-water olistholites.
3. The Hawasina sheet-pile was generated chiefly by gravity gliding into a westward migrating depression. This depression moved successively in front of the advancing Oman trench.
4. The metamorphic Series are in thrust contact with the non-metamorphic Hawasina rocks, as well as with the Semail Ophiolites.

Glennie et al. (1973) concluded that overthrusting of the Hawasina and Semail nappes onto the Arabian continental margin during Late Cretaceous probably resulted from continental drift of Arabia in the opposite direction to the spreading movement of contemporaneous oceanic plates. Therefore the presence of ophiolites, radiolarian cherts, turbidites, exotic blocks, etc. in orogenic belts is indicative of the proximity of the former edge of a continent and its transition to adjacent oceanic crust.

Reinhardt (1974) studied the primary spilitic rocks of the Oman Mountains ophiolite suite that occur in the volcanic and subvolcanic parts of the suite. He compared these rocks with fresh, subvolcanic rocks and from petrographical and field evidence concluded that the spilitic rocks have crystallized from a hydrous residual melt that approached a basaltic composition. Reinhardt showed also that, by considering the associated sediments, the spilitic lavas of the Oman Mountains Geosyncline were extruded over a long period, ranging from Late Permian to Late Cretaceous.

Glennie et al. (1974) contributed new ideas relevant to the oceanic origin of the Hawasina and Semail nappes. These nappes had been considered by both Morton (1959) and Wilson (1969) as autochthonous and

derived by small-scale gravitational sliding or slumping from a landmass NE of Oman. However, Glennie et al. convincingly show that the Hajar Super-Group, the Semeini Group and the Hawasina Series were all deposited in the same time-span of Permian to mid-Cretaceous, although they are now found one above the other. Because they are coeval, the most logical way to reconstruct their relative positions prior to nappe emplacement is to place them side-by-side. From their known, or inferred, environments of deposition, this would give a lateral sequence from west to east of: Continental shelf (Hajar) - Shelf-edge and slope (Sumaini) - Ocean basin (Hawasina). The Semail ophiolites are in turn considered as relicts of ocean crust preserved in the Semail thrust sheets which overlie the Hawasina Series. Glennie et al. introduced the concept of the Hawasina ocean basin which had been created by sea-floor spreading operative since mid-Permian times to the N and E of the Oman Mountains. In Late Cretaceous times the Hawasina ocean basin was apparently reduced in size. Since there are no proper indications of a subduction zone, most of the sedimentary series (Sumaini, Hawasina) and part of the oceanic substratum (Semail ophiolites) were overthrust or obducted onto the SE Arabian continental shelf. The order of tectonic superposition of the rock units in the Oman Mountains is

directly related to their original depositional geography in such a way that the higher the tectonic unit, the further out in the Hawasina ocean basin was its point of origin.

Carney and Welland (1974), and Welland and Mitchell (1977) have described the geology and mineral resources of the Oman Mountains, and the emplacement of the Oman ophiolite, respectively. These authors have outlined the regional geology of Oman based on field and petrographic studies, summarising their findings in the schematic diagram shown in Fig .1.2. On the basis of the diagram, the authors considered units A, B and C, which are approximately 2000 metres thick, to be essentially autochthonous. Unit A consists of a basement of low-grade metamorphic rocks, the base of which is not seen. These are overlain unconformably by a sedimentary sequence (Unit B) consisting of thick, generally featureless carbonates with minor volcanic and clastic intercalations (Hajar Super Group). Unit C is a much thinner sequence of shales and other clastic sediments, termed the Muti formation. The top of C is marked by a major tectonic contact, above which is the lowest allochthonous unit D. This consists of a thick sequence of re-deposited carbonates and is termed the Sumaini Formation. Unit E consists of a thin sequence of shales and cherty

limestones of Upper Cretaceous age. These two units, D and E, have a total thickness of approximately 700 metres. They are in turn overlain by the allochthonous unit F, which has a total thickness of 2000 metres. This consists of a sequence of cherts, cherty limestones, siltstones, shales and calcareous sediments with some intercalated volcanics of variable composition. The overlying allochthonous unit G, consists of an igneous assemblage showing a characteristic ophiolite stratigraphy of ultramafic rocks overlain by differentiated gabbros, a sheeted dolerite complex, and volcanics which include pillow lavas. The ophiolite is overlain by a thin sequence of cherts and cherty limestones which forms unit H. The two units (G and H) are approximately 2000 metres in thickness.

The major sequence may therefore be treated as an autochthon, overlain by a series of allochthonous units, the boundaries of which are major tectonic discontinuities or thrust surfaces dipping northeast.

1.3. Summary

The relationships between the Semail Ophiolite complex and underlying units are most simply explained by the progressive tectonic stacking of a series of more or less contemporaneous stratigraphic sequences derived from originally differing environments (Glennie

et al., 1973; Dewey, 1974, 1976). The assumptions that progressively higher thrust units represent progressively further-travlled allochthonous sequences leads to a reconstruction of a continental margin regime established on the north-eastern side of the Arabian shield by early Mesozoic time (Fig.1.3). The basic intrusive rocks and volcanic suites of the autochthonous units (A and B) may represent igneous activity associated with early rifting in Late Permian times. Early volcanic associations within unit F may, in turn, represent a transitional igneous phase indicative of active continental rifting but prior to full-fledged, sea-floor spreading and the generation of the ophiolite suite. The local association of gravity emplaced, exotic carbonate blocks with scattered mafic volcanic rocks does not demonstrate that the latter represent oceanic basement predating the oldest (Permian) carbonate age. By late Triassic time, a complete continental margin and ocean basin regime had been established (Carney and Welland, 1974; Glennie et al., 1973). Part of the autochthon (unit B) occupied a pre-emplacement palaeographical position typical of the continental shelf or platform and provided carbonate debris for the turbidite and breccia sequence of unit D, developing on the slope and upper rise. Lower continental-rise sediment is represented in the lower slices of unit F

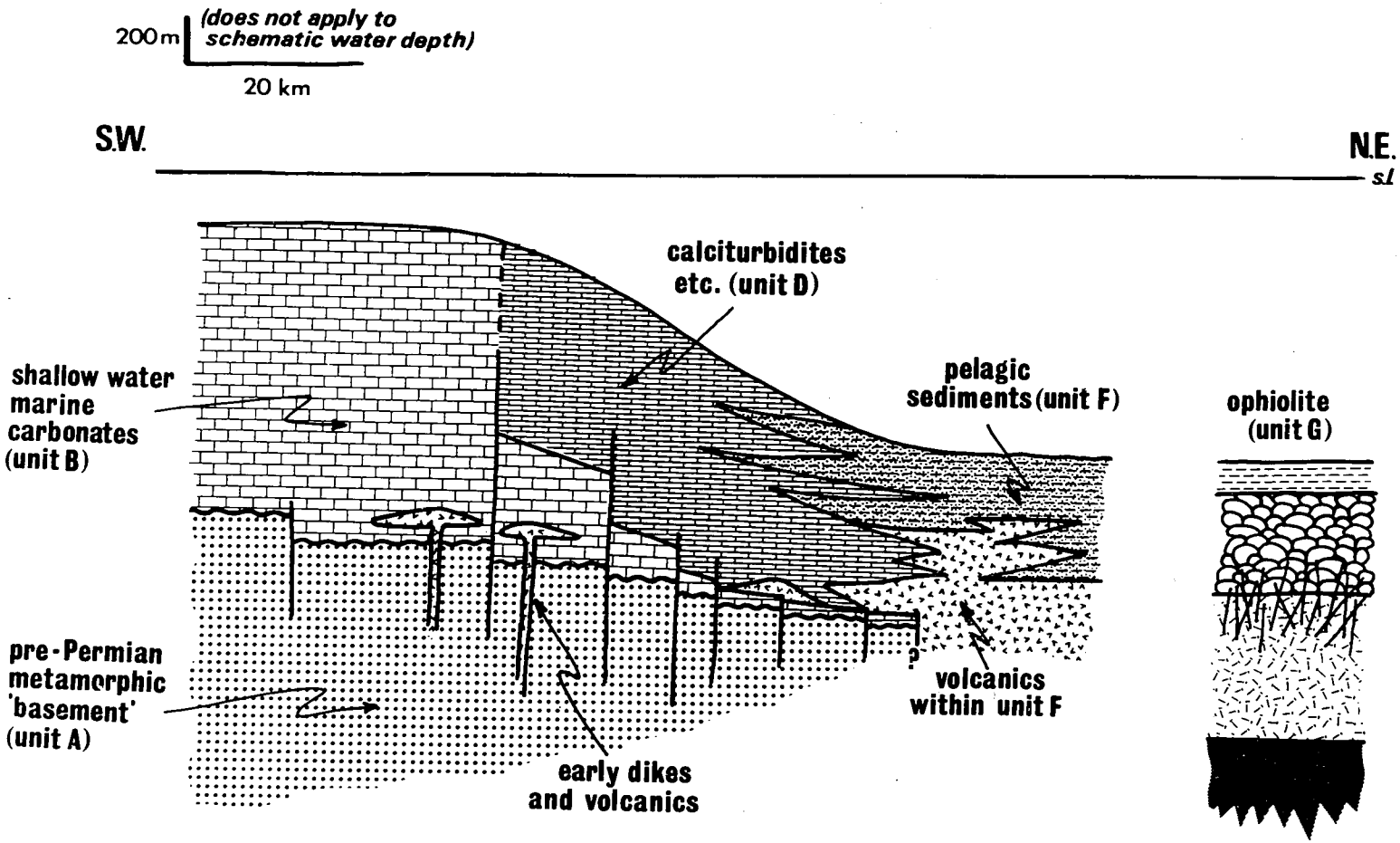

Figure 1·3 Simplified schematic palinspastic reconstruction of Arabian continental margin regime prior to Campanian flysch deposition, emplacement of exotic carbonate blocks, and tectonic compression, (Welland and Mitchell, 1977)

the upper slices constituting progressively more abyssal facies (Glennie et al., 1973). The igneous stratigraphy of the ophiolite complex is typical of that which represents oceanic crust and upper mantle at an actively spreading ridge. The continental margin, now forming the autochthon of Oman and Zagros, remained stable until Late Cretaceous time, when the platform subsidence was accompanied by clastic deposition (unit C) and gravity emplacement of the exotic carbonate blocks. There is no evidence for subduction beneath the margin.

Glennie et al. concluded that the tectonic sequence characteristic of Oman and the Zagros can be most simply explained by slicing and accretion of oceanic basement in and above a subduction zone.

CHAPTER 2: The Khawr Fakkan Area

2.1. Location

The Khawr Fakkan region is located about 120 kilometers east of the Emirate of Dubai. The area can be reached by an unpaved road up to Masafi. From the village of Masafi, a four-wheel drive vehicle is necessary to reach the coastal region of Khawr Fakkan, through the villages of Kalba and Fujairah. The area lies immediately south of the Dibba line, a tectonic belt of NE-SW orientation, which thus cuts obliquely across the Oman mountain range (Fig. 1.1). The Khawr Fakkan area includes two major wadi systems, Wadi Shi in the north and Wadi Madha to the South (see sample location map Fig. 2.1).

2.2. Physiography and geomorphology

2.2.1. Topography and drainage

Topographically, a primary and simple division of the region may be made into the elevated mountain zone and the flanking plains.

Rocks of the N-S aligned mountainous zone are practically devoid of soil and vegetation, except for strips of cultivated land on terraces bordering Wadis.

The zone as a whole is one of bold (sub-mature) topography, intensely dissected by actively eroding drainage channels. Major peaks reach elevations of some 587 metres, e.g. Jabal Uwayyin 587 metres, and unnamed peaks west of Aqabat al Khawr and west of Jabal Katalina, of 500 and 550 metres respectively. Intermediate elevations are recorded, e.g. Jabal Riyadir 342 metres, Jabal Katalina 300 metres, and Jabal Qidfa 210 metres (see sample location map Fig.2.1).

Variations in underlying lithology are clearly expressed, both in morphology of the terrain and in the character of the scree clothing many of the hill slopes.

The dark-toned gabbro hills commonly show rounded to subrounded profiles, with ridge crests flattened over widths of three to seven metres. Scree tends to be of coarse grade, ranging from blocks to boulders. Serpentinite is characterized by sharp ridges and peaks,and by numerous, closely-spaced, erosional facets of inverted chevron shape, controlled by shear and fracture planes. The scree is composed of small- to cobble-sized,angular and cuboidal fragments.

On the west side of the mountain range the inner zone of strong relief passes outwards to flanking, gravel-covered plains through a generally well-developed

zone of more subdued foothills. The passage from solid rock to alluvial plains is marked, along much of the range, by conglomeratic boulder beds. These tongue westwards, in places for several kilometres. In contrast, the eastern coastal plain is generally of more restricted width, and gabbro hills essentially reach to the sea. Only at the debouchement of major wadis, such as Wadi Madha and Wadi Shi, are more extensive spreads of rock debris and gravel found.

The mountain range is dissected into a number of blocks by major wadi systems, which provide the only means of access to much of the region. On the western side of the roughly centrally-aligned main watershed the general direction of drainage is WNW to NW, while to the east of the divide the drainage direction varies between NE and SE.

Most of the wadis appear to be fault controlled. Along most of their length the watercourses are dry, except during sporadic short periods of spate flow, and on the western side of the range all of the channels stream out in the gravel plains. Short stretches of flowing water are seen in the mountains, where bedrock is at, or near, the surface of the wadi floor.

Morphological features indicative of uplift in

relatively recent times include wadi terraces, raised beaches, and entrenched meanders. The last are well developed in wadis cutting serpentinite and draining eastwards in the region to the northwest of Khawr Fakkan.

Quaternary, fluviatile, terrace deposits are cut by major present-day wadis to depths varying from a few to several tens of metres. They are a common feature of the mountain zone (Plate 2.1). These terraces consist of material common to the present day wadis, ranging in size from boulders to gravels, with a silt matrix. The assemblage is generally chaotic, but in places the deposits display rough stratification with a tendency towards rhythmic grading. Cross bedding is sometimes well developed in the fine grain-size material.

Remnants of raised beaches or marine terraces occur along the coast line of the Gulf of Oman to the south of Khawr Fakkan. They probably represent an originally continuous terrace at about 10 to 12 metres elevation. These terraces locally reach inland for distances of up to a kilometre. Coral limestone blocks can be found in the terrace deposits in the coastal region of Khawr Fakkan. To the south of Khawr Fakkan, marine shell fragments of Recent or late Pleistocene species occur on the terrace surface. This suggests uplift in

Plate 2.1. Quaternary, fluviatile, terrace deposits consisting of material common to the present day wadis, ranging in size from boulders to gravels, with a silt matrix.

Pleistocene and sub-Recent times, perhaps in the form of gentle arching.

2.3. Geology

The region can be divided into geologically distinct units. These may be arranged in the following stratigraphic order:

Extrusives

Dolerite dykes

Gabbro cumulates

Sheared serpentinites

Ultramafic complex

2.3.1. The ultramafic complex

The peridotites in the Wadi Shi - Wadi Madha area are dissected by a number of ramifying tributaries which form the only access to them. To the west and southwest of Khawr Fakkan in the Wadi Shi - Wadi Madha area (Fig. 2.2), the ultramafic facies of the Semail ophiolite forms low-lying outcrops. The outcrops are generally discontinuous, forming detached blocks of variable dimensions, but of the order of 100 by 200 metres. The distribution of the peridotites has been controlled by the fault system, the ultramafic complex being intersected by numerous N-S faults. These faults dip to the east. N-S faulting is also evident at the contact

between the peridotites and gabbros, which is also of tectonic type.

Field observations revealed that the peridotites of the Wadi Shi - Wadi Madha area occur as blocky massive types, frequently dissected by numerous fractures filled with veins of asbestiform material, mainly chrysotile. The veins filling the fractures range in width from 2 centimetres to more than 10 centimetres. The peridotites generally do not exhibit noticeable variations in their general appearance and individual rock types are difficult to determine in the field. The original textures are not discernible in the field as all the ultramafics have a tectonic fabric. Their colour generally varies from dark green to greenish brown, although pale coloured varieties and mottled types also occur. The mottled variety is usually harzburgite, the mottled effect reflecting the presence of ortho-pyroxene. Such inhomogeneity in appearance may be accentuated locally by weathering, reflecting compositional variation.

It should, however, be mentioned that ultramafic rock types are generally not sharply separable in the field, and one type may grade imperceptibly into the other. An interesting feature observed in the Wadi Shi

sector is that part of the peridotite complex belonging to that sector has been shifted towards the gabbro complex east of Wadi Shi (Fig. 2.2), which is probably due to shearing and faulting.

2.3.2. The sheared serpentinites

Along the contact, between the main ultramafic complex of the Wadi Shi and Wadi Madha areas and the gabbro complex, the characteristics of the peridotite change. They become brownish, and locally earthy, with frequent pockets of the carbonate magnesite. They are highly impregnated with silica and are traversed by magnesite veins. The veins have an average width of a few centimetres but in a few cases they may attain half a metre in width. At the contact of some magnesite veins, the serpentinites are altered to talc carbonates. A secondary brecciated structure is frequently observed which owes its form to a network of silica enclosing extremely weathered peridotite. In general appearance the serpentinites are friable and they are highly sheared because of their close relationship to the faults.

The most striking feature characterizing the sheared serpentinites in the Wadi Shi and Wadi Madha areas is the

highly cavernous structure resulting from surface weathering of the carbonate minerals.

The shear zones encountered in the Wadi Shi and Wadi Madha areas mostly possess a N-S trend.

2.3.3. Gabbro cumulates

The outcropping gabbros are far more homogeneous and massive, in contrast to the peridotites. They constitute rather sharp massifs superimposed on the peridotites.

The gabbros are excellently exposed in the eastern Jabal Qidfa, Jabal Riyadir, Jabal Katalina, and the Jabal Khawr Fakkan areas (Figs. 2.1 and 2.2). They also occur in the eastern sector of Wadi Shi and south-eastern part of Wadi Madha, generally becoming coarser towards these two regions, and finer towards the coastal region of Khawr Fakkan.

On the whole, there is a gradual upwards decrease in grain size throughout the gabbro complex.

Layering is a marked and widespread feature in the gabbros. It is the expression of compositional variations, rendered the more obvious by weathering and colour differences, and is generally a result of the alternation of feldspathic and ferromagnesian-rich

layers. In general, layers are impersistent and many of them pinch out over relatively short distances.

Layering that is continuous over long distances, such as occur in stratiform complexes, has not been observed. Also, no rhythmic or cyclic repetition of layers has been noticed in the gabbro complex.

The attitude of the layers is fairly constant with dips ranging from 45^{o} to 65^{o} in a south-easterly direction.

2.3.4. Dolerite dykes

The dolerite dykes are well exposed in the extreme coastal region of Khawr Fakkan (Fig. 2.2), where they occur as subvertical dykes cutting each other at low angles and varying in thickness between two or three metres. The dykes strike between 35 and 40^{o} and dip steeply south-eastwards. They sometimes show faulted contacts with the overlying basaltic flows and these also occur between the dykes themselves. They become less frequent south of the village of Qidfa and immediately west of Aqabat Al-Khawr (Fig.2.2) where they cut through the gabbros. The dykes, in part at least, form the feeders to the overlying basaltic flows.

2.3.5. Extrusives

The extrusive rocks occur as massive flows, generally fine-grained and greenish to black in colour; some display crude columnar jointing. They form low-lying hills.

The basaltic flows are best exposed on the small island of Sirat Al-Khawr, north of Khawr Fakkan and separated from the latter by the Gulf of Oman (Fig. 2.2).

Other occurrences are seen at the extreme north of Khawr Fakkan (Fig. 2.2).

CHAPTER 3: Petrography

3.1. Petrography of the Ultramafic Rocks

3.1.1. Occurrence

The ultramafic rocks are exposed over wide areas of the Northern Oman Range, and occur as large sheet-like masses at least 900 metres thick. The colour of the rock types varies from dark green, almost black, to brown. They are commonly dissected by intersecting fracture planes, and appear to be sheared. Veins of asbestiform material, composed mainly of chrysotile and varying in thickness from 5 to 10 cm, intersect the ultramafic serpentinites (Plate 3.1).

The rock types are mainly dunites, harzburgites and wehrlites, with very limited feldspathic peridotite and lherzolite (Plate 3.2). They are all serpentinized to a greater or lesser degree.

The ultramafics are best exposed in the south of the area, in Wadi Madha and Wadi Sahnah although a limited development may be seen in Wadi Shi in the north (Fig. 2.2).

3.1.2. Dunites (Plate 3.3)

Dunites occur in both the south, in the area of Wadi Madha and in the north, around Wadi Shi. They

Plate 3.1. Dunite outcrop of Wadi Madha showing distribution of asbestiform material composed mainly of chrysotile.

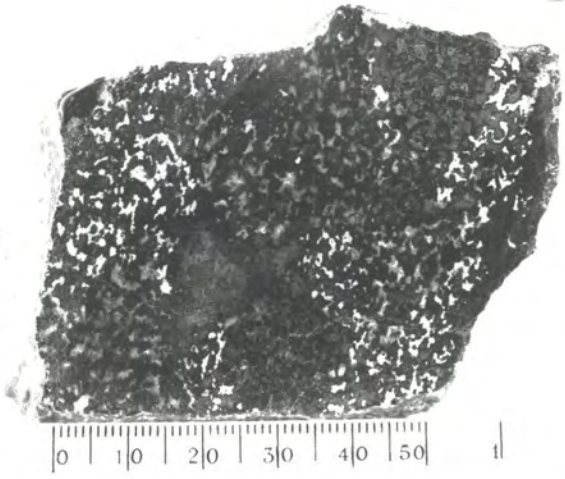

Plate 3.2. Hand specimen of sample 315: Plagioclase peridotite composed of sericitised plagioclase (white), olivine top right hand corner, and altered clinopyroxene, lower left hand corner.

are best seen, and most prevalent, around Wadi Madha.

They are found in bands of greatly varying thickness, from 100-200 metres thick, pinching out laterally. They occasionally pass into harzburgites but more commonly into wehrlites.

The dunites have a simple chemistry and mineralogy. Primary minerals include dominant olivine, together with chrome-spinel and diopsidic clinopyroxene. Serpentinization and alteration have added serpentine, talc and carbonate (magnesite) to the assemblage.

Average modal proportions of the constituents are olivine 70%, clinopyroxene 5%, chrome-spinel 3%, serpentine 20%, carbonates and talc 2%. There is, however, considerable variation depending on the degree of serpentinization.

The olivine has an average grain size of 4 by 2.5 mm. In serpentinized dunite it occurs as relict angular grains, of average diameter 3 mm, set in a mesh-textured serpentine matrix. Most of the dunites are strongly deformed, and the olivines show evidence of strain in the form of kink-banding, undulose and zone extinction (Plate 3.4). A cataclastic texture develops at the expense of an early generation of elongate, olivine megacrysts, which have a darker appearance than the later,

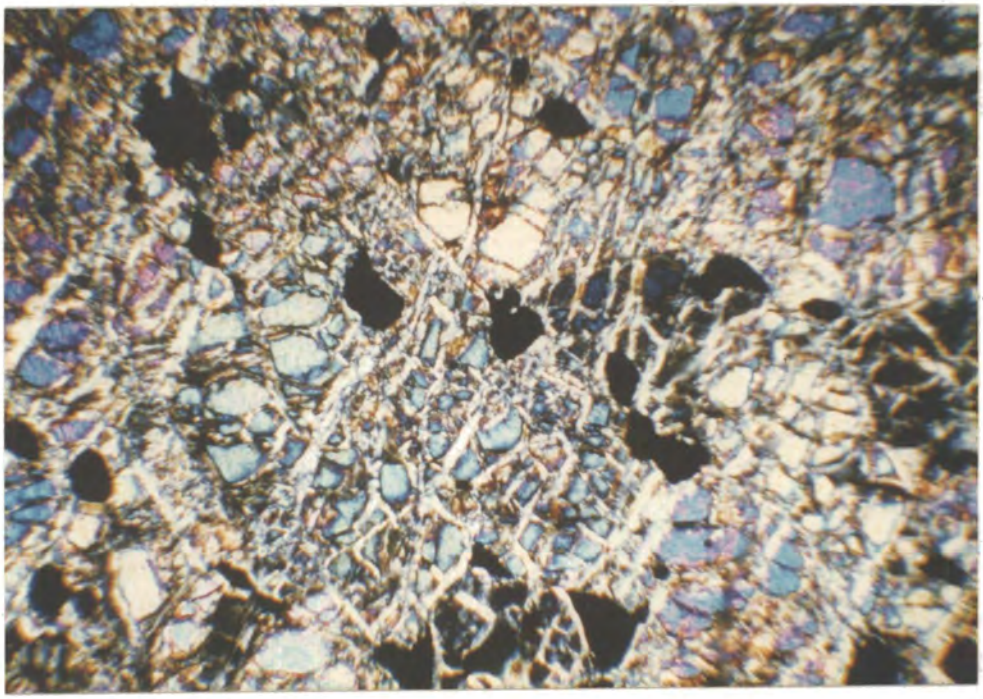

Plate 3.3. Photomicrograph: Mosaic textured dunite, moderately serpentinized by a network of chrysotile veins. Red spinels are subhedral equant (Sample 314. XP. Field width = 4 mm).

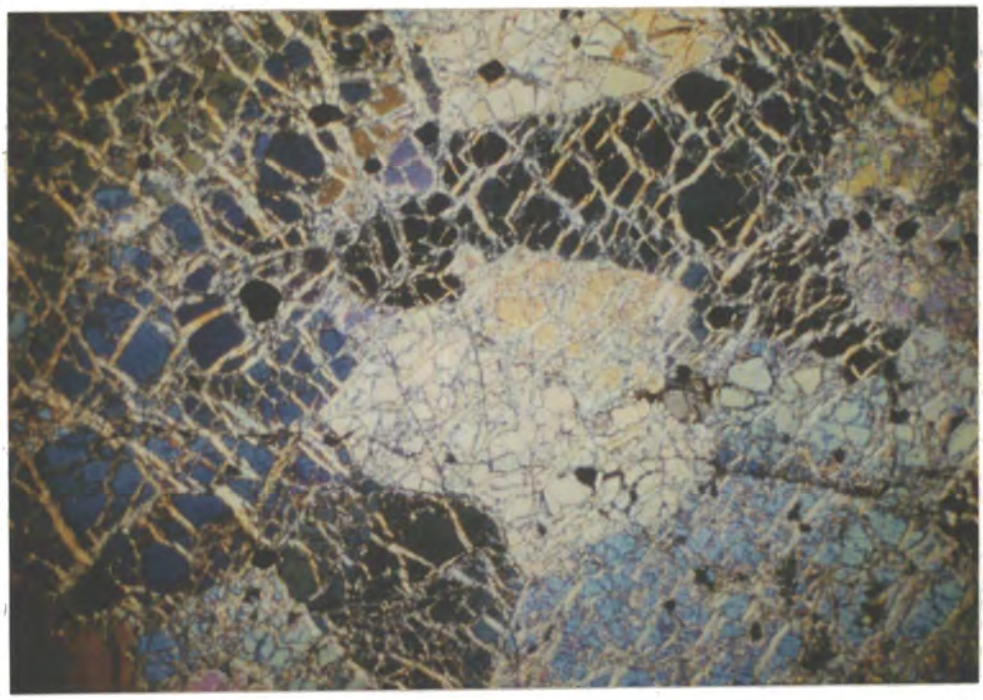

Plate 3.4. Photomicrograph: Strongly deformed dunite, showing crystallization of large, strained, prismatic olivines into a mosaic of small olivines, cut by chrysotile veining (Sample 318. XP. Field width = 4 mm).

recrystallized, mosaic-textured olivine. The elongate olivines tend to have strong directions of serpentinization normal to the elongation, while mosaic olivine is serpentinized by a network of chrysotile veinlets (Plate 3.5).

Clinopyroxenes occur as small, interstitial grains between the olivine; they have an average grain size of 1-1.5 mm diameter.

The chrome spinels occur as large, red, subhedral grains with semi-circular, embayed margins, their grain size varying between 1 and 0.5 mm diameter. Some of the spinels from strongly deformed dunites show "pull-apart" texture (Plate 3.6), the cracks in the spinel being filled by serpentine.

Within the groundmass, irregular lobate areas are sometimes present. These areas are of low birefringence and may be chlorite or clay minerals (Plate 3.7).

3.1.3. Harzburgites (Plate 3.8)

The harzburgites occur mainly in the north of the Wadi Shi area (although a limited development may be seen in Wadi Madha and Wadi Sahnah to the south of Wadi Shi). They are interbanded with dunites although the latter are subordinate in amount.

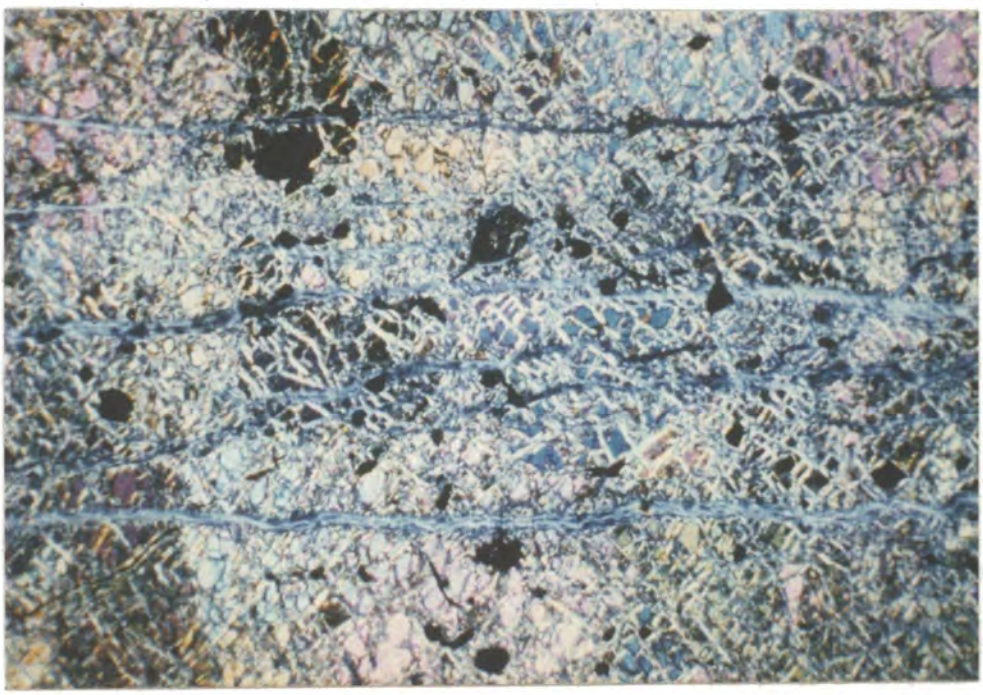

Plate 3.5. Photomicrograph: equigranular, anhedral, medium grain-size olivines, serpentinized with strong direction of serpentinization normal to elongation of olivines (Sample 528. XP. Field width = 8 mm).

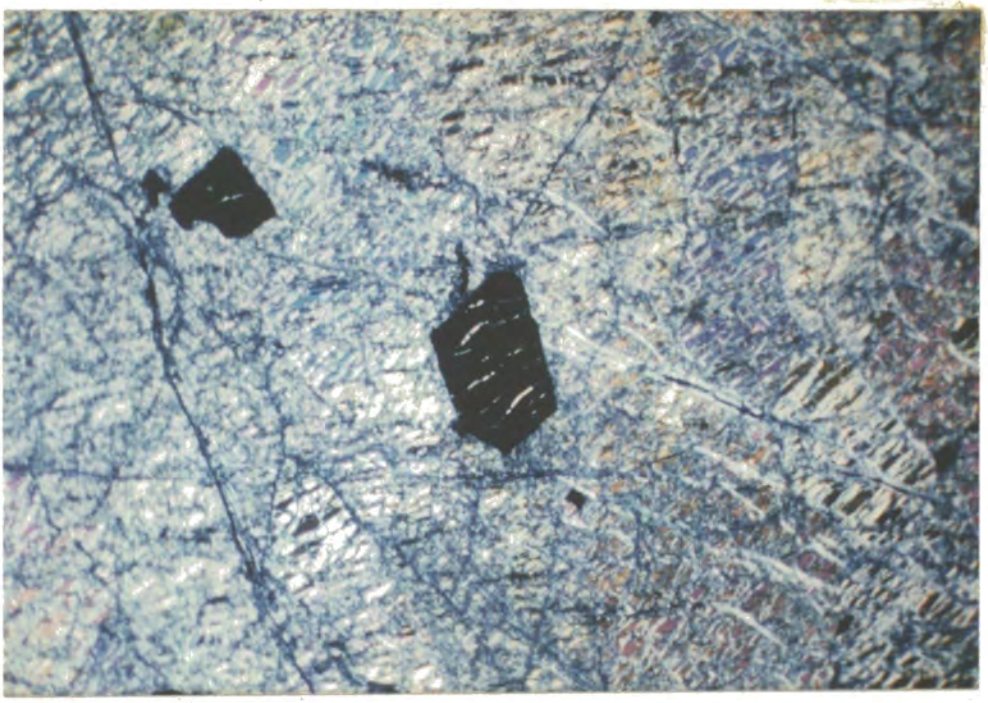

Plate 3.6. Photomicrograph: Spinel grain in a serpentinized dunite, serpentinization of olivines is reflected in the chrome spinel which shows "pull-apart" texture. The cracks in the spinel being filled with serpentine (Sample 531. XP. Field width = 4mm).

Plate 3.7. Photomicrograph: Irregular, interstitial, lobate areas of chlorite and clay minerals in a groundmass of mosaic-textured olivines, substantially serpentinized by a network of chrysotile veins, in a serpentinized dunite (Sample 515. PPL. Field width = 4mm).

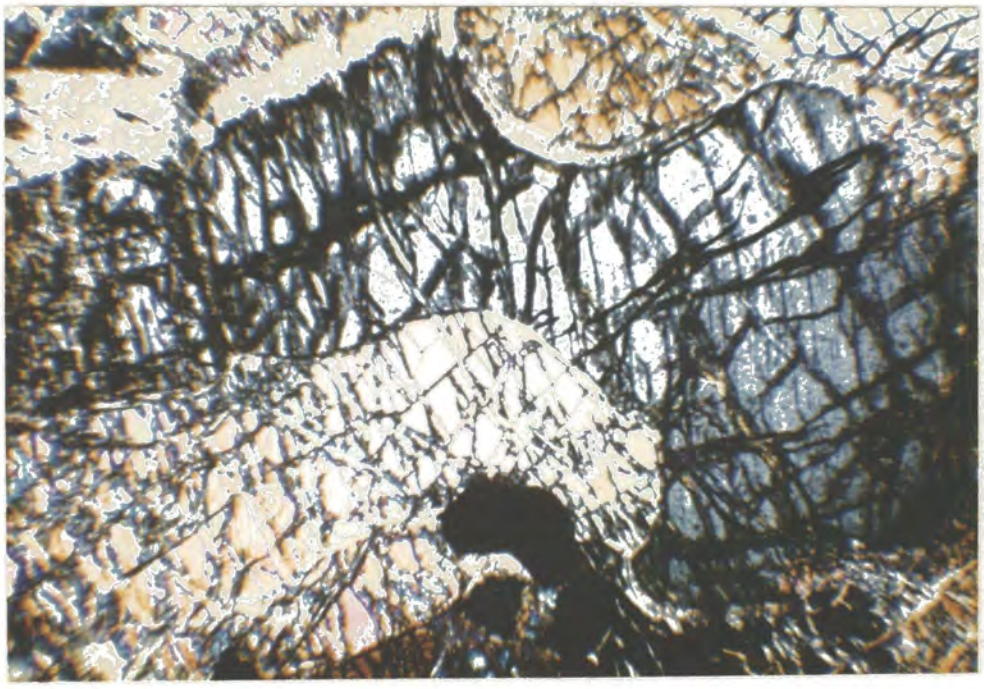

Plate 3.8. Photomicrograph: Enstatite grain in a serpentinized harzburgite. The olivines appear to be elongated and shattered. Both the enstatite and olivines show a domain and strain extinction. Note the chrysotile veining strong in one direction (Sample 328. XP. Field width = 2 mm).

Primary minerals of the harzburgites include dominant olivine and orthopyroxene, together with minor chrome spinel and diopsidic clinopyroxene. Serpentinization and alteration have added serpentine, talc and chlorite.

Average modal proportions of the constituents are olivine 85%, orthopyroxene 12%, clinopyroxene 2%, chrome spinel 2%. These modal values are usually modified by serpentine, talc and chlorite which are present in variable amounts and depend on the extent of serpentinization. The harzburgites are generally less serpentinized than the dunites. The olivines are subhedral and have an elongate appearance; there is a tendency towards preferred orientation. The elongate olivines often show evidence of cataclastic deformation; they are shattered and show domain extinction. The olivines are partly altered to serpentine, and are cut by veinlets of chrysotile, while others are traversed by irregular veins of talc. Small olivines are sometimes included within chrome spinel and pyroxene.

Orthopyroxenes occur as subhedral to euhedral crystals with an average grain size between 2x0.5 mm and 3x2 mm. The orthopyroxenes include fine clinopyroxene exsolution lamellae which are mainly parallel to the 100 cleavage trace. They occasionally enclose minute,

rounded olivines, and chrome spinel. In some areas the orthopyroxenes are replaced by fibrous chlorite, but more usually they are pseudomorphed by bastite and talc although fresh cores of the orthopyroxene usually remain.

Clinopyroxenes are very minor in amount,and in some specimens they are completely absent.

The chrome spinels are deep red in colour, with an average grain size of 2.5x1 mm and have an anhedral to subhedral texture. The chrome spinels are often fractured, with thin chrysotile veins running through the fractures. Occasionally the spinels occur within the bastite-talc groundmass. They tend to be more irregular in outline than the spinels present in the dunite.

3.1.4. Wehrlites (Plate 3.9)

The wehrlites are seen in the southern part of the area in the vicinity of Wadi Madha and Wadi Sahnah.

They are found in bands commonly associated with the dunites and often in direct contact with them.

Primary minerals of the wehrlites include dominant olivine and clinopyroxene, together with minor chrome spinel and orthopyroxene; serpentinization and alteration have added serpentine, chlorite and carbonate.

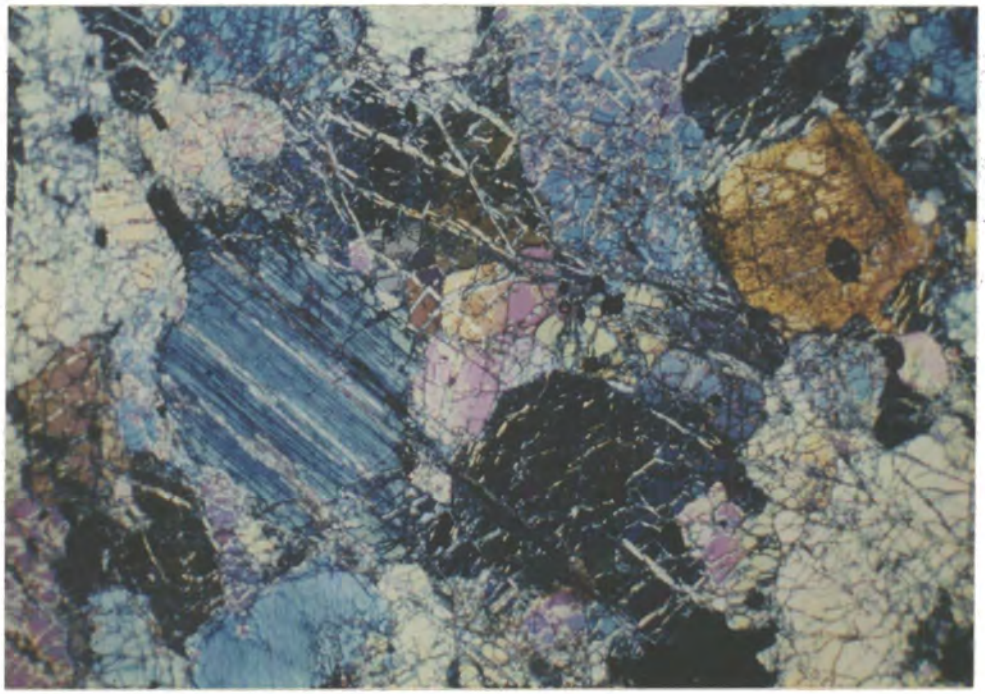

Plate 3.9. Photomicrograph: Olivine and clinopyroxene with fine-scale orthopyroxene exsolution in a wehrlite. The olivines show strong, elongate preferred orientation with a tendency for chrysotile veining to be normal to the elongation (Sample 312. XP. Field width = 4mm).

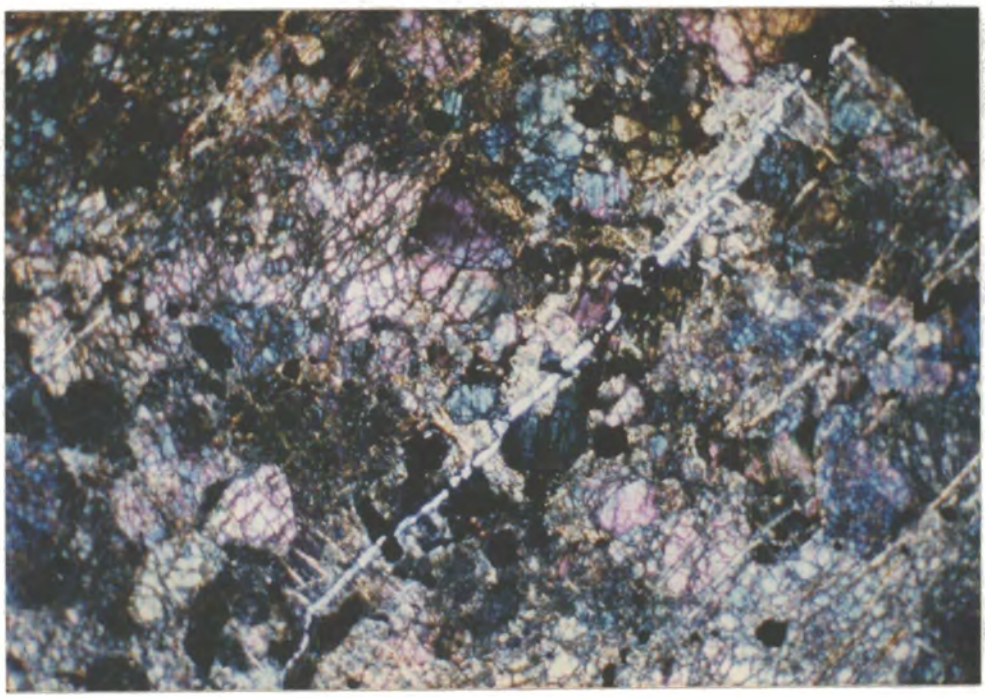

Plate 3.10. Photomicrograph: Intensely sheared wehrlite. Note late carbonate veining cutting obliquely across the clinopyroxenes and invading the adjacent olivines. (Sample 317. XP. Field width = 8 mm).

Average modal proportions of the constituents are olivine 70%, clinopyroxene 15%, chrome spinel 5%, serpentine 10%. There is, however, considerable variation depending on the degree of serpentinization.

The olivine has an average grain size of 2x1.5mm. In serpentinized wehrlites the olivines are mosaic textured with a shattered appearance, and net veined by serpentine. A cataclastic texture develops at the expense of an early generation of strongly elongate olivine. The elongate olivine tends to have a strongly preferred orientation and the tendency is for chrysotile veining to be normal to the elongation. Most of the wehrlites are strongly deformed and the olivines show evidence of strain in the form of undulose and zone extinction. Minor interstitial olivines are altered to talc. Occasionally the olivines occur as inclusions in the clinopyroxenes.

The clinopyroxenes occur as subhedral grains, with grain size ranging between 5x0.2mm and 3x1.5mm. They include fine orthopyroxene exsolution lamellae parallel to the 100 cleavage traces. The clinopyroxenes in the serpentinized wehrlites are set in a serpentine matrix, and these pyroxenes are strained and show undulose extinction. The relatively fresh clinopyroxenes are

occasionally altered and dusted with Fe oxides (magnetite) which suggests that the original clinopyroxene contained appreciable Fe. Some clinopyroxenes are altered to talc, marginally and along cleavages; occasionally a clinopyroxene will be completely replaced.

The chrome spinel is deep to pale red in colour and occurs as subhedral, equant, and in some cases rounded grains with an average grain size of 1x0.5mm. The spinels occasionally occur as inclusions in the pyroxene, sometimes contain minute inclusions of olivine, and are embayed.

Within the groundmass, some pale-green chlorite is occasionally present. In one sample, a zone of intense chlorite development is probably related to shearing. In general, however, the wehrlites are substantially fresh although late carbonate veining sometimes cuts obliquely across the clinopyroxenes and invades the adjacent olivines (Plate 3.10).

3.1.5. Rodingites

Rodingite was first defined by Bell et al. (1911) as a coarse grained, gabbro-like rock associated with dunite and containing diallage, grossularite, prehnite and/or serpentine. Bell et al. originally described this

rock type in dykes cutting through serpentinites outcropping in the region of the river Roding in New Zealand. These dykes were composed essentially of garnet (hydrogrossular), diallage and prehnite.

Glennie et al. (1974) recognised this rock type in the southern part of the Oman Mountains, and described the following features as being characteristic of rodingites in general:

1. They are calcium-rich rocks composed of (mostly hydrous) calc-silicates.
2. They occur as inclusions within serpentinized ultramafic host-rocks.
3. They are often separated from the host rock by a rim of chlorite.
4. They are lense shaped, roundish or more typically dyke-shaped.
5. They are found more commonly within assemblages that have not been affected by a regional metamorphism.

It is generally agreed that the origin of these rocks is low-temperature alteration of mostly gabbroic to basaltic igneous inclusions (layers or dykes) or sometimes of calcareous sedimentary material within the ultramafic host rock. An essential factor for the alterations to take place seems to be the serpentinization of the host

rock, since this is found to take place simultaneously with the rodingite reactions. Another factor favouring the process in many cases is contemporaneous deformation. The reaction is supposed to involve an exchange of matter between the host rock and the inclusion.

The rodingites form dykes and boudins within the sheared ultramafic rocks and dunites, and commonly occur along the contact zone between the ultramafic mass and the sheared serpentinites in Wadi Madha. The most common host rock of the rodingite is a serpentinite composed of chrysotile, chrome spinel, secondary magnetite and hematite.

The main constituents of the rodingites are pyroxenes and garnets. The garnets are most probably hydrogrossular with evidence of recrystallization and partial melting of the garnets. The garnets also occupy interstitial spaces within the pyroxenes and occur as coarse exsolution blebs in the pyroxenes (Plate 3.11). Crush zones are evident where pyroxenes have recrystallized to fine mosaic texture. The pyroxenes present are mainly monoclinic with variations in grain size ranging from medium to coarse grained. Remnants of orthopyroxene are present but with a cloudy appearance due to minute Fe oxides. Partial resorbtion and recrystallization of the rock is evident.

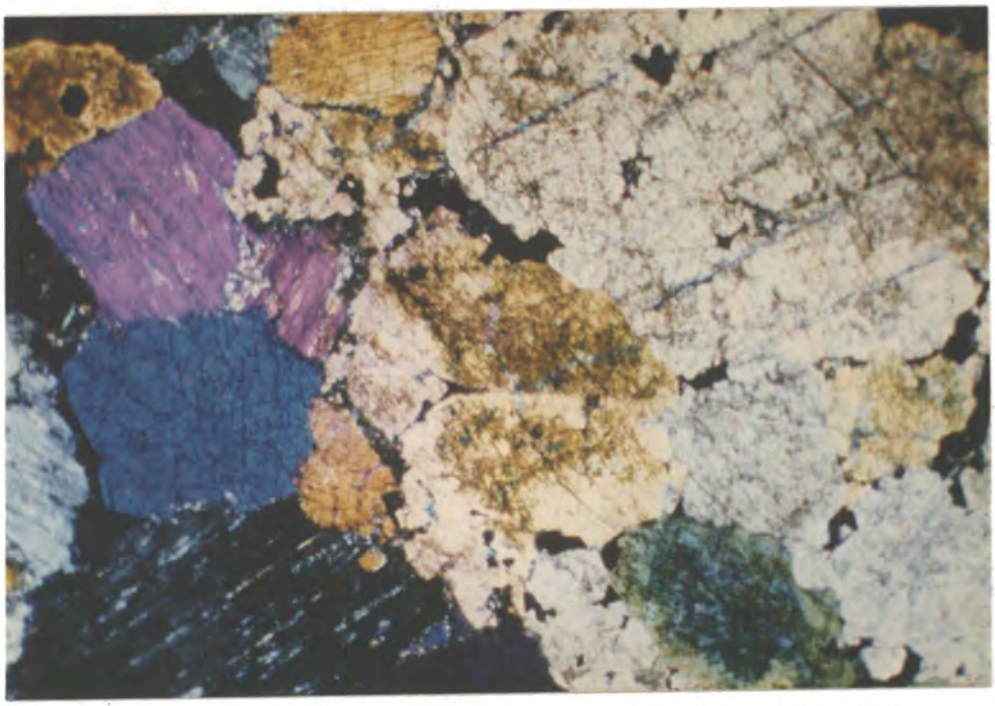

Plate 3.11 Photomicrograph: Recrystallization and partial melting of garnets in a rodingite. Garnets occupy interstitial spaces and also appear as exsolved blebs in clinopyroxene. Crush zones are evident, where the clinopyroxenes have recrystallized to fine mosaic textures (Sample 535. XP. Field width = 4mm).

Plate 3.12 Sheared, talcose serpentinite at Wadi Madha, showing cavernous structure which is due to solution of carbonates during weathering.

3.1.6. The sheared serpentinites

Along the contact zone between the ultramafics and the gabbro-cumulates, the serpentinites are highly sheared and are usually altered to talc-carbonates (Plate 3.12). These rocks are best seen in the south around Wadi Madha and Wadi Sahnah although a limited development may be seen in Wadi Shi to the north (Fig. 2.2). They show a cavernous structure which is due to solution of carbonates during weathering. Magnesite is fairly common and appears in various forms. It occurs as small cross-cutting veinlets, which give the rock a mesh-like appearance, and more often as bands running through the serpentinite (Plate 3.13). The magnesite veins disappear entirely as one approaches the ultramafic zone. Chrysotile veins are also common, both in the contact zone and in the ultramafic zone.

In thin section the most common rock-type from this zone consists of serpentine containing residual olivine granules; relict ortho- and clinopyroxenes are also present. Some areas are traversed by thick chrysotile veins and by later carbonate veins. Talc is present in the form of rims to the residual olivine granules. Ore minerals, probably magnetite, occur in a shattered skeletal form and as a fine dust in the serpentine.

Other examples from this sheared zone include meta-

Plate 3.13. Sheared serpentinite at Wadi Madha. Note the white cross-cutting veinlets of magnesite, which gives the sheared serpentinites a mesh-like appearance.

somatic talc-amphibole rocks. In thin section these rocks are a mixture of talc, pale green to brown amphibole and possibly brucite. Radiating aggregates of tremolite-actinolite (Plate 3.14) sometimes occur; these must have grown after the shearing movements ceased to be effective.

Sheared talcose serpentinite also occurs in this zone. These rocks are extremely rich in subhedral to euhedral chromite showing hexagonal and cubic outlines (Plate 3.15). Analyses of these chrome-spinels are given in Table 5.33.

3.2. Petrography of the Cumulate Rocks

3.2.1. Nomenclature and textures

The classification of igneous cumulates by Wager, Brown and Wadsworth (1960) is used in describing the cumulate rocks. Much of theoretical importance can be incorporated, and a better understanding of cumulate problems gained, by adopting this classification. The various terms used are:

An igneous cumulate: A rock formed by gravity accumulation of crystals from magma.

Cumulus minerals: Those which have settled (or, less commonly, floated) as primocrysts from the contemporary magma.

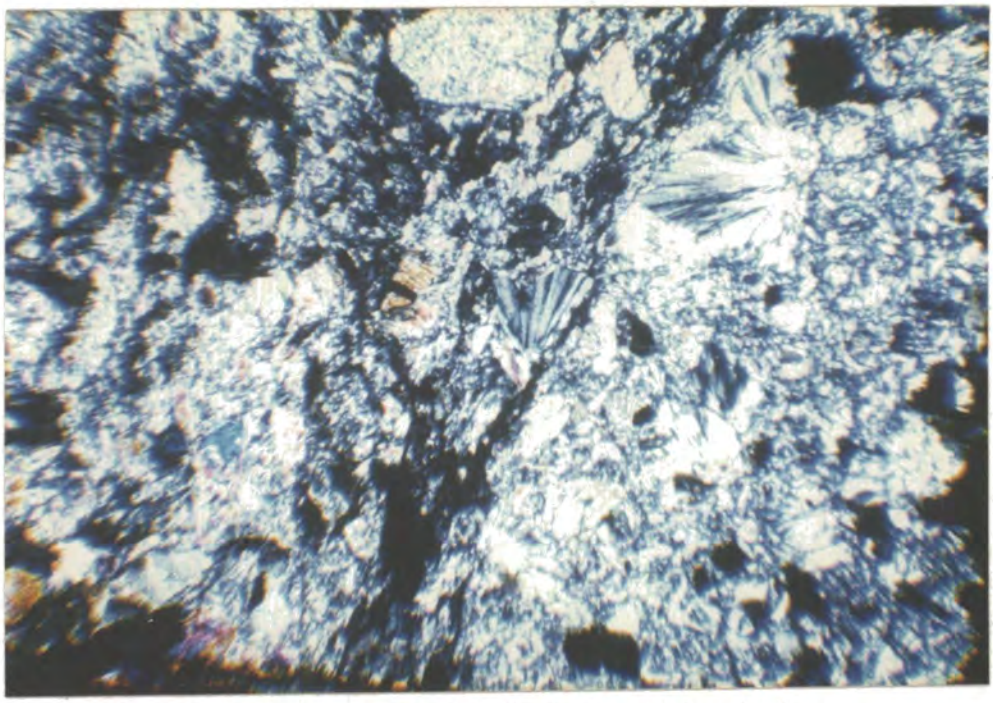

Plate 3.14 Photomicrograph: Metasomatic talc-amphibolite showing radiating aggregates of tremolite-actinolite, associated with finer grained talc and amphibole (Sample 516. XP. Field width = 4mm).

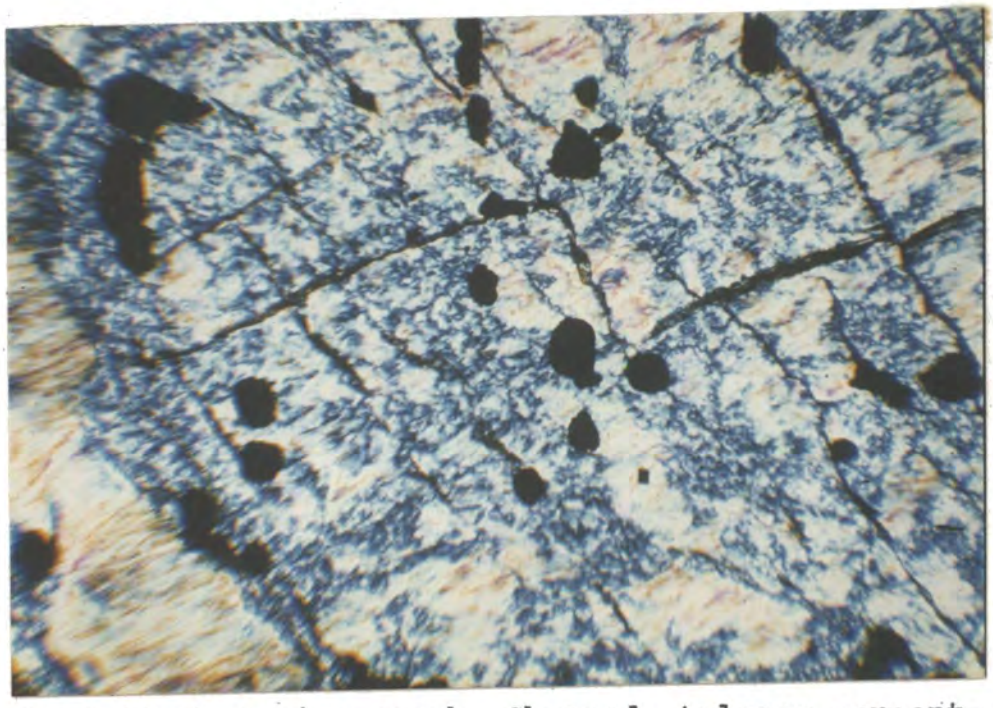

Plate 3.15 Photomicrograph: Sheared, talcose serpentinite rich in subhedral to euhedral chrome-spinels. Note the crudely hexagonal and cubic spinels (Sample 537, XP. Field width = 4 mm).

Intercumulus liquids: Contemporary magmas occupying the pore spaces between the cumulus phases.

An orthocumulate: A cumulate consisting of one or more cumulus minerals together with the products of crystallization of the "trapped" intercumulus liquid, which necessarily has the composition of the contemporary magma. The cumulus phases and their original intercumulus liquid constitute a closed system.

An adcumulate: A term used to describe the extension of the cumulus crystals at constant composition to give unzoned crystals, thus reducing the intercumulus liquid by mechanical expulsion.

Mesocumulates: Those rocks intermediate between orthocumulates and adcumulates and showing small amounts of pore material.

Postcumulus material: Primary, noncumulus material that formed (Jackson, 1961) in the spaces between the cumulus minerals. May be adcumulus or orthocumulus material.

A heteradcumulate: Contains unzoned minerals that have nucleated from intercumulus liquid but have grown by the adcumulus process.

3.2.2. Occurrence

The cumulate rocks are mainly concentrated in

the Jabal Khawr Fakkan and also south-east of Wadi Madha (Fig. 2.2). A limited development may be seen around Wadi Madha to the south and Wadi Shi to the north.

3.2.3. Rock types

The rock types are divided into:

1. Olivine pyroxenites
2. Olivine gabbros
3. Norites and hypersthene gabbros
4. Gabbros
5. Anorthosites and leucocratic gabbros
6. Gabbro mylonites

The above rock types are sub-divided in order of the abundance of the cumulus phases, with the rare phases in brackets, in the following manner:

1. Olivine pyroxenites
   - A. Clinopyroxene - olivine heteradcumulate
   - B. Clinopyroxene - olivine adcumulate

2. Olivine gabbros
   - A. Plagioclase-olivine-clinopyroxene adcumulate
   - B. Clinopyroxene-plagioclase-olivine mesocumulate
   - C. Olivine-plagioclase heteradcumulate

3. Norites and hypersthene gabbros

A. Orthopyroxene-clinopyroxene-plagioclase adcumulate

B. Plagioclase-orthopyroxene (clinopyroxene) heteradcumulate

4. Gabbros

A. Clinopyroxene-plagioclase adcumulate

B. Plagioclase-clinopyroxene mesocumulate

C. Plagioclase heteradcumulate

5. Anorthosites and leucocratic gabbros

A. Plagioclase adcumulate

6. Gabbro mylonites

The olivine-bearing cumulates are more prevalent than the other types and they are best developed in the north of the area around Wadi Shi and south of the area around Wadi Madha. The olivine-free cumulates are more common in Jabal Khawr Fakkan, and also south-east of Wadi Madha (Fig. 2.2).

3.2.3.1. Olivine pyroxenites

A. Clinopyroxene-olivine-heteradcumulate (Plate 3.16).

The following specimen is representative of this group: 1030B.

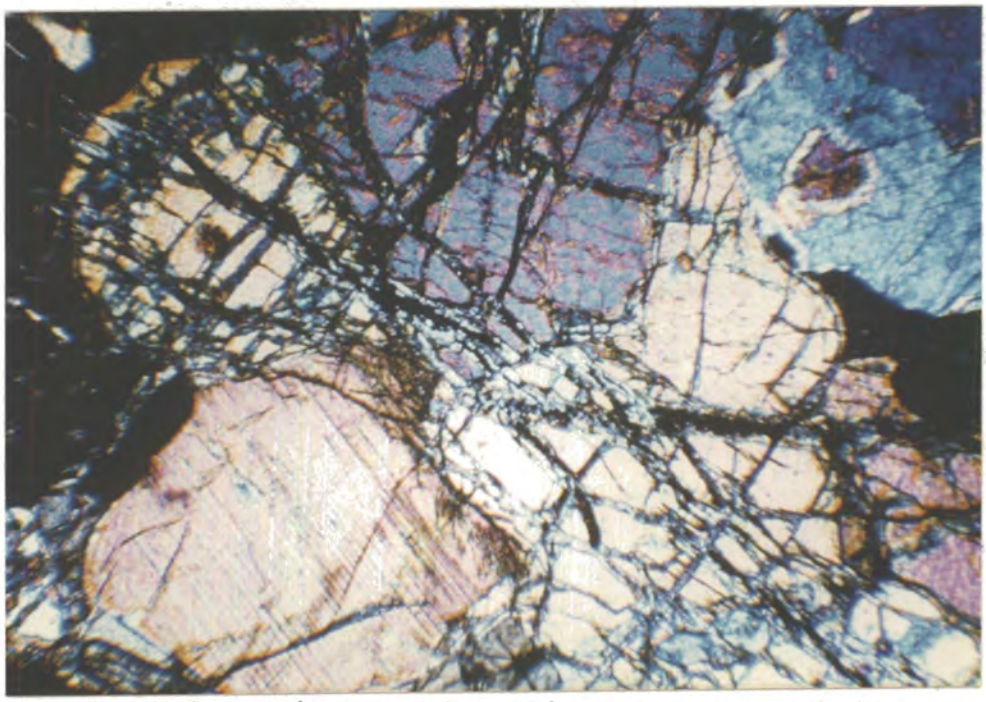

Plate 3.16 Photomicrograph: Clinopyroxene-olivine heteradcumulate, showing both cumulus clinopyroxene and cumulus olivine. The olivines are invariably traversed by a network of irregular serpentine veins outlined with magnetite (Sample 1030B. XP. Field width = 2 mm).

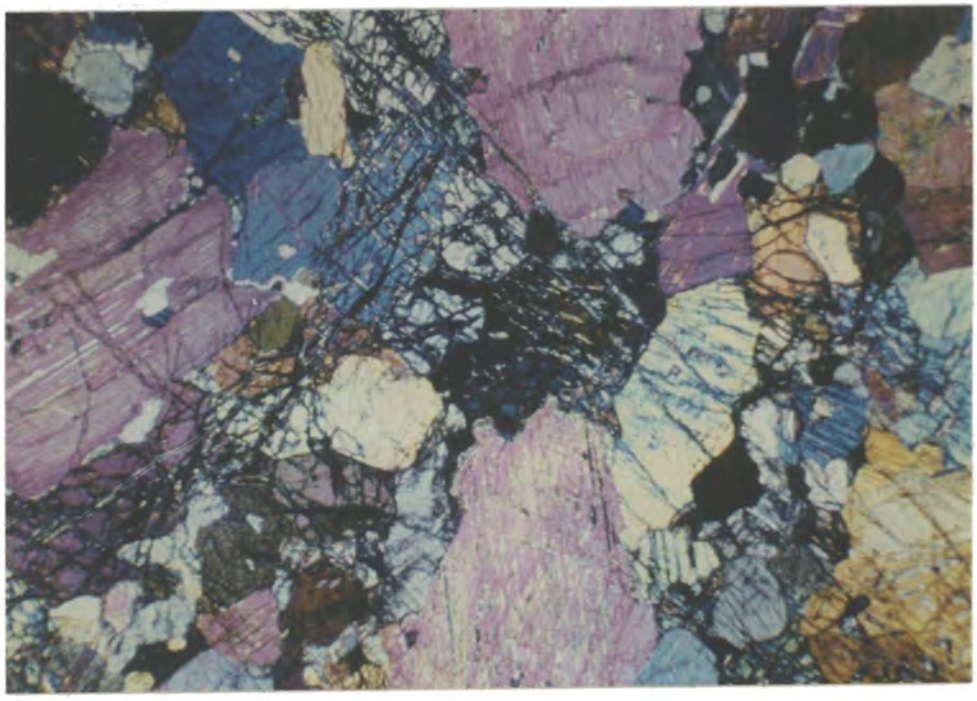

Plate 3.18 Photomicrograph: Clinopyroxene-olivine adcumulate, showing both cumulus clinopyroxene and cumulus olivine. The cumulus clinopyroxene and olivine have been extended by adcumulus growth (Sample 553. XP. Field width = 4 mm).

The main cumulus phases are diopsidic clinopyroxene and olivine. Plagioclase is rare and is an intercumulus phase. Average modal proportions are clinopyroxene 70%, olivine 19%, plagioclase 10% and spinel 1%.

Diopsidic clinopyroxenes occur as large, coarse, anhedral to subhedral crystals with an average grain size between 4x2.05mm and 10x5mm. Fine-scale exsolution lamellae of orthopyroxene parallel to (100) are common in the clinopyroxenes. Fe oxide is occasionally concentrated along the exsolved lamellae. Also present are large cumulus crystals of inverted pigeonite with clinopyroxene blebs (Plate 3.17).

Olivine is present in relatively minor amounts and occurs as large embayed crystals that appear in disequilibrium with the intercumulus liquid. The olivine crystals are highly serpentinized.

Plagioclase is rare, occurs interstitially to the clinopyroxenes and is intercumulus. The anorthite content is An_{97}. Green to brown Al-spinel is present in minor amounts.

B. Clinopyroxene - olivine adcumulates (Plate 3.18)

The following specimens are representative of this group: 553, 554, 1027 and 1028.

The main cumulus phases are diopsidic clinopyroxene and olivine. Average modal proportions are clinopyroxene 75%, olivine 24% and spinel 1%.

Diopsidic clinopyroxenes occur as large, coarse, anhedral to subhedral crystals with an average grain size between 4x2.1mm and 10x5mm. Fine-scale exsolution lamellae of orthopyroxene parallel to (100) are common. Also present are large crystals of inverted pigeonite with clinopyroxene blebs. In some samples the exsolution in the pigeonite is evident in two directions, one as broad lamellae parallel to (001) before inversion to hypersthene, and the other as broad lamellae parallel to (100) after inversion to hypersthene (Plate 3.19, Sample 553).

Olivine is present in relatively minor amounts, and occurs either as small, subhedral grains within the pyroxenes or as large grains which are invariably traversed by a network of irregular serpentine veins outlined by magnetite.

Minor brown Cr spinel is present in some samples (refer to analysis Table 5.42).

3.2.3.2. Olivine gabbros

A. Plagioclase-olivine-clinopyroxene adcumulates

The following specimens are representative of this group: 500, 501, 505, 523.

Plate 3.17 Photomicrograph: A large crystal of inverted pigeonite showing clinopyroxene blebs in a clinopyroxene-olivine heteradcumulate (Sample 1030B. XP. Field width = 2 mm).

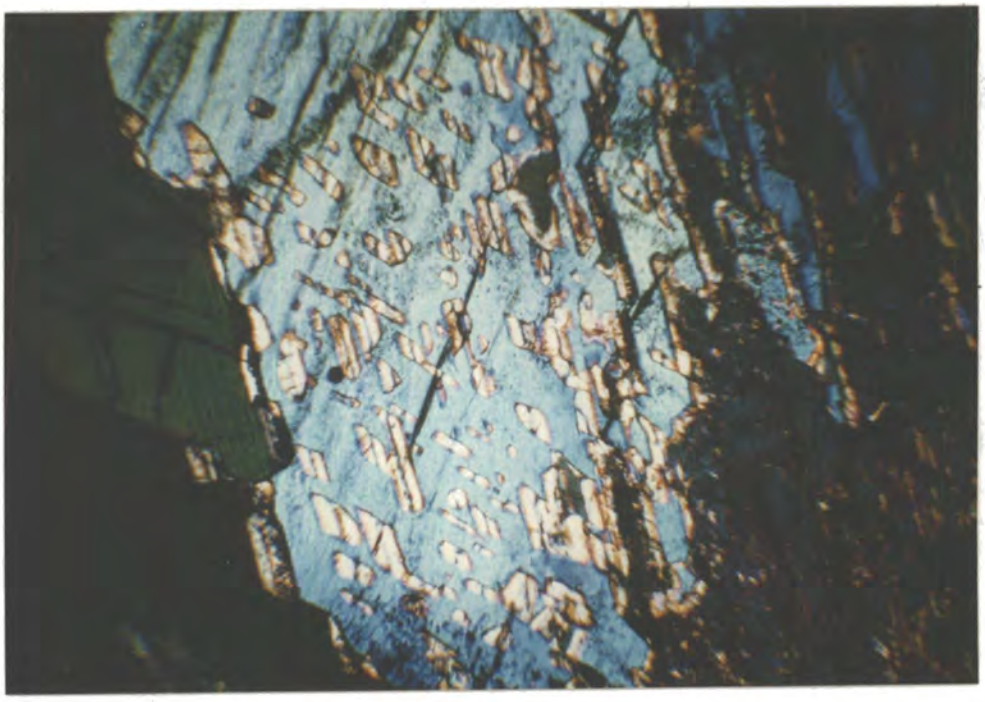

Plate 3.19 Photomicrograph: Clinopyroxene showing (001) and (100) exsolution lamellae of orthopyroxene in a clinopyroxene-olivine adcumulate (Sample 553. XP. Field width = 2 mm).

The main constituents are plagioclase, olivine, and diopsidic clinopyroxene and they form the cumulus phases. Average modal proportions are plagioclase 45%. olivine 33%, diopsidic-augite 15%, serpentine 3%, magnetite 2% and brown hornblende 2%.

Plagioclase occurs as medium-sized, anhedral to subhedral grains of average dimensions 3mm x 1.5mm. They have an anorthite content of $An_{74.8-78.7}$; they are consequently bytownite.

The olivines form rounded, corroded grains, 2x1.5mm and 1x1mm in diameter which are invariably traversed by a network of irregular serpentine veins outlined by magnetite. The texture shows evidence that serpentinization was accompanied by expansion, the effects of which are evident in strong radiate cracking of the adjacent plagioclases (Plate 3.20).

Diopsidic clinopyroxene occurs as 1.5x1mm in diameter, subhedral to anhedral crystals.

Alteration products include minor brown amphibole after pyroxene, and minor magnetite strings produced during serpentinization of olivine.

B. Clinopyroxene-plagioclase-olivine mesocumulates (Plate 3.21).

The following specimens are representative of this

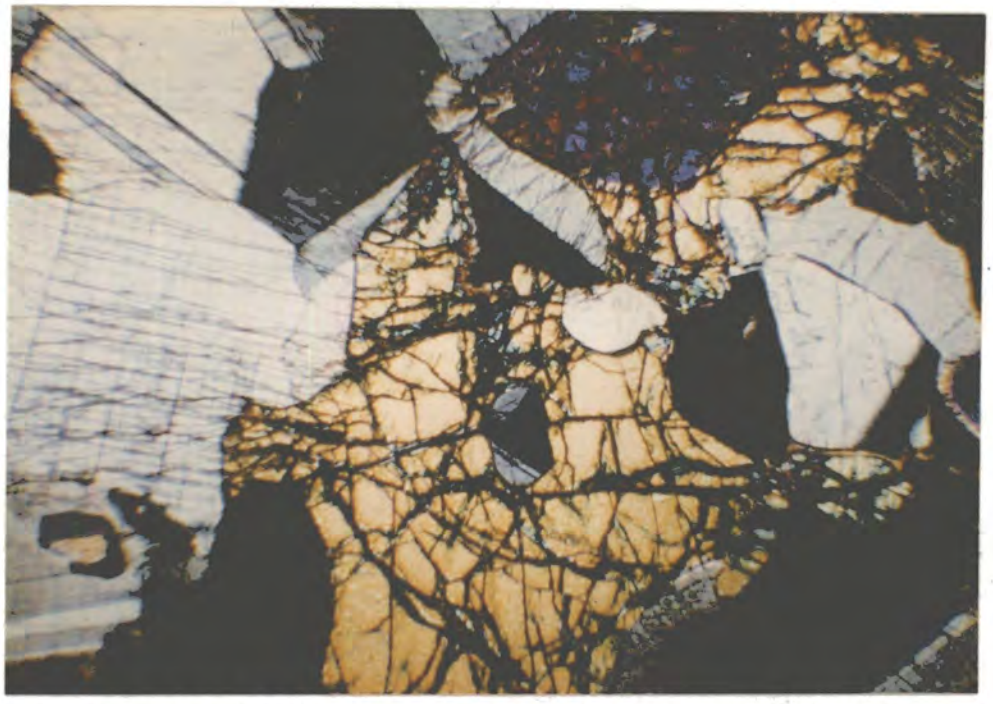

Plate 3.20 Photomicrograph: Plagioclase-olivine-clinopyroxene adcumulate. The olivines are partially serpentinized, and well-defined expansion fractures radiate from the olivine into adjacent plagioclase crystals (Sample 523. XP. Field width = 2 mm).

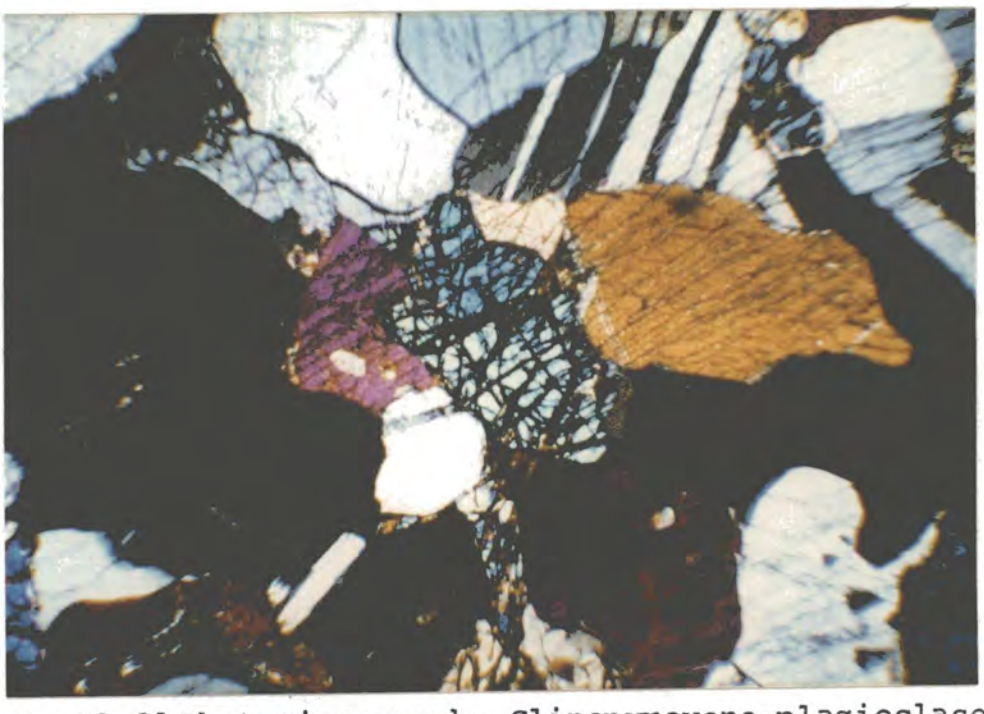

Plate 3.21 Photomicrograph: Clinopyroxene-plagioclase-olivine mesocumulate. Olivine is in reaction with hypersthene (Sample 119. XP. Field width = 4 mm).

group: 119, 555, 556, 557, 560, 562, 563, 564, 565, 1029(1), 109, 104A, 851, 871, 112, 106, 237, 846, 200, 539, 542, 567 and 568.

The main constituents are the three dominant cumulus phases - diopsidic clinopyroxene, plagioclase, and olivine. Orthopyroxene occurs as an exsolved phase or as a product of reaction between olivine and the intercumulus liquid. Average modal proportions are clinopyroxene 50%, plagioclase 30%, olivine 15%, orthopyroxene 4%, and magnetite 1%.

Diopsidic clinopyroxene occurs as anhedral crystals with an average grain-size of 3x1.5mm in diameter. The clinopyroxene contains exsolution lamellae of orthopyroxene parallel to (100).

The plagioclase is euhedral with an average grain size of 3x1.5mm in diameter and with an anorthite content of $An_{76.2-95.2}$. Occasional rosettes of ore in the plagioclase are observed by graphic texture (Plate 3.22).

Olivine is seen as anhedral, often rounded or oval crystals of average diameter 1.5mm x 1mm. Most of the olivines are traversed by a network of irregular serpentine veins outlined by magnetite.

C. Plagioclase-olivine heteradcumulates

The following specimens are representative of this

Plate 3.22 Photomicrograph: Clinopyroxene-plagioclase-olivine mesocumulate, showing occasional graphic texture of ore in the plagioclase. Olivine is in reaction with hypersthene. (Sample 560. XP. Field width = 4 mm).

group: 232, 238, 239, 234, 100, 102, and 103.

The main cumulus phases are plagioclase and olivine, the intercumulus mineral being clinopyroxene. Average modal proportions are plagioclase 60%, clinopyroxene 23%, and olivine 17%.

Plagioclase occurs as subhedral to euhedral, prismatic crystals of 3.5x1mm average dimensions. It has a tendency to a planar texture, indicative of igneous lamination. The plagioclase has an anorthite content of $An_{89.5}$ and hence is calcic bytownite.

The cumulus olivine is seen as anhedral, often rounded and oval crystals of 1.5x1mm average diameter. It is invariably traversed by a network of irregular serpentine veins outlined by magnetite. Some olivines have developed coronas separating them from plagioclase (sample 232, Plate 3.23). The coronas are formed from orthopyroxene and magnetite.

Clinopyroxene occurs as large ophitic crystals with an average grain size of 2.5x1.5mm in diameter, in patches surrounding the plagioclase crystals (Plate 3.24).

Plate 3.23 Photomicrograph: Plagioclase-olivine heteradcumulate. Coronas consisting of central olivine cores surrounded by orthopyroxene shells rimmed by magnetite granules (Sample 232. XP. Field width = 2 mm).

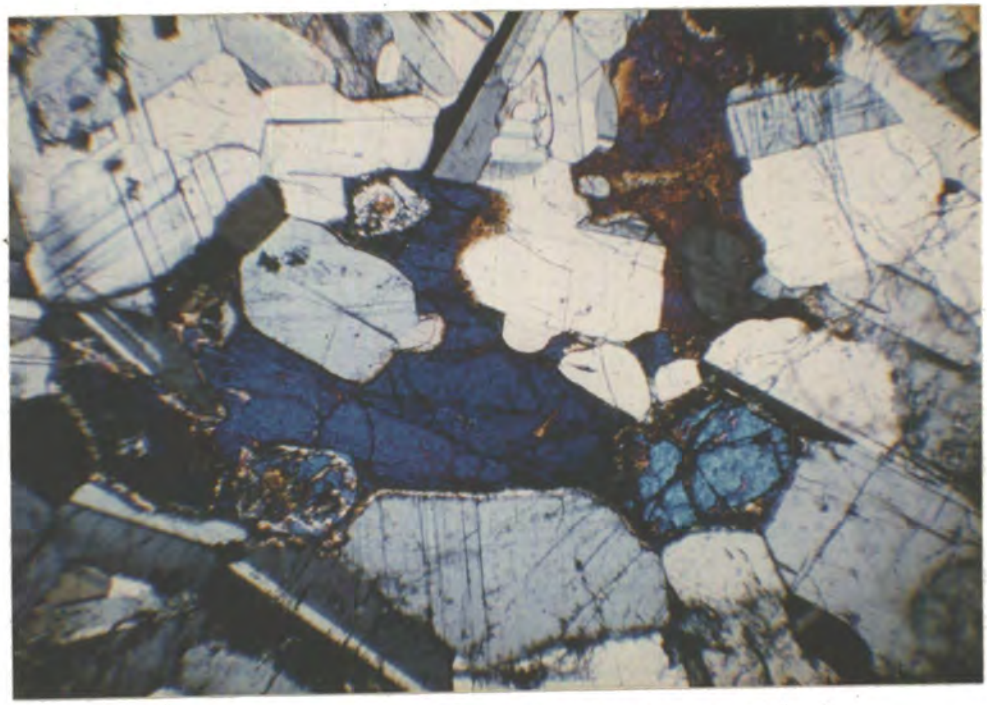

Plate 3.24 Photomicrograph: Plagioclase-olivine heteradcumulate. A large ophitic clinopyroxene enclosing plagioclase and olivine (Sample 232. XP. Field width = 4 mm).

3.2.3.3. Norites and hypersthene gabbros

Hypersthene gabbros

A. Orthopyroxene-clinopyroxene-plagioclase adcumulates.

The following specimens are representative of this group: 180, 183 and 138.

Orthopyroxene, clinopyroxene, and plagioclase are the three main cumulus phases with average modal proportions of orthopyroxene 75%, clinopyroxene 25% and plagioclase 5%.

Orthopyroxene, which is represented by hypersthene, is extremely coarse, occurring as large subhedral crystals with exsolution blebs of clinopyroxene. They have a grain-size of 4x2.5mm on average. In some samples the exsolution lamellae seem to have undergone patchy alteration to pale-green amphibole.

Clinopyroxene occurs as coarse, anhedral crystals with an average grain size of 3x2mm. The clinopyroxene contains exsolution blebs of orthopyroxene. Some of the clinopyroxenes are altered to green amphibole.

Plagioclase occurs as coarse, subhedral to anhedral crystals, varying in size between 3x2mm and 4x2.5mm in diameter, with a slight alteration to sericite.

Norites

B. Plagioclase-orthopyroxene (clinopyroxene) adcumulates (Plate 3.25).

The following specimens are representative of this group: 139, 852, 150, 138, 221, 223, 157, 201, 222, 158, 217 and 152.

Plagioclase and orthopyroxene are the main cumulus phases together with rare clinopyroxene. Average modal proportions are plagioclase 50%, orthopyroxene 40%, magnetite 3%, clinopyroxene 4%, and tremolite-actinolite 3%.

Plagioclase occurs as coarse, interlocking, subhedral to anhedral crystals of average grain size 3x2.02mm. It has an anorthite content of $An_{93.3}$.

Orthopyroxene is represented by hypersthene which occurs as coarse, subhedral crystals of average grain size 3x2mm; they show a faint reddish-pink pleochroism. Exsolved blebs of clinopyroxene, and fine exsolution lamellae parallel to (100), are present. The orthopyroxene shows varying degrees of alteration. In the least altered, tremolite is seen replacing the edges of the crystals. In the more advanced stages, the orthopyroxene is often completely converted to colourless tremolite and actinolitic amphibole.

Plate 3.25 Photomicrograph: Plagioclase-orthopyroxene -(clinopyroxene) adcumulate, showing hypersthene, plagioclase and clinopyroxene. Tremolite replaces the edges of the hypersthene crystals. (Sample 139. XP. Field width = 4 mm).

Diopsidic clinopyroxene occurs as small, anhedral crystals with an average grain size of 2x1.5mm and 1.5x1mm in diameter which are subordinate to the two major phases. Most of the clinopyroxenes are altered to pale-green amphibole.

Granular magnetite is often concentrated in the fibrous tremolite-actinolite.

3.2.3.4. Gabbros

A. Clinopyroxene-plagioclase adcumulate.

This type is considered very rare and only one sample was noticed (209). Diopsidic clinopyroxene and plagioclase are the main cumulus phases with average modal proportions of diopsidic clinopyroxene 70%, plagioclase 29%, and chrome spinel 1%.

The diopsidic clinopyroxenes occur as coarse, subhedral to anhedral crystals of average grain-size 7x6mm in diameter. They contain exsolved blebs of orthopyroxene, and fine exsolution lamellae parallel to (100).

The cumulus plagioclase crystals occur as coarse, euhedral crystals of average dimensions 5x3mm.

Chrome spinel is very minor and occurs as small crystals in the clinopyroxenes.

B. Plagioclase-clinopyroxene mesocumulates (Plate 3.26).

The following specimens are representative of this group: 859, 853, 104B, 1018, 544 and 541.

Plagioclase and clinopyroxene are the main cumulus phases with average modal proportions of plagioclase 50%, diopsidic clinopyroxene 40%, magnetite 5%, and fibrous amphibole 5%.

Plagioclase occurs as coarse, euhedral crystals with average grain size 3x2mm in diameter. In some samples such as 859, the plagioclase crystals are slightly bent or strained as shown by the twin lamellae. The anorthite content of the plagioclase crystals is $An_{80.6}$ and hence it is a bytownite.

Clinopyroxene occurs as fairly large, subhedral crystals of average diameter varying between 3x2mm and 2.5x1.5mm, with occasional reaction rims of brown basaltic hornblende (sample 859, Plate 3.27). It is also often replaced by pale green, fibrous amphibole (sample 541).

Magnetite occurs as pods and is associated with the development of the brown basaltic hornblende (sample 859, Plate 3.27).

C. Plagioclase heteradcumulate

Only sample 231 can be considered to represent this

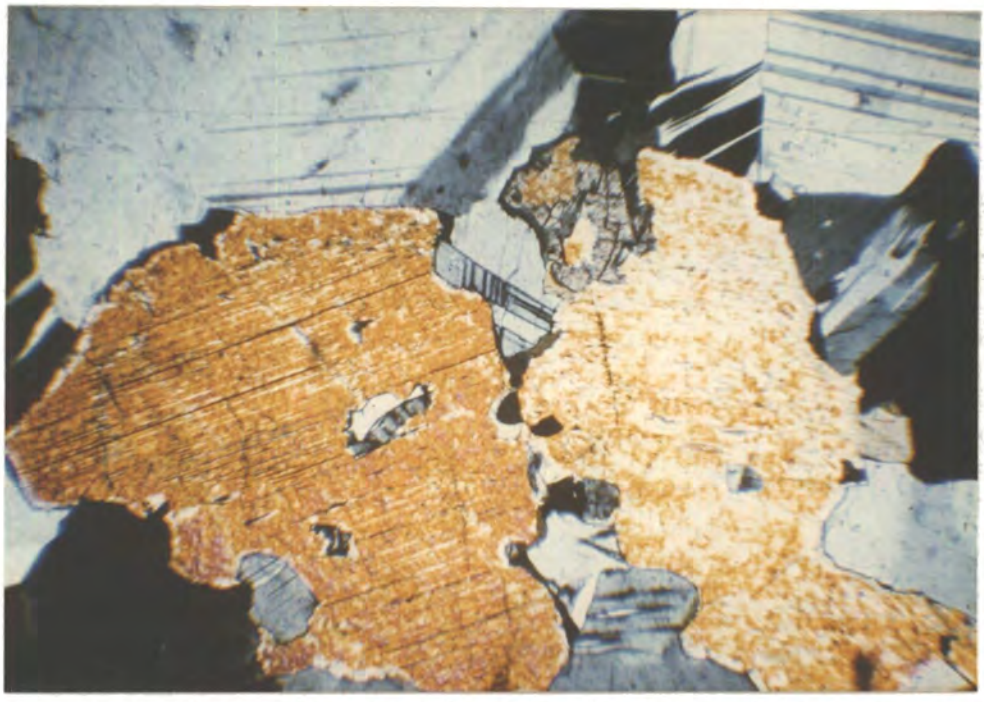

Plate 3.26 Photomicrograph: Plagioclase-clinopyroxene mesocumulate, showing large crystals of clinopyroxene enclosing small plagioclase crystals (Sample 859. XP. Field width = 4 mm).

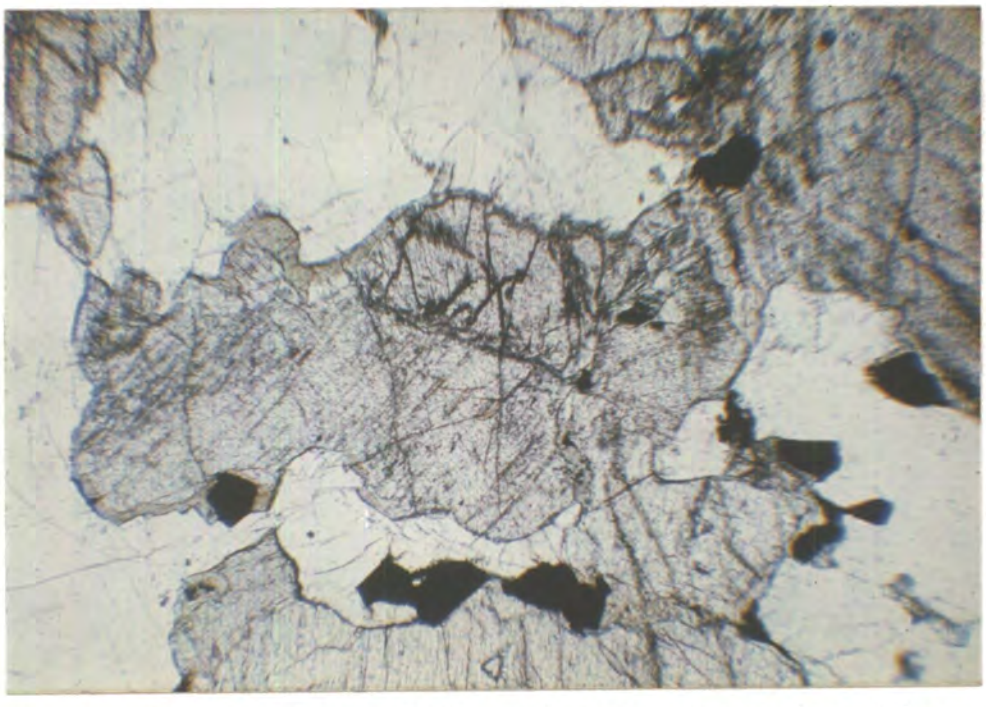

Plate 3.27 Photomicrograph: Clinopyroxene rimmed by brown basaltic hornblende. Build up of H_2O in the interstitial liquid permitted the precipitation of brown basaltic hornblende. Note magnetite associated with the development of the brown basaltic hornblende (Sample 859. PPL. Field width = 4 mm).

category. Plagioclase is the main cumulus phase with intercumulus, diopsidic clinopyroxene. Average modal proportions are plagioclase 55%, diopsidic clinopyroxene 40%, and fibrous amphibole 5%.

The plagioclase occurs as coarse, euhedral, prismatic crystals with a slight tendency to lamination; they have average dimensions of 2.5x2mm and 0.5x0.2mm. The anorthite content is $An_{86.5}$ and hence it is a bytownite. The plagioclase crystals are surrounded by very large, ophitic clinopyroxenes (Plate 3.28).

The clinopyroxenes are often replaced by fibrous amphibole, but this has not affected the texture.

3.2.3.5. Anorthosites and Leucocratic Gabbros

Anorthosites

A. Plagioclase adcumulates (Plate 3.29)

The following specimens are representative of this group: 220, 160, 151, and 146.

Plagioclase is the dominant phase, the rock approaching an extreme adcumulate. Magnetite is considered an intercumulus phase. Average modal proportions of the constituents are plagioclase 97%, magnetite 2%, and clinopyroxene 1%.

The plagioclase is coarse with an anorthite content

Plate 3.28 Photomicrograph: Plagioclase heterad-cumulate, showing euhedral to prismatic plagioclase surrounded by very large ophitic clinopyroxene. The plagioclase crystals show a slight tendency to lamination. In places the clinopyroxene is replaced by fibrous amphibole, but ophitic texture is preserved (Sample 231. XP. Field width = 4 mm).

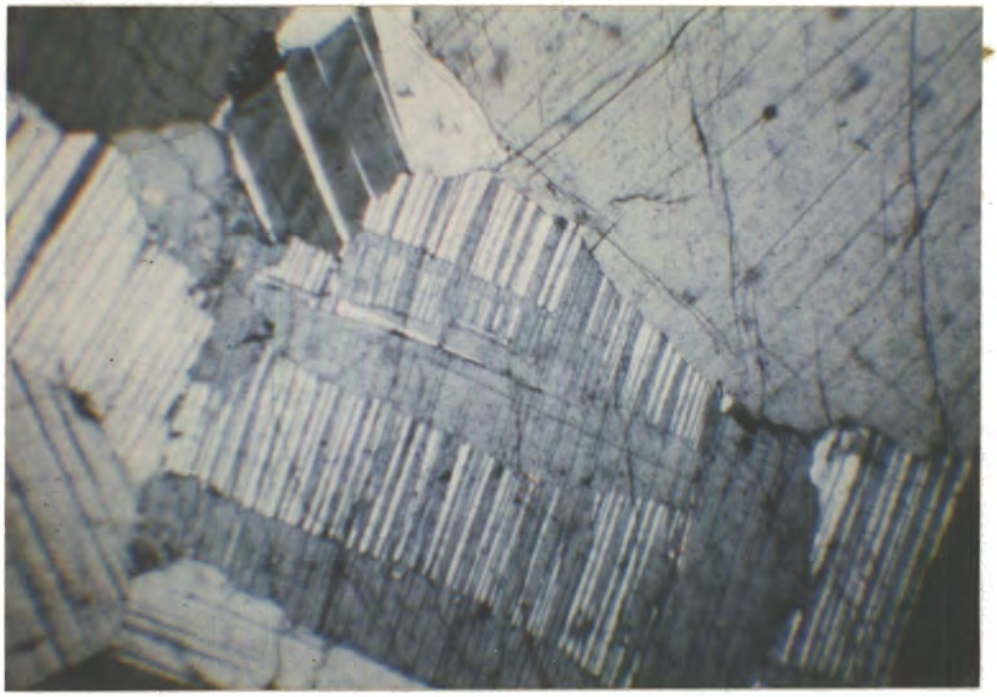

Plate 3.29 Photomicrograph: Plagioclase adcumulate. (Sample 220. XP. Field width = 2 mm).

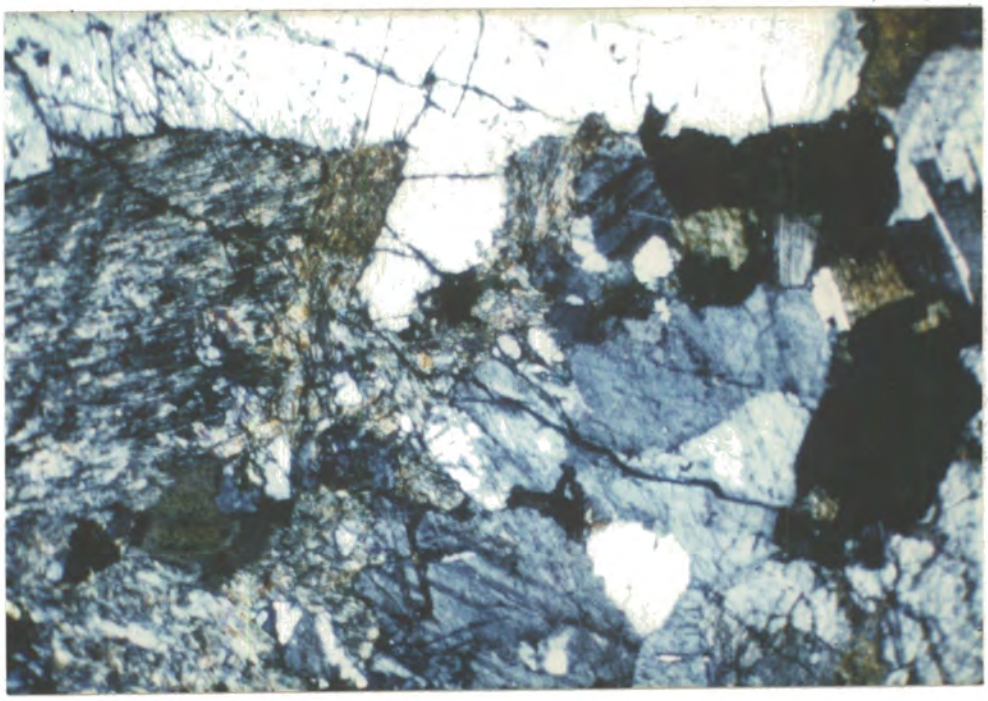

Plate 3.30 Photomicrograph: Plagioclase crystals showing evidence of brecciation, granulation and crushing due to tectonic deformation. Ilmenite and hornblende are also present (Sample 110. XP. Field width = 4 mm).

of $An_{93.1}$. It has suffered mechanical deformation (e.g. 160) and is slightly bent and strained as shown by the twin lamellae. In these crystals the twin lamellae are concentrated, and broad, in areas where the straining effect is least evident, but they pinch out and taper in the most deformed areas, due to recrystallization. The lamellae themselves are commonly bent, and they frequently terminate at cracks within the plagioclase crystals.

Magnetite is interstitial and occurs as anhedral crystals, and sometimes as stringers between the coarse plagioclase crystals.

In sample 151, a thin layer of altered plagioclase-clinopyroxene cumulate is present, where the clinopyroxene is considered a cumulus phase.

Sample 146 shows compositional layering from (a) plagioclase-clinopyroxene-orthopyroxene cumulate to (b) plagioclase adcumulate.

The overall texture of part (a) is fine grained. Clinopyroxene is concentrated into elongate patches representing brief periods of pyroxene deposition. Orthopyroxene, represented by hypersthene, is concentrated in the fine, felsic layers. The overall texture of part (b) is coarse grained. Ilmenite proved to be intercumulus

after it was checked with a reflected-light microscope and occurs as anhedral crystals and sometimes as stringers between the coarse plagioclase crystals.

Leucocratic Gabbros

This rock type is not a common member of the gabbroic rocks but occurs in the layered sequences together with the olivine gabbros and the clinopyroxene-rich cumulates. The rock-type often shows evidence of granulation and re-crystallization, due to its occurrence in highly faulted areas.

The rock type is identified as a leucocratic gabbro due to the diminished amounts of ferromagnesian minerals; it gradually passes into anorthosite.

The main constituents are plagioclase, diopsidic clinopyroxene, ilmenite, chlorite, tremolite-actinolite, and green hornblende. Modal proportions of the minerals present are: plagioclase 70%, diopsidic clinopyroxenes 10%, green hornblende 10%, ilmenite 4%, chlorite and tremolite-actinolite 6%. The overall texture of the mineral phases is extremely coarse grained.

Plagioclase occurs as coarse anhedral crystals. All the plagioclase crystals studied show evidence of brecciation, granulation, and crushing due to tectonic deformation. Undulose extinction and bent twinning are

also evident in most samples (Plate 3.30). Occasionally the large and bent plagioclase crystals pass into areas of shattering where the plagioclase forms much smaller crystals with evidence of recrystallization, e.g. sample 156(3), (Plate 3.31).

Clinopyroxenes are partly altered to chlorite and tremolite, with minor interstitial remnants evident. In rare cases the clinopyroxenes are more resistant to alteration, thus retaining their original shape.

Straw yellow-green hornblende occurs interstitially to ilmenite and as reaction rims with ilmenite (sample 110) (Plate 3.32).

Pseudomorphs after interstitial clinopyroxene, mainly forming acicular and radiate aggregates, were difficult to identify in some samples. These minerals were identified by microprobe analysis. The first type, with anomalous brownish interference colours, was chlorite. The other type, which occurs as radiate aggregates, was identified as tremolite-actinolite.

3.2.3.6. Gabbro mylonites

Mylonites occur as zones of intensely crushed and granulated rocks along clearly defined faults. The rock is of extremely fine-grained size, which makes the

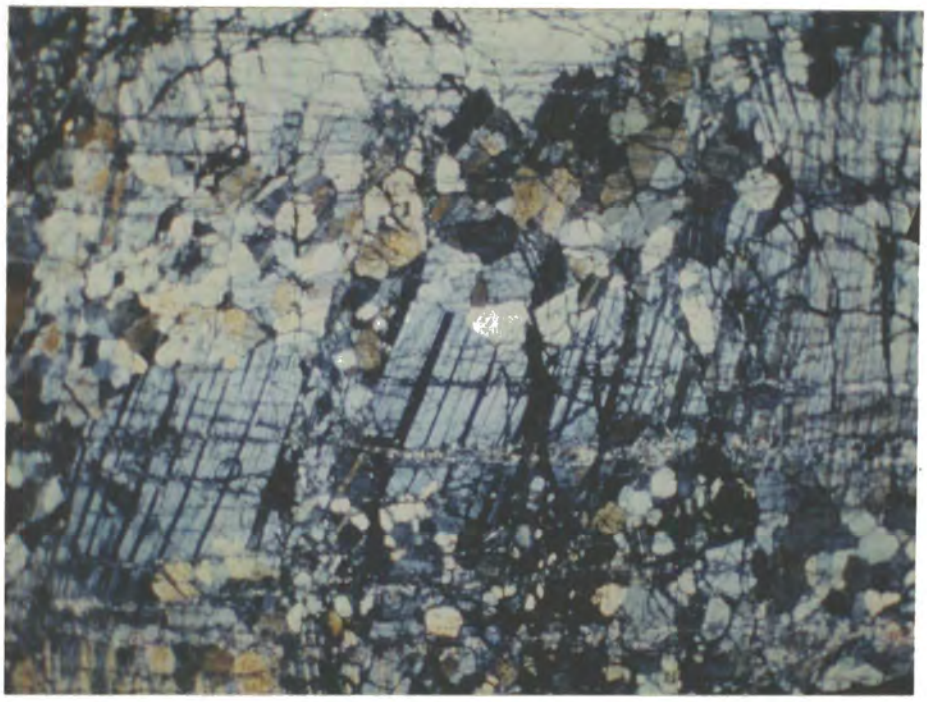

Plate 3.31 Photomicrograph: Shattered leucogabbro, showing large and bent plagioclases passing into areas of shattering, where plagioclase forms much smaller crystals (Sample 156(3). XP. Field width = 4 mm).

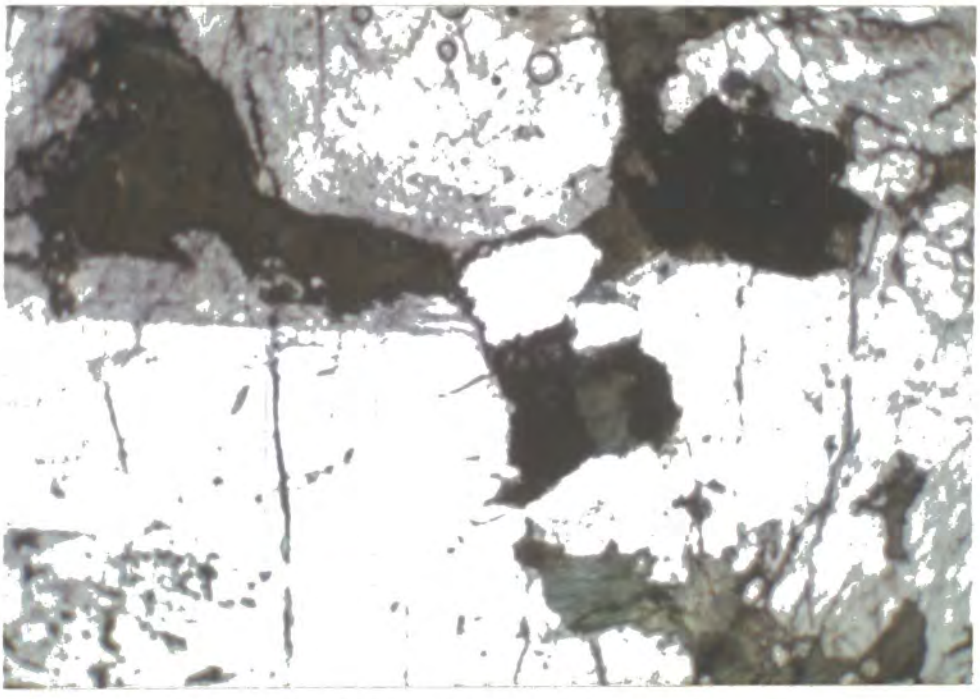

Plate 3.32 Photomicrograph: Green hornblende occurring interstitially to ilmenite and as reaction rims with ilmenite in a leucocratic gabbro. The plagioclase crystals are bent and shattered. (Sample 110. PPL. Field width = 4 mm).

optical determination of the various mineral phases extremely difficult. The main identifiable constituents are plagioclase and amphibole; clinopyroxenes are mainly altered to pale-green amphibole.

The plagioclase varies in grain-size from laths of 1.5x1mm to crystals of medium grain-size with average diameter of 2.5x2mm. Some of the plagioclase crystals are severely crushed and recrystallized, with a tendency to polygonization. Most of the plagioclase crystals show an undulose extinction due to deformation.

The clinopyroxenes are mainly altered to pale-green amphibole but the few grains remaining can be seen to be elongated, with a very strong parallel fabric. Occasionally a few residual, large and shattered clinopyroxenes can be observed as remnants in the fine-grained matrix (Plate 3.33). In some samples (e.g. 559), the pale-green amphibole occurs as porphyroblasts set in the fine-grained matrix of plagioclase laths and amphibole which show a strong alignment.

3.3. Petrography of the basaltic rocks

3.3.1. Occurrence

Rocks of basaltic composition are common within the ophiolites of the Northern Oman Range. They form massive

Plate 3.33 Photomicrograph: Fine-grained amphibolized gabbro mylonite, showing amphibole as porphyroblasts set in a fine grained matrix of plagioclase laths and amphibole which show a strong alignment. Few residual, large and shattered clinopyroxenes can be observed as remnants in the fine grained matrix (Sample 559. XP. Field width = 8 mm).

flows, sheeted dykes and occasionally near-vertical dykes that vary in thickness between two and three metres. The dykes strike between 35° and 40° and dip steeply south-eastwards. In hand specimen, the rocks are dark and massive, and contain small phenocrysts of feldspar, and ferromagnesian minerals now pseudomorphed by chlorite.

The basaltic rocks are mainly concentrated to the southeast of Jebel Qidfa where they form sheeted dykes, dissected by short and steep Wadis, and covered by coarse scree. Other basaltic rocks occur as flows, concentrated on the small island of Sirat Al-Khawr, which lies about a mile offshore from Khawr Fakkan and in the extreme north near Jabal Khawr Fakkan. Fine, vertical to sub-vertical dykes of basaltic rock also intrude the gabbros of Jabal Khawr Fakkan in the coastal region.

The following specimens are representative of this group: Lavas - 101, 103, 107, 122 and 1004. Sheeted dykes - 108, 109, 111, 117, 149A, 154, 167, 169, 170, 171, 172, 174, 176, 186, 204, 206, 230, 233, 856, 858, 165, 866, 162A, 162B and 864.

3.3.2. Petrography

The overall texture of the basaltic rocks is fine grained, varying from aphenitic to porphyritic. The

occasional phenocrysts consist of plagioclase, amphibole and chlorite embedded in a microcrystalline groundmass of plagioclase microlites, amphibole, quartz and occasional carbonates (Plate 3.34).

Average modal proportions of the constituents are plagioclase 38%, amphibole 47%, quartz 11%, carbonate 3%, and talc 1%. There is considerable variation in quartz content however, one sample, a porphyritic basalt (154) having 25% quartz. This is thus transitional to the amphibolised, quartz-rich dolerites (Section 3.3.3.).

The groundmass feldspars occur as fine, lath-shaped crystals with average dimensions of 0.6 to 0.4mm. They show slight to very good, preferred orientation. Occasional feldspar phenocrysts range up to 1.5 by 0.5mm. The fine-grained, lath-shaped feldspar is albite, while the occasional phenocrysts are andesine An_{50-46}.

Quartz occurs in patches interstitial to the feldspar laths and occasionally shows a poikilitic texture. The average diameter of the quartz crystals lies between 1 and 2mm. Some show undulose extinction, indicative of strain, and sutured boundaries.

Amphiboles and chlorite occasionally occur as phenocrysts with average dimensions of 2.5x1.5mm. More commonly the amphiboles occur as fine, lath-shaped

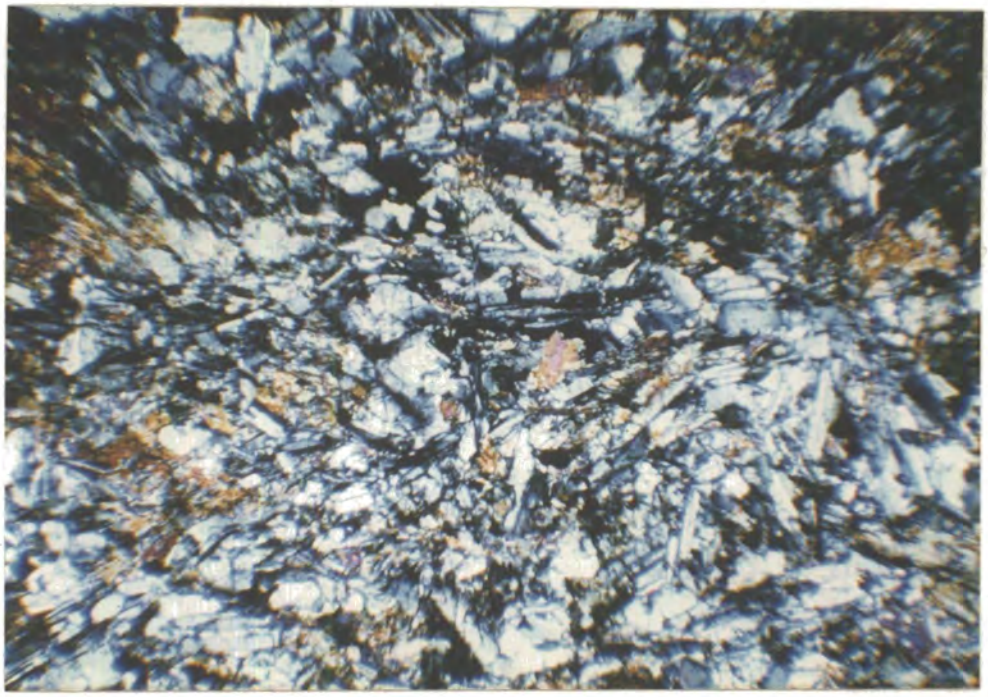

Plate 3.34 Photomicrograph: Porphyritic basalt showing fine-grained lath-shaped plagioclase set in a microcrystalline groundmass of amphibole, quartz and occasional carbonates (Sample 162A. XP. Field width = 8 mm).

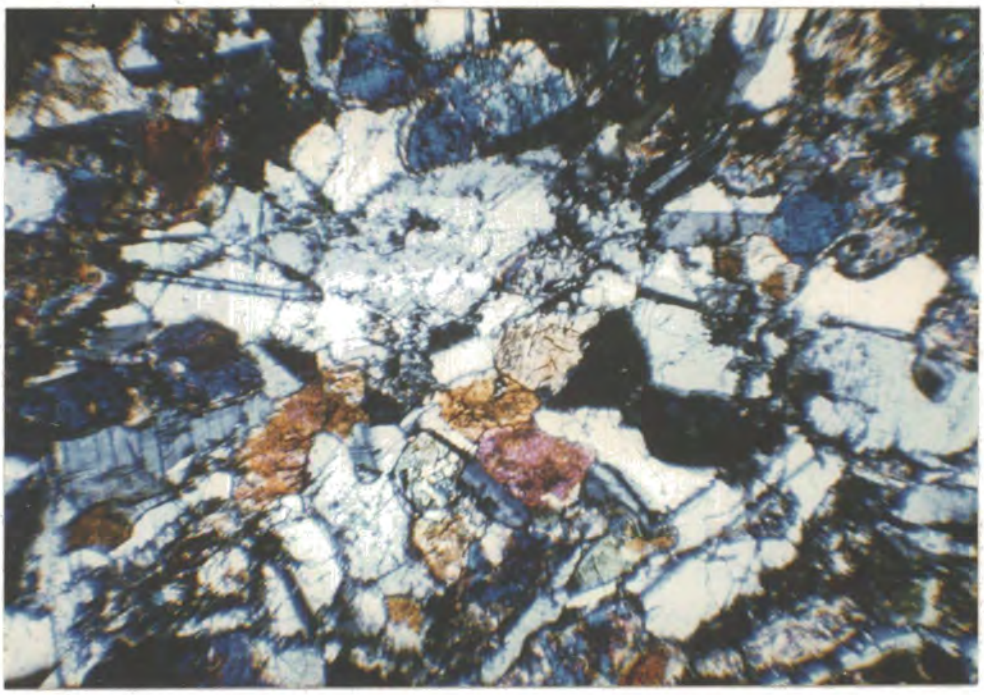

Plate 3.35 Photomicrograph: Silicified porphyritic basalt showing fine lath-shaped plagioclase and fine needle-like amphiboles projecting into quartz patches. (Sample 162A. XP. Field width = 2 mm).

crystals 0.5x0.1mm in average dimensions, or as fine, needle-like, pale-green crystals which project into the quartz patches (Plate 3.35).

Veining of the fine-grained matrix by talc and carbonates is rare, and only evident in one sample.

Pyroxenes are converted entirely to amphiboles.

3.3.3. Amphibolized, quartz-rich dolerites

The amphibolized, quartz-rich dolerites occur as sub-vertical dykes about two metres thick, within the gabbros of the Khawr Fakkan region. They are principally found in Jabal Khawr Fakkan in the coastal region near the Gulf of Oman, and more rarely to the north of Wadi Shi (Fig. 2.2). The following specimens are representative of this group: 227, 228, 184, 196, 164, 218, 137, 140 and 159.

The dolerites are medium to fine grained rocks containing subhedral, lath-shaped plagioclase, interstitial quartz, pale-green amphibole, and ilmenite. Average modal proportions of the constituents are plagioclase 40%, amphibole 30%, quartz 25% and ilmenite 5%.

The plagioclase laths have average dimensions of 4 by 2mm, and 1.5 by 1mm. They have an anorthite content of An_{50} and are thus andesine-labradorite.

Quartz occurs as clear patches interstitial to plagioclase, occasionally seeming to replace the margins of the plagioclase crystals. The quartz crystals sometimes show a shadowy, strained extinction and sutured boundaries are evident in places.

Pale-green amphibole, and straw yellow-green hornblende after pyroxene occur as needle-like to prismatic crystals; the needle-like amphiboles project into the quartz patches. A tendency to preferred orientation is evident in the straw yellow-green hornblende.

Clinopyroxene is almost entirely converted to amphibole, with the exception of one sample (196) where minor clinopyroxenes are pseudomorphed by hornblende and skeletal ilmeno-magnetite (Plate 3.36).

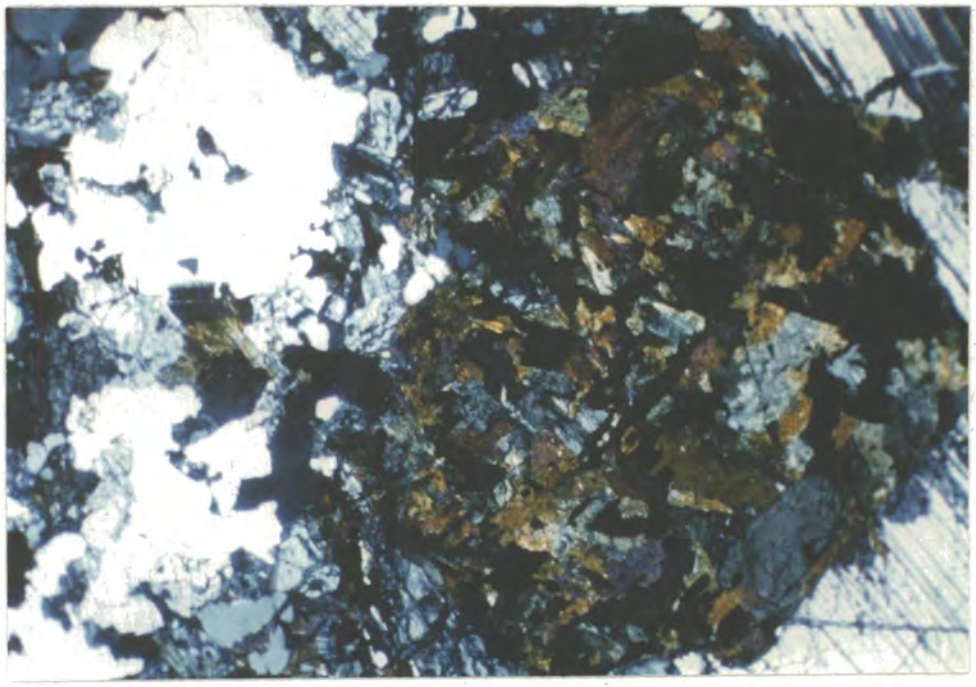

Plate 3.36 Photomicrograph: Amphibolized quartz dolerite showing clinopyroxene pseudomorphed by hornblende and skeletal ilmeno-magnetite. Clinopyroxene has been almost entirely converted to amphibole, with few remnants remaining (Sample 196. XP. Field width = 4 mm).

CHAPTER 4: Whole-rock geochemistry

4.1. Sample preparation

The specimens were split into fragments using a hydraulic splitter, and the weathered parts were cut away and discarded in order to prevent contamination. The fragments were crushed into chips using a Sturtevant Jaw crusher and this was followed by grinding in the tungsten carbide vials of a Tema Disc Mill, which reduced the samples to a powder of around 300 mesh. A few grams of the resulting powder were pelletised, using a hydraulic press, under a pressure of 5 tons per square inch; 3 drops of "Mowiol" were added as a binder.

4.2. Major element analysis

Chemical analyses for major elements were made of 358 samples, which included 86 ultramafic rocks and 272 basic rocks, composed of cumulate pyroxenites, gabbros, and fine-grained basaltic rocks. The pelletised samples were analysed on a Philips PW1212 automatic vacuum spectrometer which is capable of handling up to 108 samples in a run. The elements Si, Al, Fe, Mg, Ca, Na, K, Ti, P and S were determined using a Cr target for primary radiation, and an evacuated sample chamber. Mn was analysed separately using a W target. A "fixed counts"

operating procedure was used. In order to minimise the effects of electronic instability and voltage drift a monitor was used throughout and samples were analysed in groups of three. The samples were divided into three groups (ultramafics, gabbros and related rocks, and fine-grained basalts and dolerites). Each group was analysed separately. The international standards AGVI, W1, K211, BCR1, G, T1, S1, GR, GA, OK272, and GSP1 were used for the gabbros and related rocks, and for the fine-grained basalts and doleritic types. For the ultramafic rocks, the U.S.G.S. international standards DTS1, PCC1, UM1, UM2, UM4, RE114, and RE507 were used. The compositions of the international standards were taken from reviews by Flanagan (1969, 1973). Total Fe was calculated as Fe_2O_3. Mass-absorption corrections were made by an iterative procedure using the computer technique originally described by Holland and Brindle (1966), as modified by Reeves (1971). 75 fresh samples representing the three rock groups were chosen for the determination of FeO, using a wet-chemical, metavanadate method; these are shown in Tables 4.1 to 4.4.

4.3. Trace element analysis

The elements Ba, Nb, Zr, Y, Sr, Rb, Zn, Cu, Ni and Cr were determined using a W target, and an evacuated

sample chamber. Analytical count data were converted into concentrations (ppm) using the computer programme "Tratio" written by Dr. R.C.O. Gill. This programme uses the function (peak intensity/background intensity) -1 to compensate for matrix and mass absorption effects, using scattered background radiation as an internal standard. Corrections for contamination and also certain element interferences (e.g. Sr $k\beta$ on Zr $k\alpha$) were included in this programme.

The standards used were synthetic spiked glasses constructed for use in analysis of lunar basalts (Brown et al., 1970). The U.S.G.S. standards were also used. The samples were again arranged into the three groups described above and each group was run separately.

For analysis of the ultramafic samples, only the U.S.G.S. standards were used because the Ni and Cr values are much higher than the levels in the lunar standards. The elements Ba, Nb, Zr, Y, Sr, Rb and Zn were not determined for the ultramafics, because all of these elements were below the detection limit in a reconnaissance run of thirteen samples.

4.3.1. Ultramafic rocks

Analyses of the ultramafic rocks are given in Tables 4.5 to 4.7 together with their CIPW norms.

The analyses are all expressed on a water-free basis.

The variation in degree of serpentinisation of the ultramafic rocks makes the interpretation of their analysis difficult, owing to the possibility that the serpentinisation may have changed the proportions of the major constituents. An indication of the effects of serpentinisation is seen in samples where ferric iron contents are slightly higher than ferrous iron. This undoubtedly results from the production of magnetite during serpentinisation and oxidation of olivine. Engin and Hirst (1970) have shown, however, that the proportions of most major oxides remain relatively unaffected by serpentinisation and thus analyses expressed on a water-free basis are generally representative of unaltered rocks.

The following points may be remarked upon, on the basis of the major and trace element contents of the ultramafics. In general, the peridotites show a variation of MgO content between 39.25 and 47.62 percent, characteristic of the alpine type of peridotite, while the content of SiO_2 varies from 40.93 and 45.90 percent. The peridotites, mainly dunites, harzburgites and wehrlites can be subdivided on the basis of their significant major and trace oxide contents; mainly on the basis of SiO_2, MgO, CaO, NiO, and Cr_2O_3. The

dunites show a lower SiO_2 but higher MgO content than the harzburgites. The wehrlites have comparable SiO_2 contents to the dunites but have higher CaO and lower MgO contents than either the dunites or harzburgites. The analyses are in good agreement with values for peridotites from Burro Mountain California (Loney et al., 1971).

Total iron, shown as Fe_2O_3, varies between 10 and 12 percent for the dunites, and 8 and 9 percent for the harzburgites. Variation of total Fe as Fe_2O_3 in the wehrlites is greater, and inversely related to the MgO content. CaO contents are a reflection of the presence of major amounts of clinopyroxene in the wehrlites, and conversely, a minor presence in the dunites and harzburgites. It is possible that some CaO has been removed during serpentinisation; this would be most extensive for the wehrlites (Barnes et al., 1967; Page, 1967b). Some harzburgites have moderate levels of CaO despite the absence of accessory, discrete clinopyroxene. These levels are due to the calcium contents of the orthopyroxene in the harzburgites.

Orthopyroxene, clinopyroxene and chromian spinel are the Al_2O_3-bearing minerals in the harzburgites and wehrlites. In the dunites, accessory chromian spinel

is virtually the only Al_2O_3-bearing phase.

Alkalis are present only in trace amounts, but in general the Na_2O value is higher in the harzburgites and wehrlites than in the dunites, which suggests that the Na_2O is probably in the clinopyroxenes. K_2O is truly depleted in the peridotites.

The Cr_2O_3 in the peridotites is mainly a function of the modal amount of chromian spinel present in these rocks. In general, the harzburgites have a range of 0.35 to 0.52 percent, the dunites 0.40 to 1.33 percent and the wehrlites from 0.47 to 0.59 percent Cr_2O_3. In rare cases, wehrlites have higher Cr_2O_3 contents than either the dunites or harzburgites. This is most probably due to chrome-rich clinopyroxene in the wehrlites, a conclusion confirmed by electron-probe analysis of clinopyroxenes whose Cr_2O_3 content varies between 0.98 and 1.43 percent (see Chapter 5).

The NiO levels in the dunites vary between 0.19 and 0.37 percent, in the wehrlites between 0.16 and 0.30 percent and in the harzburgites occupy a very narrow range between 0.29 and 0.30 percent. The Ni of the ultramafics is mainly concentrated in the olivines and the high uniform level in the harzburgites reflects their refractory nature. The whole-rock distribution of Ni is confirmed by electron probe analysis of the olivines in

the harzburgites and dunites which gives a distinctly higher Ni content for the olivine from harzburgite. Some variation in content may be a reflection of variable serpentinisation of these rocks. However, during partial melting, Ni would enter the refractory crystals of olivine and thus variation in the ultramafics may well reflect variation in the degree of partial melting, in temperature and pressure, or the extent to which the process approached equilibrium.

4.3.2. Cumulate pyroxenites

Analyses of the cumulate pyroxenites are given in Table 4.8, expressed on a water-free basis. The cumulate olivine pyroxenites are characterised by high MgO varying from 22 to 26 percent, while SiO_2 varies between 43 and 52 percent. Al_2O_3 contents are very low, generally between 1.11 and 1.77 percent; although in rare cases, Al_2O_3 amounts to 11 and 9 percent. CaO is present in relatively high amounts, varying between 14 and 18 percent. This is clearly due to the high modal proportions of clinopyroxene present in these rocks. The pyroxenites are depleted in alkalis and TiO_2.

Chromium and nickel are the only trace elements present in significant amounts. For instance Cr_2O_3, in

the pyroxenites, varies between 0.40 and 1.01 percent. The chromium is present in significant amounts because Cr^{3+} substitutes in the octahedral sites of pyroxenes. The abundance is confirmed by electron-probe analysis of clinopyroxenes whose Cr_2O_3 content varies between 0.32 to 0.86 percent. The Cr is depleted in the magma early in fractional crystallization (Taylor, 1965).

NiO varies between 0.03 and 0.06 percent levels which are very much less than those of the ultramafic rocks described above. The chief host for Ni is olivine and thus part of the difference between the cumulate pyroxenite and ultramafic Ni levels may be due to the lower proportion of olivine in the cumulates. However, the cumulates themselves have been formed by fractional crystallisation of a basic magma which was generated by partial melting of the upper mantle. During the latter process, as seen above, Ni is partitioned into the refractory residuum, the crystalline phase, and thus depleted in the melt. Consequently the olivine-pyroxenite cumulates have formed from a liquid from which Ni has been previously extracted.

4.3.3. Gabbro cumulates, norites and anorthosites

Analyses of these rocks are given in Tables 4.9 to 4.10 expressed on a water-free basis.

Many of the rock types, especially the olivine-rich types, are altered with serpentinisation of olivine widespread and to a much lesser extent, alteration of pyroxenes to tremolite-actinolite. Serpentinisation of the olivines, in the olivine gabbros, has led to adjacent cracking of the plagioclases in some samples. Alteration can make the bulk-rock chemistry difficult to interpret if constituents have been added or removed from the original rock. The volume increase shown by the olivine as a result of serpentinisation suggests, however, that the process may have been essentially isochemical except for addition of H_2O. Based on 100xMgO/(MgO+FeO) ratios one can differentiate between the mantle rocks, the cumulates, and the basaltic rocks. The ultramafics have ratios of 87 to 92, the cumulates 60 to 73, and the basaltic rocks between 34 and 59.

4.3.4. Basaltic rocks

Analyses of the basaltic rocks are given in Table 4.11. These rocks include dykes (sheeted dykes) and extrusive lavas. They may in part be silicified and have relatively high silica values in the range 55 to 60 percent. Al_2O_3 contents vary from 8 to 14 percent, MgO from 4 to 10 percent, and CaO from 6 to 12 percent.

General characteristics are their low potassium and titanium contents which are invariably less than 1 percent. In some extrusive samples, Na_2O reaches 2 to 4% and the rocks are spilites, but generally Na_2O values lie in the range 0.39 to 1.53 percent. Based on the modes and chemical composition, the primary magma, from which the extrusive rocks are derived, is regarded as tholeiitic basalt.

4.4. Variation in major elements.

Variation is illustrated by means of AFM diagrams, and plots of total alkalis versus SiO_2 and of oxides versus MgO and versus 100xMgO/(MgO+FeO). The samples chosen to illustrate chemical variation were the freshest samples, based on petrographic examination. Those diagrams involving FeO and Fe_2O_3 result from plotting only those samples on which FeO determinations were made.

4.4.1. AFM diagram

In figure 4.1 the trend shown by the Oman ophiolites is compared with those for the Bay of Islands ophiolites (Malpas, 1978), the Troodos Plutonic Complex of Cyprus (Allen, 1975), the Bett's Cove ophiolite complex

Figure 4.1.(A) AFM variation diagram for the ultramafics, gabbros and basaltic rocks. B, C, D, E and F are those of the Bay of Islands ophiolites (Malpas, 1978), the Troodos Plutonic Complex of Cyprus (Allen, 1975), the Bett's Cove ophiolite complex (Upadhyay, 1973) and the ophiolites of Papua and New Caledonia (Rodgers, 1975).

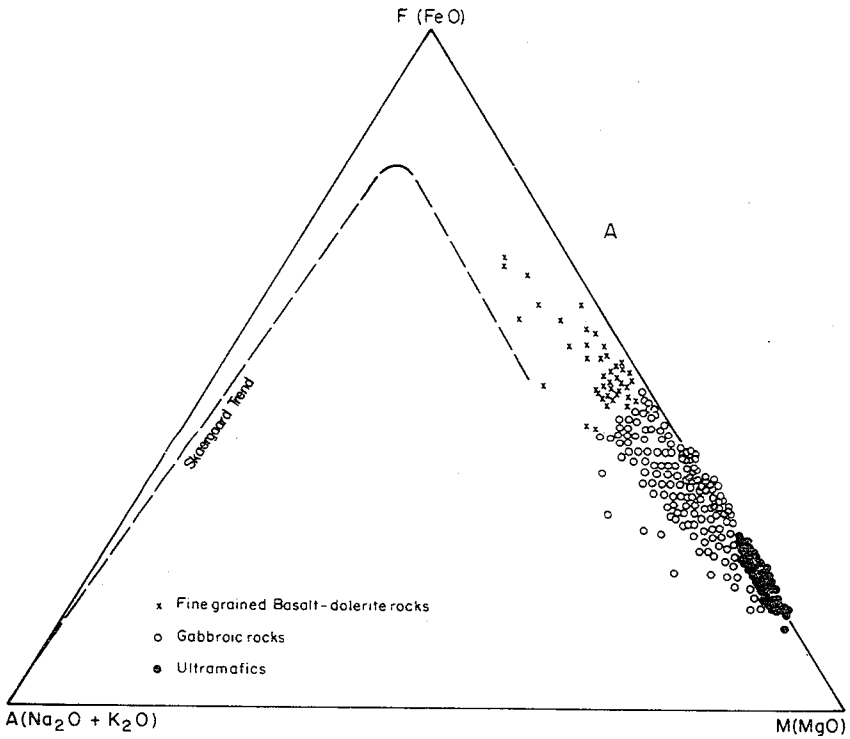
F (Fe O)
A
Skaergard Trend
x Fine grained Basalt-dolerite rocks
o Gabbroic rocks
Ultramafics
A(Na2O + K2O)
M(MgO)

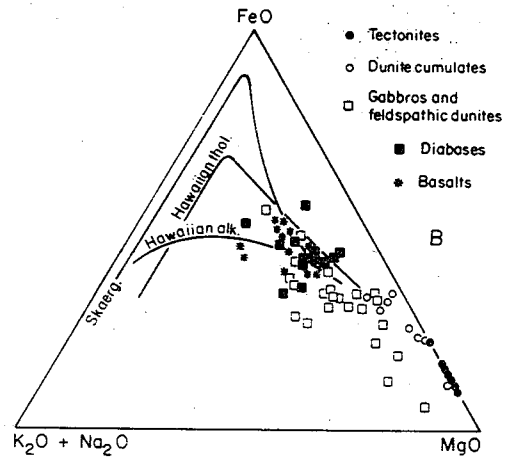
FeO
Tectonites
Dunite cumulates
Gabbros and feldspathic dunites
Diabases
Basalts
Hawaiian thol.
Hawaiian alk.
Skaerg.
B
K2O + Na2O
MgO

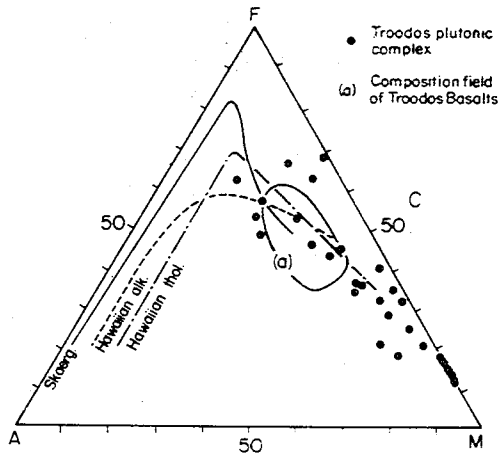
F
Troodos plutonic complex
(a) Composition field of Troodos Basalts
50
C
50
(a)
Skaerg.
Hawaiian alk.
Hawaiian thol.
A
50
M

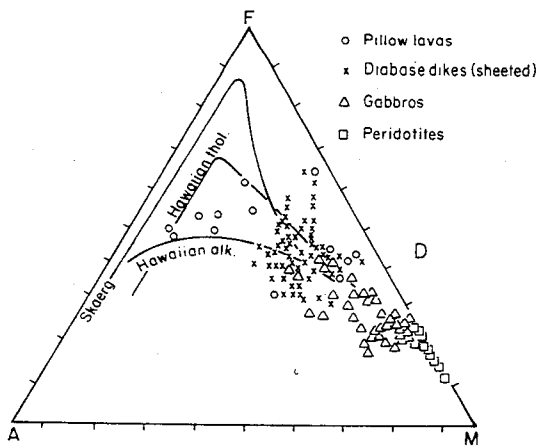
F
Pillow lavas
Diabase dikes (sheeted)
Gabbros
Peridotites
Hawaiian thol.
Hawaiian alk.
Skaerg.
D
A
M

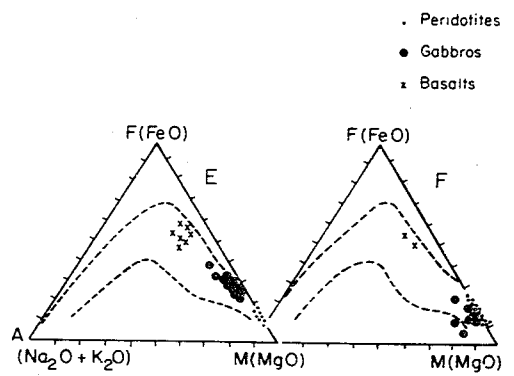
Peridotites
Gabbros
Basalts
F(FeO)
E
F(FeO)
F
A
(Na2O + K2O)
M(MgO)
M(MgO)

(Upadhyay, 1973), and trends exhibited by the recognised ophiolites of Papua and New Caledonia (Rodgers, 1975).

The general ultramafic-mafic fractionation trend of the ophiolite rocks of the Khawr Fakkan area is similar to the above-mentioned ophiolite complexes, and also similar to the general ophiolite trend given by Thayer (1967). All the rock types plot along a trend of iron enrichment typical of tholeiitic suites. However, fractionation has been such that there is a decrease in iron from some ultramafic rocks to the cumulate gabbros, the most pronounced enrichment being in the basaltic rocks. The spread of the gabbroic rocks, apparently indicating their enrichment in alkalis, is probably explained by their variable concentration of cumulate plagioclase (Malpas, 1978). The basalt fractionation trends of Skaergaard and the Hawaiian lavas are more pronounced than in the ophiolite series. This may be due to the fact that the ophiolite series did not develop from a single magma reservoir, but from basaltic magma generated more or less continuously by partial melting of the mantle (Alleman and Peters, 1972).

4.4.2. Total alkalis versus SiO_2

On the diagram (Fig. 4.2), all crustal rock types from the ophiolite suite studied can be classified as

Figure 4.2. Total alkali versus SiO_2 plot, showing the alkali-subalkali basalt divide proposed by MacDonald (1968), and the calc-alkali tholeiitic basalt divide proposed by Kuno (1968).

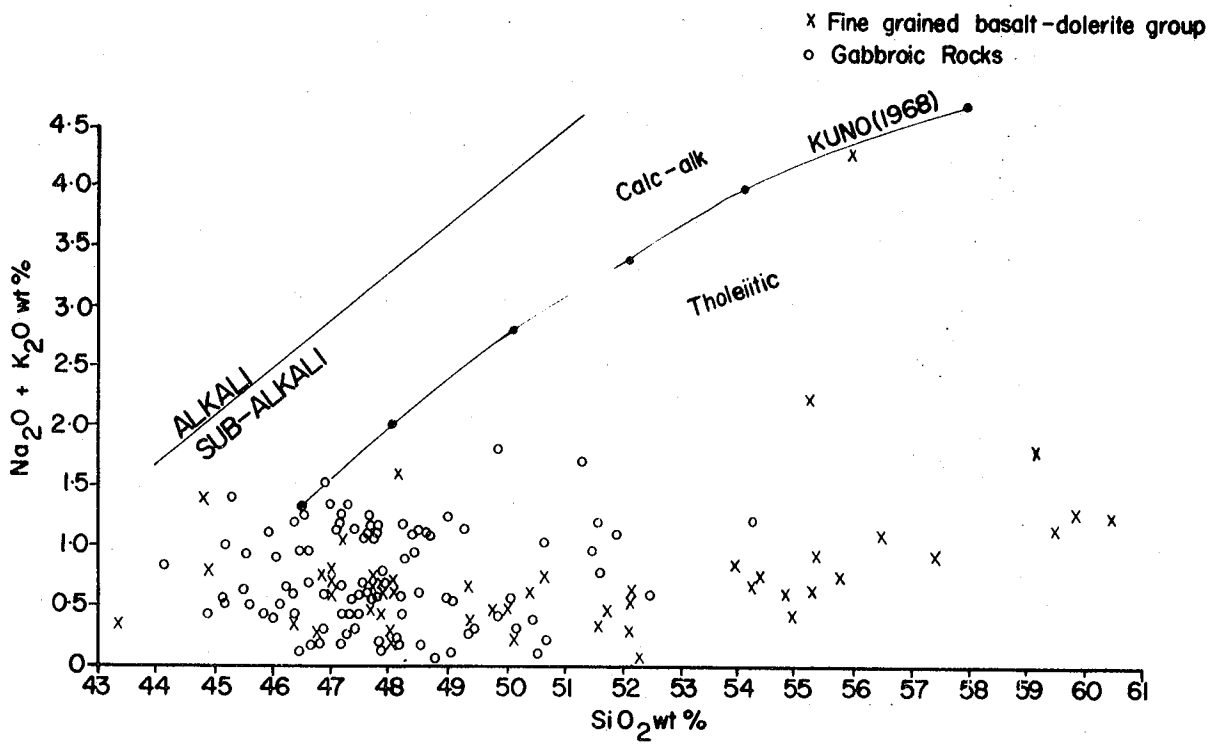
x Fine grained basalt-dolerite group
o Gabbroic Rocks
KUNO(1968)
Calc-alk
Tholeiitic
ALKALI
SUB-ALKALI
$Na_2O + K_2O$ wt %
SiO_2 wt %
0
0·5
1·0
1·5
2·0
2·5
3·0
3·5
4·0
4·5
43
44
45
46
47
48
49
50
51
52
53
54
55
56
57
58
59
60
61

tholeiitic, since both populations (cumulate gabbros and basaltic rocks) plot below the alkali/sub-alkali dividing line proposed by MacDonald (1968) and also plot below the calc-alkaline trend of Kuno (1968). The rock types are similar to the ophiolitic rocks of the Baie Verte Group of Newfoundland described by Norman and Strong (1975).

4.4.3. SiO_2, Al_2O_3, CaO, Fe_2O_3 and FeO versus MgO

Figs. 4.3, 4.4, 4.5, 4.6 and 4.7 show plots of the major-element oxides against MgO. In most instances there is a clear separation between the plots of the upper mantle rocks (dunite, harzburgite and wehrlite) and the cumulate gabbros and associated basaltic rocks. The plot for "pyrolite" (Ringwood, 1966), lherzolite (Boudier, 1972), estimated Upper Mantle (Harris et al., 1967) and lherzolite (Dickey, 1970) are also shown. The position of the wehrlites in relation to this plot clearly demonstrates their less refractory nature in comparison to dunite and harzburgite. Most of the wehrlites are, nevertheless, more refractory than pyrolite.

The evolution of the liquid phase of the partial melting process is only shown by the fine-grained basaltic rocks, variation in the gabbros being clearly controlled by the relative proportions of the cumulate

Figure 4.3. SiO_2 versus MgO diagram for the ultramafic-mafic rocks. The field of olivine, orthopyroxene, clinopyroxene and pure anorthosite is also plotted.

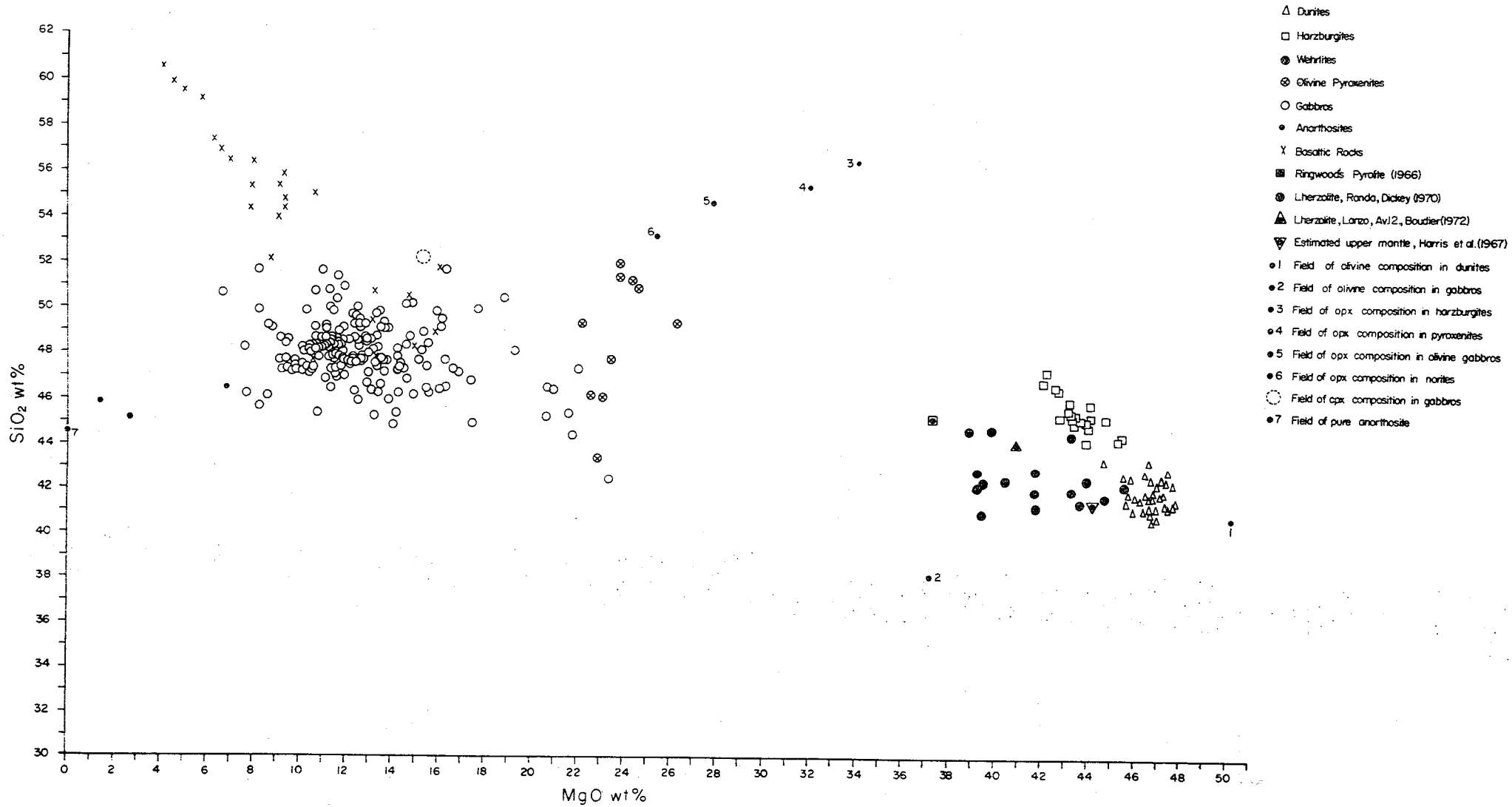
Δ Dunites
□ Harzburgites
⊛ Wehrlites
⊗ Olivine Pyroxenites
○ Gabbros
• Anorthosites
Y Basaltic Rocks
▣ Ringwood's Pyrolite (1966)
⊛ Lherzolite, Ronda, Dickey (1970)
▲ Lherzolite, Lanzo, Av.12., Boudier(1972)
▽ Estimated upper mantle, Harris et al.(1967)
•1 Field of olivine composition in dunites
•2 Field of olivine composition in gabbros
•3 Field of opx composition in harzburgites
•4 Field of opx composition in pyroxenites
•5 Field of opx composition in olivine gabbros
•6 Field of opx composition in norites
○ Field of cpx composition in gabbros
•7 Field of pure anorthosite
SiO2 wt%
MgO wt%
62
60
58
56
54
52
50
48
46
44
42
40
38
36
34
32
30
0
2
4
6
8
10
12
14
16
18
20
22
24
26
28
30
32
34
36
38
40
42
44
46
48
50

Figure 4.4. Al_2O_3 versus MgO diagram for the ultramafic-mafic rocks. The field of olivine, orthopyroxene, clinopyroxene and pure anorthosite is also plotted.

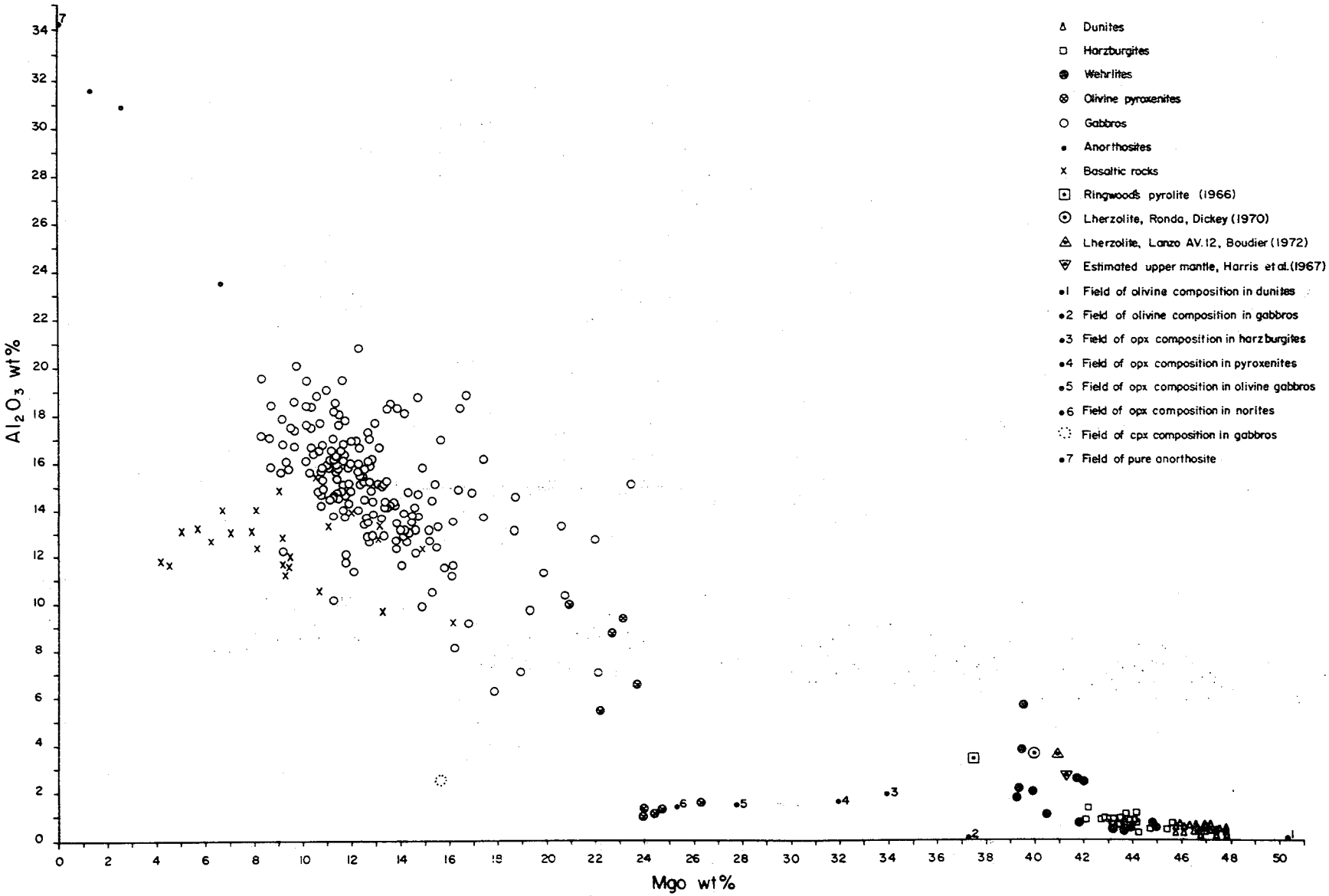
Dunites
Harzburgites
Wehrlites
Olivine pyroxenites
Gabbros
Anorthosites
Basaltic rocks
Ringwood's pyrolite (1966)
Lherzolite, Ronda, Dickey (1970)
Lherzolite, Lanzo AV.12, Boudier (1972)
Estimated upper mantle, Harris et al.(1967)
•1 Field of olivine composition in dunites
•2 Field of olivine composition in gabbros
•3 Field of opx composition in harzburgites
•4 Field of opx composition in pyroxenites
•5 Field of opx composition in olivine gabbros
•6 Field of opx composition in norites
Field of cpx composition in gabbros
•7 Field of pure anorthosite
Al_2O_3 wt%
Mgo wt%

Figure 4.5. CaO versus MgO diagram for the ultramafic-mafic rocks. The field of olivine, orthopyroxene, clinopyroxene and pure anorthosite is also plotted.

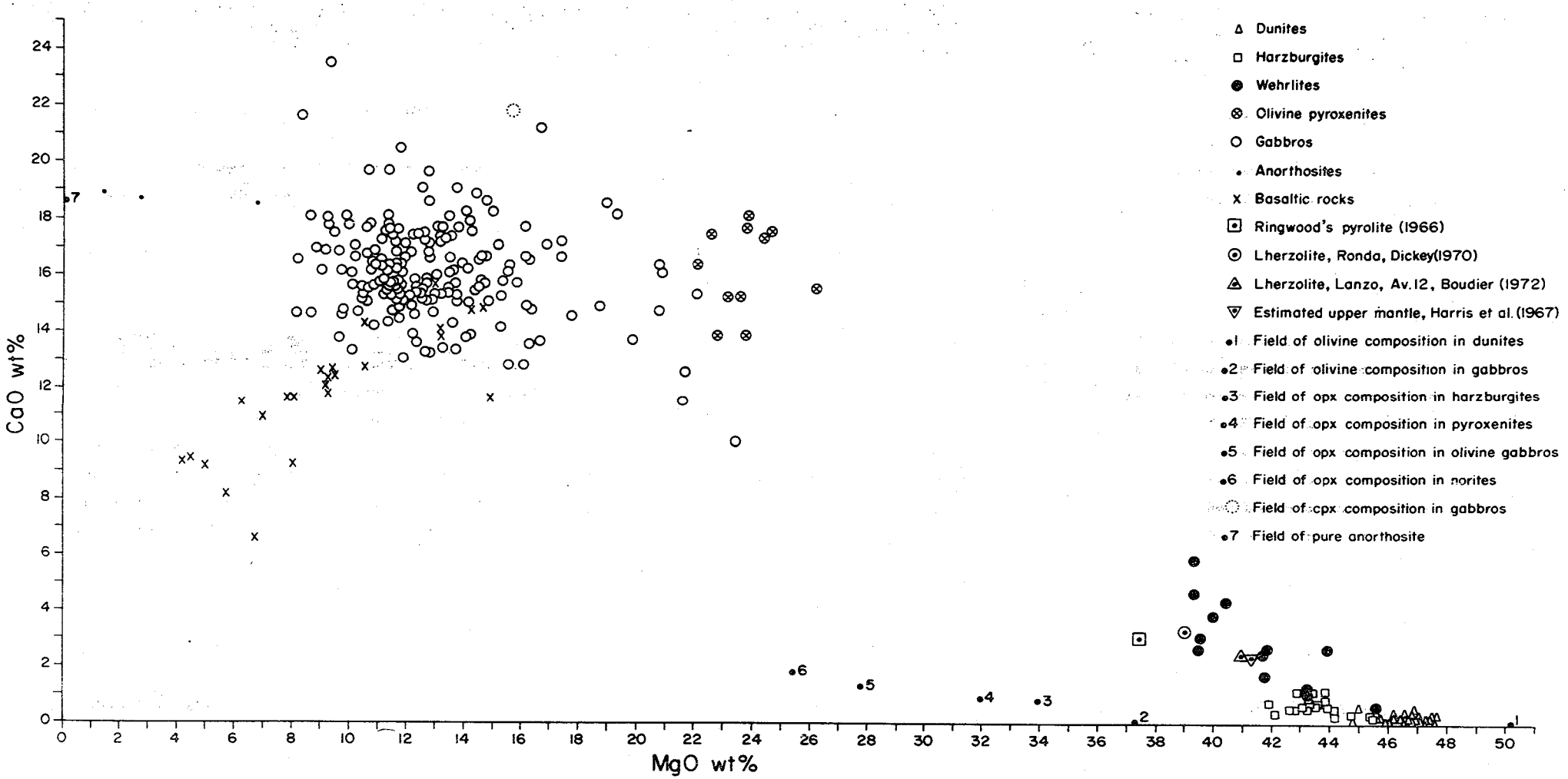
CaO wt%
MgO wt%
Dunites
Harzburgites
Wehrlites
Olivine pyroxenites
Gabbros
Anorthosites
Basaltic rocks
Ringwood's pyrolite (1966)
Lherzolite, Ronda, Dickey(1970)
Lherzolite, Lanzo, Av.12, Boudier (1972)
Estimated upper mantle, Harris et al.(1967)
1 Field of olivine composition in dunites
2 Field of olivine composition in gabbros
3 Field of opx composition in harzburgites
4 Field of opx composition in pyroxenites
5 Field of opx composition in olivine gabbros
6 Field of opx composition in norites
Field of cpx composition in gabbros
7 Field of pure anorthosite

Figure 4.6. Fe_2O_3 versus MgO diagram for the ultramafic-mafic rocks.

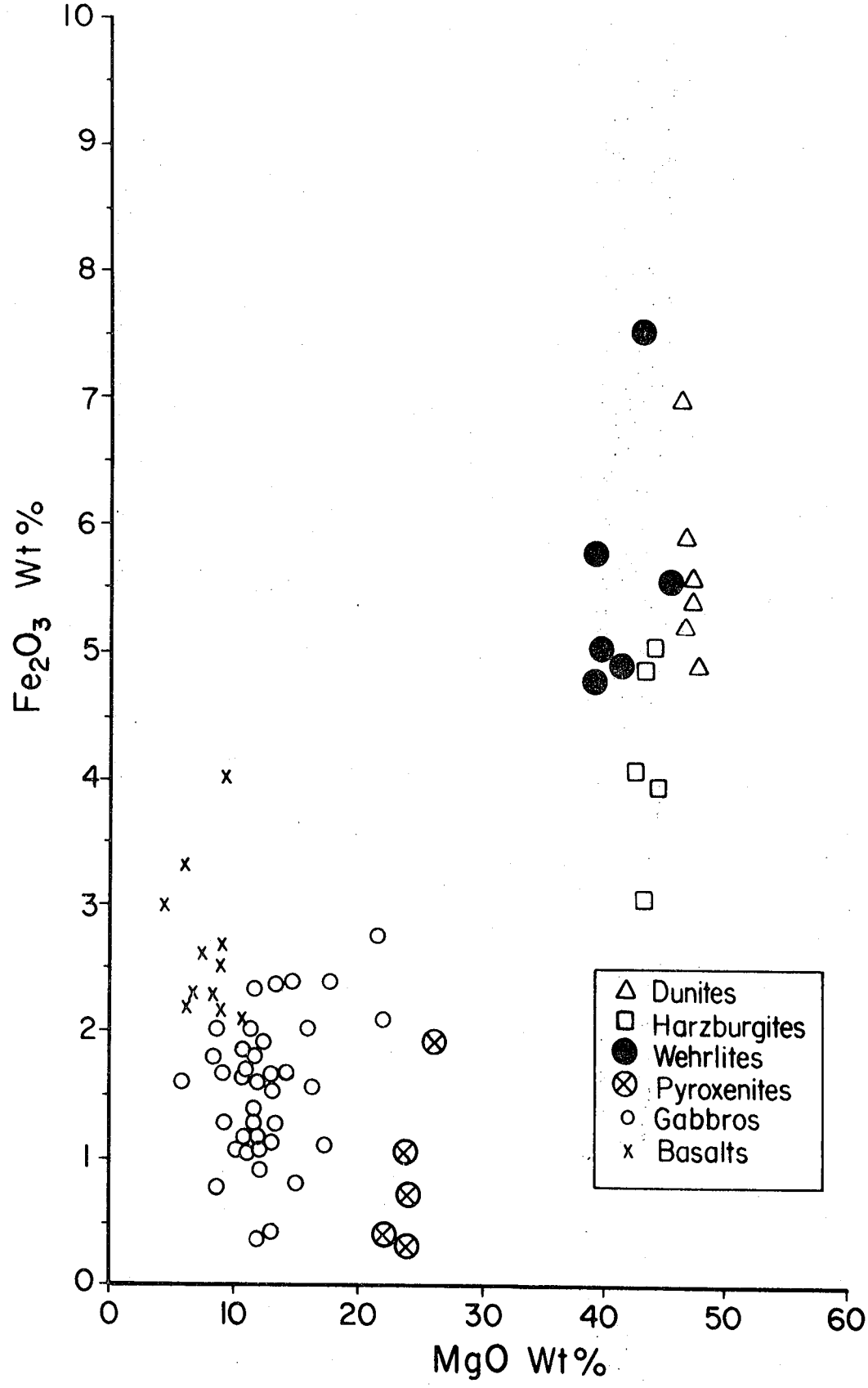
10
9
8
7
6
5
4
3
2
1
0
Fe_2O_3 Wt %
0
10
20
30
40
50
60
MgO Wt %
Dunites
Harzburgites
Wehrlites
Pyroxenites
Gabbros
Basalts

Figure 4.7. FeO versus MgO diagram for the ultramafic-mafic rocks.

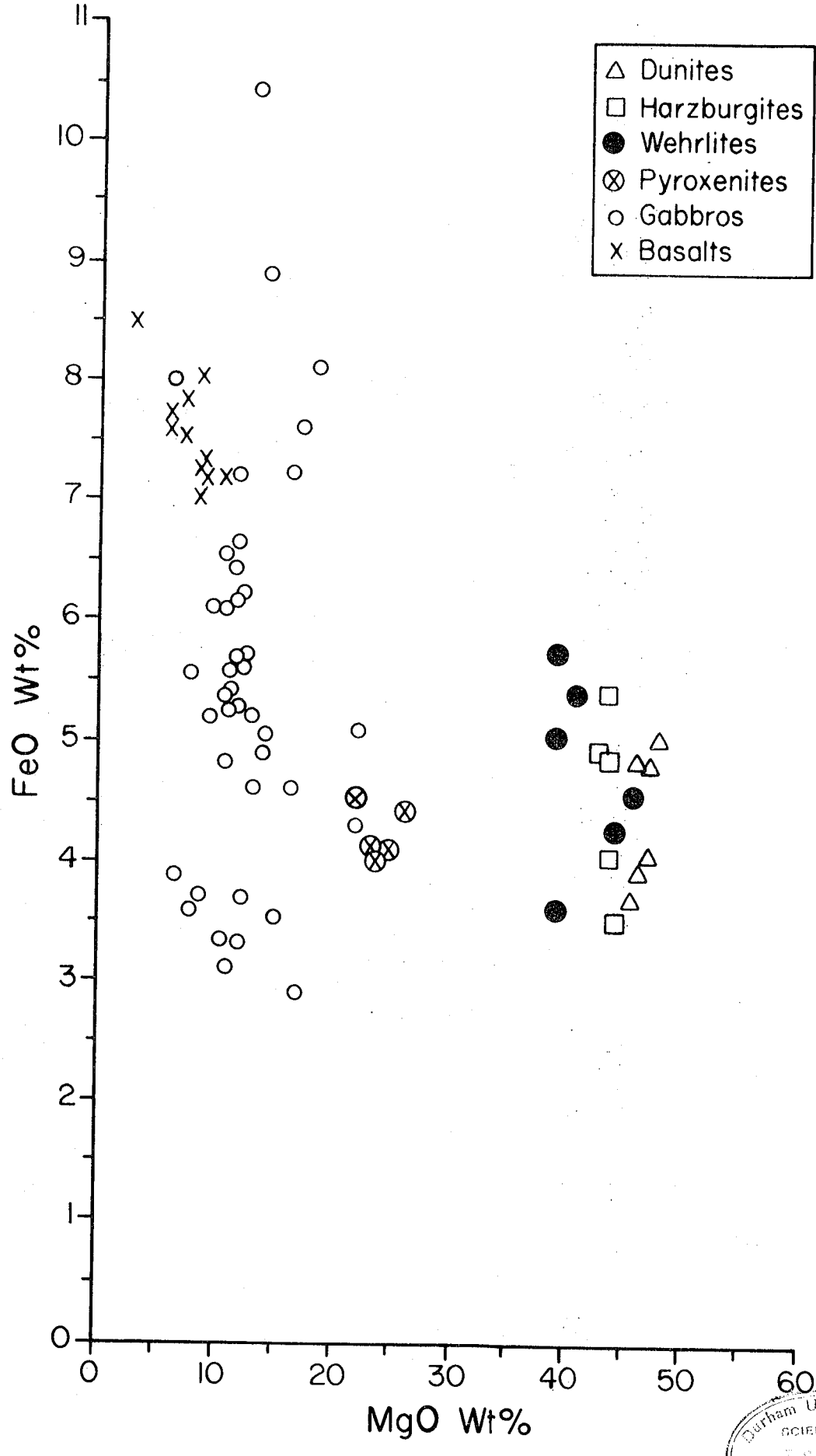

minerals olivine, pyroxene and plagioclase. The basalts themselves are thus clearly not partial melts from the upper mantle but have evolved from a partial melt magma through the crustal process of fractional crystallisation.

An estimate of the composition of the gabbroic, partial-melt magma can be made by back-extrapolating the line of liquid descent shown by the fine-grained basaltic rocks, the line of plagioclase fractionation (towards anorthosite), and a line joining the cluster of dunite and harzburgite plots (at a point representing a mixture of approximately 9 parts olivine to 1 part orthopyroxene) and "pyrolite". The point of intersection of these evolutionary trend lines gives an estimate of partial melt composition, and further suggests a ratio of liquid to refractory residuum of the order of 1 to 3.

Many of the gabbros plot close to this point, the remainder having plots which are influenced by the dominant cumulus minerals. Olivine and pyroxene-rich cumulates show relative increase in MgO at fairly constant SiO_2 and CaO, olivine gabbros show increase in MgO and decrease in SiO_2 and CaO relative to the

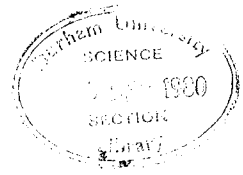

partial melt magma, and plagioclase enrichment is clearly shown by the trend towards anorthosite.

The line of liquid descent is reflected by a fairly smooth curve through the fine-grained rocks in both Figs. 4.3 and 4.5. These show that both SiO_2 and CaO decrease as MgO increases, a normal result of fractionation of olivine and/or pyroxene together with plagioclase.

Although Al_2O_3 increases into the anorthosites, the gabbros and fine-grained basaltic rocks show no systematic variation reflecting the ubiquitous presence of plagioclase feldspar in these rocks. Although FeO increases with decreasing MgO from mantle rocks to the cumulate gabbros and pyroxenites, the sharpest increase is in the basaltic rocks. Fractionation of olivine and clinopyroxene account for depletion of MgO relative to FeO and iron enrichment in the basalts is thus probably due to crystallisation of magnetite. Ferric iron is relatively abundant in the harzburgites and dunites compared to the cumulate gabbros and basaltic rocks. Breakdown of olivine to magnetite due to serpentinisation and oxidation, and the presence of considerable spinel, probably account for the high ferric content of the mantle rocks.

4.5. Variation in trace elements

4.5.1. Cr versus Ni (Fig. 4.8)

Irvine and Findlay (1972) used Cr and Ni variation to discriminate between alpine peridotites and cumulate rock associations in layered complexes. Their boundaries were drawn from the Bay of Islands Complex which contain an ultramafic transition zone of feldspathic dunite and troctolite. They suggested a similarity between alpine peridotites and the tectonic harzburgites and lherzolites of the Bay of Islands Complex, attributing a mantle origin to the latter. The peridotites of the present study supplement this view.

The studied dunites, harzburgites and wehrlites fall within Irvine and Findlay's general alpine-peridotite field, while most of the cumulate gabbros occupy the layered-series field. However, some of the cumulate pyroxenites and wehrlites have an unusually high concentration of Cr, in the range 6000-7000 ppm. Substitution of Cr in the clinopyroxenes and its concentration in early crystal phases during fractional crystallisation explains the maximum concentration of Cr in the cumulate pyroxenites. The concentration of Cr in the pyroxene of wehrlites is, however, probably representative of relatively primitive mantle material in which the degree of partial melting is

Figure 4.8. Cr versus Ni logarithmic plot for the ultramafic-mafic rocks.

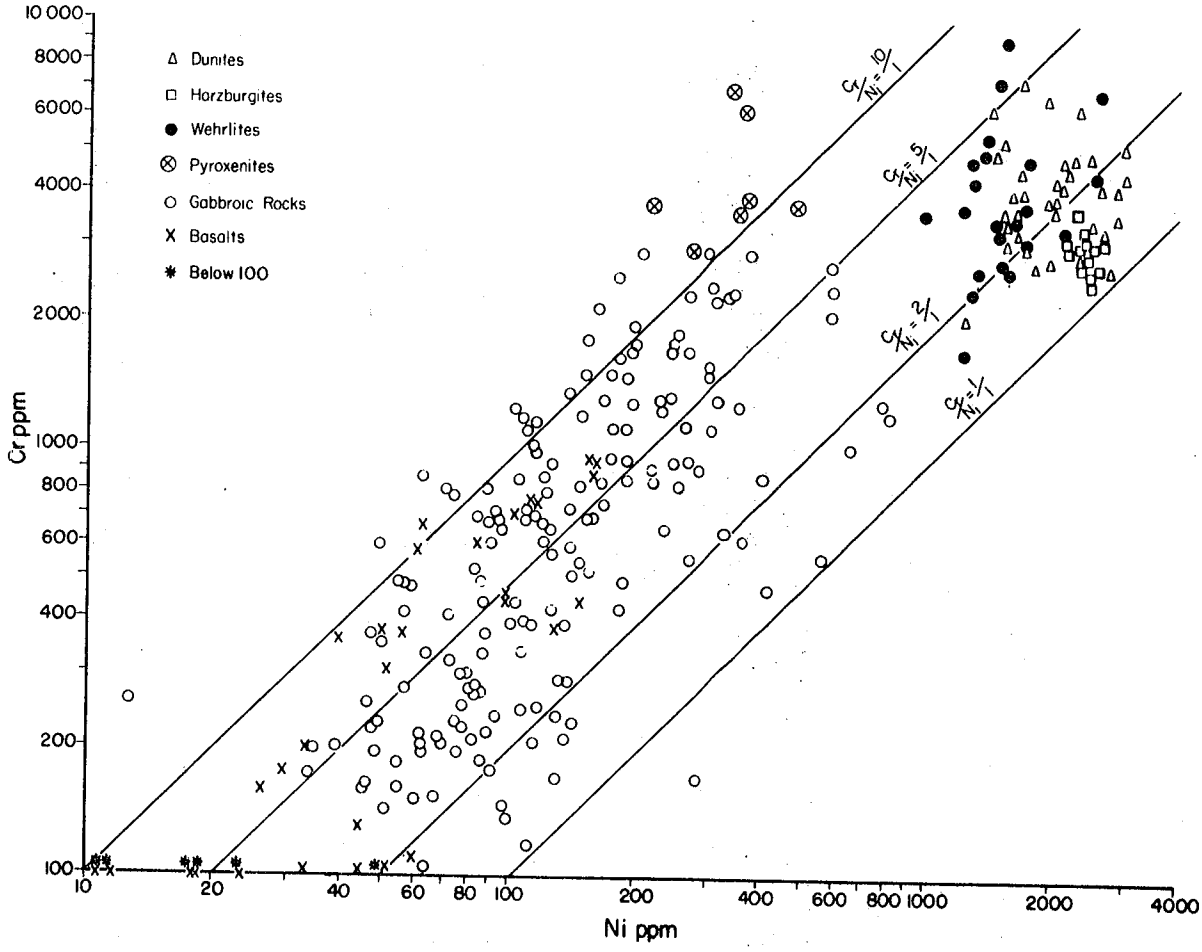
Dunites
Harzburgites
Wehrlites
Pyroxenites
Gabbroic Rocks
Basalts
Below 100
Cr/Ni = 10/1
Cr/Ni = 5/1
Cr/Ni = 2/1
Cr/Ni = 1/1
Cr ppm
Ni ppm
10 000
8000
6000
4000
2000
1000
800
600
400
200
100
10
20
40
60
80
100
200
400
600
800
1000
2000
4000

insufficient for Cr to be redistributed into chromite - a situation very clearly shown by the harzburgites and dunites.

Once the partial-melt magma has been generated, concentration of Cr and Ni into the early crystal phases of the olivine and pyroxene-rich cumulates results in depletion in the basaltic rocks.

4.5.2. Cr_2O_3 and NiO versus 100xMgO/(MgO+FeO)

The cation Cr^{3+} is virtually identical in size to Fe^{3+} but the more ionic nature of the bond with oxygen leads to preferential entry into Fe^{3+} positions, and consequent depletion at the early stage of fractional crystallisation (Taylor, 1965). According to Taylor, the larger size of V^{3+} causes it to enter rather later fractions than Cr^{3+}. The Cr^{3+}/V^{3+} ratio decreases with fractionation and is a good index of fractionation; Cr/Ni ratio is not a good index of fractionation as Cr and Ni enter different sites and different minerals. Cr abundance follows the series:

Spinel $\gg$ early Cpx $>$ late Mt $>$ Opx $>$ late Cpx $\gg$ Ol.

The Cr content of the parent magma decreased rapidly during fractionation (Fig. 4.9), but the separation of a discrete Cr-rich phase into the cumulus rocks makes this trend less apparent than for Ni in the range 100xMgO/

Figure 4.9. Cr_2O_3 versus 100xMgO/(MgO+FeO) for the ultramafic-mafic rocks.

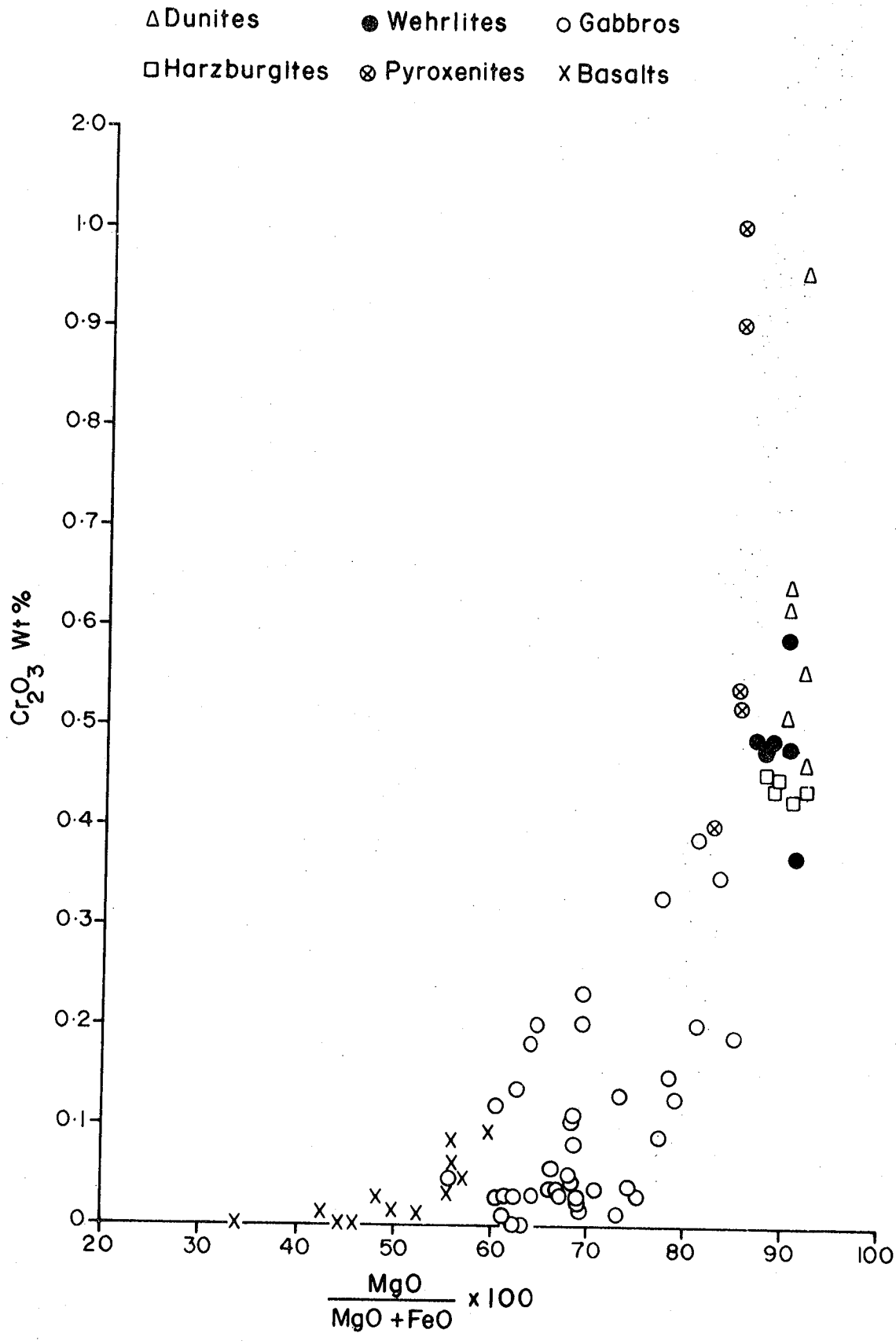
Δ Dunites
● Wehrlites
○ Gabbros
□ Harzburgites
⊗ Pyroxenites
X Basalts
2·0
1·0
0·9
0·8
0·7
0·6
0·5
0·4
0·3
0·2
0·1
0
Cr_2O_3 Wt %
20
30
40
50
60
70
80
90
100
$\frac{MgO}{MgO + FeO} \times 100$

(MgO+FeO)= 87-92.

A large gap in Cr_2O_3 concentration, at 0.23 to 0.29 percent in the present study shown in Fig. 4.9, and at 0.14-0.25 percent in the Troodos Plutonic Complex reported by Allen (1975), occurs between mantle rocks and most cumulate gabbros. The gap corresponds to the partitioning of Cr between refractory residuum (crystal phase) and magma (liquid) attendant on partial melting. The gap is partly bridged by concentration of Cr into the early crystal phases, olivine and pyroxene, and the resulting relatively high contents of these cumulates.

The well-known enrichment of Ni in early mineral fractionsof magmatic crystallisation has been explained by Burns (1970). He considers that Ni^{2+} has high octahedral-site preference energy, and occupies the same sites as Mg^{2+} and Fe^{2+}. Burns postulates that the solidus-liquidus relations in the binary Ni_2SiO_4-forsterite system are inverted in melts containing large proportions of tetrahedral-coordinated sites, so that enrichment of Ni results in early, rather than late formed, olivine.

Hakli and Wright (1967) showed the K_D liquid/olivine for Ni to be 0.10, 0.074 and 0.059 at 1250, 1160 and 1050°C, respectively. The appreciable difference between NiO contents of harzburgite and dunite, shown in Fig. 4.10

Figure 4.10. NiO versus 100xMgO/(MgO+FeO) for the ultramafic-mafic rocks.

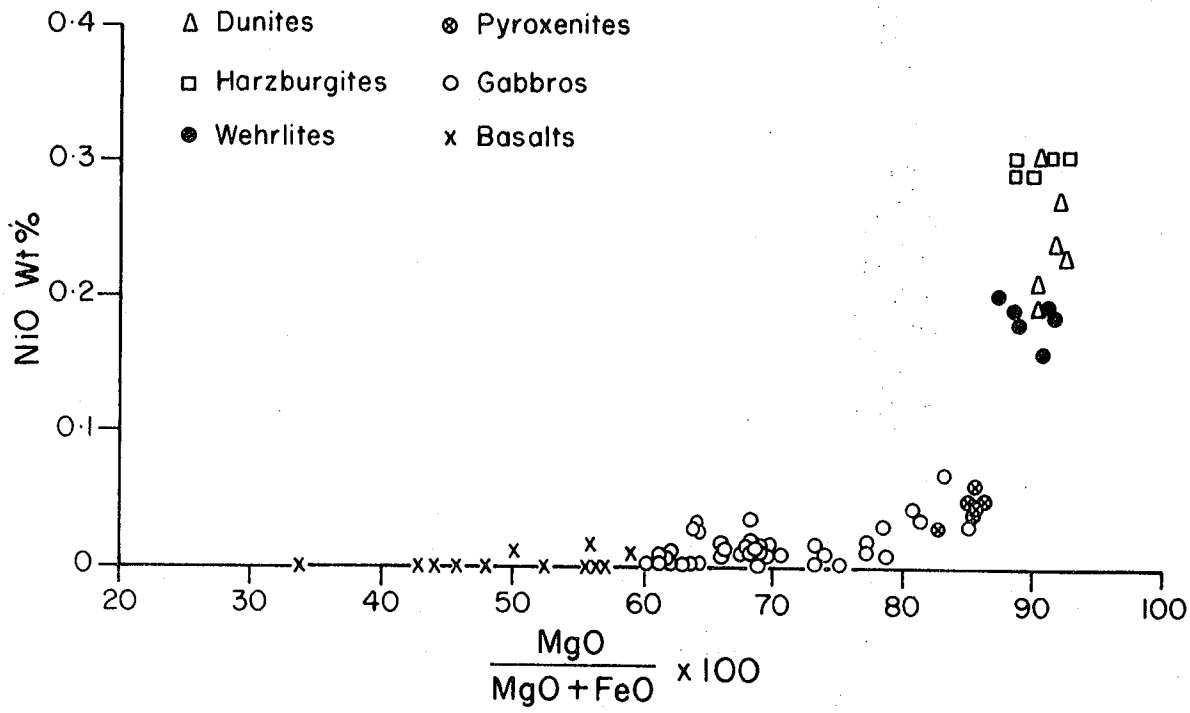
Δ Dunites
□ Harzburgites
● Wehrlites
⊗ Pyroxenites
○ Gabbros
x Basalts
NiO Wt%
0·4
0·3
0·2
0·1
0
20
30
40
50
60
70
80
90
100
MgO / MgO+FeO x 100

suggests that K_D may be substantially influenced by pressure and temperature.

As seen in Fig. 4.10, the harzburgites contain from 0.29 to 0.30 percent NiO, the range of concentration being very limited in comparison to the other ultramafics. The uniformity of NiO in the harzburgites suggests that crystal-liquid partitioning has gone to equilibrium and that the temperature may be somewhat lower than for partial melting which produced dunite as a residuum. For the dunites, the range suggests either compositional variation in the starting material or a range of temperatures and pressures for partial melting, some of which were greater than for the harzburgites. Dunites contain 0.19 to 0.30 percent NiO, and overlap with wehrlites which contain 0.16 to 0.20 percent NiO. Concentration of Ni into the refractory residuum of partial melting results in a low NiO content in the magma generated by this process, and also in the cumulate olivine-pyroxenites resulting from fractionation of this magma. Cumulate olivine gabbros contain higher values of NiO than do the cumulate gabbros due to the absence of olivine in the latter, since the NiO content of the rocks is closely related to their olivine content. Ni thus correlates with Mg in the cumulates and in the basaltic rocks is

extremely low, approaching almost complete depletion.

4.6. Ti-Zr-Y and Ti-Zr-Sr discrimination diagrams

Pearce and Cann (1973), using two sets of discriminant analysis, outlined the fields shown on Figs. 4.11 and 4.12 corresponding to different volcanic environments.

The first set is based on the comparatively immobile elements Ti, Zr and Y. The second set is based on an additional element Sr, which gives a better discrimination plot. However, use of Sr is only strictly valid for fresh or slightly altered rocks.

The authors subdivide basalt populations in the following manner:

1. "Within Plate" basalts (Ocean Island or Continental basalts).
2. Ocean-floor basalts (Tholeiitic and Alkalic).
3. Volcanic-arc basalts (Low-potassium tholeiites).
4. Calc-alkali basalts (High K Basalts).

Although fresh basalts from different tectonic settings show distinctive chemical features for some major and trace elements, such an approach is difficult to apply when the rocks are chemically altered. It is well known that weathering, spilitisation and other

Figure 4.11. Y-Zr-Ti triangular diagram Pearce and Cann (1973) with selected basalts and gabbros plotted. Within Plate Basalts = D, Low K Tholeiites = A+B, Calc-alkali Basalts = C+B, and Ocean Floor Basalts = B.

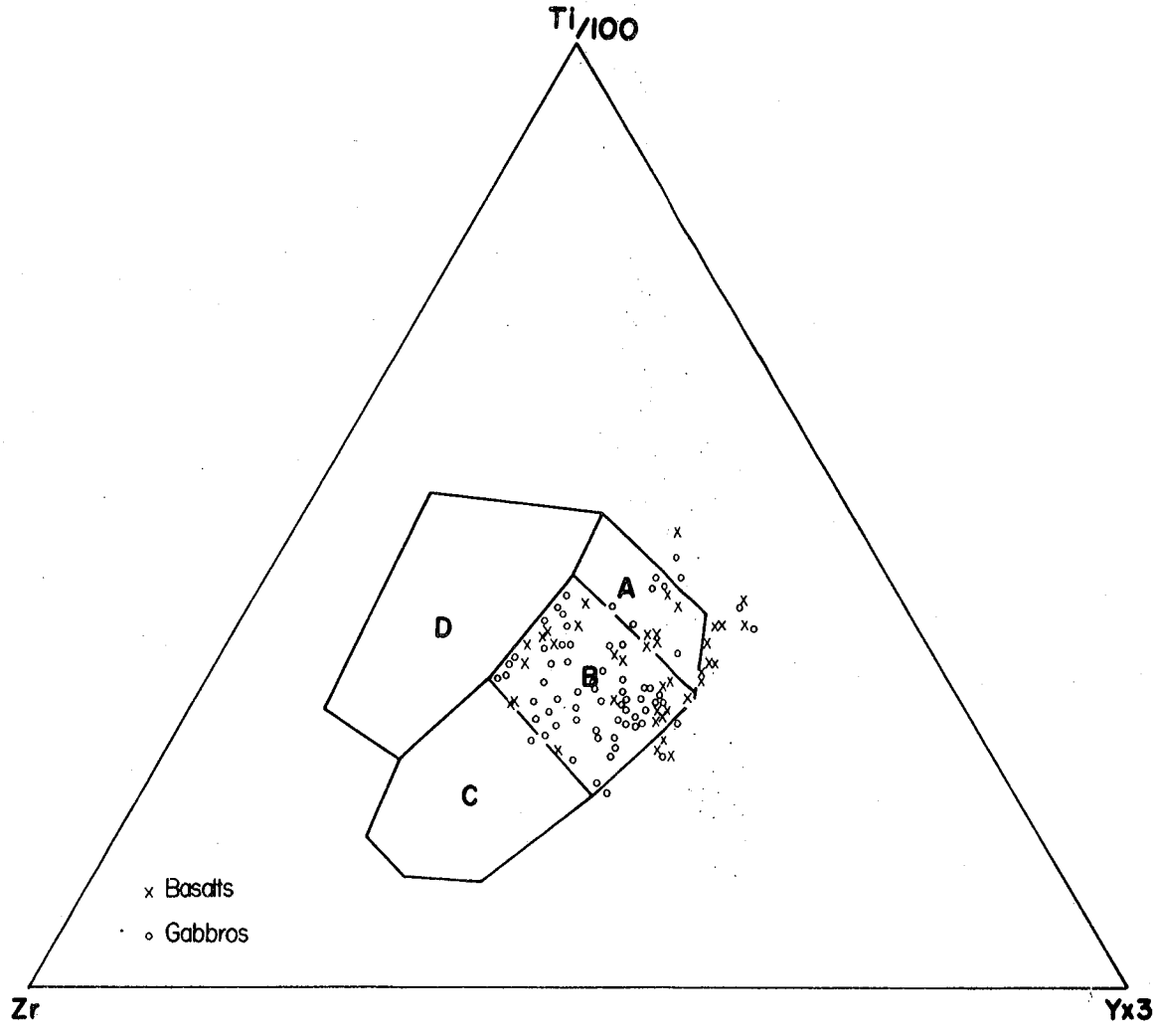
Ti/100
A
B
C
D
x Basalts
o Gabbros
Zr
Yx3

Figure 4.12 Sr-Zr-Ti triangular diagram Pearce and Cann (1973) with selected basalts and gabbros plotted. Ocean Floor Basalts = C, Low K Tholeiites = A, and Calc-alkali Basalts = B.

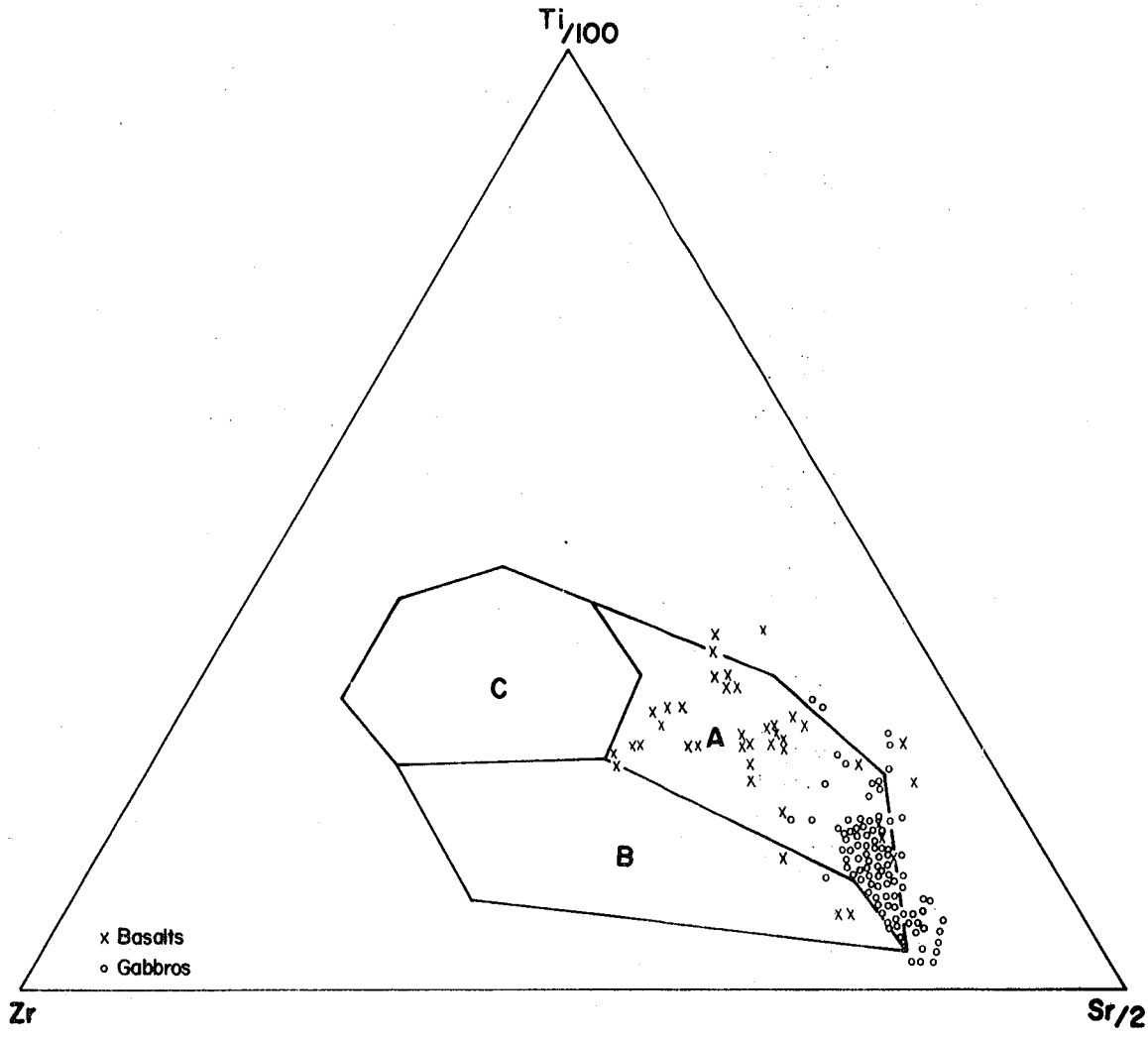
Ti/100
C
A
B
x Basalts
o Gabbros
Zr
Sr/2

metamorphism induce strong chemical mobilisation, particularly of the alkali and alkaline-earth elements. Ophiolites, presumed to have formed in an oceanic environment, are often strongly altered and have undergone secondary element mobilisation (Montigny et al., 1973; Pearce, 1975). The present study supplements this view.

Fig. 4.11 discriminates against "Within Plate Basalts" on the basis of Y content. From the diagram it is concluded that both the gabbros and basaltic rocks of the present study lie within the field of ocean-floor-basalts, although a minor proportion of both types fall within field A (low-K tholeiites). Fig. 4.12 is based on Sr, which is probably remobilised, and Sr appears to concentrate in the gabbros. However, the two populations fall distinctly in field A (Low-K tholeiites)

4.7. Discussion

Evidence from field relationships, petrography and geochemistry has been presented that the ultramafic-gabbroic basaltic rock sequences of the Khawr Fakkan-Wadi Shi-Wadi Madha are genetically related, having been the result of partial melting of the upper mantle followed by fractional crystallisation of the basaltic

magmas generated by this process.

The trend of the rocks on the AFM diagram is similar to that of other ophiolites which have been referred to as alpine-type ultramafic complexes, with a lower Fe/Mg ratio and lower alkalis than that found in typical basalt fractionation trends of continental layered intrusions. Variation diagrams further reveal the chemical relationship between the various rock types, with trends in cumulates due mainly to the fractionation in various proportions of olivine, orthopyroxene, clinopyroxene, and plagioclase. The variation in iron, with low Fe/Mg ratios in the peridotites and cumulate pyroxenites, and higher Fe/Mg ratio in the cumulate gabbroic and basaltic rocks, can be explained by fractional crystallisation of magma for the gabbros and basalts under conditions of low oxygen fugacity. The parent magma for the studied ophiolitic rocks appears also to have been a low-Ti and low-K tholeiite type basaltic magma that crystallised under conditions of low oxygen fugacity, probably in the upper crustal zones beneath a mid-oceanic ridge.

CHAPTER 5: Mineralogy

5.1. Electron Microprobe analysis methods.

The mineral analyses listed in Tables 5.9-5.75 were obtained by electron microprobe analysis, using a Cambridge Instrument Company "Geoscan Mark II" electron microprobe. They were obtained from polished thin sections, 30-50 microns in thickness, the analysed samples being chosen on the basis of mineralogy and texture. Where possible, all the main coexisting phases were analysed.

Efforts were made to standardize operating conditions, and in order to avoid undue bias all the coexisting phases were analysed for the same elements, under the same conditions. The general methods employed are those described by Sweatman and Long (1969).

The "Geoscan" was operated under a high vacuum, at an accelerating voltage of 15 kV and a specimen current of 0.04A. The electron beam was kept focussed throughout, giving an analysis spot of 1-4 μM diameter.

Secondary X-rays were analysed using a wavelength dispersive system. The spectrometer has a take-off angle of 75° and was used with LiF, K.A.P. and P.E.T. analysing crystals. Table 5.1 shows the optimum analysing conditions for the nine main elements, and

TABLE 5.1

Electron microprobe analysing conditions and standards

Atomic Number	Element	Line	Analysing Crystal	Counter	Peak 2θ	Background Location	Standard
11	Na	$K\alpha_1$	K.A.P.	Flow	52° 58'	+ 1°30'	Jadeite
12	Mg	"	"	"	43° 23'	+/-2°	MgO
13	Al	"	"	"	36° 16'	+/-2°	Al_2O_3
14	Si	"	"	"	30° 44'	+1°30'	Wollastonite (Wo-2)
19	K	"	P.E.T.	"	50° 17'	-2°	Orthoclase (AF-15)
20	Ca	"	LiF	"	113° 2'	+/-2°	Wollastonite (Wo-2)
22	Ti	"	"	"	86° 7'	+/-2°	TiO_2
24	Cr	"	"	"	69° 17'	+/-2°	Cr_2O_3
25	Mn	"	"	"	62° 52'	+/-2°	Mn
26	Fe	"	"	"	57° 22'	+/-2°	Fe
28	Ni	"	"	"	48° 27'	+/-2°	Ni

also conditions for the alkalis, Na and K.

The wavelength dispersive system is based on a comparative technique, and the standards used for each elements are also given in Table 5.1. The standards comprise metals, oxides and simple silicates of known composition. Both they and the polished thin sections were carbon coated simultaneously, prior to use, to ensure equal thickness of carbon coat.

Data from the "Geoscan" were corrected for the effects of atomic number (Duncumb and Reed, 1968), mass absorption (Heinrich, 1966), and fluorescence (Reed, 1965). Corrections were made using an on-line Varian 620-100 computer. The correction procedure was applied using the computer programme "Tim 3" written by Dr. A. Peckett. The on-line computer stores the data and also performs a dead-time correction, and subtracts background from peaks. Machine drift was readily detected.

The following procedure was adopted in setting up the "Geoscan" at the start of a probe session:

1. Standard peaks were located and analysed (3.5 x 10 second counts).
2. Standard backgrounds were analysed, above and below the peak (2-3 x 10 second counts each).

3. Unknown backgrounds were taken, above and below the peak (4-5 x 10 second counts each).

4. Unknown peaks were analysed (3-4 x 10 second counts each).

5. Results were calculated.

6. If the results were satisfactory, further unknown peaks were recorded, and the process was continued. If the results were not satisfactory, standard peaks were re-located and re-analysed. Background values, obtained for each peak, were used throughout a session, and they were not re-determined for each individual mineral.

Detection limits are calculated from the formula:

$$\sqrt{\frac{3}{M}} = {}^{Rb}/_{Tb}$$

where M = mean peak counts/sec.

Rb = mean background, counts per second.

Tb = counting time on the background.

Calculated detection limits are in the range 200-500 ppm (0.02-0.05%).

The overall precision, taking into account the counting precision and uncertainties in the correction procedure, is probably in the order of $\pm$2% of the amount

of the major constituent present.

The probe analyses given in Tables 5.9-5.75 are all spot analyses each made at one point. Lobate areas from a serpentinized dunite were the phases which readily deteriorated under the electron beam, due to the presence of high amounts of H_2O. In all other cases it was possible to complete analysis before this occurred.

Corrected analyses were tabulated, with Fe (total) taken as Fe^{2+}, except that Fe^{2+} and Fe^{3+} were distributed stoichiometrically for the spinel minerals. Hydrated minerals are presented on a water-free basis, and the apparent percentage deficiency is taken to be the water content.

5.2. Olivine

Microprobe analyses were performed on olivines from peridotites, cumulate olivine pyroxenites, and cumulate olivine gabbros; the analyses are given in Tables 5.9-5.13 and 5.35, 5.37, 5.39, 5.41, 5.43, 5.54, 5.58, 5.60, and 5.62.

5.2.1. Peridotite olivines

Olivine compositions of Alpine-type peridotites and peridotites from various ophiolites are listed in Table 5.2.

Location	Source	Fo%
1. Wadi Madha and Wadi Shi areas.		88-92
2. Burrow Mountain	Loney et al. (1971)	91.1-91.4
3. Vulcan Peak	Himmelberg and Loney (1973)	90.7
4. Papua, New Guinea	England and Davies (1973)	91.6-93.6
5. Bay of Islands, Newfoundland	Irvine and Findley, (1972); Malpas (1978)	89.4-91.8 91.1
6. Orthris, Greece	Menzies (1974)	90-92
7. Troodos Plutonic Complex, Cyprus	Allen (1975)	90.3-91.4
8. Red Mountain Peridotite, New Zealand.	Sinton (1977)	89.9-90.6

TABLE 5.2

Olivine compositions of Alpine-type peridotites and peridotites from various ophiolites.

There is little variation in major-element chemistry between the harzburgite olivines, and those from dunites, wehrlites, and dunite-wehrlites. In harzburgites the Fo content, as defined by Mgx100/(Mg+Fe) ratio, varies between 90 and 92; in dunites between 89.7 and 91.6; and in wehrlites between 88 and 90. The intermediate type, classified as dunite-wehrlite because of the presence of minor amounts of small, interstitial clinopyroxene, varies

in Fo content between 90.2 and 91.6. The range of olivine compositions in the peridotites of the Wadi Madha and Wadi Shi areas is thus virtually identical to that of other peridotites of the harzburgite sub-type, in particular to the range given by Allen (1975) for the Troodos Plutonic Complex and to that given by Menzies (1974) for the ophiolites of Orthris, Greece. The majority of the olivines contain negligible amounts of Ti and Ca, and Cr is below detection by conventional techniques (0.005%). The CaO contents of the dunite-wehrlite type, and of typical wehrlites show slight enrichment relative to other types, CaO varying between 0.01-0.8. This is to be expected in view of their higher clinopyroxene content. Al is almost completely absent in all samples probed. The amount of Al allowed in the olivine structure is negligible, and no significance is attached to the Al traces observed in some samples. Similarly, as the amount of Fe^{3+} in the olivine structure is limited, total Fe is expressed as FeO.

Dunite olivines can be discriminated from harzburgite olivine by their lower NiO content. This varies between 0.06 and 0.34% NiO while harzburgite olivines have contents between 0.24 and 0.46%. Variation of NiO and Fo content is displayed in fig. 5.1. The high NiO content of the olivine in harzburgites is consistent with their residual

Figure 5.1. NiO-Forsterite content relationships of olivine in mantle peridotites, olivine pyroxenites, and olivine gabbros.

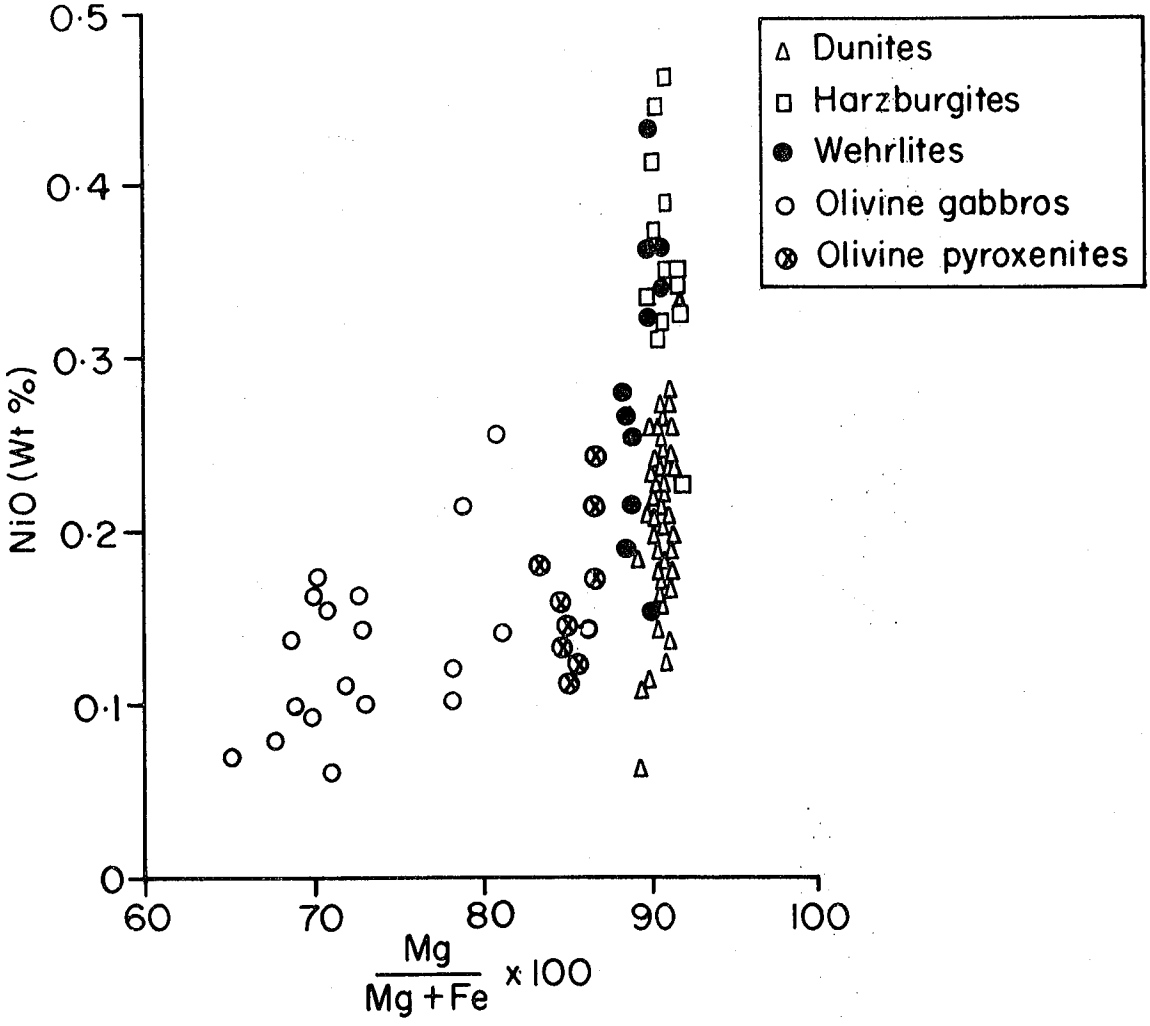
0·5
0·4
0·3
0·2
0·1
0
NiO (Wt %)
60
70
80
90
100
Mg / Mg + Fe x 100
Dunites
Harzburgites
Wehrlites
Olivine gabbros
Olivine pyroxenites

nature, Ni being partitioned into the solid phase rather than the liquid during partial melting.

Olivines from wehrlites overlap with those from dunites and harzburgites with respect to NiO, but have slightly lower Fo contents (Fig. 5.1).

5.2.2. Cumulus olivines

The olivines of the pyroxenites are clearly different from those of the peridotites in their Fo content, which ranges between Fo_{84} and Fo_{87}. The NiO content, on the other hand, varies between 0.11 and 0.24% and is similar to that in the majority of the dunitic olivines, as seen from Fig. 5.1. The distribution coefficient K_D, between olivine and orthopyroxene may be expressed by the function $(Mg^{ol}/Fe^{ol})(Fe^{opx}/Mg^{opx})$. The K_D for two pairs of olivine and orthopyroxene from olivine pyroxenite is 0.97, and is identical to values obtained in harzburgites. The values are also similar to those reported by Allen (1975), who obtained a figure of 0.96 for two pairs of olivine and orthopyroxene from pyroxenites. The K_D value of the two pairs suggests that Mg-Fe equilibrium was established.

Olivine compositions of ophiolite gabbros are listed on the following page in Table 5.3.

Location	Source	Fo%
1. Wadi Madha and Wadi Shi areas		65-86
2. Greenhill, New Zealand.	Mossman (1973)	65-79
3. Bay of Islands, New Foundland.	Irvine and Findley (1972)	69.6-84.8
4. Orthris, Greece	Menzies (1974)	77-86
5. Papua, New Guinea	England and Davies (1973)	78.3-87.7
6. Troodos Plutonic Complex.	Allen (1975)	69.8-83.9
7. New Caledonia	Rodgers (1975)	78-89

TABLE 5.3

Olivine compositions of ophiolite gabbros

The composition of olivines from olivine gabbros in the Wadi Madha and Wadi Shi areas in Fig. 5.1 shows clearly that their iron-rich nature is reflected in their lower NiO contents. The K_D value for two pairs of coexisting olivine and orthopyroxene is 0.95, clearly similar to values in harzburgites, and again suggesting that Mg-Fe equilibrium was established.

5.3. Orthopyroxenes

Orthopyroxene analyses from harzburgites, olivine pyroxenites, olivine gabbros, norites, and hypersthene gabbros are listed in Tables 5.14-5.17 and 5.44, 5.46, 5.48, 5.50 and 5.52.

5.3.1. Peridotite orthopyroxenes

Orthopyroxene compositions from harzburgites of Alpine-type peridotites and peridotites from various ophiolites are listed in Table 5.4.

Location	Source	Mgx100/ (Mg+Fe+Ca)
1. Wadi Madha and Wadi Shi areas		88.8-91.6
2. Troodos Plutonic Complex	Allen (1975)	90-92
3. Orthris, Greece	Menzies (1974)	89-90
4. Papua, New Guinea	England and Davies (1973)	90-92
5. Bay of Islands New Foundland	Malpas (1978)	88.5-92.1
6. Red Mountain Peridotite, New Zealand.	Sinton (1977)	89.5-90.7
7. Vulcan Peak, Oregon	Himmelberg and Loney (1973)	89-90
8. Burrow Mountain	Loney et al. (1971)	89.8-91.1

TABLE 5.4

Orthopyroxene compositions from harzburgites of Alpine-type peridotites and ophiolites

The orthopyroxenes from harzburgites show little compositional variation with respect to Mgx100/(Mg+Fe)

ratio, which ranges from 90-92, while enstatite values expressed by the ratio Mgx100/(Mg+Fe+Ca) range between 88.8 and 91.6. These values are consistent with the compositions of orthopyroxenes reported from Alpine-type peridotites and ophiolites of the harzburgite sub-types listed above. As clinopyroxene exsolution lamellae are present in the orthopyroxenes, the CaO values of 0.48 and 1.15 percent represent the host composition, and not the bulk pyroxene composition.

The Al_2O_3 content of the orthopyroxenes from the harzburgites varies from 1.59 to 2.68 percent, which is in the range of Al_2O_3 values (1.0 to 3.0 percent) reported for orthopyroxenes from other harzburgite subtype peridotites (Challis, 1965; Himmelberg and Coleman, 1968; Loney et al., 1971; Jackson and Thayer, 1972).

5.3.2. Pyroxenite orthopyroxenes

The orthopyroxenes from cumulate olivine pyroxenites range in Mgx100/(Mg+Fe) ratio from 85 to 87 and in Mgx100/(Mg+Fe+Ca) from 84 to 86. They have less Al_2O_3 than orthopyroxenes from harzburgites (1.38 to 1.92 percent) and CaO is also slightly lower with a range of 0.58 to 1.04 percent. The average Cr_2O_3 and NiO contents of the orthopyroxenes are less than those of harzburgite orthopyroxenes, and they are also depleted in TiO_2. Zoning

within grains is not evident.

5.3.3. Gabbroic orthopyroxenes

The orthopyroxenes from cumulate olivine gabbros range in Mgx100/(Mg+Fe) ratio between 73 to 82 and in Mgx100/(Mg+Fe+Ca) from 72 to 80. The values are consistent with the compositions of orthopyroxenes from olivine gabbros reported by Allen (1975) for the Troodos Plutonic Complex. Allen obtained Mgx100/(Mg+Fe) ratios ranging between 72 and 83.9 and Mgx100/(Mg+Fe+Ca) of 70 to 82. Al_2O_3 is lower than for orthopyroxenes from either harzburgite or pyroxenite (1.13 to 1.76 percent) but is consistent with values reported by Allen (1975) of 0.99 to 1.51 percent Al_2O_3 for the Troodos Plutonic Complex. CaO is higher than in orthopyroxenes of harzburgites and pyroxenites (0.97 to 1.60 percent) but again similar to those of the Troodos Plutonic Complex which range between 1.03 to 1.83 percent CaO. The orthopyroxenes from the olivine gabbros are higher in TiO_2 and MnO than those of the harzburgites and pyroxenites, but are depleted in Cr_2O_3.

5.3.4. Noritic and gabbroic orthopyroxenes

Orthopyroxene compositions from norites and gabbros of various ophiolites are listed in Table 5.5.

Rock Type	Mgx100/(Mg+Fe)	Mgx100/(Mg+Fe+Ca)	Al_2O_3	CaO	Source
Norite	71-73	67-71	1.30-1.72	1.31-3.18	This study
Norite (Cyprus)	68.53-80.64	58.27-78.14	0.99-1.46	1.06-1.85	Allen (1975)
Norite (Papua, New Guinea)	70-85	69-83	1.7 -1.8	0.8 -1.5	England & Davies (1973)
Norite	-	75-80	-	-	Coleman (1977)

TABLE 5.5

Orthopyroxene compositions from norites and gabbros of various ophiolites.

The orthopyroxenes from the norites range in Mgx100/(Mg+Fe) ratio between 71 and 73 and of Mgx100/(Mg+Fe+Ca) ratio between 67 and 71.

Average Al_2O_3 of the orthopyroxenes from the norites varies between 1.30 to 1.72% similar to values for those from the olivine gabbros.

CaO content of the orthopyroxenes from the norites are distinctly higher than those of the olivine gabbros, ranging from 1.31 to 3.18%. Cr_2O_3 is negligible in the orthopyroxenes from the norites, but MnO occurs in significant amounts ranging from 0.28 to 0.41%, distinctly higher than in the olivine gabbros, pyroxenites and harzburgites.

5.4. Clinopyroxenes

Clinopyroxene analyses from harzburgite, wehrlite, plagioclase peridotite (one sample), olivine pyroxenite, olivine gabbro, and hypersthene gabbro are listed in Tables 5.18-5.22 and 5.55, 5.64, 5.59, 5.65, 5.57, 5.61, 5.66, 5.63, 5.51 and 5.53.

On a plot of SiO_2 versus Al_2O_3 shown in fig. 5.2 it is clearly seen that the clinopyroxenes from the mantle rocks and cumulates fall in the tholeiitic field, as defined by Le Bas (1962), with the exception of one sample which is slightly alkaline.

Figure 5.2. Plot of SiO_2/Al_2O_3 for clinopyroxenes from mantle peridotites, pyroxenites and gabbros.

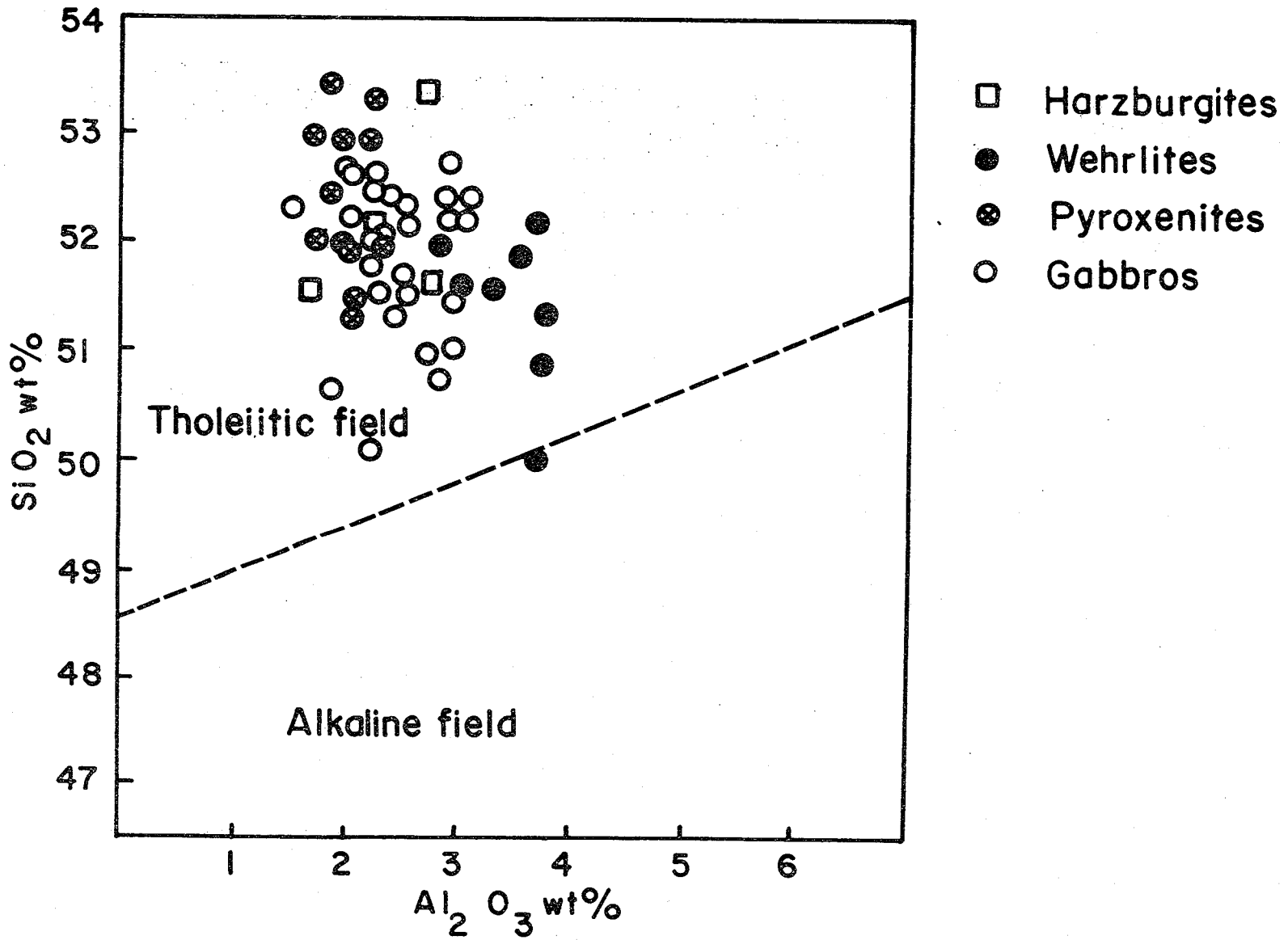
54
53
52
51
50
49
48
47
SiO_2 wt%
Tholeiitic field
Alkaline field
1
2
3
4
5
6
Al_2O_3 wt%
Harzburgites
Wehrlites
Pyroxenites
Gabbros

5.4.1. Peridotite clinopyroxenes

In the harzburgites the clinopyroxenes occur as small interstitial crystals and are relatively rare. They are essentially Cr-bearing diopsides with Mgx100/(Mg+Fe) ratio of 92 and 94, with the exception of sample 1031C which contains more iron and shows an Mgx100/(Mg+Fe) ratio of 90. The Al_2O_3 content has a small range (1.8 to 2.8%), comparable to that in the coexisting orthopyroxenes. In all aspects the clinopyroxenes are similar to those reported from other harzburgite subtype bodies (Challis, 1965; Himmelberg and Coleman, 1968; Loney et al., 1971; Allen, 1975; Himmelberg and Loney, 1973).

The clinopyroxenes from wehrlites range in Mgx100/(Mg+Fe) ratio between 90 and 93 and are distinctly higher in Cr_2O_3 than those of the harzburgite clinopyroxenes, ranging between 0.98 and 1.43 percent. Al_2O_3 ranges between 2.89 and 3.89 percent, also distinctly higher than in clinopyroxenes of the harzburgites.

5.4.2. Pyroxenite clinopyroxenes

The clinopyroxenes from cumulate olivine pyroxenites show a limited spread of Mgx100/(Mg+Fe) ratio, ranging from 89 to 91. The Al_2O_3 and Cr_2O_3 contents are distinctly

lower than those of the harzburgites and wehrlites ranging between 1.85 and 2.44 percent Al_2O_3 and 0.32 to 0.86 percent Cr_2O_3. FeO contents are higher than in clinopyroxenes from harzburgites and wehrlites.

5.4.3. Gabbroic clinopyroxenes

In general, clinopyroxenes from the cumulate olivine gabbros vary in Mgx100/(Mg+Fe) ratio from 73 to 85. Al_2O_3 varies from 1.70 to 3.20 percent and is higher than in clinopyroxene from the pyroxenites and harzburgites, but is lower than in the wehrlites. Cr_2O_3 varies between 0.06 and 0.36 percent.

The clinopyroxenes from the olivine gabbros are generally distinguishable from those of the harzburgites, wehrlites and pyroxenites by their more iron-rich composition and higher TiO_2 contents, although there is some overlap.

However, in two olivine gabbros (sample 232 and 539) chrome-rich clinopyroxene is noted. In sample 232 it appears to be a xenocryst, possibly derived from a wehrlite. In summary, Mgx100/(Mg+Fe) ratio in the chrome-rich clinopyroxene varies from 84 to 88 in sample 232 and from 88 to 90 in sample 539. Cr_2O_3 varies from 0.33 to 1.14 percent in 232 and from 0.34 to 0.53 in 539. TiO_2

values in these samples are lower than in the bulk of gabbroic clinopyroxenes and are comparable to wehrlite clinopyroxenes.

Clinopyroxenes from the pyroxene gabbros range in Mgx100/(Mg+Fe) ratio between 75 and 86. Al_2O_3 content varies between 2.15 and 2.82 percent. They show relative Ti enrichment and depletion in Cr.

5.5. Clinopyroxene-orthopyroxene-olivine relations

Fig. 5.3 shows element variation between and within the clinopyroxenes and orthopyroxenes. TiO_2 is observed to increase with decreasing Mgx100/(Mg+Fe) ratio in both pyroxenes but is enriched in the clinopyroxenes by a factor of approximately 2 over its concentration in the orthopyroxenes.

The high TiO_2 present in the clinopyroxenes from the cumulate gabbros compares closely with the earliest analysed clinopyroxenes of the Skaergaard intrusion (Brown, 1957, analysis 1), and shows a similar trend as in the Bushveld, Stillwater, and Skaergaard clinopyroxenes.

Cr_2O_3, as would be expected, shows a rapid decrease in both pyroxenes as Mgx100/(Mg+Fe) ratio decreases, and like TiO_2, it is enriched in the clinopyroxenes relative to the coexisting orthopyroxenes by a factor of about

Figure 5.3. Plots of TiO_2, Cr_2O_3, and MnO against Mgx100/(Mg+Fe) for pyroxenes from the ultramafic and mafic rocks.

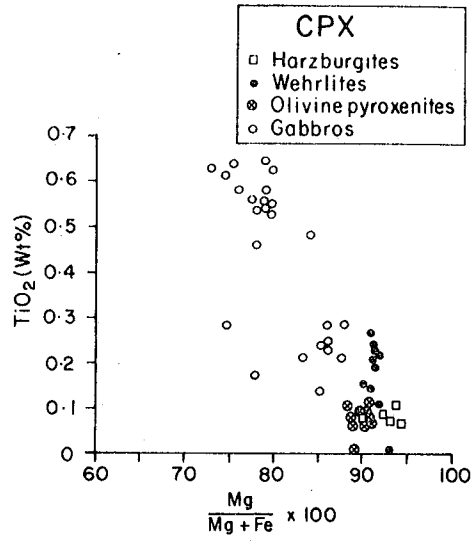
CPX
Harzburgites
Wehrlites
Olivine pyroxenites
Gabbros
TiO2 (Wt%)
0·7
0·6
0·5
0·4
0·3
0·2
0·1
0
60
70
80
90
100
Mg / Mg+Fe x 100

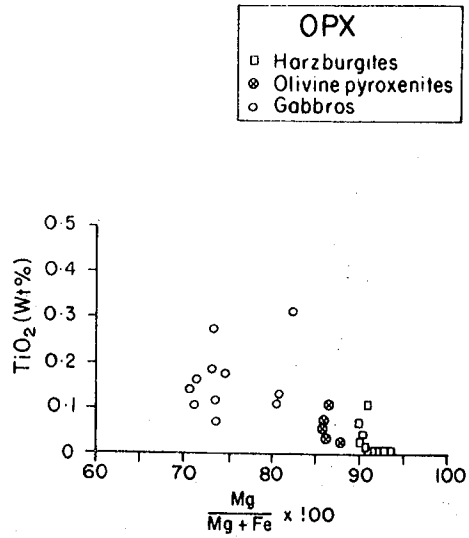
OPX
Harzburgites
Olivine pyroxenites
Gabbros
TiO2 (Wt%)
0·5
0·4
0·3
0·2
0·1
0
60
70
80
90
100
Mg / Mg+Fe x 100

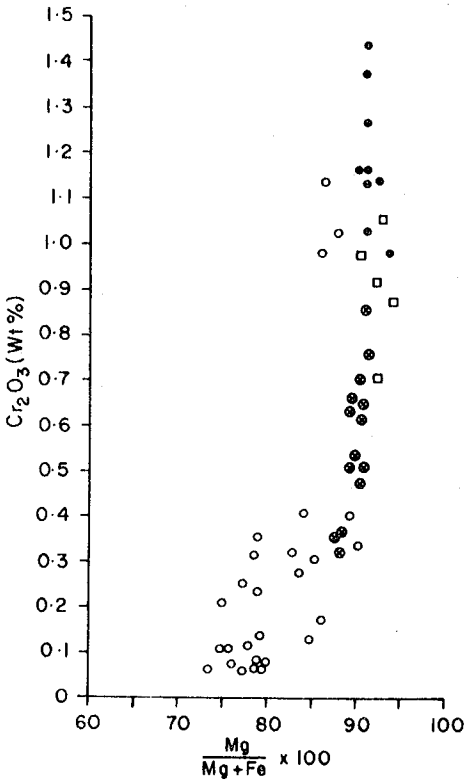
Cr2O3 (Wt%)
1·5
1·4
1·3
1·2
1·1
1·0
0·9
0·8
0·7
0·6
0·5
0·4
0·3
0·2
0·1
0
60
70
80
90
100
Mg / Mg+Fe x 100

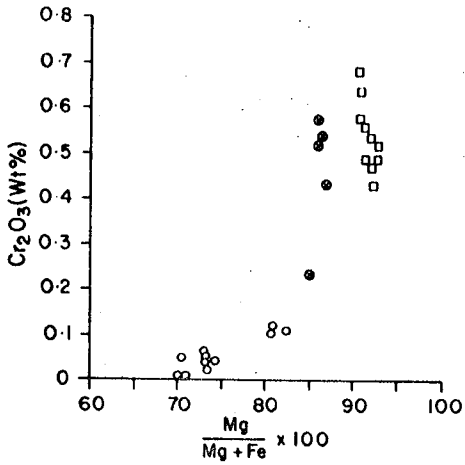
Cr2O3 (Wt%)
0·8
0·7
0·6
0·5
0·4
0·3
0·2
0·1
0
60
70
80
90
100
Mg / Mg+Fe x 100

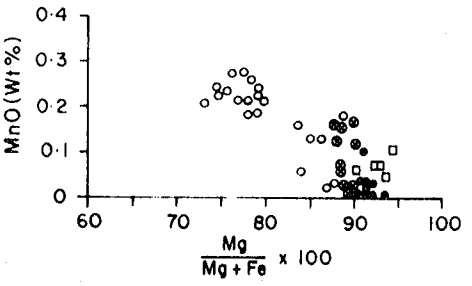
MnO (Wt%)
0·4
0·3
0·2
0·1
0
60
70
80
90
100
Mg / Mg+Fe x 100

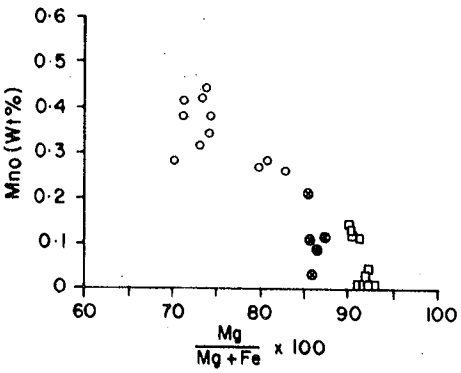
Mno (Wt%)
0·6
0·5
0·4
0·3
0·2
0·1
0
60
70
80
90
100
Mg / Mg+Fe x 100

1.5 to 2.0 for equivalent rock groups.

Mn increases with Fe^{2+}, for which it substitutes, in both pyroxenes but in view of the greater Fe^{2+} in the orthopyroxenes, shows an enrichment in them relative to its concentration in clinopyroxenes. MnO occurs in about the same abundance as in the Skaergaard clinopyroxenes.

Figs. 5.4 and 5.5 show the major element inter-relationship between and within the pyroxenes. Within the clinopyroxenes, CaO is enriched in those from harzburgites. Also there is a pronounced compositional gap within the gabbroic clinopyroxenes.

In the orthopyroxenes there is a slight tendency for Ca to increase with decreasing Mg/(Mg+Fe). The compositional gap between the pyroxenes, assuming they equilibrated on the pyroxene solvus, is indicative of an equilibration below 1000°C (Boyd and Schairer, 1964; Davis and Boyd, 1966; Boyd, 1970).

The tie-line relationships, illustrated in Fig. 5.4 also indicate equilibration of the pyroxenes due to their parallel nature, although some tie-lines do cross.

Figs. 5.6 and 5.7 summarise the relations between olivine and clinopyroxene for the various rock types. Again the tie-lines, representing Mg-Fe partitioning,

Figure 5.4. Pyroxene compositional variation in pyroxene quadrilateral for harzburgites, olivine pyroxenites and gabbros.

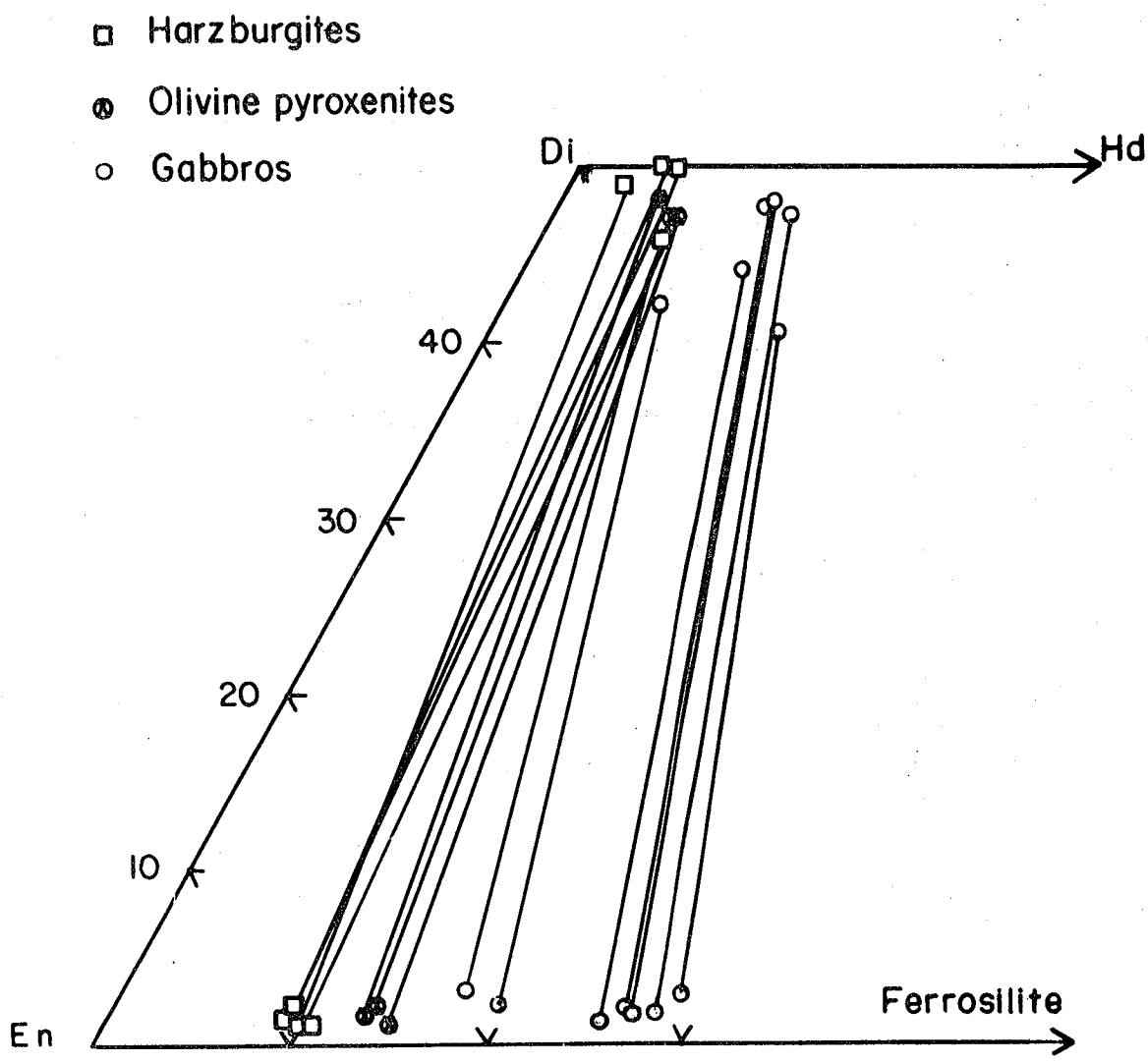
Harzburgites
Olivine pyroxenites
Gabbros
Di
Hd
40
30
20
10
En
Ferrosilite

Figure 5.5. Clinopyroxene compositions of harzburgites, wehrlites, olivine pyroxenites and gabbros.

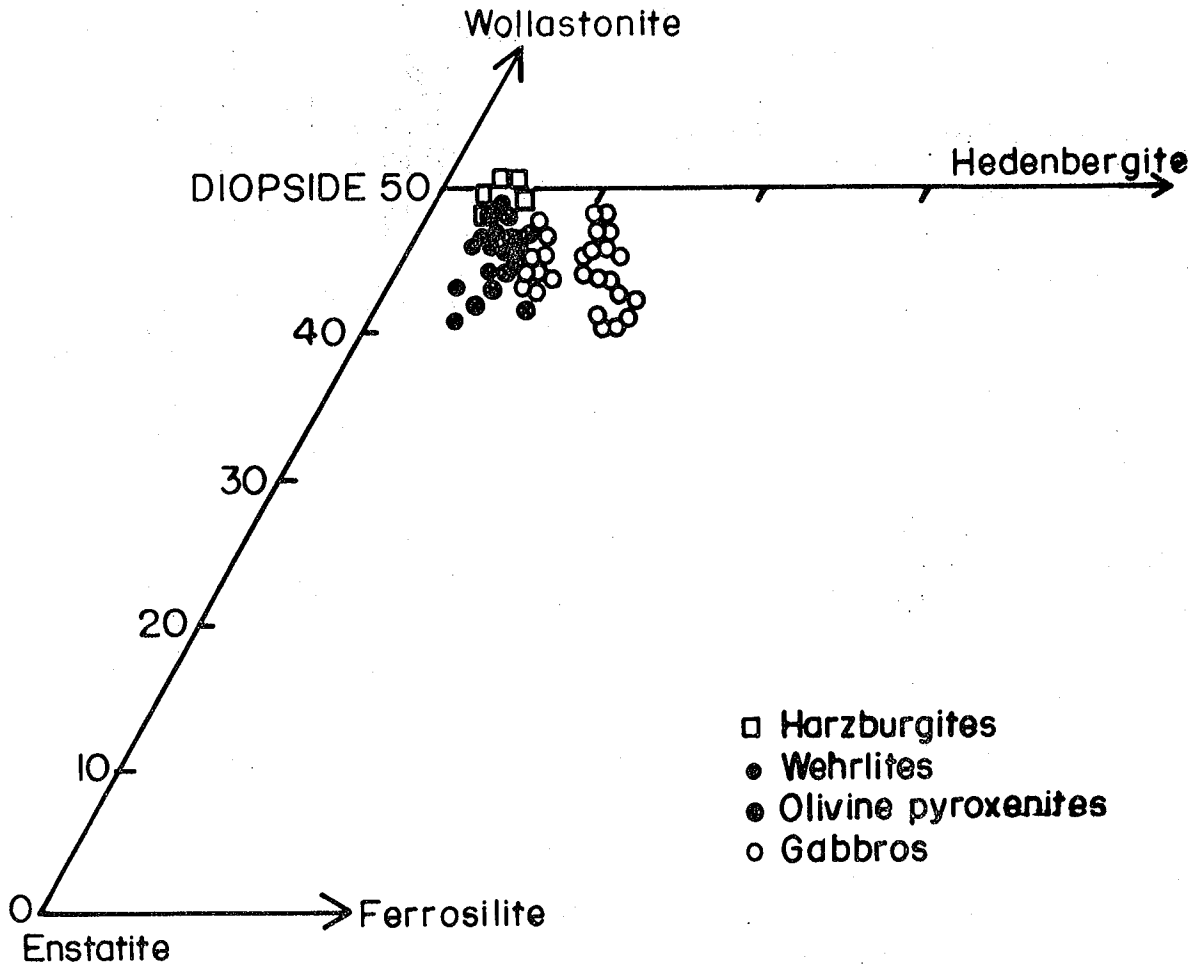
Wollastonite
DIOPSIDE 50
Hedenbergite
40
30
20
10
0
Enstatite
Ferrosilite
Harzburgites
Wehrlites
Olivine pyroxenites
Gabbros

Figure 5.6. Compositional ranges of pyroxenes and olivines from mantle rocks.

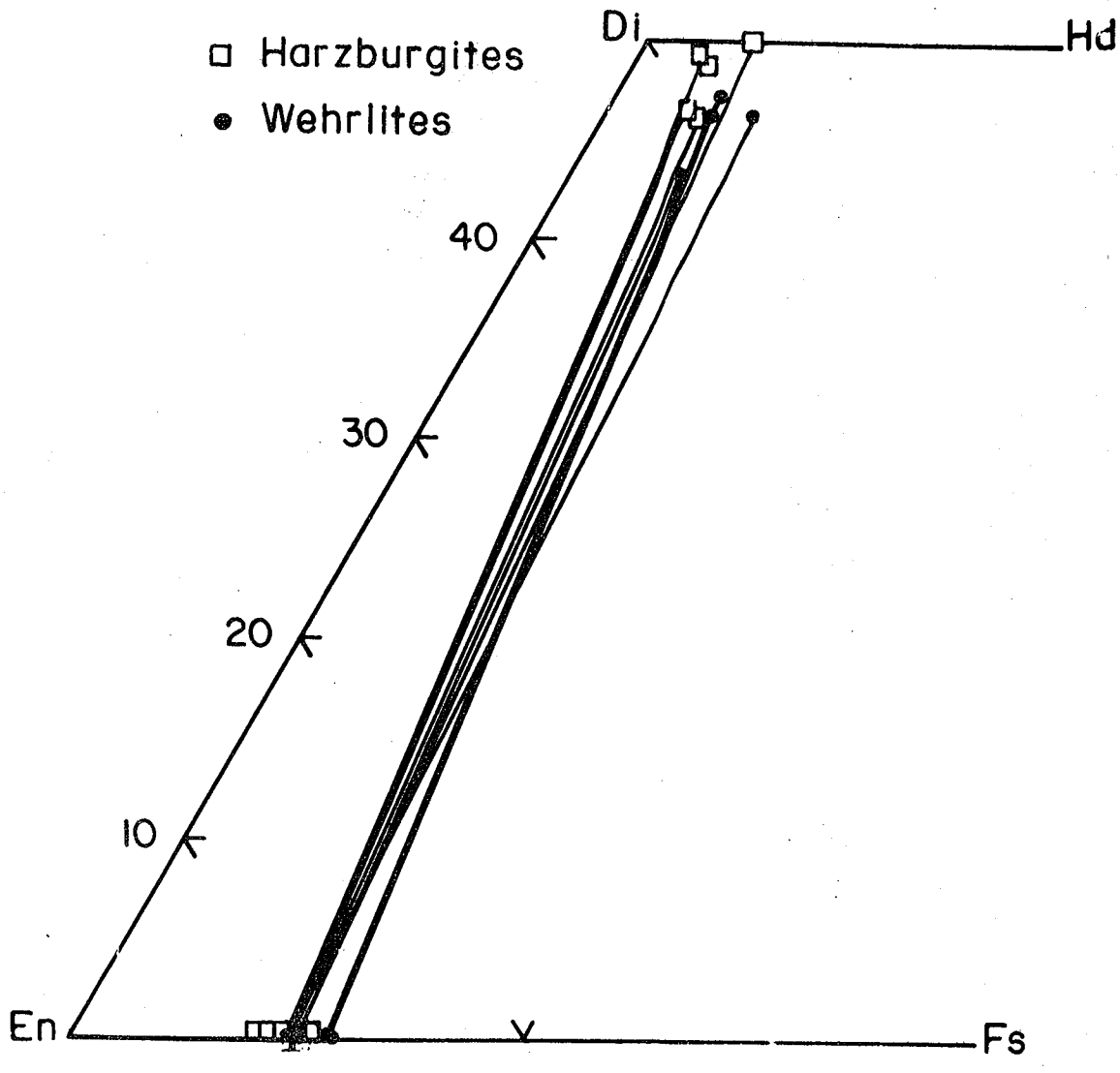
Harzburgites
Wehrlites
Di
Hd
40
30
20
10
En
Fs

Figure 5.7. Compositional ranges of pyroxenes and olivines from olivine pyroxenites and olivine gabbros.

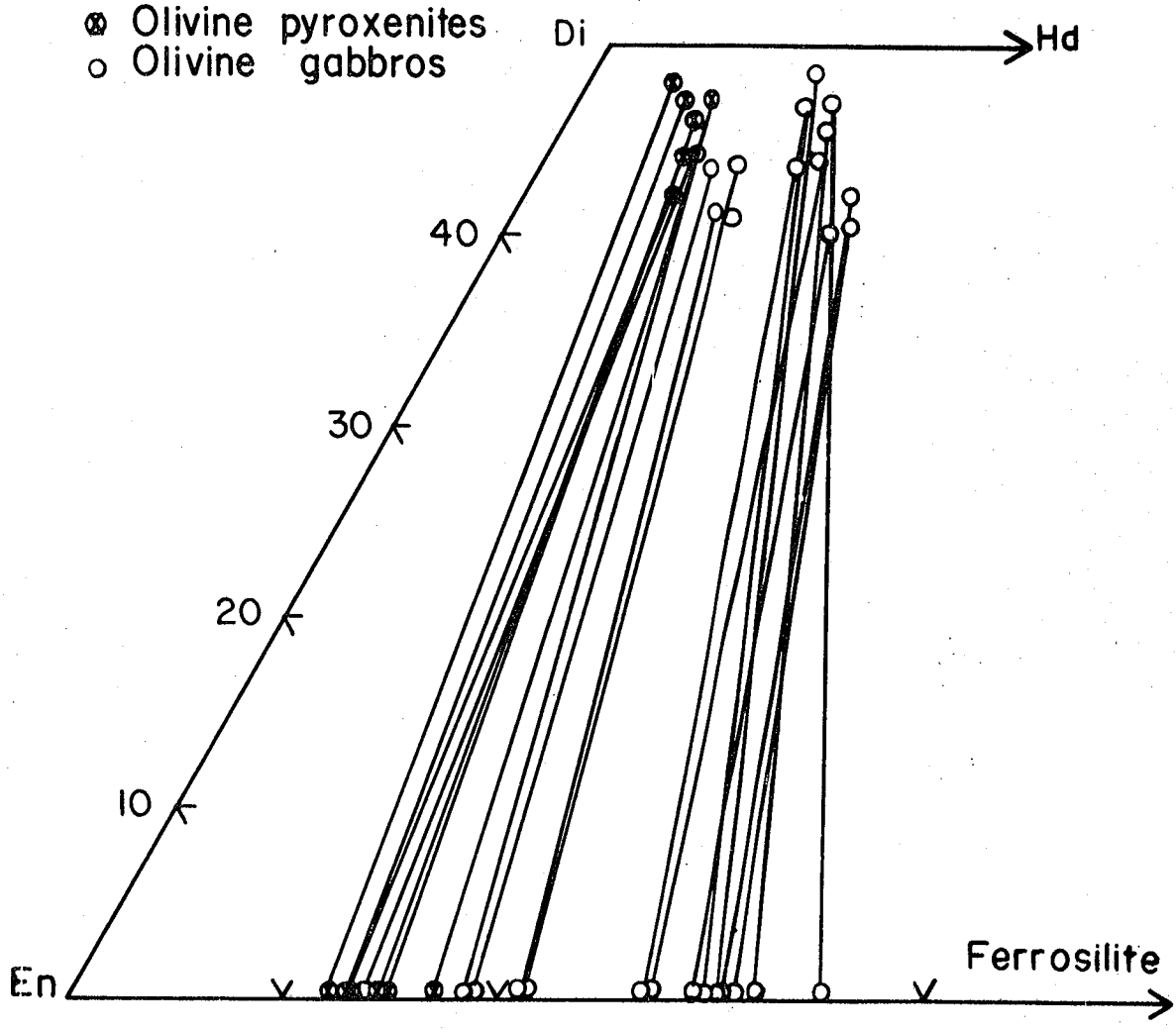
Olivine pyroxenites
Olivine gabbros
Di
Hd
40
30
20
10
En
Ferrosilite

are sub-parallel and indicate equilibration between these two phases.

The compositional relationship between the pyroxenes and olivines will be further discussed in the geothermometry and goebarometry section (5.9.2).

In summary:

1. The compositional gap, exhibited in Figs. 5.4, 5.5 and 5.7, within the gabbroic pyroxene could be explained in the following way:

When the asthenosphere melts partially beneath a mid-ocean ridge it produces residual crystals, which accrete to the lithosphere, together with melt which may enter an axial magma chamber. This primary magma may then mix with more evolved magma already in the chamber. A pyroxene subsequently crystallizing from this melt will have a composition which is more evolved than the composition of either residual pyroxenes or pyroxenes which crystallized directly from the primary magma. A compositional gap might thus be expected between pyroxenes related to primary magmas and those related to magma whose composition is buffered in a large magma chamber (Pearce, J.A., pers. comm., 1977).

2. The small amount of clinopyroxenes present in the harzburgites probably formed at a late stage, precipitating from a trapped melt. They are very calcic clinopyroxenes representing relatively primitive magma.

5.6. Plagioclase

Cumulus plagioclase compositions were determined by microprobe analysis from olivine gabbros, norites, olivine-free gabbros, and anorthosites. The results are tabulated in Tables 5.23-5.28, and Table 5.6.

Intercumulus plagioclase was determined from one olivine pyroxenite and one plagioclase peridotite. Saussuritization of plagioclase in the peridotite and olivine pyroxenite make analyses of these samples impossible.

Intercumulus plagioclase in the peridotite and pyroxenite, and core compositions in all coarse-grained gabbros and norites are exceptionally calcic, generally in the range An_{94-97} for olivine gabbros, and $An_{90.62}$ to $An_{95.22}$ for norites. Coarse grained, olivine-free gabbros are generally in the range $An_{80.59}$ to $An_{88.08}$ while medium and fine grained olivine gabbros are less calcic, generally in the range of $An_{78.8}$ to $An_{89.70}$ for the medium-grained olivine gabbros, and $An_{74.82}$ to

TABLE 5.6 Plagioclase Analyses

Rock Type	Sample No.	Core An%
Coarse Grained Gabbro	231A	88.08
" " "	231B	84.88
" " "	859A	80.59
" " "	526AA	86.55
Coarse Grained Anorth.	160A	93.30
" " "	160B	92.83

Plagioclase compositions of various ophiolites

Rock Type	Core An%	Source	Location
Wehrlite	94.2	Allen (1975)	Troodos Plutonic Complex
Olivine Gabbro	90.9	"	"
Pyroxene Gabbro	91.67	"	"
Troctolites and Eucrites	90-95	Coleman (1977)	-
Olivine Gabbro	88.3-91.0	Mossman (1973)	Greenhills ophiolite, New Zealand

$An_{79.02}$ for the fine-grained ones. Coarse-grained anorthosites range from $An_{92.83}$ to $An_{93.30}$. The intercumulus plagioclase in the peridotite has a composition of $An_{89.31}$ and that of the olivine pyroxenite has a composition of $An_{97.43}$.

Throughout the sections studied, no core-to-margin zoning was noticed.

5.7. Spinels

Electron microprobe analyses of spinels from harzburgites, dunites, wehrlites, plagioclase peridotites, sheared talcose serpentinites, and olivine pyroxenites are listed in Tables 5.29-5.33 and 5.36, 5.34, 5.38, 5.40 and 5.42. End member compositions have been calculated according to the method or Irvine (1965). Iron was determined as total iron, and the amount of FeO and Fe_2O_3 calculated by assuming the RO/R_2O_3 ratio in the chromian spinels to be 1:1. The validity of this assumption for natural chromian spinel has been demonstrated by Stevens (1944) and Irvine (1965). All analyses plot close to the chromite-picrochromite plane of Irvine (1965, 1967) Fig. 5.8. Projections of these data points onto the two planes expressing $Crx100/(Cr+Al)$ and $Fe^{3+}x100/(Cr+Al+Fe^{3+})$ versus $Mgx100/(Mg+Fe^{2+})$ in figures 5.9 and 5.10.

Figure 5.8. A spinel compositional prism, from Irvine (1965). The prism shows the principle compositional end members, and the main spinel ratio plots.

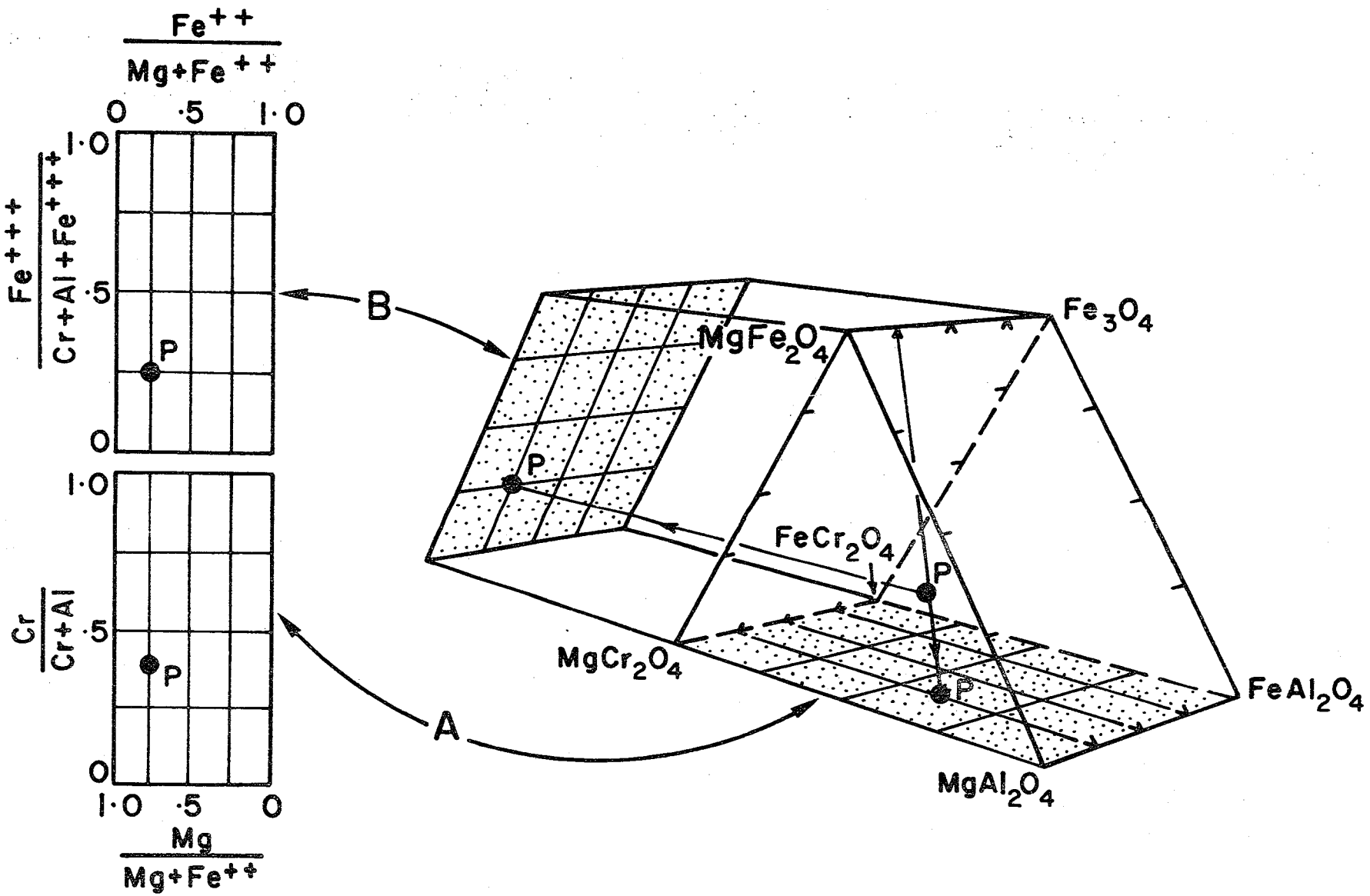
Fe++ / Mg+Fe++
0
·5
1·0
Fe+++ / Cr+Al+Fe+++
P
Cr / Cr+Al
Mg / Mg+Fe++
B
A
MgFe2O4
Fe3O4
FeCr2O4
MgCr2O4
FeAl2O4
MgAl2O4

Figure 5.9. Variation of chromian spinel compositions.

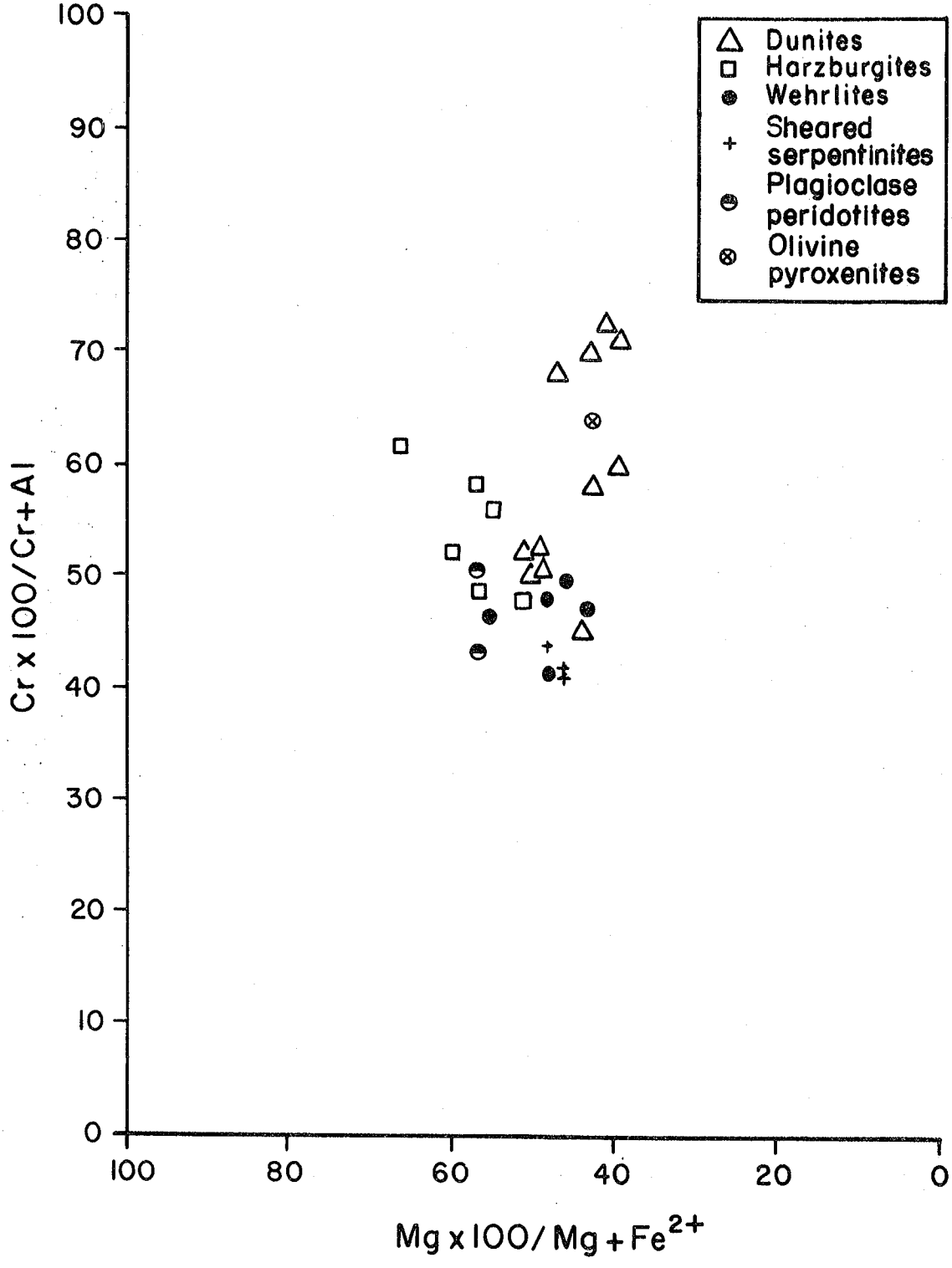
Dunites
Harzburgites
Wehrlites
Sheared serpentinites
Plagioclase peridotites
Olivine pyroxenites
Cr x 100/Cr+Al
Mg x 100/Mg + Fe2+
100
90
80
70
60
50
40
30
20
10
0
100
80
60
40
20
0

Figure 5.10. Variation of chromian spinel compositions.

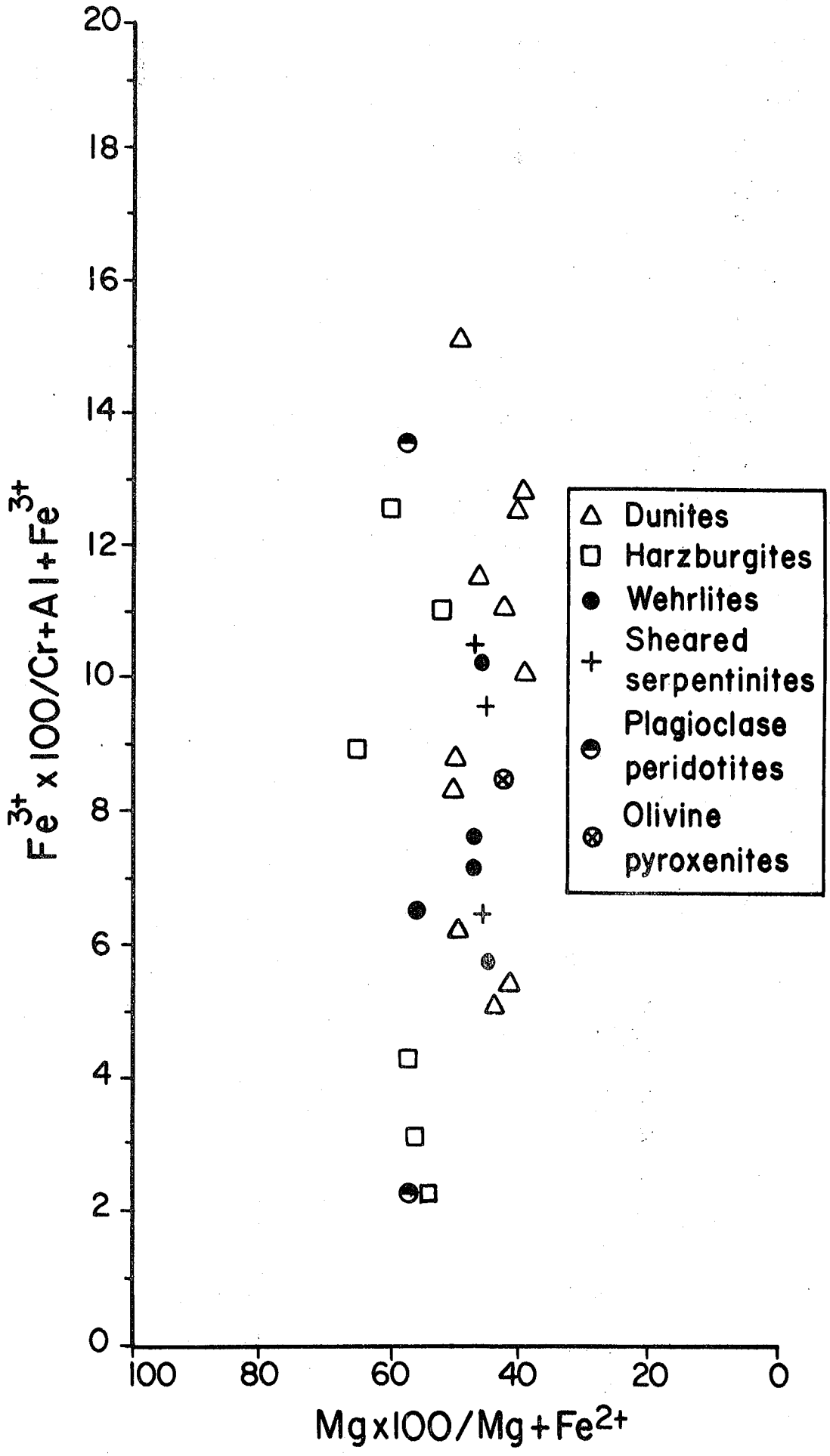
20
18
16
14
12
10
8
6
4
2
0
100
80
60
40
20
0
$Fe^{3+} \times 100/Cr+Al+Fe^{3+}$
$Mg \times 100/Mg+Fe^{2+}$
Dunites
Harzburgites
Wehrlites
Sheared serpentinites
Plagioclase peridotites
Olivine pyroxenites

5.7.1. Peridotite spinels

Spinel compositions of Alpine-type peridotites and peridotites from various ophiolites are listed on the following page (Table 5.7)

The chromian spinels of harzburgite show considerable range in chemical composition, the ratio Crx100/(Cr+Al) varying from 47 to 62 and Mgx100/(Mg+Fe^{2+}) from 52.82 to 66.54. Values for the cation ratio Fe^{3+}x100/(Cr+Al+Fe^{3+}) range between 2 and 12.5 which seems to be characteristic of chromian spinels from Alpine-type peridotites (Irvine, 1967; Loney et al., 1971; Medaris, 1972).

It is apparent from Fig. 5.9 that there is a gap in Mgx100/(Mg+Fe^{2+}) between the spinels of dunites and harzburgites. Crx100/(Cr+Al) values are somewhat higher in the dunites with a range between 46.71 and 73.66 Mgx100/(Mg+Fe^{2+}), however, is invariably lower than in the harzburgites spinels, ranging from 41.08 to 52.53. In general the dunite spinels contain more iron in the Fe^{3+} state than those of the harzburgites.

Fig. 5.9 shows that chromian spinels of the wehrlites have a somewhat lower range of Crx100/(Cr+Al) and Mgx100/(Mg+Fe^{2+}) ratios than those of the harzburgites; they have ranges of 42 to 50 and 45.62 to 56.92 respectively. Fe^{3+} values overlap with those of the dunites and

Location	Source	Crx100/(Cr+Al)	Mgx100/(Mg+Fe^{2+})	Rock-Type
Troodos Plutonic Complex	Allen (1975)	51.85-74.76	44.38-61.14	Harzburgite
" "	"	56.90-85.52	35.06-48.83	Dunite
" "	"	57.84-80.43	34.23-50.36	Wehrlite
Vulcan Peak, Oregon	Himmelberg & Loney (1973)	53.6-59.43	57-60	Harzburgite
" "	"	42-70	45-55	Dunite
Burro Mountain	Loney et al., (1971)	37-55	57-67	Harzburgite
" "	"	30-73	51-73	Dunite
Red Mountain Peridotite, New Zealand	Sinton (1977)	30.4-62.8	45-69	Harzburgite

TABLE 5.7

Spinel compositions of Alpine-type peridotites and peridotites from various ophiolites.

harzburgites although average values of Fe^{2+} are slightly less than in spinel from harzburgite. The spinels from wehrlite have a distinctly lower range of Crx100/(Cr+Al) ratios than those from dunite. Both dunite and wehrlite populations overlap with respect to Mgx100/(Mg+Fe^{2+}) and Fe^{3+}x100/(Cr+Al+Fe^{3+}), but the Fe and Cr rich dunite-spinels appear to have lower Mgx100/(Mg+Fe^{2+}) ratios.

Spinels from plagioclase peridotites range in Crx100/(Cr+Al) between 43 and 50 and Mgx100/(Mg+Fe^{2+}) between 57 and 58; they plot close to spinels from the harzburgites. The Fe^{3+} contents overlap with those of the harzburgites, high Fe^{3+} in one sample being attributed to secondary oxidation.

Chromian spinels from sheared serpentinites range in Crx100/(Cr+Al) between 41 and 44 and Mgx100/(Mg+Fe^{2+}) between 46 and 48, overlapping with spinels from wehrlites with respect to both ratios. Similarly the Fe^{3+} content also overlaps with those of the wehrlites.

5.7.2. Pyroxenite spinel

Only one analysis was obtained from spinel in olivine pyroxenite;it has a Crx100/(Cr+Al) ratio of 64.2 and Mgx100/(Mg+Fe^{2+}) ratio of 43.42.

5.8. Magnetites and ilmenites

Iron-titanium oxides are present in trace amounts in the olivine and olivine-free gabbros, in reaction relationship with brown basaltic hornblende; they appear to have formed as primary magmatic phases. The oxide species present include ilmenite-hematite, permitting an estimate of temperature and f_{O_2} of formation of the coexisting pairs (Buddington and Lindsley, 1964). Buddington and Lindsley's magnetite-ilmenite, geothermometer-oxygen barometer is based on the distribution of iron and titanium between coexisting magnetite and ilmenite. The geothermometer has been used on oxide pairs in which the ilmenites contain less than 5 weight percent MnO. The influence of manganese on the stability of ilmenite has been discussed by Neumann (1974), but is not known quantitatively. The oxidation process in the Buddington and Lindsley hypothesis can be presented by the following equation (Vincent, 1960):

$3Fe_2TiO_4$	+	$O = 3FeTiO_3$	+	Fe_3O_4
Ulvospinel in the spinel-magnetite solid solution.		Ilmenite in the ilmenite-hematite solid solution.		Magnetite in magnetite-ulvospinel solid solution.

Ilmenite and magnetite are generally pure end-member compositions, and the final equilibrium for two ilmenite-

magnetite assemblages seems to have been under oxygen fugacities between those defined by the QFM and the wüstite-magnetite buffers near 600°C, $f_{O_2} = 10^{-21.5}$ bars

5.9. Geothermometry

Simple experimental systems have yielded potential geothermometers and geobarometers, particularly for mineral assemblages characteristic of many ultramafic and mafic rocks. Therefore it is of interest to trace the pressure-temperature history of the ultramafic and cumulate rock assemblage. Methods and results for determination of temperatures and pressures of equilibration for the peridotites and cumulate rocks of this study are shown in Appendix I.

5.9.1. Method of Jackson (1969)

Partitioning of Mg and Fe^{2+} between olivine and spinel.

Cation distribution between coexisting olivine and chromian spinel has been discussed by Irvine (1965), Jackson (1969) and Loney et al. (1971). Irvine has shown that, while the effect of pressure over moderate ranges may be negligible, the relative distribution of

ferrous iron and magnesium between olivine and spinel may be expected to vary significantly with temperature.

The distribution of Mg and Fe^{2+} is complicated by the presence of trivalent cations in the spinel structure. The Mg-Fe^{2+} exchange reaction between coexisting olivine and chromian spinel can be written:

$$Fe^{2+}Si_{0.5}O_2 + Mg(Cr\alpha\ ,\ Al\beta\ ,\ Fe^{3+}\gamma\ )_2O_4 =$$

$$MgSi_{0.5}O_2 + Fe^{2+}\ (Cr\alpha\ ,\ Al\beta\ ,\ Fe^{3+}\gamma\ )_2O_4$$

The values α , β , and γ are the respective fractions of Cr, Al, and Fe^{3+} in chromian spinel. The thermodynamic equilibration coefficient (K_D) may be defined by the following equation, assuming ideal solid solution behaviour (Irvine, 1965; Jackson, 1969).

$$K_D = \frac{\left(X_{Mg}^{Ol}\right)\ \left(X_{Fe^{2+}}^{Sp}\right)}{\left(X_{Fe^2}^{Ol}\right)\ \left(X_{Mg}^{sp}\right)}$$

where X_{Mg}^{Ol} and $X_{Fe^{2+}}^{Ol}$ are mole fractions of the end members $MgSi_{0.5}O_2$ and $FeSi_{0.5}O_2$ respectively, and X_{Mg}^{sp} and $X_{Fe^{2+}}^{sp}$ are the mole fractions of divalent cations in the spinels.

Using Jackson's formula (1969), it is possible to calculate the equilibration temperature for olivine-spinel pairs, using Gibbs free-energy data. It is also possible to calculate the theoretical compositions of all spinels, coexisting with an olivine of fixed composition at a given temperature, by substituting different values for α , β , and δ in the following equation:

$$T^{o} = \frac{5580\,\alpha + 1018\,\beta - 1720\,\delta + 2400}{0.90\,\alpha + 2.56\,\beta - 3.08\,\delta - 1.47 + 1.987\,\ln K}$$

where T is in degrees Kelvin. Possible errors may be introduced due to uncertainties in Gibbs free energy values. Possible maximum errors in the free energies of formation of the spinels alone could affect the temperatures by as much as 300°C. However, these errors are equivalent to standard state errors and should not affect the relative temperatures. Temperatures derived from the above equation are, geologically, quite reasonable.

It appears from Appendex I that the dunites have temperatures of 872-1075°C, harzburgites of 1099-1167°C, and wehrlite (one sample) of 1104°C, the plagioclase peridotite (one sample) an unusually high value of 1263°C,

and the olivine pyroxenite (one sample) of 879°C.

Temperature ranges of Alpine-type peridotites and peridotites from various ophiolites are listed in Table 5.8.

Location	Temperature in °C	Source
Wadi Shi-Wadi Madha Area	872 - 1263	This study
Blue River ultramafics	1030 - 1231	Pinsent, R.H. Ph.D. Thesis (1974) Univ. of Durham.
Burro Mt., USA	1098 - 1335	Loney et al., (1971) Himmelberg and Loney (1973).
Oregon, USA	1200 - 1410	Medaris (1972)
New Caledonia	1180 - 1300	Rodgers (1973)
Bay of Islands Newfoundland	1200 - 1300	Malpas (1978)
Red Mountain Peridotite, New Zealand	930 - 1140	Sinton (1977)
Troodos Plutonic Complex	913 - 1256	Allen (1975)

TABLE 5.8

Temperature ranges of Alpine-type peridotites and peridotites from various ophiolites

Temperatures are based on thermodynamic data from Irvine (1965) and Jackson (1969).

The temperature ranges listed above were derived using the same method. Those of the Troodos Plutonic Complex (Allen, 1975), the Red Mountain Peridotite (Sinton, 1977), and the Vulcan Peak Peridotite (Himmelberg and Loney, 1973) are reasonably similar to those for the Wadi Shi-Wadi Madha area.

Median compositions of spinels are plotted in Fig. 5.11 and the actual mole fraction, X_{Mg}^{ol} of coexisting olivine shown, after Loney et al. (1971). The agreement between the actual and theoretical composition is relatively good, especially for assemblages low in Al and Mg. Fig.5.11 has been contoured according to spinel compositions which, at a given P and T, will equilibrate with olivine or pyroxene of fixed Mg/Fe ratio. Fig. 5.12 after Irvine (1965) and Rodgers (1973) shows the mole fraction of Cr in spinel, Y_{Cr}^{sp} plotted against the Fe-Mg distribution coefficient

$$K_D = \ln \left[\frac{X_{Mg}^{ol} . (1-X_{Mg}^{Sp})}{(1-X_{Mg}^{ol}) . X_{Mg}^{Sp}} \right]$$

According to theory, when spinels are plotted as in Fig. 5.12 they should lie on a straight line with slope equal to lnK. However this relationship is not perfect, and Rodgers (1973) for example quotes a range of lnK from 2.25 to 3.5.

Figure 5.11. A spinel cation ratio plot, after Loney et al. (1971). The plot has been contoured to give the theoretical coexisting olivine Mg cation fraction at 1200°C. The contours are for values of 0.900, 0.915, 0.930. Observed olivine Mg cation fractions are given for each analysed coexisting pair. Sample numbers are: 1=300A, 2=300B, 3=304A, 4=305A, 5=528A, 6=531A, 7=531B, 8=517A, 9=517B, 10=325A, 11=325C, 12=1037A, 13=1044A, 14=503A, 15=315A, 16=1027A.

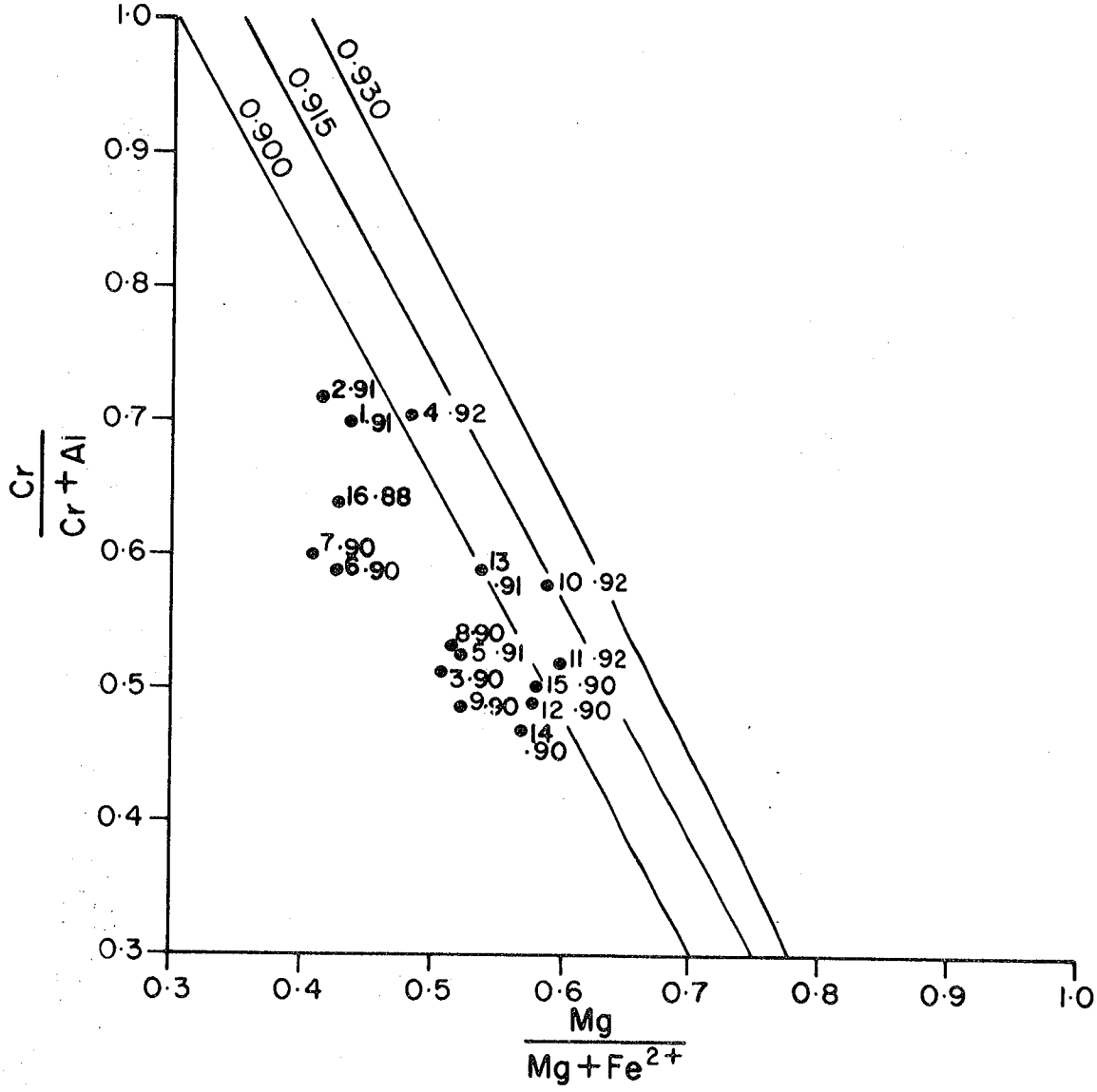
1·0
0·9
0·8
0·7
0·6
0·5
0·4
0·3
0·3
0·4
0·5
0·6
0·7
0·8
0·9
1·0
Cr / Cr + Al
Mg / Mg + Fe2+
0·900
0·915
0·930
2·91
1·91
4·92
16·88
7·90
6·90
13 ·91
10·92
8·90
5·91
11·92
3·90
15·90
9·90
12·90
14 ·90

Figure 5.12. An olivine-spinel equilibration plot, after Irvine (1965), and Rodgers (1973). An Mg-Fe distribution coefficient is plotted against the Cr cation fraction in spinel. The two lines with slopes of 3.7 and 2.6 are shown for reference purposes only. Sample numbers are: 1=300A, 2=300B, 3=304A, 4=305A, 5=528A, 6=531A, 7=531B, 8=517A, 9=517B, 10=325A, 11=325C, 12=1037A, 13=1044A, 14=503A, 15=315A, 16=1027A.

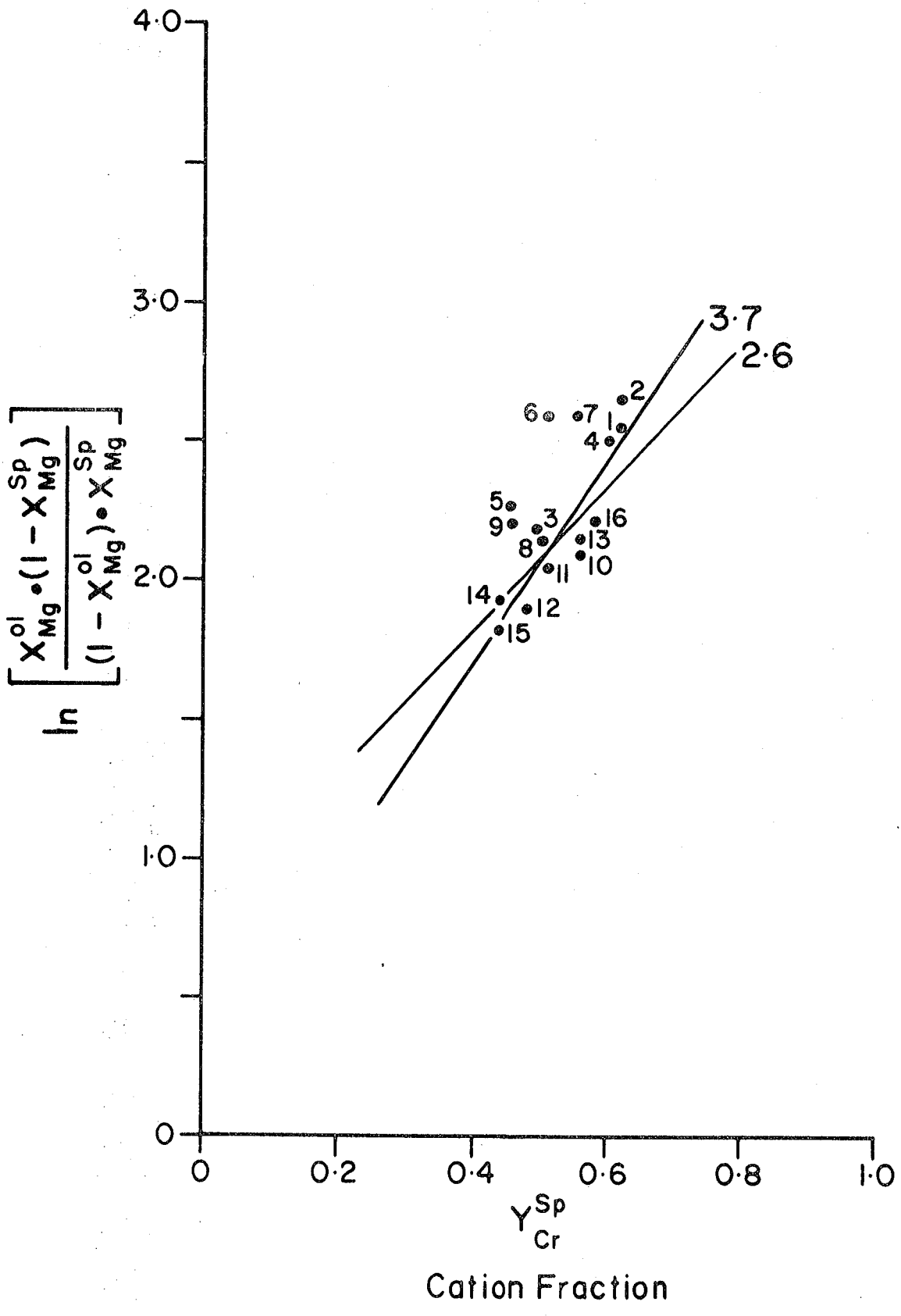
4·0
3·0
2·0
1·0
0
0
0·2
0·4
0·6
0·8
1·0
3·7
2·6
6
7
2
1
4
5
9
3
16
8
13
10
11
14
12
15
$\ln \left[\frac{X^{ol}_{Mg} \cdot (1 - X^{Sp}_{Mg})}{(1 - X^{ol}_{Mg}) \cdot X^{Sp}_{Mg}} \right]$
Y^{Sp}_{Cr}
Cation Fraction

The two lines in Fig. 5.12, with slopes of 3.7 and 2.6 are shown for reference purposes only and do not represent best-fits.

5.9.2. Method of Wood and Banno (1973)

The use of partition coefficients of Mg^{2+} and Fe^{2+} between coexisting orthopyroxenes and clinopyroxenes has been shown to give reasonable results when applied to the present study. Wood and Banno (1973) suggest that values agree with experimental data to within $\pm$ 60°C although errors of $\pm$ 100°C are probably not unreasonable. The results of the application of this method to the present study are listed in Appendix I. Appendix I shows that harzburgites indicate equilibration temperatures between 969 and 989°C. Tie lines indicate equilibrium between orthopyroxene and clinopyroxene in Fig. 5.4. Since clinopyroxene is a late-stage mineral, therefore these temperatures represent the lower limits of equilibration and not the upper temperature limit of olivine plus orthopyroxene equilibration. Since the activity-composition relations of Wood and Banno (1973) have been adopted to account for the solution of Fe, Al, Ti, Cr, Mn and Na in the pyroxene phases, one harzburgite sample (1044A) was not used, because of the high Na content in the clino-

pyroxene, thus resulting in a negative

$$\left(X_{Mg}^{M_2}\right)^{cpx}$$

Cumulate pyroxenites indicate equilibration temperatures between 927 and 974°C, and cumulate gabbros and norite between 839 and 999°C.

5.9.3. Method of Mysen and Boettcher (1975)

The orthopyroxene-clinopyroxene geothermometer of Mysen and Boettcher (1975) is based on variation in the ratios $(X_{Al}^{VI}/X_{Cr})^{opx}/(X_{Al}^{VI}/X_{Cr})^{cpx}$ with temperature. It has been calibrated against the clinopyroxene limb of the solvus (Davis and Boyd, 1966; Warner and Luth, 1974). Application of this geothermometer generally gives temperatures that are higher than those derived by the method of Wood and Banno (1973). The results of the application of this method to the present study are listed in Appendix I. Appendix I shows that harzburgites indicate equilibration temperatures between 978 and 1088°C, cumulate pyroxenites between 985 and 1168°C, and cumulate gabbros and norite between 729 and 1118°C. This method, however, was not applicable for two gabbros and one pyroxenite because $(X_{Cr})^{opx} = 0$.

5.9.4. Method of Hakli and Wright (1967)

Nickel partition between coexisting clinopyroxene and olivine can be used as a geothermometer (Hakli and Wright, 1967; Hakli, 1968). Temperature varies with the distribution coefficient K = ol Ni/cpx Ni, values in ppm, according to the equation $\ln K = -A/T+B$, where A = 8647, B = 7.838. Sample values and equilibration temperatures for harzburgites, plagioclase peridotite, wehrlites, cumulate olivine pyroxenites, and gabbros are listed in Appendix I. The temperatures are fairly consistent though somewhat higher than those obtained from the method of Wood and Banno (1973). Appendix I shows that harzburgites range between 994 and 1330°C, plagioclase peridotite 972°C, wehrlites between 879 and 1045°C, pyroxenites between 911 and 1369°C, and the cumulate gabbros between 849 and 1291°C. This method, however, was not applicable for one wehrlite, two pyroxenites, and one olivine gabbro because ppm Ni in clinopyroxene = 0.

Using the same method, Menzies (1973) obtained temperatures between 1000 and 1150°C for the ultramafic peridotites of Greece and Allen (1975) obtained temperatures of 1121 and 1126°C for the harzburgites of the Troodos Plutonic Complex, and 1104 and 1166°C for the

wehrlites.

5.9.5. Method of O'Hara (1967)

O'Hara (1967) developed a useful pressure-temperature grid based on the chemistry of clinopyroxenes. In Fig. 5.13, α_c and β_c parameters for clinopyroxenes are plotted for ultramafic harzburgites, wehrlites and cumulate olivine pyroxenites. The values for α_c and β_c are listed in Appendix I. α_c and β_c values are determined by the relationships:

$$\alpha_c = \frac{\text{wt\% } CaSiO_3 \times 100}{\text{wt\%}(CaSiO_3 + MgSiO_3)}$$

$$\beta_c = \frac{\text{wt\% } Al_2O_3 \times 100}{\text{wt\%}(CaSiO_3 + MgSiO_3 + Al_2O_3)}$$

β_c takes into account the pressure-dependent solid solution of Al_2O_3 in the clinopyroxene. Examination of Fig. 5.13 indicates that the harzburgites equilibrated at pressures less than 7Kb and temperatures in the range 950 to 1250°C, and wehrlites 1050 to 1250°C, near the solidus. The pressures correspond to a depth of about 22km in oceanic regions. The olivine-pyroxenites equilibrated under closely similar conditions, at temperatures of about 1020°C and pressures of less than 7kb. One wehrlite sample (804D), however, gave anomalous

Figure 5.13. Pyroxene Grid of O'Hara (1967) with plotted values α_c and β_c of analysed clinopyroxenes from harzburgites, wehrlites and olivine pyroxenites.

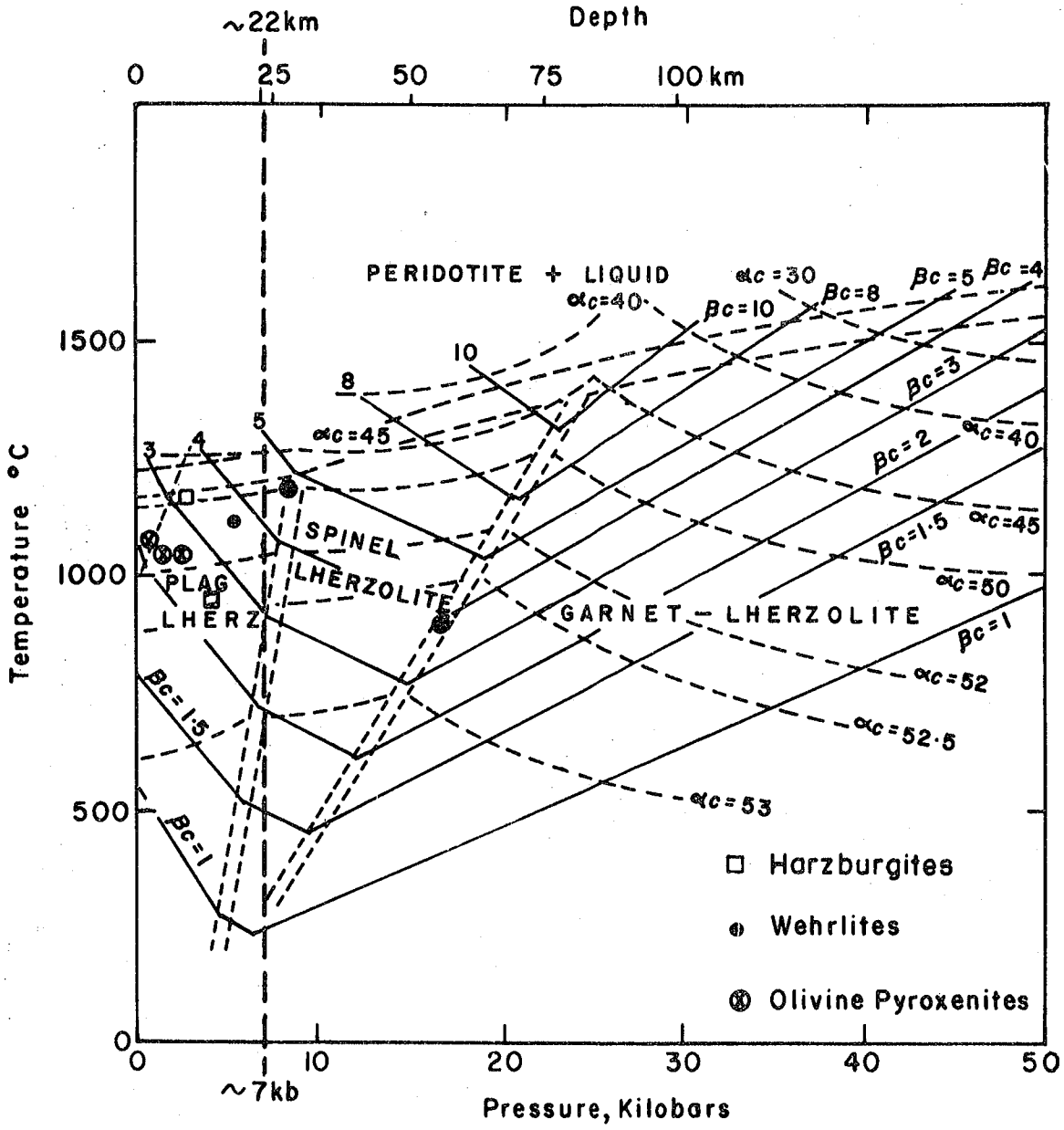
~22km
Depth
0
25
50
75
100 km
PERIDOTITE + LIQUID
αc=40
αc=30
Bc=10
Bc=8
Bc=5
Bc=4
10
8
5
4
3
αc=45
Bc=3
Bc=2
αc=40
Bc=1·5
αc=45
αc=50
SPINEL
LHERZOLITE
PLAG
LHERZ
GARNET – LHERZOLITE
Bc=1
αc=52
αc=52·5
Bc=1·5
αc=53
Bc=1
Harzburgites
Wehrlites
Olivine Pyroxenites
1500
1000
500
0
Temperature °C
0
10
20
30
40
50
~7kb
Pressure, Kilobars

results with a pressure of about 18kb, and temperature of 930°C, the pressure corresponding to a depth of about 55km! The Bay of Islands peridotites reported by Malpas (1978) equilibrated at temperatures of 1000to 1100°C and pressures of about 18-20 kb. Peridotites from the Troodos Plutonic Complex reported by Allen (1975), and those of the Lanzo peridotite Massif reported by Boudier (1978), however, appear to have equilibrated at temperatures of 1150 to 1200°C and 1150 to 1250°C, and pressures of 2 to 4 kb, and less than 5 kb respectively (closely similar values to those reported here).

Stroh (1976) has devised a procedure for calculation of equilibration pressures in harzburgites. Application of this technique gave anomalous results with calculated pressures of -2 to -3 Kb. Sinton (1977) has also attempted to calculate equilibration pressures for peridotites from the Red Mountain, using Stroh's procedure. He also derived anomalous values of -1 to +1 Kb.

5.9.6. Method of Powell and Powell (1974)

The olivine-clinopyroxene geothermometer of Powell and Powell (1974) was derived on the basis of exchange of Mg and Fe between olivine and clinopyroxene according to the reaction:

$$2CaMgSi_2O_6 + Fe_2SiO_4 = 2CaFeSi_2O_6 + Mg_2SiO_4$$

The clinopyroxene M1 site is non-ideal, and it is expressed as a regular solution. Mixing parameters were calculated, and calibrated against iron-titanium oxide temperatures. These enable equilibrium olivine-clinopyroxene pairs to be used as geothermometers. The pressure dependence of the geothermometer has been calculated as $5^{o}C$ per Kilobar. The following equation may be used to determine temperature (T), in degrees Kelvin, at a given pressure (P) in bars.

$$T = \frac{-2X_{Al}\ (920000+3.6P)-0.0435(P-1)+10100}{8+2R\ln K\left(\frac{X^{ol}_{Mg}}{X^{ol}_{Fe}}\right)\left(\frac{X^{Ml}_{Fe}}{X^{Ml}_{Mg}}\right)^{cpx} - 714.3\ (2X_{Al})}$$

The symbols X_{Mg}, X_{Fe} and X_{Al} denote the mole fractions of these elements in olivine, and in the clinopyroxene M1 site. The value for Al includes other trivalent cations in octahedral coordination. The value for R is the gas constant (1.987 cals/mole/^{o}K). The equation defines P-T lines, and assuming a pressure of 5 kbars, it is possible to estimate olivine-clinopyroxene equilibration temperatures. The results of the application of this method to the present study are listed in Appendix I.

Appendix I shows that the range in temperatures calculated for the various rock types is very narrow with a total range of only 1019 to 1048°C.

Wood (1976) has discussed in detail the reason for the narrow temperature estimates for both lherzolite nodules and for the lavas used by Powell and Powell (1974) in calibrating their technique. Wood considered a clinopyroxene with an occupancy of 0.1 aluminium in the M1 site. This figure is close to the average value in the lavas used for calibration and is also similar to that in lherzolite clinopyroxenes discussed by Wood (1976).

According to Wood, if the distribution coefficient K is 0.1 then the temperature derived from the Powell and Powell equation would be 974°C, while a value of 10 changes the estimated temperature to 1062°C. A change in the distribution coefficient K of two orders of magnitude, much greater than the range in the calibration lavas, only alters the one bar temperature by 88°C. Wood concluded therefore that temperatures derived by the Powell and Powell technique are virtually independent of K, but that K depends primarily on the aluminium content at M1 sites in the clinopyroxene. Further, all 1 bar temperature estimates should fall within the very small temperature range of 915-1060°C. Only 3 of 62

temperatures, at 1 bar, given by Powell and Powell (1974) fall outside this range, while all the lherzolite nodules discussed by Wood (1976) had temperatures, at 1 bar, in the middle of the calibration range, 1010-1017^{o}C.

CHAPTER 6. Summary

6.1. The ophiolite sequence

The field relationships, petrography, geochemistry and phase chemistry of the peridotite-gabbro-basalt sequence of the Khawr Fakkan-Wadi Shi-Wadi Madha area suggest that the various components are genetically related. They result from partial melting of the upper mantle, followed by fractional crystallisation of the basic magma generated by this process. The rocks comprise a typical ophiolite sequence and are similar to assemblages from other Alpine-type ultramafic complexes.

The area studied may be broadly subdivided into two major zones. In the west the rocks are principally tectonised ultramafics, while to the east of these a series of cumulate gabbros, with dolerite dykes particularly prevelant in the east, passes upwards into basaltic lavas. The latter are only exposed in the extreme coastal region. The tectonised ultramafics are separated from the gabbroic and basaltic rocks by an easterly-dipping thrust-fault zone, which strikes approximately north-south. At no point was a normal passage from ultramafic rocks to cumulate gabbros observed. Furthermore, the thrust-fault zone is invariably intensely serpentinised and heavily impregnated with magnesite in veins and pockets. The area can thus be

conveniently subdivided by this fault.

6.2. The area to the west of the major thrust fault

The rock types exposed in this area are harzburgites, dunites and wehrlites. They are all, to some extent, serpentinised. Those exposed in the north are principally harzburgites, although a discrete area of tectonised dunite occurs to the east of the main fault. This block is fault-bounded and probably owes its present position to thrusting.

In the southern part of the area the principal rock types are dunites and wehrlites. The two are intimately associated, and form a banded sequence. The strike of the banding is approximately north-northeast and thus oblique to the main thrust-fault.

The harzburgites have an intensely tectonised fabric with large elongate olivine showing strain and domain extinction. They consist of an assemblage of highly refractory chemistry, with a whole-rock MgOx100/(MgO+FeO) ratio of 90.5 and an Mgx100/(Mg+Fe) ratio of 91.0 in the olivines. Whole-rock NiO levels vary from 0.29 to 0.30 percent, while the olivines contain from 0.24 to 0.46 percent NiO. The high NiO contents of the olivines in the harzburgites are consistent with their residual nature, Ni being partitioned into the solid phase, rather than the liquid, during partial melting. Na_2O, K_2O, CaO and Al_2O_3 are each generally less than 1 percent in content, and

TiO_2 values are low.

The dunites also show a strong tectonic fabric and a total absence of cumulus textures. They have a closely similar bulk chemistry to the harzburgites, with an overall MgOx100/(MgO+FeO) ratio of 91.4 and an identical average Mgx100/(Mg+Fe) ratio of 91.0 in the olivines. Whole-rock NiO levels range from 0.19 to 0.37 percent, while the olivines themselves contain from 0.06 to 0.34 percent NiO.

Textural evidence shows that most of the wehrlites are strongly deformed, with their olivines showing evidence of strain in the form of undulose and zone extinction. The olivines are elongate and have a strong preferred orientation. The whole-rock chemistry of the wehrlites indicates that they are only slightly less magnesium-rich than the harzburgites and dunites. Their whole-rock MgOx100/(MgO+FeO) ratio varies from 88 to 91 and the ratio Mgx100/(Mg+Fe) in the olivines averages 89.3. Whole-rock NiO levels vary from 0.16 to 0.20 percent. The NiO content of olivine from wehrlite varies over a wide range (Fig.5.1), but the NiO versus MgOx100/(MgO+FeO) plot, shown in Fig. 4.10 indicates that the NiO contents of the wehrlites are generally lower than those of either the harzburgites or dunites.

The high, and uniform, NiO content of the harzburgites is consistent with their origin as a refractory residuum

of partial melting. The evidence for a similar origin for the dunite is less certain. A residual origin is perhaps supported by their closely similar whole-rock geochemistry to that of the harzburigtes, MgOx100/(MgO+FeO) ratios being almost identical in the two rock types, and considerably more magnesian than any of the clearly-defined cumulates. More indirectly, their tectonised fabric and absence of cumulate texture could be used as an argument for a residual origin, although it would clearly be possible to thoroughly tectonise a cumulate and obliterate the original fabric.

The whole-rock geochemistry shows that the dunites have higher Cr contents than the harzburgites, but lower Ni contents. As dunites are generally considered to represent the partial melt residue of more intense partial melting than that required to generate harzburgite, their lower Ni contents are anomalous. The more extreme partial melting necessary to produce a dunite residuum should have resulted in more extreme fractionation of Ni into residual olivine.

The wehrlites also have lower Ni contents than the harzburgites, or indeed the dunites, but this could result from less advanced partial melting. These rocks, by definition, contain considerable clinopyroxene, which has high Cr_2O_3 contents, up to 1.5 percent. Partial melting should result in the elimination of clinopyroxene first,

the Cr released in the process possibly being recombined in spinel. Several plots, e.g. Figs. 4.3, 4.4 and 4.5, show that the wehrlites are less refractory than either the harzburgites or dunites, but more refractory than pyrolite. The intimate association of the wehrlite and dunite in the south of the ultramafic area suggests they must have a common origin, indeed, within this area the two rock types appear to grade into each other in places.

The relatively low Ni contents of the dunites remain something of an enigma. Absence of a cumulate texture and presence of a tectonic fabric are not, in themselves, evidence of a residual origin, as indicated above. Generation of large volumes of cumulus olivine could arise by rapid upwards movement of a picritic partial melt - a process which should promote olivine crystallisation and fractionation (O'Hara, 1968). If this is the case, then a cumulus origin must also be postulated for the wehrlites, the banding of these two rock types thus reflecting phase layering which has been partially obliterated by later tectonism.

6.3. The area to the east of the major thrust fault.

6.3.1. Cumulates

The gabbro cumulates to the east of the major thrust-fault form a clearly identifiable unit. Phase-layering is evident within these rocks although individual layers cannot

be traced laterally for more than a few metres. The petrographic criteria used to define the cumulates are those proposed by Wager, Brown and Wadsworth (1960). The cumulus types recognised include olivine pyroxenites, olivine gabbros, norites and hypersthene gabbros, gabbros and anorthosites and leucocratic gabbros. Where transected by faults gabbro mylonites are developed. Cumulus textures include heteradcumulates, adcumulates and mesocumulates.

The rocks have lower Fe/Mg ratios and alkalis than are found in typical basalt fractionation trends of continental layered intrusions. Variation diagrams show that trends in the cumulates are due mainly to the fractionation of various proportions of olivine, orthopyroxene, clinopyroxene and plagioclase. The parent magma for the gabbroic, and basaltic, rocks studied here appears to have been of low-Ti and low-K tholeiitic type. The gabbros, themselves however, are clearly not representative of their liquids but are cumulates formed from the low-pressure crystallisation of (a) olivine (b) olivine and plagioclase (c) olivine, plagioclase and clinopyroxene.

6.3.2. Basaltic rocks

The basaltic rocks occur both as intrusive dolerite dykes and as lava flows, the latter being restricted to the coast and the offshore island of Sirat al Khawr. The basalts are invariably altered, with ferromagnesian minerals

being represented by amphibole in the most part. They are also silicified, with quartz occurring in interstitial patches or pools, into which project fine,lath-shaped plagioclases and needle-like amphiboles.

Evidence for silicification is supported by the high SiO_2 contents, which range up to 60 percent. These values are virtually the levels expected in a dacite, yet no other petrographic or chemical characteristics support differentiation to dacite. The silica content thus probably reflects a net addition. This is born out by the alkali-silica plot, shown in Fig. 4.2. In this diagram the crustal members of the ophiolite suite (gabbros and basaltic rocks) plot below the alkali/sub-alkali field boundary proposed by MacDonald (1968) and also below the calc-alkaline/tholeiitic field boundary of Kuno (1968). They thus possess tholeiitic characteristics. The high SiO_2 bearing members, however, do not have the correspondingly high alkalis expected had they resulted from fractional crystallisation alone. Further evidence for metasomatism may be deduced from Fig. 4.12. This figure shows that both basalts and gabbros are within the field of low-K tholeiite, but that Sr contents are distinctly lower in the basalts than the gabbros. Although this distribution may result from Sr depletion with differentiation, Sr being concentrated into cumulus plagioclases, it could also be

partly due to mobilisation of Sr from the basalts during metasomatism and alteration.

6.4. Primary, mantle-derived, liquids and magma evolution.

Figs. 4.3, 4.4 and 4.5 are plots of major-element oxides against MgO, and show a clear separation between the ultramafic rocks, dunite, harzburgite and wehrlite, and the cumulate gabbros and basaltic rocks. The composition of pyrolite is also shown in the figures.

The evolution of the liquid phase is only shown by the fine grain-size basaltic rocks, although even these are probably modified by subsequent silicification. The gabbro compositions are clearly controlled by the relative proportions of the cumulate minerals olivine, pyroxene and plagioclase, and thus the basalts cannot represent direct partial melts from the upper mantle, but rather have evolved through the crustal process of fractional crystallisation.

An estimate of the composition of the partial-melt magma can be made by back-extrapolating the line of liquid descent shown by the basaltic rocks, the line of plagioclase fractionation (towards, or from, anorthosite), and a line joining the cluster of harzburgite and dunite plots, at a point representing a mixture of 9 parts olivine to 1 part orthopyroxene, and pyrolite. The point of intersection of these trend lines gives an estimate of partial melt

composition, and suggests a ratio of liquid to refractory residuum of about 1 to 3. A large number of the gabbro analyses cluster around this point, suggesting the possibility that they lie near the cotectic.

The remaining gabbros have plots which are clearly influenced by the dominant cumulus minerals. Olivine and pyroxene-rich cumulates show an increase in MgO, and decrease in SiO_2 and CaO, relative to the partial-melt magma. Plagioclase enrichment is shown by the trend towards anorthosite.

The line of liquid descent is reflected by the fairly smooth curve through the fine-grained rocks in both figures 4.3 and 4.5. These show that both SiO_2 and CaO increase as MgO decreases. This would normally result from fractionation which principally involves ferromagnesian minerals such as olivine and orthopyroxene. Although Al_2O_3 increases into the fine-grained basaltic rocks, the variation is not as systematic and probably reflects the ubiquitous presence of feldspar.

FeO increases with decreasing MgO from the tectonised ultramafics to the gabbros. The most pronounced increase, however, is in the basaltic rocks. Fractionation of olivine and pyroxene would account for depletion of MgO relative to FeO, and iron enrichment in the basalts is doubtless due to this effect, and to the crystallisation of magnetite.

The relatively high ferric iron contents of the harzburgites and dunites, when compared to the cumulate gabbros and the basalts, is probably related to release of magnetite during serpentinisation of olivine, together with the presence of considerable spinel.

A selection of analyses have been plotted in CMAS projections, following O'Hara (1968). Fig. 6.1 shows that many gabbros lie near the 1 atmosphere cotectic and that the basaltic rocks lie along the control line for advanced partial melting. This control line passes through the dunites and harzburgites, and also through garnet lherzolite (Ito and Kennedy, 1967), below the orthopyroxene-clinopyroxene-plagioclase piercing point. The clustering of basalt points suggests that olivine fractionation was important in controlling their composition. The position of the 30kb cotectic in relation to the plot for garnet lherzolite, shown in Fig. 6.2, suggests that the residue of partial melting would be a harzburgite. The position of the wehrlites, in this figure, indicates that they fall on a single control line relative to the gabbros and dunites, although the harzburgites lie slightly off this line. The basaltic rocks plot near the 1 atmosphere cotectic, but lie exclusively to the orthopyroxene side of the orthopyroxene-olivine boundary confirming their silica over-saturated character. Their plot in this diagram would undoubtedly

Figure 6.1. Projections in the C-M-A-S system of O'Hara (1968), showing compositions of selected peridotites, cumulate gabbros and basaltic rocks projected from, or towards, olivine into the plane CS-MS-A.

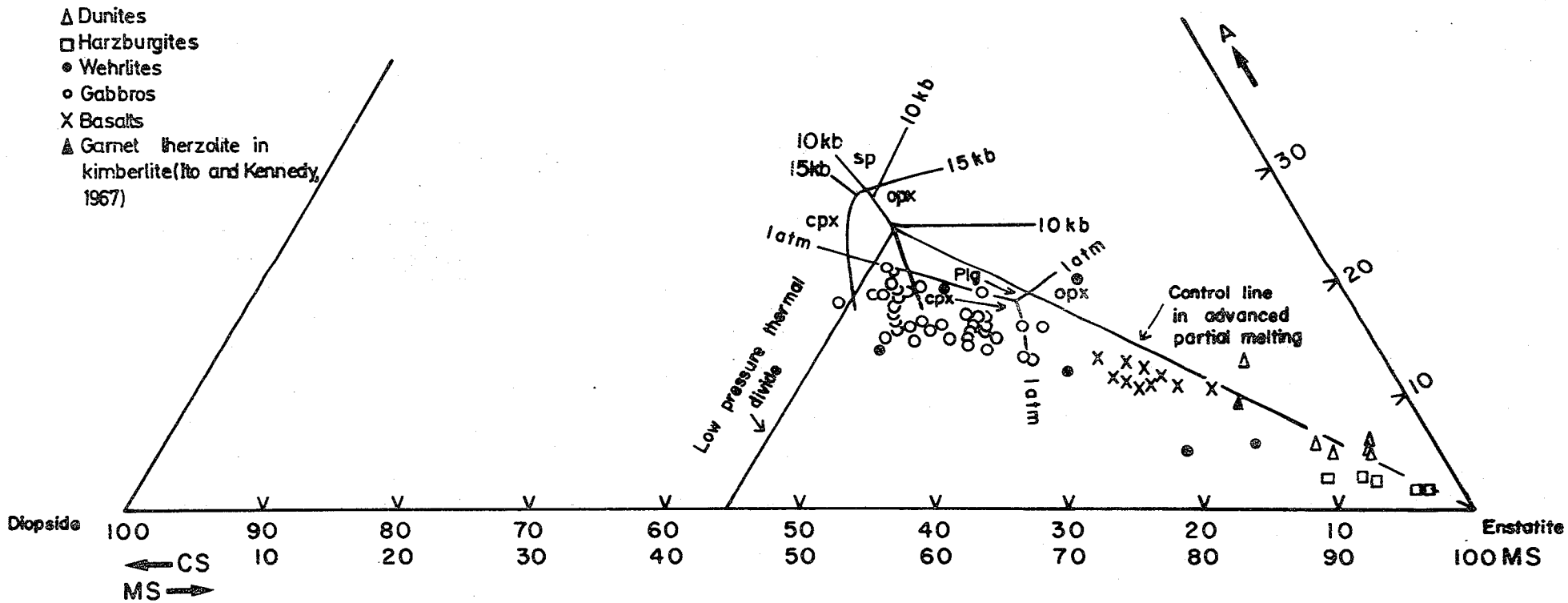
Δ Dunites
□ Harzburgites
● Wehrlites
○ Gabbros
X Basalts
▲ Garnet lherzolite in kimberlite(Ito and Kennedy, 1967)
10kb
15kb
sp
10kb
15kb
opx
cpx
10 kb
1atm
Plg
cpx
opx
1atm
1atm
Low pressure thermal divide
Control line in advanced partial melting
A
30
20
10
Diopside
100
90
80
70
60
50
40
30
20
10
Enstatite
100MS
10
20
30
40
50
60
70
80
90
CS
MS

Figure 6.2. Projections in the C-M-A-S system of O'Hara (1968), showing compositions of selected peridotites, cumulate gabbros and basaltic rocks projected from, or towards, clinopyroxene into the plane C_3A-M-S.

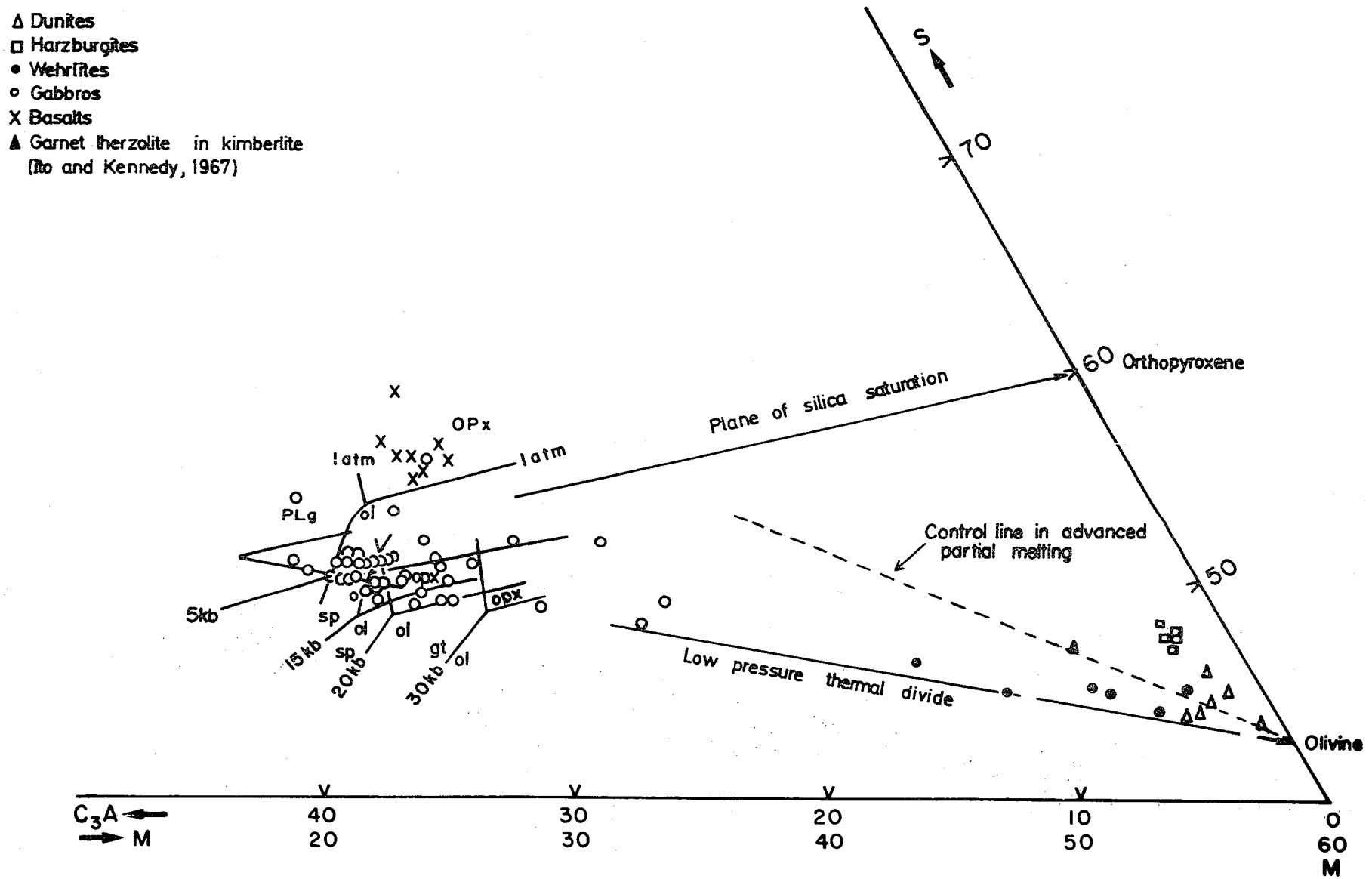
Δ Dunites
□ Harzburgites
• Wehrlites
o Gabbros
X Basalts
▲ Garnet lherzolite in kimberlite (Ito and Kennedy, 1967)
S
70
60
Orthopyroxene
50
Olivine
Plane of silica saturation
Control line in advanced partial melting
Low pressure thermal divide
1atm
1atm
OPx
PLg
ol
5kb
sp
15kb
sp
ol
ol
20kb
gt
ol
30kb
opx
C_3A
M
40
20
30
30
20
40
10
50
0
60
M

be influenced by their silicification, and might thus have little petrogenetic significance

6.5. Pressure-temperature conditions of equilibration.

A variety of methods have been used in an attempt to estimate the equilibration temperatures of the ultramafic rocks and the cumulate gabbros. These techniques include the olivine-spinel geothermometer (Jackson, 1969), the orthopyroxene-clinopyroxene methods of Wood and Banno (1973) and Mysen and Boettcher (1975), the olivine-clinopyroxene geothermometers of Powell and Powell (1974) and Hakli and Wright (1967) and the pressure-temperature grid, based on clinopyroxene chemistry, developed by O'Hara (1967).

Application of all, or most, of these techniques to each investigated sample would provide an ideal basis for comparison. In many instances, however, this did not prove possible for a variety of reasons.

The method most widely applicable to the tectonised ultramafic rocks was the olivine-spinel geothermometer. This gave values for dunite of 872 to 1075°C, for harzburgite of 1099 to 1167°C, for a wehrlite of 1104°C and for the rare rock-type plagioclase peridotite, the somewhat higher value of 1263°C. An olivine pyroxenite cumulate rock gave a temperature of 879°C. The olivine-clinopyroxene geothermometer of Powell and Powell (1974)

produced the extremely narrow temperature range of 1019-1048°C. Reasons for this have been extensively discussed above, in Chapter 5, section 5.9.6.

Hakli and Wright (1967) also used the mineral pair olivine-clinopyroxene, their method depending on the partitioning of Ni between co-existing olivine and clinopyroxene. The method was subject to some limitations, principally in the gabbros where some of the clinopyroxenes are totally depleted in Ni. Harzburgite clinopyroxenes are also usually badly altered and, further, are considered to represent crystallisation of residual dregs of trapped liquid. Equilibration with olivine, in harzburgite, may thus be at a lower temperature than that indicated by the olivine-spinel geothermometer of Jackson (1969). Despite this the overall range indicated for the harzburgites is greater by the Hakli and Wright method, 994-1330°C, than by the olivine-spinel method. In cumulate rocks the technique must also be used carefully in order to avoid any clinopyroxene resulting from exsolution. Temperatures derived using such clinopyroxene would clearly relate to subsolidus reactions. This might also apply to the plagioclase peridotite which gave a value of 972°C, almost 300°C lower than the temperature derived from the olivine-spinel geothermometer. Temperature ranges for the cumulates, of 911-1369°C for pyroxenites, and 849-1291°C

for gabbros and norites, again show a large temperature range with some unusually high values.

The orthopyroxene-clinopyroxene method of Wood and Banno (1973) is obviously subject to the same considerations as those given above regarding the origins of the clinopyroxene in the various rocks. In harzburgite the range of 909-989°C is much lower than that given by other techniques and may thus reflect the late, lower temperature, crystallisation of clinopyroxene from trapped liquid. Temperatures for the cumulate pyroxenites of 927-974°C and for gabbros and norites of 839-999°C are similar to the lower end of the ranges given by the techniques of Mysen and Boettcher (1975) and Hakli and Wright (1967). It is interesting to note that they show similarity to the temperature recorded by this technique for harzburgite. Again, in rocks with pyroxene exsolution, care must be taken that the temperature recorded is not that related to this subsolidus event.

The two pyroxene method of Mysen and Boettcher (1975) gives temperatures in the range 978-1088°C for harzburgite, 985-1168°C for cumulate pyroxenites and 729 to 1118°C for gabbros and norites. The method is limited in the gabbros because $X_{Cr}^{opx} = 0$ in some of these rocks.

Temperature and pressure estimates made using the grid developed by O'Hara (1967) indicate that the harzburgites

equilibrated at temperatures in the range 950 to 1250°C, the wehrlites from 1050 to 1250°C and the olivine pyroxenites at 1020°C. In all cases pressures were less than 7kb and correspond to a depth of about 22km in the oceanic setting. As this technique is applied to clinopyroxene only, the values recorded for harzburgite may thus only refer to equilibration during crystallisation of the trapped liquid at a late stage. Gabbros investigated by the technique of O'Hara (1967) indicate equilibration pressures in the range 5 to 10kb - the results are thus far from conclusive.

TABLE 4-1 ULTRAMAFIC MAJORS TRACES AND NORMS, NORM FE AS FEO

	Δ300	Δ304	Δ305	•312	Δ313	Δ314	•315	Δ316	•319	□324
PERCENT										
SIO2	41.26	41.57	42.71	40.93	41.67	41.94	42.23	40.70	41.92	45.20
AL2O3	0.30	0.52	0.46	3.57	0.35	0.66	5.86	0.47	0.63	0.76
FE2O3	4.86	5.47	5.28	5.84	5.61	7.01	5.07	5.94	7.55	4.90
FEO	5.00	4.80	3.95	5.75	4.08	3.67	3.61	4.84	4.35	4.09
MGO	47.62	46.25	46.42	39.42	46.95	45.78	39.46	46.99	43.23	43.58
CAO	0.13	0.39	0.26	3.10	0.52	0.23	2.74	0.23	1.38	0.72
NA2O	0.02	0.04	0.04	0.02	0.02	0.03	0.19	0.03	0.02	0.03
K2O	0.02	0.02	0.02	0.05	0.02	0.02	0.02	0.02	0.02	0.02
TIO2	0.04	0.04	0.04	0.05	0.04	0.05	0.05	0.04	0.05	0.04
MNO	0.15	0.16	0.15	0.18	0.15	0.17	0.13	0.17	0.17	0.14
S	–	0.21	0.19	–	–	–	0.14	–	0.13	0.10
P2O5	0.07	0.06	0.06	0.07	0.15	0.06	0.06	0.06	0.07	–
CR2O3	0.51	0.62	0.55	0.49	0.46	0.95	0.37	0.64	0.59	0.43
NIO	0.19	0.30	0.24	0.20	0.27	0.23	0.19	0.21	0.16	0.30
PPM										
CR	3510	4239	3779	3350	3183	6543	2557	4423	4082	2948
NI	1530	2417	1950	1586	2151	1880	1518	1703	1260	2372
CU	1	5	–	23	–	73	20	27	125	–
CIPW NORM										
OR	0.10	0.10	0.10	0.30	0.10	0.10	0.10	0.10	0.10	0.10
AB	0.20	0.30	0.30	0.20	0.20	0.30	1.00	0.30	0.20	0.30
AN	0.20	1.20	0.90	10.60	0.80	0.70	13.10	0.70	1.60	1.90
DI	–	0.10	–	3.40	0.60	–	–	–	3.70	1.30
HY	14.50	17.70	22.70	13.30	17.30	23.50	18.30	14.10	23.10	34.50
OL	76.80	71.10	66.90	62.80	71.70	63.40	57.60	75.00	59.00	53.90
MT	7.00	7.90	7.60	8.50	8.10	10.10	7.30	8.60	10.90	7.10
CM	0.70	0.90	0.80	0.70	0.70	1.40	0.50	0.90	0.90	0.60
IL	0.10	0.10	0.10	0.10	0.10	0.10	0.10	0.10	0.10	0.10
AP	0.20	0.10	0.10	0.20	0.40	0.10	0.20	0.10	0.20	–

Δ DUNITES
□ HARZBURGITES
• WEHRLITES

TABLE 41 ULTRAMAFIC MAJORS TRACES AND NORMS, NORM FE AS FEO

	▫ 325	▫ 327	▫ 329	• 502	• 603	• 605	▫ 1031
PERCENT							
SIO2	45.16	45.27	45.90	41.96	42.11	41.94	44.78
AL2O3	0.53	0.91	0.81	0.53	3.13	2.66	0.95
FE2O3	5.05	4.09	3.12	5.07	4.84	4.93	3.81
FEO	3.51	4.91	5.48	4.66	5.06	5.42	4.92
MGO	44.74	42.89	43.23	45.59	39.25	41.62	43.47
CAO	0.35	1.11	0.53	0.78	4.68	2.50	1.26
NA2O	0.03	0.02	0.03	0.03	0.04	0.01	0.04
K2O	0.02	0.02	0.01	0.02	0.02	0.02	0.02
TIO2	0.04	0.04	0.04	0.04	0.06	0.05	0.04
MNO	0.13	0.14	0.12	0.16	0.16	0.17	0.14
S	–	–	0.08	–	–	–	–
P2O5	0.06	0.07	0.06	0.07	0.13	0.07	0.06
CR2O3	0.44	0.43	0.45	0.48	0.47	0.48	0.45
NIO	0.30	0.29	0.30	0.19	0.19	0.18	0.29
PPM							
CR	3007	2949	3104	3306	3235	3300	3089
NI	2423	2287	2413	1570	1556	1451	2313
CO	–	3	–	–	84	30	8
CIPW NORM							
OR	0.10	0.10	0.10	0.10	0.10	0.10	0.10
AB	0.30	0.20	0.30	0.30	0.30	0.10	0.30
AN	1.20	2.30	2.00	1.50	8.30	7.20	2.30
DI	0.10	2.10	0.10	1.70	11.00	3.80	2.70
HY	34.90	33.30	36.80	18.80	10.70	16.20	28.80
OL	55.20	55.10	55.40	68.80	61.40	64.60	59.30
MT	7.30	5.90	4.50	8.20	7.00	7.10	5.50
CM	0.60	0.60	0.70	0.70	0.70	0.70	0.70
IL	0.10	0.10	0.10	0.10	0.10	0.10	0.10
AP	0.10	0.20	0.10	0.20	0.30	0.20	0.10

TABLE 4-2 PYROXENITE MAJORS TRACES AND NORMS, NORM FE AS FEO

	1014(3)	1028	1030B	553	554
PERCENT					
SIO2	49.33	51.36	49.32	51.91	51.32
AL2O3	1.77	1.23	0.51	1.11	1.19
FE2O3	1.96	1.09	0.49	0.33	0.77
FEO	4.41	4.01	4.55	4.04	4.26
MGO	26.20	23.94	22.19	23.86	24.32
CAO	15.54	17.65	16.35	18.08	17.36
NA2O	-	-	0.03	-	0.02
K2O	0.01	0.01	0.01	0.01	0.01
TIO2	0.07	0.07	0.07	0.07	0.07
MNO	0.14	0.14	0.14	0.13	0.14
S	-	-	-	-	-
P2O5	0.06	0.06	0.06	0.01	0.06
CR2O3	0.54	0.52	0.40	1.01	0.90
NIO	0.06	0.04	0.03	0.04	0.05
PPM					
BA	6	6	-	20	23
NB	2	-	1	1	3
ZR	-	-	-	-	-
Y	1	-	1	-	1
SR	13	5	21	-	2
RB	-	1	1	-	-
ZN	23	17	21	17	18
CU	701	-	165	-	-
NI	495	350	272	344	358
CR	3717	3577	2745	6879	6170
CIPW NORM					
OR	0.10	0.10	0.10	0.10	0.10
AB	-	-	0.30	-	0.20
AN	4.80	3.30	15.00	3.00	3.10
DI	56.50	65.90	52.40	67.80	64.70
HY	10.20	11.80	10.60	11.10	11.60
OL	24.60	16.30	20.10	16.00	17.60
MT	2.90	1.60	0.70	0.50	1.10
CM	0.80	0.80	0.60	1.50	1.30
IL	0.10	0.10	0.10	0.10	0.10
AP	0.10	0.10	0.10	-	0.10

TABLE 4-3 GABBRO MAJORS TRACES AND NORMS, NORM FE AS FEO

	104A	131	134	139	146	150	151	152	156(1)	173
PERCENT										
SIO2	49.80	47.77	47.71	47.31	47.21	48.34	50.99	48.74	48.20	48.56
AL2O3	17.14	15.19	17.09	17.51	18.71	16.26	15.32	15.22	16.85	17.07
FE2O3	1.85	1.30	1.79	1.69	2.04	1.46	2.30	1.57	1.82	1.06
FEO	3.67	6.14	5.64	6.13	5.62	5.48	0.43	4.65	4.82	5.23
MGO	8.21	9.29	11.23	10.41	8.99	11.56	4.01	13.31	10.93	12.80
CAO	16.62	17.88	15.28	15.61	16.22	15.73	25.24	15.51	16.36	14.20
NA2O	1.79	0.25	0.19	0.20	0.14	0.12	0.24	0.08	0.19	0.20
K2O	0.02	0.02	0.01	0.01	0.02	0.02	0.02	0.01	0.01	0.01
TIO2	0.24	0.16	0.13	0.13	0.11	0.11	0.15	0.11	0.09	0.07
MNO	0.16	0.16	0.14	0.16	0.13	0.15	-	0.13	0.14	0.14
S	0.01	0.01	0.01	0.01	0.02	0.01	0.01	0.01	-	-
P2O5	0.15	0.14	0.14	0.14	0.15	0.14	0.25	0.13	0.05	0.05
CR2O3	0.04	0.12	0.04	0.14	0.01	0.03	-	0.04	0.02	0.04
NIO	-	-	0.01	-	0.01	0.01	-	0.01	0.01	0.01
PPM										
BA	-	27	52	38	35	-	-	25	3	12
NB	1	1	2	1	1	1	1	1	2	1
ZR	19	4	6	9	6	10	7	1	1	4
Y	7	2	1	4	3	3	2	2	1	-
SR	179	68	91	97	71	123	104	55	62	53
RB	1	-	-	-	-	-	-	-	-	1
ZN	18	10	30	34	23	27	-	23	25	25
CU	19	341	159	42	106	234	-	-	495	64
NI	46	62	87	29	114	84	-	79	67	81
CR	252	826	269	99	118	86	55	245	156	297
CIPW NORM										
QTZ	-	-	-	-	0.90	0.20	7.00	-	0.20	-
OR	0.10	0.10	0.10	0.10	0.10	0.10	0.10	0.10	0.10	0.10
AB	15.20	2.10	1.60	1.70	1.20	1.00	2.00	0.70	1.60	1.70
AN	38.80	43.20	46.00	47.10	50.70	44.00	40.70	41.30	45.30	45.90
DI	34.20	36.30	23.50	24.00	23.60	26.80	21.50	27.90	28.70	19.60
WO	-	-	-	-	-	-	25.10	-	-	-
HY	5.30	14.20	24.90	22.50	19.90	25.10	-	26.50	21.20	25.90
OL	2.80	1.20	0.70	1.30	-	-	-	0.60	-	1.90
MT	2.70	1.90	2.60	2.50	3.00	2.20	0.90	2.30	2.70	1.60
CM	0.10	0.20	0.10	0.20	-	-	-	0.10	-	0.10
IL	0.50	0.30	0.20	0.20	0.20	0.20	0.30	0.20	0.20	0.10
AP	0.40	0.30	0.30	0.30	0.40	0.30	0.60	0.30	0.10	0.10

TABLE 4-3 GABBRO MAJORS TRACES AND NORMS, NORM FE AS FEO

	175	180
PERCENT		
SIO2	47.66	49.10
AL2O3	14.30	11.21
FE2O3	1.97	2.08
FEO	5.39	7.24
MGO	11.97	16.08
CAO	17.10	12.89
NA2O	0.62	0.23
K2O	-	0.01
TIO2	0.20	0.12
MNO	0.14	0.19
S	-	-
P2O5	0.05	0.05
CR2O3	0.11	0.20
NIO	0.01	0.02
PPM		
BA	25	32
NB	1	1
ZR	8	2
Y	7	3
SR	98	52
RB	-	-
ZN	25	43
CU	75	57
NI	107	173
CR	801	1426
CIPW NORM		
QTZ	-	-
OR	-	0.10
AB	5.30	2.00
AN	36.40	29.70
DI	38.70	27.40
WO	-	-
HY	7.10	33.00
OL	9.00	4.20
MT	2.90	3.00
CM	0.20	0.30
IL	0.40	0.20
AP	0.10	0.10

TABLE 4.3 GABBRO MAJORS TRACES AND NORMS, NORM FE AS FEO

	183	190	200	209	211	221	223	231	232	500
PERCENT										
SIO2	49.87	47.48	44.88	50.62	54.23	48.51	48.10	47.15	46.91	44.43
AL2O3	6.30	13.54	13.92	8.18	15.86	16.87	15.82	19.48	19.49	12.79
FE2O3	2.46	2.41	2.44	1.64	1.66	1.70	1.77	2.03	1.22	2.62
FEO	7.68	5.06	8.83	4.61	3.86	5.26	6.52	3.35	3.16	4.32
MGO	17.79	14.36	14.09	16.21	5.94	9.57	10.80	10.16	11.60	21.79
CAO	14.54	15.40	13.97	17.79	16.29	16.96	15.74	16.03	16.30	12.58
NA2O	0.09	0.65	0.48	0.12	1.19	0.24	0.19	1.12	0.70	0.39
K2O	-	0.01	-	0.01	0.03	-	-	0.01	0.01	-
TIO2	0.16	0.32	0.17	0.13	0.37	0.10	0.11	0.14	0.13	0.10
MNO	0.21	0.14	0.20	0.14	0.10	0.15	0.16	0.08	0.07	0.12
S	-	-	-	-	-	-	-	-	-	0.11
P2O5	0.05	0.05	0.07	0.06	0.07	0.06	0.05	0.06	0.05	0.05
CR2O3	0.23	0.13	0.03	0.33	0.03	0.03	0.03	0.03	0.13	0.35
NIO	0.02	0.02	0.01	0.02	-	-	0.01	-	0.03	0.07
PPM										
BA	36	21	31	24	13	35	-	-	-	30
NB	1	1	2	2	2	2	2	2	1	1
ZR	5	9	6	3	24	6	1	16	9	8
Y	6	5	3	1	7	1	-	3	3	3
SR	67	109	76	24	188	78	49	146	91	89
RB	1	-	1	2	1	1	-	1	1	-
ZN	43	32	41	25	22	24	31	14	20	31
CU	51	113	114	169	9	-	326	13	84	109
NI	178	214	136	177	34	39	61	93	249	591
CR	1582	881	216	2315	196	204	218	248	905	2395
CIPW NORM										
QTZ	-	-	-	-	10.50	1.30	0.10	-	-	-
OR	-	0.10	-	0.10	0.20	-	-	0.10	0.10	-
AB	0.80	5.50	4.10	1.00	10.10	2.00	1.60	9.50	5.90	3.30
AN	16.90	34.10	36.20	21.60	38.00	45.20	42.60	48.30	50.10	33.20
DI	44.20	33.50	26.80	52.40	34.20	31.30	28.70	24.70	24.20	22.60
HY	29.30	10.70	7.80	18.80	3.70	17.30	24.00	4.20	5.60	3.50
OL	4.50	11.60	21.00	2.70	-	-	-	9.90	11.80	32.10
MT	3.60	3.50	3.60	2.40	2.40	2.50	2.60	3.00	1.80	4.10
CM	0.30	0.20	-	0.50	-	-	-	-	0.20	0.50
IL	0.30	0.60	0.30	0.20	0.70	0.20	0.20	0.30	0.20	0.20
AP	0.10	0.10	0.20	0.10	0.20	0.10	0.10	0.10	0.10	0.10

TABLE 4-3 GABBRO MAJORS TRACES AND NORMS, NORM FE AS FEO

	523	526A	868	869	871	1014(1)	1017	1029(1)	1033
PERCENT									
SIO2	42.08	47.53	48.14	48.59	48.30	49.11	49.29	47.59	47.57
AL2O3	14.67	11.38	15.07	15.23	14.20	18.49	16.06	15.95	15.55
FE2O3	5.62	3.68	0.85	2.43	1.30	0.81	0.46	1.20	1.23
FEO	8.10	6.21	3.54	7.23	4.81	3.73	3.71	6.24	5.69
MGO	18.82	12.08	15.38	11.92	13.49	8.61	12.72	11.41	12.43
CAO	8.77	15.99	15.88	13.01	16.65	18.12	16.88	15.21	15.47
NA2O	0.70	0.48	0.50	0.38	0.40	0.47	0.21	1.30	1.04
K2O	-	0.01	0.01	0.02	0.02	0.01	0.01	0.01	0.03
TIO2	0.10	0.73	0.11	0.11	0.10	0.07	0.07	0.19	0.19
MNO	0.19	0.19	0.07	0.21	0.12	0.09	0.11	0.13	0.13
S	-	-	-	-	-	-	-	-	-
P2O5	0.08	0.04	0.07	0.07	0.06	0.07	0.06	0.07	0.05
CR2O3	0.01	0.07	0.20	-	0.01	0.03	0.09	0.20	0.08
NIO	0.03	0.01	0.04	-	-	0.01	0.01	0.03	0.03
PPM									
BA	19	40	-	-	5	-	20	-	-
NB	1	1	3	-	2	1	2	-	-
ZR	9	9	11	7	7	4	4	16	14
Y	1	11	3	4	3	2	2	4	3
SR	105	96	111	76	73	87	62	125	114
RB	-	-	-	-	-	1	2	-	-
ZN	58	38	18	54	25	17	16	29	25
CU	50	50	142	41	161	97	172	111	158
NI	267	86	301	19	71	75	89	240	262
CR	85	493	1359	-	77	220	620	1351	556
CIPW NORM									
QTZ	-	-	-	0.90	-	0.90	-	-	-
OR	-	0.10	0.10	0.10	0.10	0.10	0.10	0.10	0.20
AB	6.00	4.10	4.20	3.20	3.40	4.00	1.80	11.10	8.80
AN	37.20	29.00	38.90	40.10	37.10	48.50	43.00	37.80	37.90
DI	4.90	44.20	31.20	19.70	36.20	33.00	32.20	30.10	31.10
HY	13.00	12.90	9.90	32.00	12.10	12.00	19.00	2.80	4.20
OL	30.30	2.70	13.70	-	8.80	-	2.80	15.60	15.40
MT	8.20	5.40	1.20	3.60	1.90	1.20	0.70	1.70	1.80
CM	-	0.10	0.30	-	-	-	0.10	0.30	0.10
IL	0.20	1.40	0.20	0.20	0.20	0.10	0.10	0.40	0.40
AP	0.20	0.10	0.20	0.20	0.10	0.20	0.10	0.20	0.10

TABLE 4.3 GABBRO MAJORS TRACES AND NORMS, NORM FE AS FEO

	526B	539	541	544	552	555	556	557	850	852
PERCENT										
SIO2	44.27	47.25	44.93	49.78	47.11	46.92	47.04	48.54	47.13	47.99
AL2O3	14.26	7.13	16.[illegible]	15.71	16.41	16.51	15.70	15.42	17.62	16.91
FE2O3	1.68	2.14	1.1[illegible]	0.41	1.64	1.32	1.17	1.12	1.54	0.96
FEO	10.42	5.15	2.97	3.39	6.63	6.48	5.64	5.43	5.36	5.53
MGO	13.22	22.04	17.41	12.49	11.69	11.62	12.21	10.62	11.42	12.14
CAO	13.48	15.56	16.73	17.43	15.13	14.47	15.53	16.73	14.73	15.30
NA2O	0.80	0.08	0.11	0.18	0.52	1.37	1.09	1.13	1.24	0.26
K2O	-	-	0.01	0.01	0.02	0.01	0.01	0.01	0.01	0.01
TIO2	0.45	0.08	0.07	0.07	0.10	0.18	0.19	0.22	0.17	0.06
MNO	0.20	0.15	0.08	0.10	0.16	0.13	0.12	0.12	0.12	0.13
S	-	-	-	-	-	-	-	-	-	-
P2O5	0.05	0.06	0.06	0.07	0.07	0.07	0.07	0.07	0.07	0.07
CR2O3	0.05	0.39	0.19	0.15	-	0.18	0.10	0.06	0.05	0.04
NIO	0.01	0.04	0.03	0.01	-	0.03	0.02	0.02	0.01	0.01
PPM										
BA	12	8	-	23	17	18	23	21	1	10
NB	1	1	2	2	1	2	1	1	1	2
ZR	11	1	4	4	7	13	12	14	14	2
Y	4	3	-	2	3	2	5	5	4	1
SR	101	23	69	34	101	124	106	125	133	56
RB	-	2	-	-	2	-	1	-	-	-
ZN	50	32	9	15	34	29	23	22	23	28
CU	31	101	2	172	68	106	136	142	-	61
NI	108	306	223	113	60	232	162	125	112	82
CR	332	2692	1308	1002	37	1199	703	429	379	276
CIPW NORM										
QTZ	-	-	-	-	-	-	-	-	-	-
OR	-	-	-	0.10	0.10	0.10	0.10	0.10	0.10	0.10
AB	6.80	0.70	-	1.50	2.70	11.70	9.30	9.60	10.50	2.20
AN	35.80	19.10	43.70	42.10	45.60	39.10	38.10	37.20	42.70	45.20
NE	-	-	0.50	-	-	-	-	-	-	-
DI	25.60	44.80	27.90	34.90	25.40	26.20	31.10	36.70	24.20	24.50
HY	1.60	5.90	-	19.70	18.50	1.30	4.10	4.50	4.70	21.20
OL	26.70	24.50	24.60	0.60	7.00	19.00	15.00	9.70	15.00	5.00
CA-OR	-	-	1.10	-	-	-	-	-	-	-
MT	2.50	3.10	1.70	0.60	2.40	1.90	1.70	1.60	2.20	1.40
CM	0.10	0.60	0.30	0.20	-	0.30	0.10	0.10	0.10	0.10
IL	0.90	0.20	0.10	0.10	0.20	0.30	0.40	0.40	0.30	0.20
AP	0.10	0.10	0.10	0.20	0.20	0.20	0.20	0.20	0.20	0.20

TABLE 4.4 BASALT- DOLERITE MAJORS TRACES AND NORMS, NORM FE AS FEO

	101	122	140	154	159	162A	162B	856	864	866
PERCENT										
SIO2	55.88	52.14	59.89	57.34	54.20	55.75	54.93	54.30	53.94	54.75
AL2O3	14.07	13.66	11.62	12.67	12.06	11.21	10.51	13.18	12.80	11.53
FE2O3	3.30	2.30	3.05	2.28	4.03	2.30	2.12	2.74	2.88	2.55
FEO	7.75	8.02	6.51	7.65	7.22	7.25	7.21	7.86	7.06	7.36
MGO	6.63	8.97	4.50	6.25	9.47	9.26	10.67	7.98	9.19	9.41
CAO	6.51	12.56	9.44	11.44	12.68	12.08	12.75	11.70	11.84	12.36
NA2O	4.24	0.59	1.13	0.78	0.60	0.66	0.39	0.68	0.80	0.52
K2O	0.04	0.04	0.16	0.12	0.06	0.07	0.05	0.08	0.06	0.07
TIO2	0.48	0.28	0.41	0.30	0.24	0.28	0.26	0.27	0.29	0.30
MNO	0.18	0.18	0.19	0.17	0.18	0.19	0.18	0.19	0.19	0.18
S	0.01	-	-	0.01	0.01	0.01	-	-	0.01	-
P2O5	0.16	0.14	0.13	0.14	0.14	0.14	0.13	0.14	0.14	0.14
CR2O3	-	0.01	-	-	0.05	0.08	0.09	0.01	0.04	0.06
NIO	-	-	-	-	-	-	0.01	0.01	0.01	-
PPM										
BA	9	40	48	19	35	30	12	26	31	38
NB	5	4	5	4	4	4	5	5	6	6
ZR	26	12	21	14	10	10	8	13	12	9
Y	14	6	11	84	5	7	5	8	8	7
SR	87	72	74	195	61	51	62	64	71	44
RB	1	-	3	1	2	-	-	-	-	2
ZN	92	57	95	80	73	70	64	73	64	67
CU	134	162	25	19	122	58	139	196	133	123
NI	16	56	3	16	55	58	62	44	51	56
CR	25	112	17	27	370	579	659	100	303	417
CIPW NORM										
QTZ	5.30	8.60	24.80	19.00	11.80	14.20	12.20	13.40	11.40	13.10
OR	0.20	0.20	1.00	0.70	0.50	0.40	0.30	0.50	0.50	0.40
AB	36.10	5.00	9.70	6.70	5.00	5.60	3.30	5.80	6.80	4.40
AN	19.40	35.40	26.40	31.00	29.70	27.60	27.00	33.00	31.30	29.10
DI	9.90	21.60	16.80	20.80	25.50	25.70	28.90	20.10	21.70	25.70
HY	22.90	24.80	15.90	17.60	20.80	22.00	24.20	22.40	23.10	22.40
MT	4.80	3.40	4.50	3.30	5.80	3.40	3.10	4.00	4.20	3.70
CM	-	-	-	-	0.10	0.10	0.10	-	0.10	0.10
IL	0.90	0.50	0.80	0.60	0.50	0.50	0.50	0.50	0.60	0.60
AP	0.40	0.30	0.30	0.30	0.30	0.30	0.30	0.30	0.30	0.30

TABLE 44 BASALT- DOLERITE MAJORS TRACES AND NORMS, NORM FE AS FEO

	1004	196
PERCENT		
SIO2	56.42	47.36
AL2O3	13.06	16.26
FE2O3	2.35	3.43
FEO	7.55	8.02
MGO	7.00	6.03
CAO	10.99	13.95
NA2O	1.03	1.09
K2O	0.07	0.03
TIO2	0.35	0.69
MNO	0.18	0.18
S	0.01	-
P2O5	0.15	0.06
CR2O3	0.02	0.01
NIO	-	-
PPM		
BA	232	29
NB	4	2
ZR	22	10
Y	11	5
SR	106	115
RB	-	-
ZN	89	61
CU	208	-
NI	26	-
CR	162	76
CIPW NORM		
QTZ	16.30	2.30
CR	0.40	0.20
AB	8.80	9.30
AN	31.00	45.20
DI	18.70	19.80
HY	20.20	15.60
MT	3.40	5.00
CM	-	-
IL	0.70	1.30
AP	0.40	0.10

TABLE 45 DUNITE MAJORS TRACES AND NORMS

	300	301	302	303	304	305	306	307	308	309
PERCENT										
SIO2	41.26	41.24	42.16	42.35	41.57	42.71	42.75	42.39	42.40	43.25
AL2O3	0.30	0.39	0.44	0.26	0.52	0.46	0.32	0.38	0.21	0.26
FE2O3	10.42	10.32	9.15	9.59	10.81	9.68	9.08	9.68	10.33	9.36
MGO	47.62	47.47	47.65	47.32	46.25	46.42	47.34	47.05	46.28	46.59
CAO	0.13	0.30	0.35	0.22	0.35	0.26	0.24	0.24	0.51	0.31
NA2O	0.02	0.02	0.03	0.03	0.04	0.04	0.02	0.04	0.02	0.02
K2O	0.02	0.02	0.02	0.02	0.02	0.02	0.02	0.02	0.02	0.02
TIO2	0.04	0.04	0.04	0.04	0.04	0.04	0.04	0.04	0.04	0.04
MNO	0.15	0.15	0.14	0.14	0.16	0.15	0.14	0.15	0.15	0.14
S	-	-	-	-	0.21	0.19	-	-	-	-
P2O5	0.07	0.07	0.06	0.07	0.06	-	0.06	0.06	0.06	0.03
CR2O3	0.51	0.42	0.74	0.48	0.62	0.55	0.60	0.61	0.49	0.40
NIO	0.19	0.22	0.37	0.30	0.30	0.24	0.33	0.33	0.19	0.33
PPM										
CR	3510	2900	5060	3337	4239	3779	4158	4193	3385	2766
NI	1530	1736	2939	2415	2417	1950	2631	2616	1506	2602
CO	1	-	-	-	5	-	-	-	-	-
CIPW NORM										
OR	0.10	0.10	0.10	0.10	0.10	0.10	0.10	0.10	0.10	0.10
AB	0.20	0.20	0.30	0.30	0.30	0.30	0.20	0.30	0.20	0.20
AN	0.20	0.90	1.00	0.50	1.20	1.00	0.70	0.80	0.40	0.80
DI	-	0.10	0.30	0.10	0.10	0.20	0.10	-	1.40	0.60
HY	7.00	5.20	9.50	11.50	9.30	14.20	13.30	11.70	12.20	16.00
OL	90.10	90.50	86.40	85.40	86.10	81.70	83.40	84.70	83.50	80.70
MT	1.30	1.20	1.10	1.10	1.30	1.20	1.10	1.20	1.20	1.10
CM	0.80	0.60	1.10	0.70	0.90	0.80	0.90	0.90	0.70	0.60
IL	0.10	0.10	0.10	0.10	0.10	0.10	0.10	0.10	0.10	0.10
AP	0.20	0.20	0.10	0.20	0.10	-	0.10	0.10	0.10	0.10

TABLE 4.5 DUNITE MAJORS TRACES AND NORMS

	310	311	313	314	316	317	320	321	322	517
PERCENT										
SIO2	41.46	41.21	41.67	41.94	40.70	41.64	41.25	41.40	41.04	41.68
AL2O3	0.69	0.40	0.35	0.66	0.47	0.56	0.52	0.35	0.56	0.53
FE2O3	11.24	11.22	10.15	11.09	11.32	9.91	11.48	12.08	11.98	10.58
MGO	45.50	46.09	46.95	45.78	46.99	45.98	45.74	45.69	45.99	46.00
CAO	0.64	0.20	0.52	0.23	0.23	1.42	0.72	0.19	0.14	0.95
NA2O	0.01	0.04	0.02	0.03	0.03	0.01	0.03	0.02	0.02	0.03
K2O	0.02	0.02	0.02	0.02	0.02	-	0.02	0.02	0.02	0.02
TIO2	0.04	0.04	0.04	0.05	0.04	0.05	0.04	0.04	0.05	0.04
MNO	0.17	0.16	0.15	0.17	0.17	0.15	0.17	0.16	0.17	0.16
S	0.16	-	-	-	-	0.20	-	-	-	-
P2O5	0.07	0.07	0.15	0.06	0.06	0.07	0.06	0.06	0.06	0.04
CR2O3	0.57	0.45	0.46	0.95	0.64	0.40	0.59	0.29	0.89	0.72
NIO	0.20	0.19	0.27	0.23	0.21	0.25	0.21	0.15	0.28	0.18
PPM										
CR	3927	3019	3183	6543	4423	2750	4052	2018	6104	4896
NI	1616	1537	2151	1860	1703	1988	1699	1252	2243	1449
CU	33	58	-	73	27	10	74	19	64	-
CIPW NORM										
OR	0.10	0.10	0.10	0.10	0.10	-	0.10	0.10	0.10	0.10
AB	0.10	0.30	0.20	0.30	0.30	0.10	0.30	0.20	0.20	0.30
AN	1.60	0.50	0.80	0.70	0.80	1.50	1.20	0.60	0.30	1.30
DI	0.70	-	0.60	-	-	4.00	1.50	-	-	2.50
HY	9.20	7.40	8.50	12.50	4.70	6.10	6.70	10.00	8.60	7.20
OL	85.30	89.20	87.40	83.10	91.50	85.90	87.70	86.90	87.40	86.10
MT	1.30	1.30	1.20	1.30	1.40	1.20	1.40	1.50	1.40	1.50
CM	0.80	0.70	0.70	1.40	0.90	0.60	0.90	0.40	1.30	1.10
IL	0.10	0.10	0.10	0.10	0.10	0.10	0.10	0.10	0.10	0.10
AP	0.20	0.20	0.40	0.10	0.10	0.20	0.10	0.10	0.10	0.10

TABLE 4:5 DUNITE MAJORS TRACES AND NORMS

	528	531	538	545	546	800	801	808	809	817
PERCENT										
SIO2	41.32	41.12	43.38	41.63	41.86	42.62	41.63	41.11	40.68	42.01
AL2O3	0.39	0.33	0.49	0.56	0.26	0.48	0.51	0.40	0.46	0.49
FE2O3	10.67	12.04	10.95	10.44	10.14	10.37	10.27	11.31	11.36	11.14
MGO	46.94	45.94	44.69	46.58	47.25	45.59	47.03	46.71	46.96	45.81
CAO	0.28	0.14	0.15	0.37	0.09	0.66	0.29	0.21	0.22	0.48
NA2O	0.03	0.03	0.02	0.04	0.03	–	0.02	0.04	0.03	0.02
K2O	0.02	0.02	0.02	0.02	0.02	0.02	0.02	0.02	0.02	0.02
TIO2	0.04	0.04	0.04	0.04	0.04	0.04	0.04	0.04	0.04	0.04
MNO	0.16	0.16	0.16	0.16	0.15	0.15	0.15	0.15	0.16	0.15
S	0.13	0.16	–	0.10	0.13	–	–	–	–	–
P2O5	0.06	0.05	0.12	0.10	0.06	0.07	0.06	0.06	0.09	0.05
CR2O3	0.61	0.80	0.41	1.04	0.58	0.67	0.67	0.50	0.53	1.05
NIO	0.26	0.17	0.20	0.21	0.21	0.28	0.27	0.33	0.21	0.19
PPM										
CR	4220	5480	2840	7140	3994	4603	4635	3462	3679	7178
NI	2054	1397	1551	1619	1675	2266	2124	2614	1689	1494
CU	–	8	12	–	2	–	–	393	49	27
CIPW NORM										
OR	0.10	0.10	0.10	0.10	0.10	0.10	0.10	0.10	0.10	0.10
AB	0.30	0.30	0.20	0.30	0.30	–	0.20	0.30	0.30	0.20
AN	0.90	0.40	–	1.20	0.10	1.30	1.00	0.70	0.50	1.20
DI	0.10	–	–	–	–	1.20	–	–	–	0.70
HY	7.50	9.00	21.50	9.50	10.50	14.00	8.70	6.60	5.00	11.80
OL	88.60	87.00	75.50	85.60	86.30	80.90	87.50	89.90	91.50	82.90
MT	1.30	1.40	1.30	1.20	1.20	1.20	1.20	1.40	1.40	1.30
CM	0.90	1.20	0.60	1.50	0.90	1.00	1.00	0.70	0.80	1.50
IL	0.10	0.10	0.10	0.10	0.10	0.10	0.10	0.10	0.10	0.10
AP	0.10	0.10	0.30	0.20	0.10	0.20	0.10	0.10	0.20	0.10

TABLE 4.5 DUNITE MAJORS TRACES AND NORMS

	820	821	823	825	829	830	831	836	1019	1020
PERCENT										
SIO2	41.44	42.11	41.57	41.38	41.54	41.66	42.47	41.25	41.67	42.33
AL2O3	0.28	0.50	0.42	0.32	0.43	0.51	0.48	0.58	0.57	0.32
FE2O3	10.18	9.86	10.74	10.44	10.55	10.83	10.56	10.85	10.26	10.24
MGO	47.67	45.99	46.83	47.41	46.86	46.54	45.79	46.54	46.83	45.69
CAO	0.16	0.25	0.18	0.18	0.34	0.17	0.38	0.53	0.35	0.16
NA2O	0.03	0.03	0.03	0.02	0.03	0.03	0.03	0.03	0.03	0.03
K2O	0.01	0.02	0.01	0.02	0.02	0.02	0.02	0.02	0.01	0.02
TIO2	0.04	0.04	0.04	0.04	0.04	0.04	0.04	0.04	0.04	0.04
MNO	0.15	0.15	0.15	0.16	0.16	0.16	0.15	0.16	0.15	0.15
S	-	-	-	-	-	-	-	-	-	-
P2O5	0.06	0.07	0.06	0.07	0.06	0.07	0.10	0.03	0.06	0.06
CR2O3	0.64	0.65	0.60	0.45	0.65	0.69	0.55	0.74	1.33	0.47
NIO	0.21	0.31	0.26	0.22	0.27	0.17	0.25	0.18	0.19	0.20
PPM										
CR	4400	4500	4120	3083	4500	4735	3820	5073	9137	3224
NI	1648	2441	2055	1794	2133	1403	1959	1461	1535	1654
CU	-	-	-	-	-	-	-	-	-	-
CIPW NORM										
OR	0.10	0.10	0.10	0.10	0.10	0.10	0.10	0.10	0.10	0.10
AB	0.30	0.30	0.30	0.20	0.30	0.30	0.30	0.30	0.30	0.30
AN	0.40	0.80	0.50	0.40	1.00	0.40	1.10	1.40	1.30	0.40
DI	-	-	-	-	0.20	-	0.10	0.80	-	-
HY	7.50	11.00	9.20	7.50	8.00	10.40	14.00	6.30	9.20	12.70
OL	89.40	85.30	87.40	89.50	87.90	86.00	82.10	88.60	85.70	84.20
MT	1.20	1.20	1.30	1.30	1.30	1.30	1.30	1.30	1.20	1.20
CM	0.90	1.00	0.90	0.70	1.00	1.00	0.80	1.10	1.90	0.70
IL	0.10	0.10	0.10	0.10	0.10	0.10	0.10	0.10	0.10	0.10
AP	0.10	0.20	0.10	0.20	0.10	0.20	0.20	0.10	0.10	0.10

TABLE 4.5 DUNITE MAJORS TRACES AND NORMS

	1036
PERCENT	
SIO2	40.93
AL2O3	0.60
FE2O3	11.73
MGO	46.20
CAO	0.22
NA2O	0.02
K2O	0.01
TIO2	0.04
MNO	0.16
S	-
P2O5	0.10
CR2O3	0.69
NIO	0.27
PPM	
CR	4755
NI	2141
CU	65
CIPW NORM	
OR	0.10
AB	0.20
AN	0.40
DI	-
HY	7.80
OL	88.40
MT	1.40
CM	1.00
IL	0.10
AP	0.20

TABLE 4.6 HARZBURGITE MAJORS TRACES AND NORMS

	323	324	325	326	327	328	329	550	822	1031
PERCENT										
SIO2	45.87	45.20	45.18	46.46	45.27	46.30	45.90	45.26	44.14	44.78
AL2O3	1.19	0.76	0.53	0.99	0.91	0.97	0.81	0.86	0.57	0.95
FE2O3	8.29	9.45	8.95	9.09	9.55	9.05	9.21	9.36	9.12	9.26
MGO	44.12	43.58	44.74	42.70	42.89	42.09	43.23	43.27	45.34	43.47
CAO	0.29	0.72	0.35	0.51	1.11	0.59	0.53	0.90	0.44	1.26
NA2O	0.04	0.03	0.03	0.03	0.02	0.03	0.03	0.01	0.13	0.04
K2O	0.02	0.02	0.02	0.02	0.02	0.02	0.01	0.02	0.02	0.02
TIO2	0.04	0.04	0.04	0.04	0.04	0.04	0.04	0.04	0.04	0.04
MNO	0.12	0.14	0.13	0.13	0.14	0.14	0.12	0.14	0.13	0.14
S	-	0.10	-	-	-	-	0.08	0.07	-	-
P2O5	0.06	-	0.06	0.06	0.07	0.21	0.06	0.06	0.07	0.06
CR2O3	0.49	0.43	0.44	0.36	0.43	0.39	0.45	0.40	0.39	0.45
NIO	0.31	0.30	0.30	0.30	0.29	0.29	0.30	0.29	0.30	0.29
PPM										
CR	3357	2948	3007	2466	2949	2718	3104	2800	2690	3089
NI	2444	2372	2423	2386	2287	2287	2413	2296	2420	2313
CU	7	-	-	-	3	-	-	5	-	8
CIPW NORM										
OR	0.10	0.10	0.10	0.10	0.10	0.10	0.10	0.10	0.10	0.10
AB	0.30	0.30	0.30	0.30	0.20	0.30	0.30	0.10	1.10	0.30
AN	1.00	1.90	1.30	2.10	2.30	1.60	2.00	2.20	0.90	2.40
DI	-	1.30	0.10	-	2.10	-	0.20	1.40	0.60	2.80
HY	32.30	27.40	27.40	35.70	27.60	36.10	32.50	28.10	19.80	23.40
OL	63.60	67.00	68.90	59.80	65.80	59.40	62.90	65.90	75.50	69.10
MT	1.00	1.10	1.10	1.10	1.10	1.10	1.10	1.10	1.10	1.10
CM	0.70	0.60	0.60	0.50	0.60	0.60	0.70	0.60	0.60	0.70
IL	0.10	0.10	0.10	0.10	0.10	0.10	0.10	0.10	0.10	0.10
AP	0.10	-	0.10	0.10	0.20	0.50	0.10	0.10	0.20	0.10

TABLE 4·6 HARZBURGITE MAJORS TRACES AND NORMS

	1035(1)	1035(2)	1037	1038	1039	1040	1041	1042	1043	1044
PERCENT										
SIO2	45.10	44.71	47.18	45.05	44.23	46.79	44.19	45.50	45.13	45.33
AL2O3	0.79	0.91	1.44	1.01	0.60	0.87	0.80	0.73	0.74	0.46
FE2O3	9.27	9.30	8.56	9.25	9.08	9.30	9.62	9.70	9.71	9.26
MGO	43.92	43.96	42.14	43.68	45.52	41.98	43.90	43.15	43.37	44.15
CAO	0.64	0.86	0.44	0.75	0.34	0.82	1.15	0.67	0.71	0.56
NA2O	0.03	0.02	0.04	0.03	0.02	0.03	0.03	–	–	–
K2O	0.02	0.02	0.02	0.02	0.02	0.02	0.02	–	–	–
TIO2	0.04	0.04	0.04	0.04	0.04	0.04	0.04	0.04	0.04	0.04
MNO	0.13	0.13	0.12	0.14	0.13	0.13	0.14	0.13	0.13	0.13
S	–	–	–	–	–	–	–	–	0.10	–
P2O5	0.09	0.06	0.06	0.06	0.05	0.06	0.14	0.07	0.07	0.05
CR2O3	0.35	0.43	0.39	0.52	0.40	0.47	0.40	0.44	0.45	0.37
NIO	0.29	0.30	0.30	0.28	0.30	0.29	0.29	0.31	0.31	0.30
PPM										
CR	2424	2939	2700	3553	2774	3218	2741	3013	2937	2502
NI	2317	2392	2372	2258	2419	2302	2306	2454	2440	2366
CU	–	–	3	–	4	10	6	7	–	2
CIPW NORM										
OR	0.10	0.10	0.10	0.10	0.10	0.10	0.10	–	–	–
AB	0.30	0.20	0.30	0.30	0.20	0.30	0.30	–	–	–
AN	2.00	2.30	1.80	2.60	1.40	2.20	2.00	2.00	2.00	1.30
DI	0.50	1.20	–	0.60	–	1.20	2.20	0.70	0.80	0.90
HY	27.30	24.40	40.50	20.80	22.20	36.80	21.40	30.70	28.80	26.70
OL	66.00	69.70	54.70	67.60	74.30	57.40	71.90	64.50	66.10	67.20
MT	1.10	1.10	1.00	1.10	1.10	1.10	1.20	1.20	1.20	1.10
CM	0.50	0.60	0.60	0.80	0.60	0.70	0.60	0.60	0.60	0.50
IL	0.10	0.10	0.10	0.10	0.10	0.10	0.10	0.10	0.10	0.10
AP	0.20	0.10	0.10	0.10	0.10	0.10	0.30	0.20	0.20	0.10

TABLE 4-7 WEHRLITE MAJORS TRACES AND NORMS

	312	315	318	319	502	503	504	515	527	532
PERCENT										
SIO2	40.93	42.23	42.46	41.92	41.96	42.48	42.38	41.55	44.44	44.81
AL2O3	3.97	5.66	1.08	0.63	0.53	0.64	0.75	1.07	0.69	2.12
FE2O3	12.21	9.09	11.01	12.39	10.85	9.92	10.68	11.54	10.26	8.82
MGO	39.42	39.46	40.39	43.23	45.59	43.94	45.23	44.91	43.24	39.96
CAO	3.10	2.74	4.47	1.38	0.78	2.74	0.68	0.63	1.08	3.96
NA2O	0.02	0.19	0.04	0.02	0.03	0.04	0.05	0.02	0.02	0.04
K2O	0.05	0.02	0.02	0.02	0.02	0.02	0.02	0.02	0.02	0.02
TIO2	0.05	0.05	0.07	0.05	0.04	0.05	0.04	0.04	0.05	0.07
MNO	0.18	0.13	0.21	0.17	0.16	0.14	0.15	0.17	0.15	0.12
S	-	0.14	0.16	0.13	-	-	-	-	-	0.05
P2O5	0.07	0.08	0.13	0.07	0.07	0.07	0.07	0.06	0.07	0.07
CR2O3	0.49	0.37	0.67	0.59	0.48	0.36	0.75	0.42	1.13	0.54
NIO	0.20	0.19	0.15	0.16	0.19	0.17	0.19	0.22	0.34	0.15
PPM										
CR	3350	2557	4648	4082	3306	2455	5166	2896	7735	3756
NI	1586	1518	1253	1260	1570	1334	1503	1744	2675	1227
CU	25	20	702	125	-	-	-	109	3527	61
CIPW NORM										
OR	0.30	0.10	0.10	0.10	0.10	0.10	0.10	0.10	0.10	0.10
AB	0.20	1.60	0.30	0.20	0.30	0.30	0.40	0.20	0.20	0.30
AN	10.60	13.10	2.70	1.60	1.30	1.50	1.80	2.70	1.70	5.60
DI	3.40	-	14.70	3.80	1.70	9.20	0.90	-	2.50	10.80
HY	4.20	10.40	4.50	11.20	10.00	5.90	12.60	9.90	23.60	17.30
OL	78.80	71.80	74.60	80.20	84.40	81.00	81.50	84.90	68.70	63.70
MT	1.50	1.10	1.30	1.50	1.30	1.20	1.30	1.40	1.20	1.10
CM	0.70	0.50	1.00	0.90	0.70	0.50	1.10	0.60	1.70	0.80
IL	0.10	0.10	0.10	0.10	0.10	0.10	0.10	0.10	0.10	0.10
AP	0.20	0.20	0.30	0.20	0.20	0.20	0.20	0.10	0.20	0.20

TABLE 4-7 WEHRLITE MAJORS TRACES AND NORMS

	537	802	803	804	805	806	807	810	811	812
PERCENT										
SIO2	46.65	47.71	42.11	42.82	41.94	41.20	41.54	42.20	45.24	41.31
AL2O3	0.68	2.02	3.13	1.99	2.66	2.54	0.57	0.50	1.60	0.42
FE2O3	7.26	5.19	10.47	9.66	10.96	12.26	10.34	10.89	7.59	11.29
MGO	43.91	29.91	39.25	39.24	41.62	41.79	44.79	45.56	35.52	43.61
CAO	1.04	14.61	4.68	5.96	2.50	1.87	2.45	0.54	9.73	3.11
NA2O	0.02	0.07	0.04	0.03	0.01	0.04	0.04	0.02	0.02	0.02
K2O	0.02	0.03	0.02	0.02	0.02	0.02	0.02	0.01	0.02	0.02
TIO2	0.04	0.10	0.06	0.07	0.05	0.05	0.06	0.04	0.06	0.04
MNO	0.13	0.11	0.16	0.15	0.17	0.18	0.16	0.16	0.14	0.12
S	–	–	–	–	–	–	–	–	–	–
P2O5	0.06	0.05	0.13	0.07	0.07	0.07	0.07	0.08	0.07	0.07
CR2O3	0.47	0.86	0.47	0.46	0.48	0.52	0.66	0.60	0.51	0.40
NIO	0.17	0.18	0.19	0.19	0.18	0.21	0.21	0.22	0.12	0.19
PPM										
CR	3235	5012	3235	3200	3300	3600	4540	4150	3506	2736
NI	1392	1399	1556	1516	1451	1676	1690	1730	980	1516
CU	485	472	84	220	30	26	54	65	231	211
CIPW NORM										
OR	0.10	–	0.10	0.10	0.10	0.10	0.10	0.10	0.10	–
AB	0.20	–	0.30	0.30	0.10	0.30	0.30	0.20	0.20	–
AN	2.30	5.10	8.30	5.20	7.20	6.70	1.30	1.20	4.20	1.00
DI	2.00	50.80	11.10	18.90	3.80	1.70	8.20	0.70	34.40	11.10
HY	32.50	–	3.20	0.40	8.70	7.20	1.60	12.50	0.50	–
OL	61.20	40.50	74.50	72.90	77.90	81.40	85.60	82.80	58.60	85.50
MT	0.90	0.60	1.30	1.20	1.30	1.50	1.20	1.30	0.90	1.40
CM	0.70	1.30	0.70	0.70	0.70	0.80	1.00	0.90	0.80	0.60
IL	0.10	0.20	0.10	0.10	0.10	0.10	0.10	0.10	0.20	0.10
AP	0.10	0.10	0.30	0.20	0.20	0.20	0.20	0.20	0.20	0.20

TABLE 4.7 WEHRLITE MAJORS TRACES AND NORMS

	852	634
PERCENT		
SIO2	42.87	41.67
AL2O3	0.62	0.63
FE2O3	11.51	11.52
MGO	41.77	44.74
CAO	2.72	1.13
NA2O	0.03	0.02
K2O	0.01	0.02
TIO2	0.07	0.05
MNO	0.15	0.17
S	–	–
P2O5	0.07	0.06
CR2O3	0.25	0.33
NIO	0.16	0.16
PPM		
CR	1705	2275
NI	1245	1283
CU	129	28
CIPW NORM		
OR	0.10	0.10
AB	0.30	0.20
AN	2.10	1.60
DI	8.70	2.90
HY	11.30	8.40
OL	75.50	84.70
MT	1.40	1.40
CM	0.40	0.50
IL	0.10	0.10
AP	0.20	0.10

TABLE 4-8 PYROXENITE MAJORS TRACES AND NORMS

	553	554	1024	1030B	1014(3)	1027	1028	1013	1029(3)	1030C
PERCENT										
SIO2	51.91	51.32	46.01	49.32	49.33	50.96	51.36	47.71	46.14	43.38
AL2O3	1.11	1.19	9.46	5.51	1.77	1.35	1.23	6.71	8.89	11.59
FE2O3	4.82	5.51	6.05	6.32	6.88	5.18	5.55	6.46	4.72	7.89
MGO	23.86	24.32	23.01	22.19	26.20	24.61	23.94	23.55	22.57	22.85
CAO	18.08	17.36	15.20	16.35	15.54	17.64	17.65	15.30	17.45	13.96
NA2O	–	0.02	–	0.03	–	–	–	0.02	–	0.03
K2O	0.01	0.01	0.01	0.01	0.01	0.01	0.01	0.01	0.01	0.01
TIO2	0.07	0.07	0.06	0.07	0.07	0.08	0.07	0.06	0.06	0.07
MNO	0.13	0.14	0.12	0.14	0.14	0.13	0.14	0.12	0.09	0.16
S	–	–	–	–	–	–	–	–	–	–
P2O5	0.01	0.06	0.06	0.06	0.06	0.06	0.06	0.07	0.06	0.07
PPM										
BA	20	23	63	–	6	–	6	–	–	–
NB	1	3	1	1	2	3	–	2	–	–
ZR	–	–	2	–	–	–	–	–	1	1
Y	–	1	2	1	1	3	–	–	1	1
SR	–	2	34	21	13	6	5	26	16	40
RB	–	–	–	1	–	1	1	–	–	1
ZN	17	18	9	21	23	18	17	21	16	21
CU	–	–	64	165	701	–	–	135	234	–
NI	344	358	334	272	495	374	350	371	305	284
CR	6879	6170	2230	2745	3717	3792	3577	2930	2254	170
CIPW NORM										
QR	0.10	0.10	0.10	0.10	0.10	0.10	0.10	0.10	–	–
AB	–	0.20	–	0.30	–	–	–	0.20	–	–
AN	3.00	3.10	25.90	14.90	4.80	3.70	3.30	18.30	24.30	31.70
NE	–	–	–	–	–	–	–	–	–	0.10
DI	68.30	65.30	39.00	52.20	57.00	65.90	66.30	45.40	39.90	24.20
HY	11.00	12.00	0.50	10.90	9.00	8.90	11.80	6.60	–	–
OL	15.10	17.40	32.40	19.40	26.80	19.50	16.60	27.20	30.50	39.00
CA-OR	–	–	–	–	–	–	–	–	3.50	2.10
MT	1.50	1.70	1.90	2.00	2.10	1.60	1.70	2.00	1.50	2.40
IL	0.10	0.10	0.10	0.10	0.10	0.20	0.10	0.10	0.10	0.10
AP	–	0.10	0.10	0.10	0.10	0.10	0.10	0.20	0.10	0.27

TABLE 4-9 GABBRO MAJORS TRACES AND NORMS

	115	177	551	837	1025	516
PERCENT						
SIO2	50.44	49.35	47.67	46.99	47.57	48.66
AL2O3	9.90	11.70	13.25	13.70	12.91	9.77
FE2O3	8.86	6.92	10.99	5.23	10.96	6.24
MGO	14.71	15.56	11.03	15.09	11.24	18.95
CAO	14.96	17.27	15.60	16.03	16.17	15.97
NA2O	0.60	0.66	0.52	0.53	0.39	0.12
K2O	0.03	0.05	0.09	0.02	0.06	0.03
TIO2	0.24	0.23	0.37	0.17	0.36	0.11
MNO	0.13	0.12	0.14	0.09	0.14	0.11
S	0.01	0.01	0.01	0.01	0.01	-
P2O5	0.13	0.14	0.14	0.14	0.13	0.05
PPM						
BA	8	8	6	7	20	-
NB	6	5	5	4	3	-
ZR	8	14	25	10	20	-
Y	4	5	10	3	9	-
SR	70	154	158	122	137	-
RB	-	1	2	-	1	-
ZN	22	20	84	17	41	-
CU	-	7	-	14	-	-
NI	190	167	44	299	33	149
CR	1495	1421	153	2917	104	165
CIPW NORM						
QTZ	-	-	-	-	-	-
OR	0.20	0.20	0.50	0.10	0.50	0.20
AB	5.10	5.60	4.40	1.90	3.30	1.00
AN	24.40	29.00	33.80	35.10	33.50	26.20
NE	-	-	-	1.40	-	-
DI	39.50	44.70	34.90	42.50	37.50	42.10
HY	25.70	10.30	16.70	-	16.70	11.50
OL	1.60	7.20	3.10	16.70	4.00	17.90
MT	2.70	2.10	3.40	1.60	3.40	0.80
IL	0.50	0.40	0.70	0.30	0.70	0.20
AP	0.30	0.30	0.30	0.20	0.30	0.10

TABLE 4-9 GABBRO MAJORS TRACES AND NORMS

	124	151	1003	1006	1017	1022	1030A	1048	118	127
PERCENT										
SIO2	51.78	50.99	49.96	48.41	49.29	47.05	46.88	46.57	51.53	46.21
AL2O3	17.06	15.32	13.63	16.12	16.06	14.70	18.75	14.38	13.42	17.16
FE2O3	3.15	2.76	4.07	7.30	4.56	3.69	3.46	9.64	2.60	6.61
MGO	3.56	4.01	12.35	12.85	12.72	16.92	14.06	13.51	8.24	11.56
CAO	23.44	26.24	19.04	14.64	16.66	17.08	15.73	14.35	21.71	15.65
NA2O	0.63	0.24	0.50	0.29	0.21	0.14	0.27	0.96	1.16	0.16
K2O	0.02	0.02	0.01	0.01	0.01	0.01	0.02	0.03	0.03	0.02
TIO2	0.12	0.15	0.09	0.09	0.07	0.06	0.05	0.26	1.27	0.10
MNO	0.01	–	0.09	0.14	0.11	0.08	0.07	0.16	0.01	0.12
S	0.01	0.01	–	–	–	–	–	0.01	0.01	0.01
P2O5	0.19	0.25	0.06	0.07	0.06	0.07	0.07	0.14	–	0.15
PPM										
BA	–	–	22	49	20	13	–	–	–	25
NB	1	1	2	1	2	2	–	1	3	2
ZR	9	7	4	8	2	4	8	14	85	4
Y	2	2	3	2	2	1	–	6	29	2
SR	130	104	69	97	62	57	72	115	291	67
RB	1	–	–	–	2	–	3	–	–	1
ZN	1	–	13	33	16	11	9	35	–	26
CU	12	–	141	60	172	67	–	119	–	115
NI	–	–	111	81	89	242	74	124	37	46
CR	8	55	1136	227	620	1715	773	560	87	225
CIPW NORM										
QTZ	6.90	5.70	–	–	–	–	–	–	1.90	–
OR	0.10	0.10	0.10	0.10	0.10	0.10	0.10	0.20	0.20	0.10
AB	5.30	2.00	4.20	2.50	1.60	1.20	2.30	8.20	10.00	1.50
AN	43.80	40.70	35.00	42.90	43.00	39.60	50.00	35.10	31.30	40.30
NE	–	–	–	–	–	–	–	–	–	–
DI	25.50	27.00	46.90	23.70	32.20	35.40	21.90	28.60	45.90	24.70
WO	16.60	22.70	–	–	–	–	–	–	7.50	–
HY	–	–	8.30	25.60	19.90	3.50	9.80	6.60	–	24.30
OL	–	–	3.90	2.70	1.40	18.80	14.50	17.60	–	0.50
MT	1.00	0.90	1.50	2.30	1.40	1.20	1.10	3.00	0.80	2.10
IL	0.20	0.30	0.20	0.20	0.10	0.10	0.10	0.50	2.40	0.20
AP	0.50	0.60	0.10	0.20	0.10	0.20	0.20	0.30	–	0.30

TABLE 4-9 GABBRO MAJORS TRACES AND NORMS

	138	141	145	166	179	182	852	865	1005	1011
PERCENT										
SIO2	47.88	47.81	47.64	48.35	50.65	49.07	47.99	48.60	49.40	49.74
AL2O3	16.73	13.73	17.47	16.44	14.20	14.36	16.91	16.02	13.58	11.63
FE2O3	7.66	9.53	8.30	7.39	4.18	6.62	7.11	5.70	6.10	8.55
MGO	12.20	11.66	9.72	11.76	10.66	13.72	12.14	11.54	13.13	15.94
CAO	14.98	16.44	16.16	15.48	19.70	15.75	15.30	15.54	17.30	15.72
NA2O	0.12	0.16	0.16	0.28	0.36	0.21	0.26	0.33	0.19	0.14
K2O	0.01	0.03	0.02	-	0.01	-	0.01	0.01	0.01	0.01
TIO2	0.11	0.15	0.13	0.10	0.10	0.09	0.08	0.08	0.10	0.06
MNO	0.15	0.17	0.15	0.14	0.07	0.14	0.13	0.12	0.13	0.15
S	0.01	0.01	0.01	-	-	-	-	-	-	-
P2O5	0.14	0.14	0.14	0.05	0.05	0.05	0.07	0.07	0.06	0.06
PPM										
BA	31	18	16	-	-	19	10	-	138	3
NB	1	2	1	-	4	1	2	2	2	2
ZR	2	1	4	2	9	2	2	5	5	4
Y	-	2	3	3	1	2	1	1	1	1
SR	59	49	57	70	131	51	56	72	79	43
RB	-	2	-	1	1	-	1	1	-	-
ZN	28	36	29	27	5	22	28	22	20	[illegible]
CU	187	134	43	139	-	93	61	5	101	60
NI	55	68	35	50	71	179	82	45	86	159
CR	196	145	85	70	771	1182	276	151	682	962
CIPW NORM										
WTZ	-	-	0.50	-	1.40	-	-	-	-	-
OR	0.10	0.20	0.10	-	0.10	-	0.10	0.10	0.10	0.10
AB	1.00	1.40	2.50	2.40	3.20	1.80	2.20	2.80	1.60	1.20
AN	45.40	30.90	47.10	43.90	37.10	38.40	45.20	47.90	36.30	31.20
NE	-	-	-	-	-	-	-	-	-	-
DI	22.80	35.60	26.30	26.40	48.00	31.60	24.50	23.10	39.30	37.10
HY	26.40	19.40	21.30	23.30	8.60	23.60	22.10	23.10	16.60	25.60
OL	1.50	3.00	-	1.50	-	2.80	3.40	0.90	1.80	4.40
MT	2.40	3.00	2.60	2.30	1.30	2.10	2.20	1.80	1.90	2.60
IL	0.20	0.30	0.20	0.20	0.20	0.20	0.20	0.20	0.20	0.20
AP	0.30	0.30	0.30	0.10	0.10	0.10	0.20	0.20	0.10	0.10

TABLE 4-9 GABBRO MAJORS TRACES AND NORMS

	156(1)	156(2)	157	181	197	198	201	222	543	544
PERCENT										
SIO2	48.20	47.66	48.53	48.93	47.27	47.26	48.37	48.65	48.63	49.76
AL2O3	16.85	17.35	17.80	10.59	17.41	15.62	14.66	14.93	14.85	15.71
FE2O3	7.16	5.95	6.02	10.44	11.07	12.54	9.92	8.69	4.91	4.18
MGO	10.93	12.82	9.19	15.33	9.06	9.11	10.86	10.70	14.73	12.49
CAO	16.30	15.83	16.04	14.23	13.64	14.65	15.53	16.53	16.51	17.43
NA2O	0.19	0.14	0.18	0.09	0.37	0.39	0.30	0.16	0.15	0.18
K2O	0.01	–	–	0.01	–	–	–	–	–	0.01
TIO2	0.09	0.07	0.08	0.13	0.13	0.15	0.13	0.11	0.07	0.07
MNO	0.14	0.12	0.12	0.20	0.20	0.23	0.19	0.17	0.10	0.09
S	–	–	–	–	–	–	–	–	–	–
P2O5	0.05	0.05	0.05	0.05	0.05	0.05	0.05	0.05	0.05	0.07
PPM										
BA	3	5	7	55	3	2	–	44	21	23
NB	2	1	2	–	–	2	2	2	1	2
ZR	1	3	3	4	3	6	10	2	3	4
Y	1	2	5	3	1	3	5	1	1	2
SR	62	55	64	54	64	76	68	53	54	34
RB	–	–	–	–	2	–	–	1	–	–
ZN	25	24	18	45	62	73	48	30	11	15
CU	495	37	426	81	13	50	93	–	125	172
NI	67	164	101	127	34	72	78	57	96	115
CR	156	2256	130	1103	163	412	295	272	651	1062
CIPW NORM										
QTZ	–	–	1.10	–	0.30	0.50	0.40	1.00	–	0.30
OR	0.10	–	–	0.10	–	–	–	–	–	0.10
AB	1.60	1.20	1.50	0.80	3.20	3.30	2.60	1.40	1.10	1.50
AN	45.40	46.90	48.00	28.70	46.20	41.30	39.00	40.30	40.10	42.20
NE	–	–	–	–	–	–	–	–	–	–
DI	28.70	25.10	33.30	33.70	18.40	25.90	30.90	33.70	33.00	34.90
HY	21.30	18.80	14.00	30.00	26.10	24.70	23.60	20.60	16.90	19.50
OL	0.40	5.90	–	3.10	–	–	–	–	7.10	–
MT	2.20	1.80	1.90	3.20	3.40	3.90	3.10	2.70	1.50	1.80
IL	0.20	0.10	0.20	0.20	0.20	0.30	0.20	0.20	0.10	0.10
AP	0.10	0.10	0.10	0.10	0.10	0.10	0.10	0.10	0.10	0.20

TABLE 4-9 GABBRO MAJORS TRACES AND NORMS

	173	175	208	209	210	211	212	213	214	215
PERCENT										
SIO2	48.56	47.66	50.17	50.62	50.13	54.23	48.18	49.84	47.84	48.14
AL2O3	17.07	14.30	11.80	8.18	12.11	15.86	13.49	14.83	16.40	15.19
FE2O3	6.90	7.96	5.29	6.76	6.78	5.95	9.67	5.70	9.38	9.61
MGO	12.80	11.97	14.97	16.21	14.58	5.94	12.54	11.41	10.45	11.62
CAO	14.20	17.10	16.36	17.79	15.84	16.29	15.17	17.49	15.33	14.63
NA2O	0.20	0.62	0.22	0.12	0.36	1.19	0.42	0.46	0.25	0.26
K2O	0.01	-	0.01	0.01	-	0.03	0.01	0.01	-	-
TIO2	0.07	0.20	0.12	0.13	0.05	0.37	0.12	0.09	0.11	0.12
MNO	0.14	0.14	0.12	0.14	0.11	0.10	0.14	0.11	0.17	0.16
S	-	-	-	-	-	-	-	-	0.02	-
P2O5	0.05	0.05	0.06	0.06	0.06	0.07	0.06	0.06	0.06	0.06
PPM										
BA	12	25	39	24	22	13	-	8	16	17
NB	1	1	2	2	2	2	1	-	3	3
ZR	4	8	3	3	12	24	3	5	3	3
Y	3	7	3	1	-	7	2	2	2	3
SR	53	98	42	24	131	188	75	68	57	51
RB	1	-	-	2	-	1	1	-	-	-
ZN	25	25	16	25	12	22	30	16	40	42
CU	64	75	17	169	-	9	10	4	112	26
NI	81	107	76	177	114	34	143	109	61	65
CR	297	601	818	2315	372	196	569	569	66	60
CIPW NORM										
QTZ	-	-	-	-	-	10.60	-	0.20	0.20	-
OR	0.10	-	0.10	0.10	-	0.20	0.10	0.10	-	-
AB	1.70	5.30	1.90	1.00	3.10	10.10	3.60	3.90	2.10	2.20
AN	45.90	56.50	30.80	21.90	31.60	38.00	35.20	38.50	43.90	40.60
NE	-	-	-	-	-	-	-	-	-	-
DI	19.60	38.80	47.80	52.70	37.30	34.40	32.30	38.30	26.00	26.60
HY	29.50	6.50	14.90	16.30	23.40	4.60	20.80	16.80	24.40	26.70
OL	0.80	10.00	2.60	3.60	2.30	-	4.60	-	-	0.50
MT	2.10	2.50	1.60	2.10	2.10	1.80	3.10	1.80	2.90	3.00
IL	0.10	0.40	0.20	0.20	0.10	0.70	0.20	0.20	0.20	0.20
AP	0.10	0.10	0.10	0.10	0.10	0.20	0.10	0.10	0.10	0.10

TABLE 4-9 GABBRO MAJORS TRACES AND NORMS

	180	102	104A	105	851	853	862	868	869	1012
PERCENT										
SIO2	49.10	46.31	49.60	47.76	46.48	48.45	49.95	48.14	46.59	48.04
AL2O3	11.21	15.53	17.14	14.98	13.26	18.50	15.40	15.07	15.23	18.65
FE2O3	10.13	10.50	5.93	8.57	7.93	5.65	4.26	4.78	10.47	5.71
MGO	16.03	12.30	8.21	11.93	10.93	11.40	11.34	15.38	11.92	13.17
CAO	12.89	13.58	16.62	15.03	17.86	15.55	18.14	15.88	13.01	13.56
NA2O	0.28	1.19	1.79	1.16	0.65	0.19	0.66	0.50	0.38	0.19
K2O	0.01	0.02	0.02	0.03	0.01	0.01	0.03	0.01	0.02	0.01
TIO2	0.12	0.25	0.24	0.26	0.47	0.06	0.06	0.11	0.11	0.07
MNO	0.19	0.17	0.10	0.14	0.14	0.12	0.09	0.07	0.21	0.12
S	-	0.01	0.01	0.01	-	-	-	-	-	-
P2O5	0.05	0.15	0.15	0.14	0.06	0.07	0.06	0.07	0.07	0.07
PPM										
BA	32	-	-	20	14	24	1	-	-	119
NB	1	1	1	1	-	2	2	3	-	-
ZR	2	22	19	18	20	3	14	11	7	11
Y	3	6	7	8	9	-	1	3	4	1
SR	52	178	179	156	157	60	132	111	76	159
RB	-	1	1	2	1	-	1	-	-	-
ZN	43	42	18	32	26	21	9	16	54	20
CU	57	81	19	131	58	233	-	142	41	169
NI	173	141	46	81	90	92	47	301	19	80
CR	1426	266	252	206	594	90	368	1359	-	259
CIPW NORM										
QTZ	-	-	-	-	-	0.10	-	-	0.60	-
OR	0.10	0.10	0.10	0.20	0.10	0.10	0.20	0.10	0.10	0.10
AB	2.00	10.20	15.20	9.90	7.20	1.60	5.60	4.20	3.20	1.60
AN	29.80	37.30	38.90	35.80	32.50	49.80	39.10	39.00	40.10	44.80
NE	-	-	-	-	-	-	-	-	-	-
DI	27.50	24.00	34.40	30.70	45.00	21.60	40.20	31.30	19.70	24.90
HY	33.10	7.00	4.10	7.70	4.90	24.80	11.10	10.20	32.50	23.90
OL	4.10	17.40	4.60	12.30	6.80	-	2.20	13.40	-	2.70
MT	3.10	3.30	1.80	2.70	2.50	1.70	1.30	1.50	3.30	1.80
IL	0.20	0.50	0.50	0.50	0.90	0.10	0.20	0.20	0.20	0.10
AP	0.10	0.30	0.40	0.30	0.10	0.20	0.10	0.20	0.20	0.20

TABLE 4-9 GABBRO MAJORS TRACES AND NORMS

	183	192	231	252	500	510	526B	529	530	534
PERCENT										
SIO2	49.87	50.72	47.15	46.91	44.43	49.02	44.27	46.30	47.34	47.58
AL2O3	6.30	14.93	19.48	19.49	12.79	13.34	14.28	13.34	9.27	14.85
FE2O3	11.00	3.53	5.76	4.73	7.62	5.29	13.26	7.60	5.19	8.60
MGO	17.79	7.46	10.16	11.60	21.79	13.69	15.22	15.57	16.62	12.79
CAO	14.54	22.13	16.03	16.30	12.58	17.61	13.48	16.22	21.11	17.11
NA2O	0.09	0.90	1.12	0.70	0.39	0.55	0.60	0.57	0.10	0.72
K2O	-	-	0.01	0.01	-	0.02	-	0.01	0.10	0.01
TIO2	0.16	0.24	0.14	0.13	0.10	0.13	0.45	0.22	0.15	0.18
MNO	0.21	0.09	0.08	0.07	0.12	0.10	0.20	0.13	0.10	0.11
S	-	-	-	-	0.11	-	-	-	-	-
P2O5	0.05	0.03	0.06	0.05	0.06	0.05	0.05	0.05	0.03	0.07
PPM										
BA	38	-	-	8	30	22	12	26	29	16
NB	1	7	2	4	1	1	1	1	2	2
ZR	5	53	16	7	8	8	11	13	6	11
Y	6	11	3	3	3	3	4	6	2	5
SR	67	270	146	89	89	102	101	136	89	111
RB	1	1	1	-	-	-	-	2	1	-
ZN	43	3	14	21	31	14	50	23	11	21
CU	51	-	13	76	109	115	31	14	67	75
NI	178	85	93	266	591	270	108	243	192	153
CR	1582	425	248	905	2395	1228	352	1759	1645	1392
CIPW NORM										
QTZ	-	1.10	-	-	-	-	-	-	-	-
OR	-	-	0.10	0.10	-	0.10	-	0.10	-	0.10
AB	0.80	7.60	9.50	5.90	3.30	4.70	6.80	4.40	-	6.10
AN	16.90	36.80	46.30	50.20	33.40	34.00	35.70	34.00	24.60	37.40
NE	-	-	-	-	-	-	-	0.20	0.50	-
DI	44.30	47.10	24.80	24.30	23.00	43.10	25.40	37.00	51.20	37.70
WO	-	5.70	-	-	-	-	-	-	-	-
HY	29.10	-	2.60	5.10	1.10	7.00	3.90	-	-	2.80
OL	5.10	-	12.30	12.60	36.30	9.10	23.00	21.30	16.50	15.40
CA-OR	-	-	-	-	-	-	-	-	4.80	-
MT	3.40	1.10	1.80	1.50	2.40	1.80	4.10	2.40	1.60	2.10
IL	0.30	0.50	0.30	0.20	0.20	0.20	0.90	0.40	0.30	0.30
AP	0.10	0.10	0.10	0.10	0.10	0.10	0.10	0.10	0.10	0.20

TABLE 4-9 GABBRO MAJORS TRACES AND NORMS

	205	225	237	H3	555	556	557	1014(4)	523	189
PERCENT										
SIO2	48.01	49.39	47.79	47.68	46.92	47.64	48.54	47.72	42.08	50.73
AL2O3	12.99	12.81	14.68	14.04	16.51	15.70	15.42	19.10	14.67	10.17
FE2O3	7.58	5.36	9.61	7.53	8.52	7.44	7.15	7.41	14.63	9.59
MGO	13.22	12.96	11.32	12.25	11.82	12.21	10.62	10.80	18.82	11.27
CAO	17.66	18.56	16.25	17.43	14.47	15.53	16.73	14.26	8.77	23.65
NA2O	0.22	0.57	0.97	0.66	1.37	1.09	1.13	0.42	0.70	0.25
K2O	-	-	-	0.02	0.01	0.01	0.01	0.02	-	0.04
TIO2	0.13	0.18	0.19	0.20	0.18	0.19	0.22	0.07	0.10	0.17
MNO	0.15	0.11	0.15	0.13	0.13	0.12	0.12	0.13	0.19	0.09
S	-	-	-	-	-	-	-	-	-	-
P2O5	0.05	0.02	0.08	0.05	0.07	0.07	0.07	0.07	0.08	0.05
PPM										
BA	3	18	12	-	18	23	21	3	19	7
NB	-	1	-	1	2	1	1	2	1	3
ZR	2	8	5	10	13	12	14	5	9	18
Y	4	5	6	6	2	5	5	1	1	5
SR	63	89	72	88	124	106	125	75	105	163
RB	-	1	-	-	-	1	-	1	-	2
ZN	26	16	34	29	29	23	22	34	58	4
CU	132	63	106	136	106	136	142	4	50	-
NI	177	207	149	213	232	162	125	80	267	97
CR	1111	2924	839	838	1199	703	429	303	85	663
CIPW NORM										
QTZ	-	-	-	-	-	-	-	-	-	-
OR	-	-	-	0.10	0.10	0.10	0.10	0.10	-	0.20
AB	1.90	4.80	8.30	5.60	11.70	9.30	9.60	3.60	6.00	1.10
AN	34.70	32.50	35.90	35.50	39.10	38.10	37.20	50.50	37.30	26.60
NE	-	-	-	-	-	-	-	-	-	0.50
DI	42.40	47.50	35.80	40.80	26.20	31.00	36.60	16.20	4.90	66.10
WO	-	-	-	-	-	-	-	-	-	1.90
HY	10.30	6.00	6.10	3.60	2.20	4.90	5.30	25.10	8.20	-
OL	8.10	7.10	10.60	11.50	17.60	13.80	8.50	2.00	38.60	-
MT	2.30	1.70	2.70	2.50	2.60	2.30	2.20	2.30	4.60	1.10
IL	0.20	0.30	0.40	0.40	0.30	0.40	0.40	0.10	0.20	0.30
AP	0.10	-	0.20	0.10	0.20	0.20	0.20	0.20	0.20	0.10

TABLE 4-9 GABBRO MAJORS TRACES AND NORMS

	216	217	505	506	507	509	511	835	838	839
PERCENT										
SIO2	51.59	49.16	42.44	46.26	50.60	46.54	48.00	48.00	48.20	46.56
AL2O3	14.97	16.65	15.25	12.77	16.11	14.96	6.64	18.11	13.13	14.[illegible]
FE2O3	4.51	5.33	8.20	12.21	5.24	6.55	9.16	4.02	4.46	4.70
MGO	10.96	10.64	23.[illegible]	14.20	6.76	16.32	27.04	11.30	15.09	13.[illegible]
CAO	16.94	17.62	10.12	13.46	20.00	14.78	8.75	17.63	18.27	18.11
NA2O	0.77	0.16	0.53	0.40	1.03	0.56	-	0.71	0.55	0.64
K2O	0.01	-	0.01	0.13	0.03	0.01	-	0.01	0.02	0.01
TIO2	0.08	0.09	0.06	0.27	0.12	0.12	0.07	0.09	0.15	0.16
MNO	0.10	0.11	0.13	0.25	0.06	0.11	0.11	0.06	0.10	0.09
S	-	-	0.04	-	-	-	-	-	-	-
P2O5	0.06	0.06	0.06	0.09	0.06	0.06	0.05	0.07	0.08	0.06
PPM										
BA	6	-	33	41	-	2	15	9	4	12
NB	2	3	2	3	2	2	1	1	1	2
ZR	10	7	15	38	17	16	-	11	13	15
Y	-	-	2	15	1	2	1	1	1	4
SR	119	93	156	229	175	136	2[illegible]	123	124	112
RB	1	-	-	2	-	1	-	-	-	-
ZN	15	16	59	64	8	20	31	11	17	12
CU	-	117	118	13	80	26	585	54	27	65
NI	57	59	654	134	81	251	822	156	290	172
CR	472	472	1015	66	826	810	1204	1485	2850	1449
CIPW NORM										
QTZ	2.30	1.00	-	-	1.80	-	-	-	-	-
OR	0.10	-	0.10	0.80	0.20	0.10	-	0.10	0.10	0.10
AB	6.50	1.40	2.80	3.40	8.70	4.80	-	6.00	4.00	5.40
AN	37.50	44.90	40.40	33.00	44.80	38.50	16.80	46.30	33.40	36.00
NE	-	-	-	-	-	-	-	-	0.30	-
DI	36.80	34.60	7.70	27.30	43.10	27.60	19.40	32.40	45.10	42.50
HY	15.10	16.30	1.80	17.10	-	5.70	33.20	4.20	-	2.70
OL	-	-	44.30	13.90	-	21.00	25.60	9.40	15.20	11.40
MT	1.40	1.60	2.50	3.80	1.00	2.00	2.80	1.20	1.40	1.50
IL	0.20	0.20	0.20	0.50	0.20	0.20	0.10	0.20	0.20	0.30
AP	0.10	0.10	0.10	0.20	0.10	0.10	0.10	0.20	0.10	0.10

TABLE 4-9 GABBRO MAJORS TRACES AND NORMS

	223	1007	125	126	128	129	131	134	135	136
PERCENT										
SIO2	48.10	46.07	47.41	48.62	48.55	48.92	47.77	47.71	48.07	47.31
AL2O3	15.82	17.17	18.54	16.29	15.20	14.91	16.19	17.09	15.91	16.96
FE2O3	9.02	12.63	7.05	6.28	5.80	6.68	8.13	8.06	7.63	7.49
MGO	10.80	8.54	10.08	11.00	12.43	11.68	9.29	11.23	11.85	10.55
CAO	15.74	14.60	15.71	17.30	17.48	17.27	17.88	15.28	16.04	15.15
NA2O	0.19	0.46	0.19	0.14	0.16	0.15	0.25	0.19	0.08	0.17
K2O	-	0.01	0.02	0.02	0.02	0.02	0.02	0.01	0.01	0.02
TIO2	0.11	0.23	0.11	0.11	0.11	0.11	0.16	0.13	0.11	0.10
MNO	0.16	0.22	0.14	0.12	0.11	0.13	0.16	0.14	0.15	0.14
S	-	-	0.01	0.01	0.01	0.01	0.01	0.01	0.01	0.01
P2O5	0.05	0.07	0.14	0.13	0.14	0.13	0.14	0.14	0.14	0.14
PPM										
BA	-	34	17	63	11	25	27	52	44	13
NB	2	1	-	2	2	2	1	2	2	1
ZR	1	7	4	2	4	2	4	6	5	2
Y	-	4	2	2	2	3	2	1	-	2
SR	49	84	83	54	73	49	68	91	91	60
RB	-	2	-	-	-	2	-	-	-	-
ZN	31	65	28	21	21	23	10	30	26	22
CU	326	73	126	206	149	115	341	159	244	114
NI	61	28	30	117	112	88	62	87	68	60
CR	218	72	51	691	691	671	626	269	207	173
CIPW NORM										
QTZ	0.30	-	-	0.30	-	0.20	-	-	-	-
OR	-	0.10	0.10	0.10	0.10	0.10	0.10	0.10	0.10	0.10
AB	1.60	3.90	1.60	1.20	1.40	1.30	2.10	1.60	0.70	1.40
AN	42.60	45.20	49.40	44.00	40.90	40.20	43.30	46.00	43.30	51.20
NE	-	-	-	-	-	-	-	-	-	-
DI	28.70	22.50	22.50	33.00	36.60	36.00	36.30	23.50	28.60	18.80
HY	23.60	20.90	23.10	18.90	16.10	19.70	15.00	24.70	23.60	24.70
OL	-	2.90	0.30	-	3.20	-	0.10	1.00	0.80	0.90
MT	2.80	3.90	2.40	1.90	1.80	2.10	2.50	2.50	2.40	2.30
IL	0.20	0.40	0.40	0.20	0.20	0.20	0.30	0.20	0.20	0.20
AP	0.10	0.20	0.30	0.30	0.30	0.30	0.30	0.30	0.30	0.30

TABLE 4-9 GABBRO MAJORS TRACES AND NORMS

	229	846	849	1053	1034	H1	114	234	560	561
PERCENT										
SIO2	51.21	49.20	47.46	47.57	48.60	47.28	48.46	48.19	48.49	47.62
AL2O3	14.97	12.25	14.21	15.55	14.54	13.26	15.83	15.82	15.60	13.66
FE2O3	3.99	6.79	7.99	7.55	7.47	7.54	7.27	6.98	10.36	8.20
MGO	7.21	12.76	13.47	12.43	11.17	14.51	9.41	14.98	11.30	12.75
CAO	20.53	17.39	15.49	15.47	16.68	16.63	17.55	15.06	14.44	15.95
NA2O	1.61	1.13	0.91	1.04	1.09	0.44	0.95	0.63	1.30	1.09
K2O	0.15	0.01	0.02	0.03	0.05	0.02	0.02	0.01	0.01	0.02
TIO2	0.23	0.28	0.22	0.19	0.25	0.14	0.25	0.15	0.27	0.28
MNO	0.08	0.14	0.15	0.13	0.14	0.15	0.13	0.12	0.16	0.15
S	-	-	-	-	-	-	0.01	-	-	-
P2O5	0.04	0.05	0.07	0.05	0.05	0.05	0.13	0.05	0.07	0.07
PPM										
BA	30	-	1	-	-	1	-	7	20	71
NB	2	2	1	-	-	-	1	1	2	3
ZR	31	15	14	14	16	6	16	10	16	16
Y	5	6	6	3	5	4	7	5	5	5
SR	210	152	133	114	109	74	137	99	146	140
RB	3	-	-	-	-	-	-	1	-	1
ZN	7	19	29	25	28	33	27	28	33	39
CU	-	58	41	158	112	99	16	84	22	15
NI	14	124	167	262	234	246	39	145	43	89
CR	255	791	833	558	647	933	353	504	78	357
CIPW NORM										
QTZ	-	-	-	-	-	-	-	-	-	-
OR	0.80	0.10	0.10	0.20	0.20	0.10	0.10	0.10	0.10	0.10
AB	12.70	9.60	7.70	8.90	9.30	3.70	8.10	5.40	11.10	9.30
AN	33.30	25.30	34.80	37.90	34.90	34.30	39.10	40.50	37.00	35.10
NE	0.50	-	-	-	-	-	-	-	-	-
DI	40.90	46.00	38.50	31.10	38.40	38.40	38.20	27.20	28.00	30.60
WO	4.00	-	-	-	-	-	-	-	-	-
HY	-	1.80	5.50	5.00	5.30	5.60	6.80	3.80	3.00	2.20
OL	-	11.30	15.20	14.20	9.10	15.10	4.70	20.40	17.00	15.30
MT	1.20	2.10	2.50	2.30	2.30	2.30	2.30	2.20	3.20	2.50
IL	0.40	0.50	0.40	0.40	0.50	0.30	0.50	0.30	0.50	0.50
AP	0.10	0.10	0.20	0.10	0.10	0.10	0.30	0.10	0.20	0.20

TABLE 4.9 GABBRO MAJORS TRACES AND NORMS

	236	524	526A	549	123	139	143	144	148	153
PERCENT										
SIO2	46.63	47.95	47.53	46.50	48.52	47.31	47.01	47.47	48.19	49.05
AL2O3	14.45	12.39	11.38	10.31	16.08	17.51	16.82	15.95	17.59	16.19
FE2O3	9.52	8.09	10.58	5.65	8.74	8.51	8.86	9.32	8.76	8.69
MGO	12.92	13.97	12.08	20.76	12.29	10.41	9.18	12.19	10.15	11.10
CAO	15.33	16.41	16.99	16.32	15.87	15.61	16.90	14.52	16.72	17.56
NA2O	0.70	0.95	0.48	0.15	0.09	0.20	0.17	0.11	0.16	0.05
K2O	-	0.01	0.01	0.01	0.02	0.01	0.02	0.01	0.02	0.01
TIO2	0.26	0.28	0.73	0.09	0.11	0.13	0.14	0.11	0.11	0.10
MNO	0.13	0.14	0.19	0.13	0.13	0.16	0.16	0.17	0.12	0.11
S	-	0.05	-	-	0.01	0.01	0.01	0.01	0.01	0.01
P2O5	0.05	0.05	0.04	0.06	0.14	0.14	0.14	0.13	0.14	0.13
PPM										
BA	4	24	40	9	160	38	73	-	-	16
NB	3	2	1	2	2	1	1	1	1	1
ZR	13	14	9	2	2	9	7	3	6	5
Y	4	6	11	2	2	4	2	3	2	4
SR	126	128	96	50	65	97	90	65	76	76
RB	-	-	-	-	1	-	-	-	2	1
ZN	34	27	38	25	20	34	27	37	21	18
CU	20	170	50	131	121	42	103	266	46	210
NI	79	155	86	332	102	29	33	64	23	35
CR	222	688	493	2164	457	99	64	85	93	666
CIPW NORM										
QTZ	-	-	-	-	-	-	0.70	-	0.60	1.10
OR	-	0.10	0.10	0.10	0.10	0.10	0.10	0.10	0.10	0.10
AB	6.00	8.10	4.10	0.30	0.80	1.70	1.40	0.90	1.40	0.40
AN	36.60	29.70	29.10	27.60	43.60	47.20	45.40	43.30	47.50	44.10
NE	-	-	-	0.50	-	-	-	-	-	-
DI	31.80	41.40	44.70	42.10	27.50	24.00	30.70	22.80	28.00	33.80
HY	7.40	0.70	10.20	-	25.10	22.70	16.30	27.20	19.80	15.10
OL	14.60	15.80	7.10	27.40	0.10	1.20	-	2.20	-	-
MT	3.00	2.50	3.30	1.70	2.10	2.60	2.70	2.90	2.10	1.60
IL	0.50	0.50	1.40	0.20	0.20	0.20	0.30	0.20	0.20	0.20
AP	0.10	0.10	0.10	0.10	0.30	0.30	0.30	0.30	0.30	0.30

TABLE 4.9 GABBRO MAJORS TRACES AND NORMS

	536	614	819	824	826	828	833	110	147	156(3)
PERCENT										
SIO2	44.97	46.13	45.59	47.01	47.79	45.13	46.21	45.30	49.62	45.91
AL2O3	12.52	20.98	16.39	15.87	13.50	18.83	14.11	17.68	17.68	16.59
FE2O3	5.39	5.65	6.08	7.88	5.16	4.99	3.57	11.22	5.75	6.03
MGO	20.29	12.23	16.30	14.56	16.17	16.69	14.55	10.77	8.33	13.75
CAO	16.44	13.94	12.53	15.59	16.55	13.61	18.92	12.36	19.85	15.02
NA2O	0.09	0.83	0.84	0.70	0.52	0.50	0.38	1.39	0.40	0.44
K2O	0.02	0.03	0.02	0.02	0.01	0.04	0.02	0.06	0.01	0.01
TIO2	0.12	0.06	0.08	0.19	0.14	0.07	0.12	0.95	0.13	0.09
MNO	0.10	0.08	0.09	0.12	0.09	0.06	0.06	0.12	0.06	0.13
S	–	–	–	–	–	–	–	0.01	0.01	–
P2O5	0.07	0.07	0.07	0.07	0.06	0.07	0.06	0.14	0.15	0.06
PPM										
BA	9	–	–	50	15	24	17	24	–	–
NB	2	3	2	2	2	1	3	–	1	2
ZR	10	17	22	19	10	21	11	19	13	13
Y	3	3	–	3	2	–	2	6	3	3
SR	96	190	212	174	91	196	111	160	154	147
RB	–	3	–	–	1	2	1	1	–	–
ZN	16	25	22	24	17	22	10	19	7	27
CU	62	51	2	111	312	57	74	79	–	–
NI	317	331	403	183	341	416	215	91	1	143
CR	1439	651	875	913	2688	474	1526	177	47	233
CIPW NORM										
QTZ	–	–	–	–	–	–	–	–	3.90	–
OR	–	0.20	0.10	0.10	0.10	0.20	0.10	0.40	0.10	0.10
AB	–	7.10	7.10	6.00	4.40	4.20	3.10	11.90	3.40	3.70
AN	35.80	55.70	46.60	34.90	34.60	49.20	36.60	42.20	46.60	46.40
NE	0.40	–	–	–	–	–	0.10	–	–	–
DI	31.40	12.20	12.20	33.80	37.50	14.30	44.60	15.10	41.30	20.70
WO	–	–	–	–	–	–	–	–	–	–
HY	–	9.10	6.70	4.80	4.10	4.60	–	8.40	2.30	7.50
OL	29.80	15.80	25.10	17.50	17.40	25.60	13.60	16.40	–	17.40
CA-OR	2.40	–	–	–	–	–	–	–	–	–
MT	1.70	1.70	1.90	2.40	1.60	1.50	1.10	3.50	1.80	1.90
IL	0.20	0.10	0.10	0.40	0.30	0.10	0.20	1.80	0.20	0.20
AP	0.20	0.20	0.20	0.20	0.10	0.20	0.10	0.30	0.40	0.10

TABLE 4-9 GABBRO MAJORS TRACES AND NORMS

	539	542	1023	10300	200	512	516	519	520	522
PERCENT										
SIO2	47.25	45.55	46.40	45.22	44.88	47.59	50.33	47.05	47.05	37.45
AL2O3	7.13	10.15	10.08	13.39	13.92	14.12	13.29	16.53	14.70	10.86
FE2O3	7.86	5.62	6.01	4.65	12.25	5.91	6.14	8.91	6.34	14.10
MGO	22.04	14.19	20.91	20.65	14.09	10.20	13.01	8.35	15.59	27.28
CAO	15.36	15.28	16.08	15.78	13.97	15.36	15.90	15.55	15.24	3.92
NA2O	0.08	0.21	0.16	0.08	0.46	0.53	0.93	0.83	0.75	-
K2O	-	-	0.01	0.01	-	0.02	0.06	0.09	0.01	0.01
TIO2	0.08	0.07	0.10	0.06	0.17	0.12	0.19	0.49	0.15	0.09
MNO	0.15	0.10	0.13	0.12	0.20	0.10	0.11	0.16	0.11	0.20
S	-	-	-	-	-	-	-	-	-	-
P2O5	0.05	0.05	0.06	0.06	0.07	0.06	0.07	0.07	0.05	0.06
PPM										
BA	8	13	21	1	31	-	17	9	-	-
NB	1	2	2	-	2	2	3	6	1	2
ZR	1	3	3	2	6	11	15	32	13	-
Y	3	2	8	-	3	3	6	25	3	2
SR	23	61	49	55	76	125	141	190	141	3
RB	2	2	-	-	1	1	1	3	1	-
ZN	32	18	24	19	41	21	20	49	19	33
CU	101	14	62	10	114	35	-	-	156	-
NI	306	162	259	248	136	266	155	58	242	740
CR	2692	507	2305	1739	216	901	1455	66	1140	1291
CIPW NORM										
QTZ	-	-	-	-	-	-	-	-	-	-
OR	-	-	0.10	-	-	0.10	0.40	0.50	0.10	0.10
AB	0.70	1.80	0.80	-	4.10	4.50	7.90	7.10	6.40	-
AN	19.20	48.80	26.90	36.50	36.20	36.30	52.10	46.90	36.90	19.10
NE	-	-	0.30	0.40	-	-	-	-	-	-
DI	45.20	25.30	41.70	30.40	26.80	31.60	37.10	24.50	30.70	-
WO	-	-	-	-	-	-	-	-	-	-
HY	5.80	2.80	-	-	6.20	8.30	10.10	13.10	3.70	18.80
OL	26.40	19.30	28.10	30.20	20.50	17.10	4.10	4.00	19.90	47.40
CA-OR	-	-	-	1.00	-	-	-	-	-	-
MT	2.40	1.70	1.90	1.40	3.80	1.80	1.90	2.80	2.00	4.40
IL	0.20	0.10	0.20	0.10	0.30	0.20	0.40	0.90	0.30	0.20
AP	0.10	0.10	0.10	0.10	0.20	0.10	0.20	0.20	0.10	0.20

TABLE 4.9 GABBRO MAJORS TRACES AND NORMS

	562	564	565	566	106	119	185	188	194	203
PERCENT										
SIO2	46.22	47.26	47.15	52.49	45.97	47.06	46.38	48.02	47.36	49.05
AL2O3	15.37	16.68	16.62	12.26	15.34	12.68	15.28	16.12	14.06	15.82
FE2O3	7.85	8.62	8.62	1.63	11.10	8.54	8.81	8.93	8.22	7.54
MGO	10.85	10.39	9.70	9.24	12.59	15.16	13.02	10.07	11.72	8.75
CAO	16.01	15.24	14.85	23.50	13.81	17.07	15.97	17.77	17.67	16.99
NA2O	1.25	1.36	1.31	0.00	1.11	0.07	0.19	0.71	0.56	1.39
K2O	0.01	0.01	0.02	0.01	0.02	0.01	0.01	–	–	–
TIO2	0.24	0.22	0.13	0.19	0.24	0.12	0.14	0.19	0.20	0.26
MNO	0.14	0.14	0.12	0.02	0.16	0.12	0.15	0.12	0.14	0.15
S	–	–	–	–	0.01	0.01	–	–	0.01	–
P2O5	0.07	0.06	0.07	0.06	0.15	0.14	0.05	0.05	0.05	0.05
PPM										
BA	1	–	23	–	10	–	–	–	19	12
NB	2	2	1	3	–	1	1	2	1	1
ZR	14	15	15	30	16	4	4	12	8	16
Y	4	3	2	2	6	2	3	5	5	6
SR	139	156	163	270	177	35	65	136	84	135
RB	–	1	–	–	–	–	1	–	1	–
ZN	23	35	24	–	40	21	28	21	24	23
CU	40	–	8	–	97	201	16	65	166	68
NI	62	61	77	50	99	181	101	84	129	50
CR	196	202	81	356	157	959	365	684	902	369
CIPW NORM										
QTZ	–	–	–	2.80	–	–	–	–	–	–
OR	0.10	0.10	0.10	0.10	0.10	0.10	0.10	–	–	–
AB	10.60	11.60	11.20	5.10	9.50	0.60	1.00	6.00	4.80	11.60
AN	36.50	39.60	45.20	30.80	37.10	34.40	41.10	41.00	36.10	37.10
NE	–	–	–	–	–	–	–	–	–	–
DI	34.40	29.00	22.90	52.60	23.00	39.50	30.70	37.80	41.50	36.00
WO	–	–	–	7.70	–	–	–	–	–	–
HY	4.80	2.60	5.60	–	7.70	11.50	11.60	6.30	4.10	5.00
OL	10.60	13.70	12.00	–	18.30	13.10	11.70	6.20	10.60	5.00
MT	2.40	2.70	2.50	0.50	3.50	2.20	2.70	2.10	2.50	2.30
IL	0.50	0.40	0.20	0.40	0.50	0.20	0.30	0.40	0.40	0.50
AP	0.20	0.10	0.20	0.10	0.30	0.30	0.10	0.10	0.10	0.10

TABLE 4-9 GABBRO MAJORS TRACES AND NORMS

	840	841	842	843	844	113	121	224	548	846
PERCENT										
SIO2	46.65	47.14	50.00	47.76	46.36	47.94	46.93	46.42	46.79	49.37
AL2O3	18.52	11.31	14.70	14.41	13.15	13.24	17.72	17.15	13.75	12.78
FE2O3	4.84	7.13	3.29	5.89	5.99	7.54	7.50	6.81	4.33	4.41
MGO	13.80	19.98	11.43	15.38	18.83	14.28	11.69	15.51	17.46	15.79
CAO	15.27	13.73	19.74	15.23	14.96	16.43	15.58	12.87	17.24	19.01
NA2O	0.65	0.34	0.55	0.96	0.41	0.17	0.18	0.94	0.22	0.34
K2O	0.02	0.02	0.03	0.04	0.01	0.02	0.02	0.03	0.02	0.01
TIO2	0.08	0.14	0.12	0.15	0.12	0.12	0.12	0.10	0.08	0.12
MNO	0.07	0.13	0.07	0.11	0.10	0.12	0.12	0.11	0.09	0.09
S	-	-	-	-	-	0.01	0.01	-	-	-
P2O5	0.07	0.07	0.06	0.07	0.07	0.13	0.14	0.06	0.06	0.07
PPM										
BA	4	16	-	41	10	20	17	21	30	1
NB	4	3	1	3	3	2	1	-	-	2
ZR	14	19	16	21	9	1	3	11	4	7
Y	-	7	2	3	2	2	3	3	1	4
SR	159	176	157	204	80	57	63	138	74	75
RB	1	-	-	-	1	-	-	-	1	-
ZN	20	24	8	18	23	27	31	45	11	13
CU	41	-	-	2	45	124	45	92	100	205
NI	93	18	2	12	77	156	138	362	241	143
CR	232	959	3875	3156	977	702	393	612	1769	718
CIPW NORM										
QTZ	-	-	-	-	-	-	-	-	-	-
OR	0.10	0.10	0.20	0.20	0.10	0.10	0.10	0.20	0.10	0.10
AB	5.50	2.90	4.70	8.20	3.50	1.40	1.50	8.00	1.40	2.90
AN	47.70	29.40	37.70	35.10	34.10	35.50	47.80	42.70	36.50	33.40
NE	-	-	-	-	-	-	-	-	0.30	-
DI	22.00	30.50	47.40	32.00	31.70	36.30	23.20	16.70	38.50	48.00
HY	6.10	11.40	5.80	3.40	2.70	15.30	18.80	8.30	-	8.70
OL	16.70	22.90	2.90	16.90	25.70	8.40	5.60	21.60	21.60	7.10
MT	1.50	2.20	1.00	1.80	1.90	2.30	2.30	2.10	1.30	1.40
IL	0.20	0.30	0.20	0.30	0.20	0.20	0.20	0.20	0.10	0.20
AP	0.20	0.20	0.10	0.20	0.20	0.30	0.30	0.10	0.10	0.20

TABLE 49 GABBRO MAJORS TRACES AND NORMS

	850	871	1000	1001	1014(2)	1016	1029(2)	100	146	176
PERCENT										
SIO2	47.13	48.30	47.48	47.92	50.45	46.26	48.08	46.97	47.21	45.42
AL2O3	17.62	14.20	20.12	15.03	7.17	18.44	9.75	20.27	18.71	10.65
FE2O3	7.50	6.65	4.00	5.67	4.56	5.10	4.37	7.95	6.29	10.37
MGO	11.42	13.49	9.83	13.11	18.82	13.48	19.26	8.15	8.99	21.65
CAO	14.73	16.65	18.09	17.82	16.66	16.15	18.15	14.70	16.22	11.56
NA2O	1.24	0.40	0.28	0.20	0.06	0.35	0.14	1.51	0.14	0.07
K2O	0.01	0.02	0.02	0.01	0.01	0.01	0.01	0.02	0.02	0.01
TIO2	0.17	0.10	0.06	0.08	0.07	0.06	0.06	0.16	0.11	0.06
MNO	0.12	0.12	0.06	0.10	0.11	0.08	0.11	0.12	0.13	0.17
S	-	-	-	-	-	-	-	0.01	0.02	-
P2O5	0.07	0.06	0.07	0.06	0.05	0.07	0.06	0.14	0.15	0.06
PPM										
BA	1	5	2	-	-	-	-	-	35	-
NB	1	2	3	2	2	1	-	2	1	3
ZR	14	7	5	2	-	4	5	17	6	2
Y	4	3	1	2	2	-	-	4	3	3
SR	133	73	62	50	35	71	38	184	71	52
RB	-	-	-	-	-	1	1	-	-	1
ZN	23	25	16	11	13	14	14	29	23	39
CU	-	161	38	128	166	-	118	8	1061	99
NI	112	71	116	129	216	146	196	64	114	571
CR	379	77	218	840	3702	531	1773	104	118	2740
CIPW NORM										
QTZ	-	-	-	-	-	-	-	-	0.60	-
OR	0.10	0.10	0.10	0.10	0.10	0.10	0.10	0.10	0.10	0.10
AB	10.60	3.40	2.40	1.70	0.50	3.00	0.90	12.90	1.20	0.60
AN	42.70	37.10	53.70	40.30	19.30	48.90	26.00	48.80	50.70	26.90
NE	-	-	-	-	-	-	0.10	-	-	-
DI	24.20	36.20	28.40	36.20	57.70	24.60	50.30	19.10	23.60	22.50
HY	4.80	12.30	9.40	9.20	9.60	6.10	-	5.20	20.60	16.30
OL	14.80	6.40	4.40	8.50	10.90	15.50	20.90	10.80	-	28.00
MT	2.30	2.10	1.20	1.80	1.40	1.60	1.40	2.50	2.60	3.20
IL	0.30	0.20	0.10	0.20	0.10	0.10	0.10	0.30	0.20	0.20
AP	0.20	0.10	0.20	0.10	0.10	0.20	0.10	0.30	0.40	0.10

TABLE 4:9 GABBRO MAJORS TRACES AND NORMS

	867	870	567	568	845	847	1010	1029(1)	1032	H2
PERCENT										
SIO2	46.66	48.67	48.35	47.27	47.40	47.10	47.30	47.59	48.46	47.62
AL2O3	14.52	15.21	14.98	18.52	14.08	14.43	15.76	15.95	13.49	14.84
FE2O3	8.01	7.72	8.02	8.05	7.43	7.72	7.04	8.13	8.41	8.09
MGO	12.47	12.64	10.72	9.74	14.23	13.62	11.41	11.41	12.54	13.49
CAO	15.49	15.01	16.30	14.69	14.99	16.20	17.66	15.21	15.56	17.31
NA2O	0.50	0.43	1.17	1.38	0.67	0.58	0.53	1.30	1.08	0.52
K2O	0.01	0.01	0.01	0.01	0.05	0.01	0.01	0.01	0.03	0.02
TIO2	0.13	0.11	0.25	0.15	0.14	0.15	0.22	0.19	0.25	0.14
MNO	0.14	0.12	0.14	0.12	0.11	0.12	0.12	0.13	0.15	0.12
S	–	–	–	–	–	–	–	–	0.01	–
P2O5	0.07	0.07	0.07	0.07	0.07	0.06	0.06	0.07	0.05	0.05
PPM										
BA	–	17	–	–	–	–	–	–	–	5
NB	1	2	1	1	–	1	1	–	–	–
ZR	4	8	12	17	6	8	5	16	–	8
Y	2	1	5	3	5	4	1	4	–	5
SR	76	77	115	160	96	104	79	125	–	81
RB	–	1	1	1	2	–	–	–	–	1
ZN	35	25	24	30	27	22	21	29	–	25
CU	169	–	137	10	136	158	121	111	82	138
NI	83	27	49	79	192	196	122	240	187	256
CR	260	–	593	98	831	1217	643	1351	427	895
CIPW NORM										
QTZ	–	–	–	–	–	–	–	–	–	–
OR	0.10	0.10	0.10	0.10	0.20	0.10	0.10	0.10	0.20	0.10
AB	4.30	3.70	10.00	11.80	5.70	4.90	2.80	11.10	9.20	4.40
AN	37.60	39.60	35.80	44.60	37.70	37.00	41.70	37.90	32.10	36.40
NE	–	–	–	–	–	–	–	–	–	–
DI	31.40	27.70	36.10	22.70	29.10	34.70	37.50	30.10	36.10	39.50
HY	19.80	23.00	5.70	5.90	10.00	6.00	7.00	3.80	8.20	4.20
OL	4.00	3.10	9.20	12.00	14.50	14.60	8.40	14.10	11.00	12.50
MT	2.50	2.40	2.50	2.50	2.30	2.40	2.20	2.50	2.60	2.10
IL	0.20	0.20	0.50	0.30	0.30	0.30	0.20	0.40	0.50	0.30
AP	0.20	0.20	0.20	0.20	0.20	0.10	0.10	0.20	0.10	0.10

TABLE 4-9 GABBRO MAJORS TRACES AND NORMS

	1002	1008	1009	132	133	150	155	158	199	221
PERCENT										
SIO2	50.20	45.65	45.19	48.26	48.35	48.34	48.29	47.87	48.08	48.51
AL2O3	9.90	19.51	17.75	16.56	16.46	16.26	15.94	15.94	16.44	16.[illegible]7
FE2O3	5.99	12.80	13.65	7.55	6.91	7.57	8.29	9.51	7.69	7.55
MGO	14.61	6.22	7.76	11.16	11.37	11.56	11.08	12.85	10.35	9.57
CAO	18.63	12.64	14.51	15.87	16.34	15.73	15.83	13.31	14.75	16.96
NA2O	0.15	0.49	0.49	0.18	0.18	0.12	0.15	0.19	0.37	0.24
K2O	0.01	0.01	0.01	0.02	0.01	0.02	0.02	-	-	-
TIO2	0.11	0.20	0.30	0.12	0.11	0.11	0.11	0.09	0.11	0.10
MNO	0.13	0.22	0.25	0.15	0.14	0.15	0.16	0.18	0.15	0.15
S	-	-	-	0.01	0.01	0.01	0.01	-	-	-
P2O5	0.05	0.07	0.07	0.13	0.13	0.14	0.13	0.05	0.05	0.06
PPM										
BA	2	15	12	168	24	-	-	60	15	35
NB	1	1	2	1	2	1	1	-	3	2
ZR	1	4	5	10	2	10	4	2	3	6
Y	3	1	2	4	4	3	3	3	2	1
SR	34	75	89	119	57	123	75	59	55	76
RB	-	2	1	-	2	-	-	-	1	1
ZN	21	57	69	27	26	27	30	18	40	24
CU	217	5	87	152	245	234	42	21	30	-
NI	141	5	15	54	87	84	97	43	47	39
CR	1238	-	-	185	334	86	444	86	197	204
CIPW NORM										
QTZ	-	-	-	0.20	-	0.30	0.50	-	0.30	1.10
OR	0.10	0.10	0.10	0.10	0.10	0.10	0.10	-	-	-
AB	1.30	4.20	4.20	1.50	1.50	1.00	1.30	1.60	3.20	2.00
AN	26.40	51.50	46.70	44.60	44.30	44.00	43.00	43.00	49.00	45.20
NE	-	-	-	-	-	-	-	-	-	-
DI	52.40	10.10	20.20	27.00	29.00	26.80	26.20	18.60	19.50	31.30
HY	14.00	27.50	19.40	23.70	22.20	24.60	23.80	31.60	25.40	17.60
OL	3.60	2.10	4.40	-	0.20	-	-	1.90	-	-
MT	1.90	4.00	4.30	2.30	2.10	2.30	2.60	3.00	2.40	2.30
IL	0.20	0.40	0.60	0.20	0.20	0.20	0.20	0.20	0.20	0.20
AP	0.10	0.20	0.20	0.30	0.30	0.30	0.30	0.10	0.10	0.10

TABLE 4-9 GABBRO MAJORS TRACES AND NORMS

	1015	1018	120	130	202	857	859	860	861	863
PERCENT										
SIO2	46.48	49.55	49.46	49.82	50.42	51.43	46.74	48.71	47.06	49.52
AL2O3	16.54	15.24	12.66	15.64	11.62	15.31	15.61	16.84	17.71	11.70
FE2O3	3.69	4.22	4.60	6.46	10.21	3.49	9.73	5.92	5.10	6.95
MGO	16.16	13.26	12.75	10.21	11.74	11.60	11.14	11.66	12.96	16.16
CAO	16.61	17.29	19.61	17.08	14.96	16.86	15.31	16.28	16.64	14.94
NA2O	0.31	0.20	0.30	0.42	0.44	0.89	0.79	0.31	0.30	0.42
K2O	0.02	0.01	0.02	0.02	0.01	0.01	0.01	0.01	0.02	0.01
TIO2	0.05	0.07	0.12	0.11	0.14	0.28	0.23	0.08	0.07	0.09
MNO	0.06	0.10	0.09	0.07	0.21	0.05	0.17	0.12	0.08	0.13
S	–	–	0.01	0.01	–	–	–	–	–	–
P2O5	0.06	0.07	0.13	0.14	0.05	0.07	0.07	0.07	0.07	0.07
PPM										
BA	7	–	5	8	9	12	7	13	4	–
NB	–	1	1	1	2	2	2	2	2	2
ZR	5	2	5	9	11	24	22	14	9	14
Y	2	1	2	3	3	3	6	2	2	1
SR	78	42	56	87	91	207	141	130	82	69
RB	2	1	1	–	1	1	–	1	–	–
ZN	8	13	11	10	40	9	42	19	17	22
CU	6	177	87	–	–	–	33	259	481	97
NI	184	116	103	57	76	99	39	47	132	127
CR	1126	1090	1253	499	185	433	162	218	289	724
CIPW NORM										
QTZ	–	–	–	1.90	2.50	1.20	–	–	–	–
OR	0.10	0.10	0.10	0.10	0.10	0.10	0.10	0.10	0.10	0.10
AB	2.60	1.70	2.50	3.60	3.80	7.60	6.70	2.60	2.50	3.60
AN	43.80	40.60	33.30	40.90	30.50	37.50	35.90	44.70	47.10	30.20
NE	–	–	–	–	–	–	–	–	–	–
DI	30.20	35.40	30.20	34.60	35.40	35.90	29.10	28.60	28.00	34.80
HY	1.10	16.50	7.30	16.30	24.20	15.70	9.40	20.40	9.10	21.30
OL	20.70	2.00	4.40	–	–	–	11.20	1.40	11.30	7.00
MT	1.10	1.30	1.50	2.00	3.20	1.10	3.00	1.80	1.60	2.20
IL	0.10	0.10	0.20	0.20	0.50	0.50	0.40	0.20	0.10	0.20
AP	0.10	0.20	0.30	0.30	0.10	0.20	0.20	0.20	0.20	0.20

TABLE 4-9 GABBRO MAJORS TRACES AND NORMS

	H4	152	101	187	190	191	193	195	207	219
PERCENT										
SIO2	46.21	46.74	49.19	46.33	47.46	47.66	50.59	47.25	46.44	49.21
AL2O3	12.99	15.22	16.05	13.73	15.54	15.14	12.05	13.16	14.76	13.67
FE2O3	5.76	6.74	5.51	5.94	6.04	6.76	4.29	7.03	9.09	7.12
MGO	14.25	13.51	11.96	14.70	14.56	13.96	11.04	14.22	11.75	11.19
CAO	17.59	15.51	16.76	16.72	15.46	17.67	20.55	17.55	15.37	16.35
NA2O	0.49	0.08	0.29	0.54	0.65	0.51	0.42	0.42	0.25	1.15
K2O	0.02	0.01	-	0.01	0.01	0.02	-	0.02	-	0.02
TIO2	0.15	0.11	0.08	0.09	0.12	0.16	0.15	0.18	0.14	0.35
MNO	0.11	0.13	0.11	0.09	0.14	0.12	0.07	0.12	0.15	0.15
S	-	0.01	-	-	-	-	-	-	-	-
P2O5	0.05	0.13	0.06	0.04	0.05	0.05	0.04	0.05	0.05	0.04
PPM										
BA	-	25	9	11	21	31	14	25	0	14
NB	-	1	2	1	1	2	2	1	1	2
ZR	8	1	5	7	9	12	16	11	5	10
Y	4	2	3	2	5	6	5	3	1	6
SR	75	55	75	101	109	127	154	114	76	99
RB	-	-	1	-	-	-	1	-	1	-
ZN	22	23	17	7	32	17	3	19	34	27
CU	169	-	366	44	115	191	-	182	107	1
NI	304	79	66	191	214	147	190	128	51	116
CR	1229	245	204	922	881	857	1697	576	136	249
CIPW NORM										
QTZ	-	-	-	-	-	-	-	-	-	-
OR	0.10	0.10	-	0.10	0.10	0.10	-	0.10	-	0.10
AB	4.20	0.70	2.50	2.90	5.50	4.30	3.60	3.60	2.10	9.60
AN	33.30	41.40	42.70	36.10	34.20	33.70	31.10	34.20	39.50	32.90
NE	-	-	-	-	-	-	-	-	-	-
DI	44.40	28.00	32.10	37.20	33.70	43.00	50.10	42.20	29.70	30.70
HY	2.60	26.30	20.20	11.00	9.30	2.20	6.80	2.00	25.40	9.20
OL	13.10	1.00	0.50	10.60	13.90	14.10	0.70	15.30	0.10	0.90
MT	1.80	2.10	1.70	1.80	2.50	2.10	1.30	2.20	2.80	2.40
IL	0.20	0.20	0.20	0.20	0.60	0.30	0.30	0.30	0.30	0.60
AP	0.10	0.30	0.10	0.10	0.10	0.10	0.10	0.10	0.10	0.10

TABLE 4.9 GABBRO MAJORS TRACES AND NORMS

	1014(1)	1026	501
PERCENT			
SIO2	49.11	48.20	43.39
AL2O3	18.49	18.62	10.93
FE2O3	4.96	6.16	9.46
MGO	8.61	7.65	24.50
CAO	18.12	18.55	10.92
NA2O	0.47	0.56	0.38
K2O	0.01	0.03	0.01
TIO2	0.07	0.08	0.10
MNO	0.09	0.10	0.15
S	-	-	0.10
P2O5	0.07	0.07	0.08
PPM			
BA	-	6	26
NB	1	2	6
ZR	4	12	6
Y	2	-	3
SR	87	142	97
RB	1	-	1
ZN	17	16	37
CU	97	115	137
NI	75	57	597
CR	220	2	2069
CIPW NORM			
QTZ	1.20	0.10	-
OR	0.10	0.20	0.10
AB	4.00	4.80	3.20
AN	48.50	48.40	28.50
NE	-	-	-
DI	32.90	35.00	20.40
HY	11.50	9.40	0.20
OL	-	-	44.30
MT	1.50	1.90	2.90
IL	0.10	0.20	0.20
AP	0.20	0.20	0.20

TABLE 4.9 GABBRO MAJORS TRACES AND NORMS

	541	552	554
PERCENT			
SIO2	44.93	47.11	48.50
AL2O3	16.18	15.41	14.07
FE2O3	4.44	9.01	9.55
MGO	17.41	11.69	13.78
CAO	16.73	15.13	13.39
NA2O	0.11	0.32	0.33
K2O	0.01	0.02	0.02
TIO2	0.07	0.10	0.11
MNO	0.08	0.16	0.18
S	-	-	-
P2O5	0.06	0.07	0.07
PPM			
BA	-	17	-
NB	2	1	3
ZR	4	7	3
Y	-	3	1
SR	69	101	63
RB	-	2	1
ZN	9	34	52
CU	2	66	100
NI	223	60	110
CR	1308	37	710
CIPW NORM			
QTZ	-	-	-
OR	-	0.10	0.10
AB	-	2.70	2.80
AN	43.80	43.60	37.10
NE	0.50	-	-
DI	27.50	25.30	25.50
WO	-	-	-
HY	-	18.90	30.00
OL	25.20	6.20	3.10
CA-OR	1.30	-	-
MT	1.40	2.80	3.00
IL	0.10	0.20	0.20
AP	0.10	0.20	0.20

TABLE 4-9 GABBRO MAJORS TRACES AND NORMS

533

PERCENT	
SIO2	48.33
AL2O3	12.42
FE2O3	6.25
MGO	15.51
CAO	16.30
NA2O	0.74
K2O	0.09
TIO2	0.18
MNO	0.12
S	-
P2O5	0.05
PPM	
BA	41
NB	2
ZR	24
Y	7
SR	174
RB	2
ZN	20
CU	297
NI	252
CR	1133
CIPW NORM	
QTZ	-
OR	0.50
AB	6.30
AN	30.50
NE	-
DI	40.00
WO	-
HY	4.10
OL	16.20
MT	1.90
IL	0.30
AP	0.10

TABLE 4-10 ANORTHOSITE MAJORS TRACES AND NORMS

	160	220	540
PERCENT			
SIO2	45.64	45.15	46.41
AL2O3	31.52	30.88	28.51
FE2O3	1.26	2.04	3.98
MGO	1.39	2.68	6.89
CAO	18.92	18.73	18.56
NA2O	0.94	0.35	0.41
K2O	-	0.01	0.01
TIO2	0.06	0.06	0.08
MNO	0.02	0.04	0.09
S	-	-	-
P2O5	0.06	0.06	0.06
PPM			
EA	-	-	4
NB	4	2	1
ZR	12	9	5
Y	2	-	1
SR	146	106	70
RB	-	1	-
ZN	-	3	14
CU	1013	62	24
NI	-	1	54
CR	53	42	164
CIPW NORM			
QTZ	-	0.20	-
OR	-	0.10	0.10
AB	7.80	3.00	3.50
AN	81.90	82.80	62.50
NE	0.10	-	-
DI	9.40	7.90	23.50
WO	-	-	-
HY	-	5.20	4.90
OL	0.20	-	4.00
CA-OR	-	-	-
MT	0.40	0.60	1.20
IL	0.10	0.10	0.20
AP	0.10	0.10	0.10

TABLE 4-11 BASALT-DOLERITE MAJORS TRACES AND NORMS

	101	107	108	116	117	122	137	140	149A	154
PERCENT										
SIO2	55.88	44.85	48.18	46.97	50.62	52.14	60.43	59.89	46.74	57.34
AL2O3	14.07	15.02	12.41	13.93	9.79	13.88	11.77	11.62	15.43	12.67
FE2O3	11.80	9.65	10.20	10.35	10.73	11.20	12.27	12.51	12.09	10.78
MGO	6.63	14.26	14.95	11.89	13.22	8.97	4.17	4.50	10.53	6.25
CAO	6.51	14.87	11.70	15.41	14.07	12.58	9.34	9.44	14.29	11.44
NA2O	4.24	0.77	1.53	0.73	0.73	0.59	1.15	1.13	0.26	0.78
K2O	0.04	0.03	0.09	0.02	0.04	0.04	0.14	0.16	0.02	0.12
TIO2	0.48	0.24	0.60	0.37	0.57	0.28	0.40	0.41	0.29	0.30
MNO	0.18	0.17	0.16	0.18	0.09	0.18	0.18	0.19	0.22	0.17
S	0.01	0.01	0.01	0.01	0.01	-	0.01	-	0.01	0.01
P2O5	0.16	0.14	0.15	0.14	0.13	0.14	0.15	0.13	0.13	0.14
PPM										
BA	9	14	15	34	-	40	23	48	27	19
NB	5	7	4	1	5	4	7	5	5	4
ZR	28	15	51	11	9	12	24	21	4	14
Y	14	6	12	8	5	6	12	11	2	84
SR	87	157	123	109	84	72	92	74	87	195
RB	1	1	-	-	-	-	1	3	-	1
ZN	92	41	44	40	9	57	82	95	63	80
CU	134	206	-	61	-	162	76	25	78	19
NI	16	104	352	63	160	58	3	3	28	16
CR	25	703	1295	331	936	112	2	17	78	27
CIPW NORM										
QTZ	4.50	-	-	-	1.50	8.70	25.60	24.40	-	19.10
OR	0.20	0.20	0.50	0.10	0.20	0.20	0.80	1.00	0.10	0.70
AB	36.20	5.50	13.10	6.20	6.20	5.00	9.80	9.70	2.20	6.70
AN	19.40	37.70	26.90	35.00	23.50	35.40	26.80	26.40	41.30	31.00
NE	-	0.60	-	-	-	-	-	-	-	-
DI	9.90	28.50	24.40	33.10	36.90	21.60	15.90	16.70	23.90	20.80
HY	24.70	-	14.10	10.80	26.90	24.60	16.20	16.90	26.10	17.50
OL	-	23.70	16.20	10.50	-	-	-	-	1.80	-
MT	3.70	3.00	3.20	3.20	3.30	3.50	3.80	3.90	3.80	3.40
IL	0.90	0.50	1.10	0.70	1.10	0.50	0.80	0.80	0.60	0.60
AP	0.40	0.30	0.40	0.30	0.30	0.30	0.40	0.30	0.30	0.30

TABLE 4.11 BASALT-DOLERITE MAJORS TRACES AND NORMS

	159	162A	162B	164	184	186	218	858	864	866
PERCENT										
SIO2	54.20	55.75	54.93	55.26	55.36	47.96	59.39	47.98	53.94	54.75
AL2O3	12.06	11.21	10.51	11.71	12.33	11.14	13.08	13.41	12.80	11.53
FE2O3	10.34	10.36	10.13	10.60	11.07	9.27	11.56	10.78	10.72	10.73
MGO	9.47	9.26	10.67	9.18	8.07	15.99	5.00	13.22	9.19	9.41
CAO	12.68	12.08	12.75	12.02	11.65	14.96	9.15	13.82	11.84	12.38
NA2O	0.60	0.66	0.39	0.54	0.86	0.23	1.08	0.24	0.80	0.52
K2O	0.08	0.07	0.05	0.08	0.08	0.02	0.03	0.02	0.08	0.07
TIO2	0.24	0.28	0.26	0.29	0.25	0.15	0.37	0.19	0.29	0.30
MNO	0.18	0.19	0.18	0.17	0.19	0.14	0.17	0.20	0.19	0.18
S	0.01	0.01	-	0.01	0.01	0.01	0.01	0.01	0.01	-
P2O5	0.14	0.14	0.13	0.14	0.14	0.13	0.16	0.13	0.14	0.14
PPM										
BA	35	30	12	57	13	11	16	22	31	38
NB	4	4	5	5	6	5	7	3	6	6
ZR	10	10	8	11	18	3	28	12	12	9
Y	5	7	5	8	9	2	14	3	8	7
SR	61	51	62	52	99	51	76	154	71	44
RB	2	-	-	2	2	-	-	-	-	2
ZN	73	70	64	74	66	31	90	48	64	67
CU	122	58	139	72	78	24	74	83	133	123
NI	55	58	62	50	33	149	18	113	51	56
CR	370	579	659	373	201	1217	21	785	303	417
CIPW NORM										
QTZ	11.30	14.00	12.30	13.90	13.80	-	22.70	-	10.70	12.80
OR	0.50	0.40	0.30	0.50	0.50	0.10	0.20	0.10	0.50	0.40
AB	5.10	5.60	3.30	4.60	7.30	2.00	9.20	2.00	6.80	4.40
AN	30.20	27.60	27.00	29.50	29.80	29.50	31.00	35.80	31.40	29.20
NE	-	-	-	-	-	-	-	-	-	-
DI	26.10	25.80	28.90	24.00	22.50	35.40	11.40	26.10	21.80	25.80
HY	22.80	22.40	24.20	23.20	21.80	18.80	19.80	29.20	24.50	23.10
OL	-	-	-	-	-	10.70	-	2.70	-	-
MT	3.20	3.20	3.10	3.30	3.40	2.90	3.60	3.40	3.30	3.30
IL	0.50	0.50	0.50	0.60	0.50	0.30	0.70	0.40	0.60	0.60
AP	0.30	0.30	0.30	0.30	0.30	0.30	0.40	0.30	0.30	0.30

TABLE 4.11 BASALT-DOLERITE MAJORS TRACES AND NORMS

	1004	196	227	228
PERCENT				
SIO2	56.42	47.36	55.26	59.02
AL2O3	13.06	18.26	14.06	13.17
FE2O3	10.74	12.34	10.64	11.42
MGO	7.00	6.03	8.03	5.77
CAO	10.99	13.95	9.24	8.13
NA2O	1.03	1.09	2.12	1.78
K2O	0.07	0.03	0.15	0.10
TIO2	0.35	0.69	0.25	0.34
MNO	0.18	0.18	0.17	0.17
S	0.01	-	0.02	-
P2O5	0.15	0.06	0.07	0.08
PPM				
BA	232	29	14	42
NB	4	2	3	1
ZR	22	10	24	31
Y	11	5	7	15
SR	106	115	84	69
RB	-	-	-	3
ZN	89	61	68	86
CU	208	-	21	123
NI	26	-	33	11
CR	162	76	88	53
CIPW NORM				
QTZ	16.30	1.40	9.10	19.50
OR	0.40	0.20	0.90	0.60
AB	8.80	9.30	18.10	15.20
AN	31.10	45.30	28.60	27.90
NE	-	-	-	-
DI	18.70	19.90	13.90	10.10
HY	20.30	18.50	25.30	22.20
OL	-	-	-	-
MT	3.30	3.80	3.30	3.60
IL	0.70	1.30	0.50	0.70
AP	0.40	0.10	0.20	0.20

TABLE 4-12 ALTERED DOLERITE MAJORS TRACES AND NORMS

	103	109	111
PERCENT			
SIO2	44.75	47.65	48.06
AL2O3	4.99	13.90	13.82
FE2O3	10.02	6.31	6.55
MGO	14.97	14.09	13.46
CAO	23.11	16.87	16.93
NA2O	1.39	0.76	0.68
K2O	0.03	0.03	0.03
TIO2	0.38	0.19	0.20
MNO	0.25	0.16	0.11
S	0.01	0.01	0.02
P2O5	0.11	0.14	0.13
PPM			
BA	38	21	13
NB	6	6	4
ZR	19	9	21
Y	8	5	6
SR	97	94	107
RB	-	-	2
ZN	36	19	25
CU	-	157	122
NI	123	130	149
CR	384	235	827
CIPW NORM			
QTZ	-	-	-
OR	-	0.20	0.20
AB	-	6.00	5.80
AN	7.30	34.90	34.80
LEUC	0.10	-	-
NE	6.40	-	-
DI	50.90	38.30	38.80
HY	-	2.80	5.60
OL	17.50	15.10	12.00
CA-OR	13.60	-	-
MT	3.10	2.00	2.00
IL	0.70	0.40	0.40
AP	0.30	0.30	0.30

TABLE 4-12 ALTERED DOLERITE MAJORS TRACES AND NORMS

	165	167	168	169	170	171	172	174	176	204
PERCENT										
SIO2	49.37	49.91	51.55	52.22	47.67	52.01	52.15	51.78	47.64	50.11
AL2O3	12.91	11.73	9.31	6.64	11.56	8.49	10.69	9.25	12.91	13.17
FE2O3	8.09	5.49	4.73	4.21	7.68	2.67	3.11	10.26	7.14	8.02
MGO	13.07	11.94	13.93	13.32	15.08	12.77	11.90	16.13	14.12	13.70
CAO	15.81	20.00	19.79	23.24	16.47	23.32	21.28	11.59	17.28	10.56
NA2O	0.32	0.45	0.32	0.06	0.60	0.23	0.57	0.37	0.45	0.20
K2O	0.03	0.02	0.02	0.02	0.05	0.02	0.02	0.09	0.02	0.02
TIO2	0.14	0.25	0.17	0.17	0.19	0.15	0.12	0.22	0.20	0.10
MNO	0.14	0.07	0.05	0.05	0.13	0.02	0.04	0.18	0.11	0.09
S	0.01	0.01	0.01	0.01	0.01	0.01	0.01	-	0.01	0.01
P2O5	0.13	0.14	0.13	0.12	0.14	0.12	0.13	0.13	0.13	0.14
PPM										
BA	26	14	-	22	22	18	8	31	6	6
NB	3	6	5	4	4	6	6	6	5	4
ZR	4	14	13	13	11	23	17	5	9	4
Y	-	4	2	4	3	3	2	5	3	1
SR	82	149	145	128	115	153	107	35	113	61
RB	-	-	-	-	-	-	-	2	-	-
ZN	22	1	-	1	22	-	1	53	17	12
CU	114	-	-	-	95	-	-	-	31	-
NI	47	112	153	83	149	99	83	287	152	73
CR	61	759	1823	524	440	454	600	1559	945	320
CIPW NORM										
QTZ	-	-	0.30	1.30	-	0.60	1.10	2.70	-	0.40
OR	0.20	0.10	0.10	0.10	0.30	0.10	0.10	0.50	0.10	0.10
AB	2.70	3.80	2.70	0.50	5.10	2.00	4.80	3.20	3.80	1.70
AN	33.90	30.10	24.00	17.80	28.90	22.10	26.60	23.50	33.30	35.40
NE	-	-	-	-	-	-	-	-	-	-
DI	35.20	54.50	58.20	76.50	41.70	73.10	61.70	26.80	41.40	35.90
HY	24.10	5.60	12.50	1.80	5.90	0.60	4.10	39.30	5.40	24.10
OL	0.70	2.40	-	-	15.00	-	-	-	13.00	-
MT	2.50	1.70	1.50	1.30	2.40	0.90	1.00	3.20	2.20	1.90
IL	0.30	0.50	0.30	0.30	0.40	0.30	0.20	0.40	0.40	0.20
AP	0.30	0.30	0.30	0.30	0.30	0.30	0.30	0.30	0.30	0.30

TABLE 4-12 ALTERED DOLERITE MAJORS TRACES AND NORMS

	206	230	233	855	856
PERCENT					
SIO2	46.30	46.88	47.19	49.74	54.30
AL2O3	14.40	14.75	18.47	16.25	13.16
FE2O3	7.19	7.78	6.67	6.15	11.48
MGO	14.64	16.11	9.58	9.16	7.98
CAO	16.67	13.29	16.26	17.63	11.70
NA2O	0.30	0.73	0.99	0.44	0.68
K2O	0.03	0.06	0.02	0.03	0.08
TIO2	0.14	0.16	0.16	0.17	0.27
MNO	0.12	0.09	0.10	0.09	0.19
S	0.01	0.01	0.01	0.01	-
P2O5	0.13	0.14	0.14	0.14	0.14
PPM					
BA	10	4	5	8	26
NB	5	3	4	5	5
ZR	6	12	13	8	13
Y	3	4	4	2	8
SR	78	136	145	102	64
RB	-	-	-	-	-
ZN	25	15	17	22	73
CU	129	-	110	-	198
NI	187	130	106	54	44
CR	498	174	246	870	100
CIPW NORM					
QTZ	-	-	-	2.30	13.00
OR	0.20	0.40	0.10	0.20	0.50
AB	2.60	6.20	8.40	3.70	5.80
AN	38.10	37.00	46.10	42.50	33.00
NE	-	-	-	-	-
DI	35.20	22.60	27.20	36.40	20.10
HY	4.00	11.90	5.10	12.40	23.20
OL	17.20	16.90	10.30	-	-
MT	2.20	2.40	2.10	1.90	3.60
IL	0.30	0.30	0.30	0.30	0.50
AP	0.30	0.30	0.30	0.30	0.30

TABLE 4-13 AMPHIBOLE MAJORS TRACES AND NORMS

	813	815	816	818
PERCENT				
SIO2	51.52	51.21	51.76	51.36
AL2O3	1.23	4.30	4.62	4.21
FE2O3	10.64	10.16	9.65	9.47
MGO	22.29	20.46	19.75	20.99
CAO	13.27	12.51	12.26	12.44
NA2O	0.14	0.47	0.70	0.46
K2O	0.07	0.22	0.23	0.22
TIO2	0.17	0.59	0.56	0.59
MNO	0.39	0.21	0.20	0.19
S	-	-	-	-
P2O5	0.06	0.06	0.07	0.06
PPM				
BA	-	-	5	-
NB	-	6	6	-
ZR	-	27	33	-
Y	-	62	66	-
SR	-	23	52	-
RB	-	1	1	-
ZN	-	91	80	-
CU	32	172	55	215
NI	548	463	455	386
CR	567	1380	894	1065
CIPW NORM				
OR	0.40	1.30	1.40	1.30
AB	1.20	4.00	6.00	3.90
AN	2.50	9.00	9.40	8.60
DI	50.50	41.30	40.80	42.10
HY	33.40	32.80	32.20	29.80
OL	8.10	7.10	5.90	11.40
MT	3.40	3.20	3.00	1.10
IL	0.30	1.10	1.10	1.10
AP	0.10	0.20	0.20	0.10

TABLE 5-9 OLIVINES FROM DUNITES

	300C	300D	300E	300F	300G	300H	300I	* 304B	* 305B	* 305C
WEIGHT PERCENT OXIDE										
SIO2	40.35	40.87	40.93	40.40	40.62	40.35	40.24	40.25	40.86	41.15
TIO2	-	-	0.02	0.01	-	0.05	-	-	-	-
AL2O3	-	-	-	-	-	-	-	-	0.02	0.03
CR2O3	-	-	-	-	-	-	-	-	-	-
FEO	8.60	8.82	8.73	8.59	8.45	8.73	8.71	9.05	8.15	8.16
MNO	0.06	0.05	0.09	0.07	0.02	-	-	0.05	0.10	0.10
MGO	51.71	50.74	51.66	51.53	50.94	51.11	51.02	50.87	50.13	50.68
CAO	-	-	0.02	-	-	-	-	-	-	-
NA2O	-	-	-	-	-	-	-	-	-	-
K2O	-	-	-	-	-	-	-	-	-	-
NIO	0.19	0.16	0.20	0.24	0.13	0.17	0.27	0.43	0.36	0.18
TOTAL	100.92	100.65	101.65	100.84	100.17	100.42	100.24	100.65	99.62	100.31
STRUCTURAL FORMULA ON THE BASIS OF 4 OXYGENS										
SI	0.977	0.991	0.983	0.979	0.988	0.982	0.981	0.980	0.998	0.997
TI	0.000	0.000	0.000	0.000	0.000	0.001	0.000	0.000	0.000	0.000
AL	0.000	0.000	0.000	0.000	0.000	0.000	0.000	0.000	0.000	0.000
CR	0.000	0.000	0.000	0.000	0.000	0.000	0.000	0.000	0.000	0.000
FE2	0.174	0.180	0.175	0.174	0.172	0.177	0.177	0.184	0.166	0.166
MN	0.001	0.001	0.002	0.001	0.000	0.000	0.000	0.001	0.002	0.002
MG	1.866	1.834	1.850	1.861	1.847	1.853	1.854	1.846	1.826	1.831
CA	0.000	0.000	0.000	0.000	0.000	0.000	0.000	0.000	0.000	0.000
NA	0.000	0.000	0.000	0.000	0.000	0.000	0.000	0.000	0.000	0.000
K	0.000	0.000	0.000	0.000	0.000	0.000	0.000	0.000	0.000	0.000
NI	0.003	0.003	0.004	0.004	0.002	0.003	0.005	0.008	0.007	0.003
END MEMBER COMPOSITIONS										
MG	91.46	91.11	91.33	91.44	91.48	91.25	91.26	90.92	91.64	91.69
FE	8.54	8.88	8.66	8.55	8.52	8.75	8.74	9.07	8.35	8.30

* DUNITE - WEHRLITE

TABLE 5-9 OLIVINES FROM DUNITES

	310A*	310B*	310C*	310D*	311A	311B	311C	311D	311E	311F
WEIGHT PERCENT OXIDE										
SIO2	40.67	40.19	40.38	40.25	40.73	41.03	40.77	40.30	39.78	40.06
TIO2	-	-	-	0.02	0.01	0.04	0.02	-	-	-
AL2O3	-	-	-	-	0.04	0.06	0.06	0.03	0.05	0.02
CR2O3	-	-	-	-	-	-	-	-	-	-
FEO	9.33	9.19	9.20	9.13	9.41	9.26	8.99	9.62	9.45	9.25
MNO	0.13	0.18	0.11	0.16	0.11	0.13	0.19	0.13	0.19	0.17
MGO	50.22	50.22	49.17	50.24	49.21	49.50	50.14	49.70	49.74	49.50
CAO	-	-	-	0.05	-	0.02	0.01	-	-	-
NA2O	-	-	-	-	-	-	-	-	-	-
K2O	-	-	-	-	-	-	-	-	-	-
NIO	0.25	0.18	0.18	0.32	0.21	0.20	0.12	0.17	0.19	0.26
TOTAL	100.59	99.94	99.04	100.16	99.71	100.24	100.30	99.96	99.41	99.26
STRUCTURAL FORMULA ON THE BASIS OF 4 OXYGENS										
SI	0.990	0.985	0.997	0.984	0.999	1.000	0.993	0.988	0.982	0.989
TI	0.000	0.000	0.000	0.000	0.000	0.000	0.000	0.000	0.000	0.000
AL	0.000	0.000	0.000	0.000	0.001	0.002	0.001	0.001	0.001	0.000
CR	0.000	0.000	0.000	0.000	0.000	0.000	0.000	0.000	0.000	0.000
FE2	0.190	0.188	0.190	0.186	0.193	0.188	0.183	0.197	0.195	0.191
MN	0.002	0.003	0.002	0.003	0.002	0.002	0.004	0.002	0.004	0.003
MG	1.822	1.834	1.809	1.831	1.799	1.798	1.820	1.817	1.830	1.821
CA	0.000	0.000	0.000	0.001	0.000	0.000	0.000	0.000	0.000	0.000
NA	0.000	0.000	0.000	0.000	0.000	0.000	0.000	0.000	0.000	0.000
K	0.000	0.000	0.000	0.000	0.000	0.000	0.000	0.000	0.000	0.000
NI	0.005	0.003	0.003	0.006	0.004	0.004	0.002	0.003	0.003	0.005
END MEMBER COMPOSITIONS										
MG	90.56	90.68	90.49	90.25	90.31	90.50	90.85	90.20	90.37	90.50
FE	9.44	9.31	9.50	9.25	9.69	9.50	9.14	9.80	9.63	9.49

TABLE 5-9 OLIVINES FROM DUNITES

	311G	311H	311I	314A	314B	321A	321B	321C	321D	321E
WEIGHT PERCENT OXIDE										
SIO2	40.30	40.28	40.38	40.12	40.43	40.18	41.06	39.96	40.22	40.09
TIO2	0.02	0.02	0.06	-	-	-	-	-	0.03	-
AL2O3	0.04	0.11	0.12	0.04	0.04	0.08	0.06	0.09	0.03	0.05
CR2O3	-	-	-	-	-	-	-	-	-	-
FEO	9.01	9.44	9.12	8.94	9.10	10.16	10.20	9.88	9.93	9.87
MNO	0.12	0.14	0.22	0.03	0.08	0.12	0.11	0.11	0.18	0.18
MGO	50.47	49.57	50.40	48.88	49.18	49.43	49.62	49.12	49.57	50.52
CAO	-	-	0.06	-	-	-	0.01	-	-	-
NA2O	-	-	-	-	-	-	-	-	-	-
K2O	-	-	-	-	-	-	-	-	-	-
NIO	0.24	0.20	0.21	0.17	0.16	0.10	0.11	0.18	0.06	0.14
TOTAL	100.20	99.76	100.58	98.19	98.99	100.07	101.17	99.34	100.02	100.86
STRUCTURAL FORMULA ON THE BASIS OF 4 OXYGENS										
SI	0.984	0.989	0.983	0.998	0.998	0.986	0.996	0.988	0.987	0.977
TI	0.000	0.000	0.001	0.000	0.000	0.000	0.000	0.000	0.000	0.000
AL	0.001	0.003	0.003	0.001	0.001	0.002	0.001	0.002	0.001	0.001
CR	0.000	0.000	0.000	0.000	0.000	0.000	0.000	0.000	0.000	0.000
FE2	0.184	0.194	0.185	0.185	0.188	0.208	0.206	0.204	0.204	0.201
MN	0.002	0.003	0.004	0.000	0.001	0.002	0.002	0.002	0.003	0.004
MG	1.837	1.815	1.829	1.812	1.809	1.809	1.794	1.809	1.813	1.835
CA	0.000	0.000	0.001	0.000	0.000	0.000	0.000	0.000	0.000	0.000
NA	0.000	0.000	0.000	0.000	0.000	0.000	0.000	0.000	0.000	0.000
K	0.000	0.000	0.000	0.000	0.000	0.000	0.000	0.000	0.000	0.000
NI	0.004	0.004	0.004	0.003	0.003	0.002	0.002	0.003	0.001	0.002
END MEMBER COMPOSITIONS										
MG	90.89	90.34	90.78	90.69	90.59	89.66	89.66	89.85	89.89	90.12
FE	9.10	9.66	9.21	9.30	9.41	10.33	10.34	10.14	10.11	9.88

TABLE 5-9 OLIVINES FROM DUNITES

	502A	517C	517D	517E	517F	517G	517H	517I *	517J	528B
WEIGHT PERCENT OXIDE										
SIO2	40.62	41.01	40.71	40.78	40.80	40.25	40.69	40.94	40.80	41.10
TIO2	-	0.02	-	-	-	-	-	0.02	0.07	-
AL2O3	-	-	-	-	-	-	-	-	-	0.05
CR2O3	-	0.01	-	-	-	-	-	-	-	-
FEO	8.16	9.48	9.26	9.30	8.91	9.19	9.11	9.10	9.23	8.45
MNO	0.12	0.17	0.12	0.15	0.16	0.20	0.12	0.23	0.20	0.15
MGO	50.03	48.98	49.29	49.40	49.03	49.55	49.26	49.15	49.40	50.64
CAO	-	0.03	0.06	0.06	0.02	0.08	0.01	0.04	0.05	-
NA2O	-	-	0.02	-	0.01	0.01	0.03	0.03	0.02	-
K2O	-	-	-	-	-	-	-	-	-	-
NIO	0.27	0.20	0.23	0.24	0.23	0.23	0.21	0.36	0.22	0.24
TOTAL	99.21	99.89	99.70	99.92	99.16	99.51	99.44	99.88	100.00	100.62
STRUCTURAL FORMULA ON THE BASIS OF 4 OXYGENS										
SI	0.997	1.004	0.998	0.998	1.004	0.991	1.000	1.002	0.998	0.995
TI	0.000	0.000	0.000	0.000	0.000	0.000	0.000	0.000	0.001	0.000
AL	0.000	0.000	0.000	0.000	0.000	0.000	0.000	0.000	0.000	0.001
CR	0.000	0.000	0.000	0.000	0.000	0.000	0.000	0.000	0.000	0.000
FE2	0.167	0.194	0.190	0.190	0.183	0.189	0.187	0.186	0.189	0.171
MN	0.002	0.003	0.002	0.003	0.003	0.004	0.002	0.004	0.004	0.003
MG	1.830	1.788	1.802	1.803	1.799	1.818	1.804	1.793	1.802	1.828
CA	0.000	0.000	0.001	0.001	0.000	0.002	0.002	0.001	0.001	0.000
NA	0.000	0.000	0.001	0.000	0.000	0.000	0.001	0.002	0.001	0.000
K	0.000	0.000	0.000	0.000	0.000	0.000	0.000	0.000	0.000	0.000
NI	0.005	0.004	0.004	0.004	0.004	0.004	0.004	0.007	0.004	0.004
END MEMBER COMPOSITIONS										
MG	91.62	90.20	90.46	90.44	90.74	90.57	90.60	90.58	90.51	91.44
FE	8.38	9.79	9.54	9.55	9.25	9.42	9.40	9.41	9.49	8.60

TABLE 5-9 OLIVINES FROM DUNITES

	528C
WEIGHT PERCENT OXIDE	
SIO2	41.56
TIO2	-
AL2O3	0.03
CR2O3	-
FEO	8.33
MNO	0.12
MGO	50.54
CAO	-
NA2O	-
K2O	-
NIO	0.34
TOTAL	100.93
STRUCTURAL FORMULA ON THE BASIS OF 4 OXYGENS	
SI	1.003
TI	0.000
AL	0.000
CR	0.000
FE2	0.168
MN	0.003
MG	1.816
CA	0.000
NA	0.000
K	0.000
NI	0.006
END MEMBER COMPOSITIONS	
MG	91.53
FE	8.46

TABLE 5-10 OLIVINES FROM HARZBURGITES

	325B	1031D	1037B	1037C	1037D
WEIGHT PERCENT OXIDE					
SIO2	41.18	40.60	40.66	40.82	40.86
TIO2	-	-	-	0.05	-
AL2O3	-	0.02	-	-	-
CR2O3	-	-	-	-	-
FEO	8.23	9.21	9.02	8.57	8.47
MNO	0.03	0.06	0.08	0.14	0.09
MGO	49.55	48.50	49.09	50.38	50.21
CAO	0.02	-	-	-	-
NA2O	-	-	-	-	-
K2O	0.02	-	-	-	-
NIO	0.34	0.31	0.41	0.34	0.24
TOTAL	99.37	98.71	99.44	100.29	99.88
STRUCTURAL FORMULA ON THE BASIS 4 OXYGENS					
SI	1.008	1.005	1.004	0.993	0.997
TI	0.000	0.000	0.000	0.000	0.000
AL	0.000	0.000	0.000	0.000	0.000
CR	0.000	0.000	0.000	0.000	0.000
FE2	0.168	0.191	0.185	0.174	0.173
MN	0.000	0.001	0.001	0.003	0.002
MG	1.807	1.789	1.797	1.827	1.826
CA	0.000	0.000	0.000	0.000	0.000
NA	0.000	0.000	0.000	0.000	0.000
K	0.000	0.000	0.000	0.000	0.000
NI	0.006	0.006	0.006	0.006	0.005
END MEMBER COMPOSITIONS					
MG	91.50	90.40	90.70	91.30	91.35
FE	8.52	9.63	9.34	8.71	8.64

TABLE5-11 OLIVINES FROM WEHRLITES

	503C	802A	802B	803B	803C	804B	805A
WEIGHT PERCENT OXIDE							
SIO2	40.42	40.47	40.35	40.56	40.59	40.70	40.40
TIO2	0.04	0.01	0.04	-	-	-	-
AL2O3	-	-	-	-	-	-	-
CR2O3	-	-	-	-	-	-	-
FEO	9.41	9.29	9.43	11.01	11.20	10.93	11.15
MNO	0.04	0.01	0.01	0.10	0.13	0.12	0.10
MGO	48.70	49.15	47.99	47.58	46.24	48.25	49.47
CAO	-	0.02	0.06	0.02	-	0.02	0.01
NA2O	0.01	-	-	-	-	0.03	0.04
K2O	0.02	-	-	-	-	-	0.03
NIO	0.15	0.20	0.37	0.43	0.26	0.27	0.25
TOTAL	98.80	99.15	98.24	99.69	98.43	100.32	101.44
STRUCTURAL FORMULA ON THE BASIS 4 OXYGENS							
SI	1.000	0.998	1.005	1.003	1.016	0.999	0.984
TI	0.000	0.000	0.000	0.000	0.000	0.000	0.000
AL	0.000	0.000	0.000	0.000	0.000	0.000	0.000
CR	0.000	0.000	0.000	0.000	0.000	0.000	0.000
FE2	0.195	0.192	0.200	0.227	0.234	0.224	0.227
MN	0.001	0.000	0.000	0.002	0.003	0.002	0.002
MG	1.797	1.806	1.782	1.754	1.725	1.766	1.800
CA	0.000	0.000	0.002	0.000	0.000	0.000	0.000
NA	0.000	0.000	0.000	0.000	0.000	0.001	0.001
K	0.000	0.000	0.000	0.000	0.000	0.000	0.001
NI	0.003	0.004	0.007	0.008	0.005	0.005	0.005
END MEMBER COMPOSITIONS							
MG	90.21	90.41	90.07	88.50	88.03	88.72	88.77
FE	9.76	9.60	9.93	11.49	11.97	11.27	11.22

TABLE5-12 OLIVINES FROM OLIVINE PYROXENITES

	554A	1014(3)A	1014(3)D	1014(3)E
WEIGHT PERCENT OXIDE				
SIO2	39.90	39.80	39.67	40.36
TIO2	–	0.03	0.02	0.02
AL2O3	–	–	–	–
CR2O3	–	–	0.03	0.01
FEO	12.13	13.71	13.39	13.37
MNO	0.13	0.21	0.23	0.25
MGO	46.04	45.78	45.42	45.52
CAO	0.09	0.02	0.02	0.05
NA2O	–	0.01	–	–
K2O	0.03	0.01	0.01	0.01
NIO	0.17	0.15	0.11	0.14
TOTAL	98.49	99.71	99.10	99.73
STRUCTURAL FORMULA ON THE BASIS 4 OXYGENS				
SI	1.004	0.997	1.003	1.008
TI	0.000	0.000	0.000	0.000
AL	0.000	0.000	0.000	0.000
CR	0.000	0.000	0.000	0.000
FE2	0.255	0.287	0.281	0.279
MN	0.002	0.004	0.005	0.005
MG	1.727	1.709	1.702	1.690
CA	0.002	0.000	0.000	0.001
NA	0.000	0.000	0.000	0.000
K	0.000	0.000	0.000	0.000
NI	0.003	0.003	0.002	0.002
END MEMBER COMPOSITIONS				
MG	87.12	85.61	85.80	85.85
FE	12.88	14.39	14.19	14.15

TABLE 5:13 OLIVINES FROM OLIVINE GABBROS

	119B	232A	523B	523C	232B	106A	106B	104A A	564B	528B A
WEIGHT PERCENT OXIDE										
SIO2	39.52	39.49	38.78	37.99	39.96	37.90	37.85	37.57	37.56	35.28
TIO2	0.02	0.02	0.04	0.04	0.07	0.05	0.05	0.02	0.04	0.07
AL2O3	-	-	-	-	-	0.04	-	0.02	0.08	-
CR2O3	0.02	0.02	0.04	0.01	0.04	0.04	0.05	0.04	-	0.05
FEO	19.17	17.06	23.72	25.55	16.81	26.38	26.69	26.22	27.04	31.01
MNO	0.26	0.27	0.33	0.40	0.23	0.49	0.45	0.37	0.56	0.39
MGO	40.60	43.17	36.92	37.11	42.40	34.11	34.29	36.80	36.77	32.64
CAO	0.02	0.01	-	0.01	0.09	0.09	0.09	0.05	0.12	-
NA2O	0.02	-	-	-	-	0.16	-	-	-	-
K2O	0.02	0.01	0.02	0.01	0.03	0.02	0.01	0.02	0.02	0.02
NIO	0.21	0.14	0.10	0.11	0.25	0.14	0.10	0.06	0.09	0.07
TOTAL	100.04	100.21	99.96	101.23	99.89	99.43	99.59	101.17	102.29	99.53
STRUCTURAL FORMULA ON THE BASIS 4 OXYGENS										
SI	1.010	0.999	1.014	0.992	1.012	1.012	1.010	0.985	0.979	0.968
TI	0.000	0.000	0.000	0.000	0.001	0.001	0.001	0.000	0.000	0.001
AL	0.000	0.000	0.000	0.000	0.000	0.001	0.000	0.000	0.002	0.000
CR	0.000	0.000	0.000	0.000	0.000	0.000	0.001	0.000	0.000	0.001
FE2	0.410	0.361	0.519	0.558	0.356	0.589	0.596	0.575	0.589	0.712
MN	0.005	0.005	0.007	0.008	0.005	0.011	0.010	0.008	0.012	0.009
MG	1.555	1.628	1.439	1.444	1.601	1.358	1.364	1.439	1.428	1.335
CA	0.000	0.000	0.000	0.000	0.002	0.002	0.002	0.001	0.003	0.000
NA	0.000	0.000	0.000	0.000	0.000	0.008	0.000	0.000	0.000	0.000
K	0.000	0.000	0.000	0.000	0.000	0.000	0.000	0.000	0.000	0.000
NI	0.004	0.003	0.002	0.002	0.005	0.003	0.002	0.001	0.002	0.001
END MEMBER COMPOSITIONS										
MG	79.13	81.84	73.50	72.13	81.80	69.74	69.59	71.43	70.78	65.22
FE	20.86	18.15	26.50	27.87	18.19	30.26	30.40	28.56	29.21	34.77

TABLE 5-14 ORTHOPYROXENES FROM HARZBURGITES

	325A	325B	325C	328B	328C
WEIGHT PERCENT OXIDE					
SIO2	56.18	56.47	56.94	55.69	55.76
TIO2	-	-	-	0.01	-
AL2O3	1.71	1.70	1.59	2.18	2.03
CR2O3	0.47	0.53	0.47	0.49	0.44
FEO	5.15	5.26	5.11	5.64	5.32
MNO	-	0.02	-	-	-
MGO	35.22	35.12	35.01	34.84	35.24
CAO	0.58	0.76	0.46	1.14	0.94
NA2O	0.03	-	0.01	-	0.02
K2O	0.02	0.02	0.03	0.02	0.03
NIO	0.07	0.03	0.08	0.03	-
TOTAL	99.43	99.95	99.71	100.06	99.77
STRUCTURAL FORMULA ON THE BASIS OF 6 OXYGENS					
SI	1.943	1.944	1.960	1.923	1.926
TI	0.000	0.000	0.000	0.000	0.000
AL	0.069	0.069	0.064	0.088	0.082
CR	0.013	0.014	0.013	0.013	0.012
FE2	0.149	0.152	0.147	0.163	0.154
MN	0.000	0.000	0.000	0.000	0.000
MG	1.816	1.802	1.796	1.793	1.815
CA	0.021	0.028	0.175	0.042	0.035
NA	0.002	0.000	0.000	0.000	0.001
K	0.001	0.001	0.001	0.001	0.001
NI	0.002	0.000	0.002	0.001	0.000
END MEMBER COMPOSITIONS					
CA	1.07	1.44	0.89	2.11	1.74
MG	91.42	90.86	91.59	89.73	90.58
FE	7.50	7.67	7.51	8.15	7.67

TABLE5:15 ORTHOPYROXENES FROM OLIVINE PYROXENITES

	1027C	1028A
WEIGHT PERCENT OXIDE		
SIO2	55.78	55.97
TIO2	0.11	0.01
AL2O3	1.62	1.72
CR2O3	0.54	0.43
FEO	8.57	8.04
MNO	0.09	0.11
MGO	31.83	31.62
CAO	1.00	0.85
NA2O	0.02	0.01
K2O	0.02	0.03
NIO	-	0.02
TOTAL	99.77	98.80
STRUCTURAL FORMULA ON THE BASIS OF 6 OXYGENS		
SI	1.953	1.970
TI	0.003	0.000
AL	0.070	0.070
CR	0.010	0.012
FE2	0.250	0.236
MN	0.002	0.003
MG	1.660	1.659
CA	0.037	0.032
NA	0.001	0.000
K	0.001	0.001
NI	0.000	0.000
END MEMBER COMPOSITIONS		
CA	1.93	1.65
MG	85.20	86.06
FE	12.86	12.28

TABLE 16 ORTHOPYROXENES FROM OLIVINE GABBROS

	119B	232A
WEIGHT PERCENT OXIDE		
SIO2	54.56	55.54
TIO2	0.11	0.30
AL2O3	1.43	1.13
CR2O3	0.11	0.10
FEO	11.85	11.31
MNO	0.28	0.26
MGO	27.93	29.41
CAO	1.60	1.54
NA2O	–	0.05
K2O	0.01	0.01
NIO	0.04	0.09
TOTAL	97.92	99.74
STRUCTURAL FORMULA ON THE BASIS OF 6 OXYGENS		
SI	1.978	1.972
TI	0.003	0.008
AL	0.060	0.047
CR	0.003	0.002
FE2	0.359	0.336
MN	0.008	0.007
MG	1.509	1.556
CA	0.062	0.058
NA	0.000	0.003
K	0.000	0.000
NI	0.001	0.002
END MEMBER COMPOSITIONS		
CA	3.21	3.00
MG	78.17	79.78
FE	18.60	17.21

TABLE 5.17 ORTHOPYROXENES FROM NORITES

	139A	139B	852A	221A
WEIGHT PERCENT OXIDE				
SIO2	54.40	53.88	53.04	52.45
TIO2	0.16	0.10	0.07	0.12
AL2O3	1.42	1.46	1.30	1.45
CR2O3	-	-	0.04	0.06
FEO	18.26	17.94	16.83	16.49
MNO	0.41	0.38	0.32	0.41
MGO	25.27	25.17	25.69	25.59
CAO	1.33	3.18	1.72	1.31
NA2O	0.02	-	0.01	0.01
K2O	0.04	0.03	0.02	0.02
NIO	0.02	-	0.11	0.03
TOTAL	101.32	102.14	99.14	97.94
STRUCTURAL FORMULA ON THE BASIS OF 6 OXYGENS				
SI	1.962	1.936	1.951	1.949
TI	0.004	0.002	0.002	0.003
AL	0.060	0.062	0.056	0.063
CR	0.000	0.000	0.001	0.001
FE2	0.551	0.539	0.517	0.512
MN	0.012	0.011	0.001	0.013
MG	1.358	1.349	1.408	1.417
CA	0.051	0.122	0.067	0.052
NA	0.001	0.000	0.000	0.000
K	0.001	0.001	0.001	0.001
NI	0.000	0.000	0.003	0.001
END MEMBER COMPOSITIONS				
CA	2.61	6.09	3.40	2.63
MG	69.29	67.08	70.63	71.50
FE	28.09	26.82	25.96	25.86

TABLE5-18 CLINOPYROXENES FROM WEHRLITES

	503C	804B	804C
WEIGHT PERCENT OXIDE			
SIO2	51.47	52.32	52.04
TIO2	-	0.15	0.14
AL2O3	3.38	3.86	3.60
CR2O3	0.98	1.15	1.13
FEO	2.11	3.42	3.02
MNO	-	0.01	0.04
MGO	17.39	17.67	17.41
CAO	22.41	19.17	21.20
NA2O	0.23	0.27	0.21
K2O	0.03	0.02	0.03
NIO	0.02	0.04	-
TOTAL	98.02	98.09	98.82
STRUCTURAL FORMULA ON THE BASIS OF 6 OXYGENS			
SI	1.906	1.924	1.910
TI	0.000	0.004	0.004
AL	0.147	0.167	0.156
CR	0.028	0.033	0.033
FE2	0.065	0.105	0.093
MN	0.000	0.000	0.001
MG	0.959	0.968	0.952
CA	0.889	0.755	0.834
NA	0.016	0.019	0.015
K	0.001	0.001	0.001
NI	0.000	0.001	0.000
END MEMBER COMPOSITIONS			
CA	46.45	41.30	44.37
MG	50.12	52.93	50.68
FE	3.41	5.76	4.94

TABLE 5:19 CLINOPYROXENES FROM OLIVINE PYROXENITES

	554A	554B	554C	1014(3)A	1030B(B)	1030B(C)	553A
WEIGHT PERCENT OXIDE							
SIO2	52.51	53.64	53.11	53.43	51.49	52.16	51.74
TIO2	–	0.07	0.05	0.08	0.09	0.11	0.12
AL2O3	1.99	1.98	1.89	2.31	2.15	1.85	2.26
CR2O3	0.64	0.62	0.67	0.50	0.37	0.35	0.70
FEO	3.87	3.30	3.68	3.86	3.81	3.80	2.95
MNO	0.03	0.01	0.06	0.16	0.15	0.13	0.01
MGO	18.69	16.24	17.76	17.81	17.20	16.76	16.54
CAO	21.11	22.61	21.13	21.88	24.45	23.32	23.21
NA2O	0.11	0.19	0.11	0.14	0.12	0.17	0.14
K2O	0.04	0.03	0.03	0.02	0.02	0.02	0.03
NIO	0.06	–	–	0.07	0.05	–	0.03
TOTAL	99.05	100.69	98.49	100.28	99.89	98.68	97.74
STRUCTURAL FORMULA ON THE BASIS OF 6 OXYGENS							
SI	1.930	1.940	1.957	1.940	1.899	1.936	1.932
TI	0.000	0.002	0.001	0.022	0.002	0.003	0.003
AL	0.086	0.084	0.080	0.099	0.093	0.081	0.099
CR	0.018	0.017	0.019	0.014	0.010	0.010	0.020
FE2	0.119	0.099	0.110	0.118	0.117	0.118	0.092
MN	0.000	0.000	0.001	0.005	0.005	0.004	0.000
MG	1.024	0.960	0.975	0.963	0.945	0.928	0.920
CA	0.831	0.875	0.834	0.850	0.966	0.930	0.930
NA	0.008	0.013	0.008	0.010	0.008	0.012	0.010
K	0.002	0.001	0.001	0.001	0.001	0.000	0.001
NI	0.002	0.000	0.000	0.002	0.001	0.000	0.000
END MEMBER COMPOSITIONS							
CA	42.10	44.73	43.38	44.03	47.62	46.97	47.84
MG	51.86	50.17	50.72	49.86	46.58	47.03	47.40
FE	6.02	5.09	5.90	6.10	5.79	5.97	4.75

TABLE 5.20 CLINOPYROXENES FROM OLIVINE GABBROS

	555A	555B	232A	232B	232C	232D	232E	106A	106B	539B
WEIGHT PERCENT OXIDE										
SIO2	52.36	52.41	52.52	52.01	53.54	51.56	51.87	52.56	51.71	52.49
TIO2	0.54	0.45	0.21	0.47	0.28	0.24	0.24	0.62	0.60	0.05
AL2O3	3.13	3.04	2.50	2.30	3.20	3.18	3.10	2.47	2.61	1.70
CR2O3	0.36	0.31	0.33	0.40	1.03	1.14	0.98	0.07	0.10	0.53
FEO	6.90	7.35	4.18	5.44	3.67	4.45	4.49	10.04	9.25	3.44
MNO	0.22	0.21	0.13	0.16	0.13	0.11	0.15	0.22	0.25	0.15
MGO	14.77	14.96	17.15	16.52	16.41	16.01	16.17	15.24	14.95	17.36
CAO	21.99	21.37	22.17	21.28	21.65	21.45	21.85	20.10	20.56	23.64
NA2O	0.41	0.49	0.25	0.25	0.27	0.22	0.25	0.31	0.34	0.17
K2O	0.03	0.02	0.01	0.02	0.02	0.02	0.02	0.02	0.02	0.01
NIO	0.08	0.04	0.09	0.04	0.11	0.06	0.02	0.18	0.11	-
TOTAL	100.79	100.66	99.07	98.91	99.52	98.44	99.15	101.83	100.49	99.54
STRUCTURAL FORMULA ON THE BASIS OF 6 OXYGENS										
SI	1.920	1.920	1.934	1.930	1.925	1.920	1.916	1.925	1.918	1.931
TI	0.015	0.012	0.005	0.013	0.008	0.007	0.006	0.017	0.016	0.002
AL	0.135	0.130	0.108	0.101	0.140	0.140	0.135	0.106	0.114	0.073
CR	0.010	0.009	0.009	0.012	0.029	0.033	0.030	0.002	0.003	0.015
FE2	0.210	0.226	0.130	0.170	0.118	0.138	0.139	0.307	0.287	0.105
MN	0.007	0.006	0.004	0.005	0.004	0.003	0.004	0.007	0.008	0.004
MG	0.800	0.820	0.941	0.913	0.896	0.886	0.890	0.832	0.826	0.952
CA	0.860	0.840	0.855	0.846	0.849	0.854	0.865	0.769	0.817	0.931
NA	0.029	0.035	0.018	0.018	0.020	0.016	0.018	0.022	0.024	0.012
K	0.001	0.001	0.000	0.000	0.000	0.000	0.000	0.000	0.000	0.000
NI	0.002	0.001	0.002	0.001	0.003	0.002	0.000	0.005	0.003	0.000
END MEMBER COMPOSITIONS										
CA	45.88	44.59	44.43	43.87	45.58	45.46	45.67	40.90	42.32	46.84
MG	42.67	43.43	48.88	47.36	48.05	47.18	47.00	43.14	42.81	47.64
FE	11.24	11.97	6.69	8.80	6.36	7.36	7.32	15.95	14.87	5.32

TABLE 5-20 CLINOPYROXENES FROM OLIVINE GABBROS

	539C
WEIGHT PERCENT OXIDE	
SIO2	52.12
TIO2	0.17
AL2O3	2.29
CR2O3	0.41
FEO	3.87
MNO	0.18
MGO	17.52
CAO	23.04
NA2O	0.15
K2O	0.01
NIO	0.06
TOTAL	99.82
STRUCTURAL FORMULA ON THE BASIS OF 6 OXYGENS	
SI	1.913
TI	0.004
AL	0.099
CR	0.012
FE2	0.118
MN	0.005
MG	0.958
CA	0.906
NA	0.010
K	0.000
NI	0.002
END MEMBER COMPOSITIONS	
CA	45.69
MG	48.32
FE	5.99

TABLE521 CLINOPYROXENES FROM NORMAL GABBROS

	859A	526A(b)	231A	231B
WEIGHT PERCENT OXIDE				
SIO2	52.49	52.17	52.67	52.10
TIO2	0.58	0.62	0.23	0.29
AL2O3	2.65	2.70	2.31	2.35
CR2O3	0.08	0.07	0.14	0.17
FEO	8.00	6.40	5.16	4.68
MNO	0.27	0.23	0.14	0.14
MGO	14.48	14.17	16.87	16.74
CAO	22.06	21.96	21.09	21.95
NA2O	0.32	0.30	0.24	0.27
K2O	0.02	0.07	0.02	0.02
NIO	0.03	0.09	0.10	0.07
TOTAL	100.97	98.80	98.98	98.78
STRUCTURAL FORMULA ON THE BASIS OF 6 OXYGENS				
SI	1.931	1.947	1.950	1.931
TI	0.016	0.017	0.006	0.008
AL	0.115	0.118	0.100	0.102
CR	0.002	0.002	0.004	0.005
FE2	0.246	0.200	0.159	0.145
MN	0.008	0.007	0.004	0.004
MG	0.794	0.788	0.928	0.924
CA	0.869	0.878	0.834	0.872
NA	0.022	0.022	0.017	0.019
K	0.001	0.005	0.001	0.001
NI	0.001	0.002	0.003	0.002
END MEMBER COMPOSITIONS				
CA	45.54	47.05	43.42	44.90
MG	41.56	42.22	48.29	47.62
FE	12.89	10.72	8.28	7.47

TABLE 5-22 CLINOPYROXENE FROM HYPERSTHENE GABBRO

	180A
WEIGHT PERCENT OXIDE	
SIO2	52.31
TIO2	0.17
AL2O3	2.15
CR2O3	0.25
FEO	9.35
MNO	0.27
MGO	17.76
CAO	17.27
NA2O	0.02
K2O	-
NIO	-
TOTAL	99.55
STRUCTURAL FORMULA ON THE BASIS OF 6 OXYGENS	
SI	1.937
TI	0.004
AL	0.094
CR	0.007
FE2	0.289
MN	0.008
MG	0.980
CA	0.685
NA	0.001
K	0.000
NI	0.000
END MEMBER COMPOSITIONS	
CA	35.06
MG	50.13
FE	14.81

TABLE 5-23 PLAGIOCLASES FROM ANORTHOSITES

	160A	160B
WEIGHT PERCENT OXIDE		
SIO2	44.32	44.80
TIO2	0.05	-
AL2O3	34.15	34.16
FEO	0.54	0.20
MGO	-	0.07
CAO	18.79	18.44
K2O	0.01	0.01
NA2O	0.74	0.78
TOTAL	98.61	98.50
STRUCTURAL FORMULA ON THE BASIS OF 8 OXYGENS		
SI	2.080	2.097
TI	0.001	0.000
AL	1.890	1.886
FE2	0.021	0.007
MG	0.000	0.004
CA	0.945	0.925
K	0.001	0.001
NA	0.067	0.070
END MEMBER COMPOSITIONS		
AB	6.64	7.09
AN	93.30	92.83
OR	0.08	0.08

TABLE 5.24 PLAGIOCLASES FROM NORMAL GABBROS

	859A	526A(A)	231A	231B
WEIGHT PERCENT OXIDE				
SIO2	48.70	47.30	44.76	46.48
TIO2	0.04	0.05	0.04	0.06
AL2O3	32.39	33.84	32.72	33.40
FEO	0.27	0.25	0.41	0.45
MGO	-	0.01	0.02	-
CAO	16.33	16.99	17.82	16.61
K2O	0.01	0.01	0.02	0.02
NA2O	2.16	1.45	1.32	1.62
TOTAL	99.96	99.95	97.17	98.74
STRUCTURAL FORMULA ON THE BASIS OF 8 OXYGENS				
SI	2.231	2.169	2.128	2.162
TI	0.001	0.002	0.001	0.002
AL	1.750	1.830	1.834	1.832
FE2	0.010	0.010	0.016	0.017
MG	0.000	0.001	0.001	0.000
CA	0.801	0.835	0.907	0.828
K	0.000	0.000	0.001	0.001
NA	0.192	0.130	0.122	0.146
END MEMBER COMPOSITIONS				
AB	19.33	13.37	11.52	14.97
AN	80.59	86.55	88.08	84.88
OR	0.08	0.07	0.11	0.15

TABLE 5-25 PLAGIOCLASES FROM CUMULATE NORITES

	139A	139B	139C	131A	852A
WEIGHT PERCENT OXIDE					
SIO2	44.74	44.89	45.02	43.83	43.94
TIO2	-	-	-	-	0.05
AL2O3	34.38	35.12	34.28	34.57	33.36
FEO	0.46	0.33	0.45	0.57	0.39
MGO	-	-	-	0.06	-
CAO	19.21	19.52	18.94	19.27	19.90
K2O	0.04	0.03	0.03	0.01	0.01
NA2O	0.75	0.77	0.70	1.09	0.55
TOTAL	99.57	100.66	99.42	99.47	98.22
STRUCTURAL FORMULA ON THE BASIS OF 8 OXYGENS					
SI	2.080	2.065	2.093	2.048	2.077
TI	0.000	0.000	0.000	0.000	0.002
AL	1.886	1.906	1.900	1.905	1.860
FE2	0.017	0.012	0.017	0.022	0.015
MG	0.000	0.000	0.000	0.004	0.000
CA	0.957	0.963	0.943	0.965	1.008
K	0.002	0.002	0.002	0.000	0.000
NA	0.067	0.070	0.063	0.099	0.050
END MEMBER COMPOSITIONS					
AB	6.60	6.65	6.23	9.30	4.74
AN	93.21	93.17	93.57	90.62	95.22
OR	0.21	0.18	0.20	0.06	0.05

TABLE 5-26 PLAGIOCLASES FROM CUMULATE OLIVINE GABBROS

	523E	232A	232B	106A	557A	104A A	564A	539A	113A	526B A
WEIGHT PERCENT OXIDE										
SIO2	48.62	45.36	45.66	48.82	48.32	48.89	47.50	43.20	44.69	47.48
TIO2	0.01	0.15	0.03	0.04	0.05	0.03	0.16	-	-	0.05
AL2O3	32.45	33.80	33.14	31.52	32.48	31.88	33.07	35.52	34.72	32.14
FEO	0.96	0.41	0.49	0.73	0.20	0.47	0.17	0.11	0.38	0.18
MGO	0.14	0.08	0.26	0.03	-	0.02	-	0.04	0.04	-
CAO	15.39	18.04	17.95	16.37	16.37	15.91	16.14	20.09	19.40	17.01
K2O	0.03	0.02	0.02	0.02	0.01	0.01	0.02	0.01	0.01	0.01
NA2O	2.61	1.17	1.13	2.39	2.21	2.47	2.63	0.33	0.51	2.06
TOTAL	100.28	99.09	98.73	99.96	99.72	99.71	99.70	99.39	99.75	98.98
STRUCTURAL FORMULA ON THE BASIS OF 8 OXYGENS										
SI	2.225	2.112	2.133	2.244	2.220	2.246	2.187	2.017	2.073	2.204
TI	0.000	0.005	0.001	0.001	0.002	0.001	0.005	0.000	0.000	0.001
AL	1.751	1.857	1.826	1.709	1.759	1.727	1.796	1.956	1.899	1.759
FE2	0.036	0.016	0.019	0.028	0.007	0.018	0.006	0.004	0.015	0.007
MG	0.009	0.006	0.018	0.002	0.000	0.001	0.000	0.003	0.002	0.000
CA	0.755	0.900	0.898	0.806	0.806	0.783	0.796	1.005	0.964	0.846
K	0.001	0.001	0.001	0.001	0.000	0.000	0.000	0.000	0.000	0.000
NA	0.232	0.105	0.102	0.213	0.197	0.220	0.235	0.030	0.045	0.185
END MEMBER COMPOSITIONS.										
AB	23.47	10.47	10.19	20.87	19.62	21.94	22.77	2.88	4.50	17.98
AN	76.37	89.39	89.70	79.02	80.31	77.98	77.14	97.05	95.43	81.98
OR	0.15	0.13	0.11	0.11	0.06	0.06	0.08	0.06	0.07	0.04

TABLE 5-26 PLAGIOCLASES FROM CUMULATE OLIVINE GABBROS

	555A	556A	556B	556C	119A	119B	523A	523B	523C	523D
WEIGHT PERCENT OXIDE										
SIO2	47.68	47.25	47.36	47.25	44.74	43.77	47.00	50.25	48.04	48.62
TIO2	0.05	0.02	0.05	0.02	0.04	0.04	0.16	0.07	0.03	0.02
AL2O3	32.26	32.60	31.98	32.60	34.83	34.44	30.81	31.58	31.92	32.18
FEO	0.18	0.22	0.24	0.22	0.29	0.29	2.15	0.31	1.36	1.32
MGO	0.04	-	0.01	-	0.02	0.02	0.90	0.02	0.96	1.16
CAO	16.59	17.01	16.43	17.01	19.29	19.04	14.75	14.82	14.53	14.60
K2O	0.02	0.01	0.02	0.01	0.02	0.02	0.02	0.02	0.02	0.03
NA2O	2.45	1.87	2.06	1.91	0.41	0.63	2.19	2.60	2.69	2.60
TOTAL	99.29	99.02	98.16	99.06	99.71	98.28	98.08	99.68	99.81	100.65
STRUCTURAL FORMULA ON THE BASIS OF 8 OXYGENS										
SI	2.206	2.192	2.213	2.190	2.079	2.061	2.213	2.295	2.214	2.218
TI	0.001	0.000	0.001	0.000	0.001	0.001	0.006	0.002	0.001	0.000
AL	1.760	1.780	1.760	1.780	1.904	1.913	1.711	1.700	1.735	1.732
FE2	0.006	0.008	0.009	0.008	0.010	0.010	0.084	0.012	0.052	0.050
MG	0.002	0.000	0.000	0.000	0.001	0.001	0.063	0.001	0.066	0.080
CA	0.820	0.845	0.822	0.845	0.958	0.960	0.744	0.725	0.717	0.714
K	0.001	0.000	0.001	0.000	0.001	0.001	0.001	0.001	0.001	0.001
NA	0.219	0.168	0.186	0.172	0.037	0.057	0.200	0.230	0.240	0.230
END MEMBER COMPOSITIONS										
AB	21.05	16.61	18.46	16.89	3.70	5.66	21.16	24.06	25.04	24.31
AN	78.80	83.31	81.39	83.03	96.19	94.24	78.68	75.83	74.82	75.52
OR	0.14	0.07	0.14	0.07	0.10	0.09	0.15	0.10	0.13	0.16

TABLE 5·27 PLAGIOCLASE FROM CUMULATE OLIVINE PYROXENITE

1030B(A)

WEIGHT PERCENT OXIDE

SIO2	42.77
TIO2	0.01
AL2O3	34.02
FEO	0.25
MGO	0.18
CAO	20.75
K2O	0.02
NA2O	0.29
TOTAL	98.42

STRUCTURAL FORMULA ON THE BASIS OF 8 OXYGENS

SI	2.026
TI	0.000
AL	1.901
FE2	0.010
MG	0.013
CA	1.053
K	0.001
NA	0.026

END MEMBER COMPOSITIONS

AB	2.47
AN	97.43
OR	0.09

TABLE 5.28 PLAGIOCLASE FROM PLAGIOCLASE BEARING PERIDOTITE

	315A
WEIGHT PERCENT OXIDE	
SIO2	45.90
TIO2	0.04
AL2O3	35.03
FEO	0.08
MGO	-
CAO	18.63
K2O	0.01
NA2O	1.23
TOTAL	100.94
STRUCTURAL FORMULA ON THE BASIS OF 8 OXYGENS	
SI	2.097
TI	0.001
AL	1.887
FE2	0.003
MG	0.000
CA	0.912
K	0.000
NA	0.108
END MEMBER COMPOSITIONS	
AB	10.62
AN	89.31
OR	0.06

TABLE 5.29 SPINELS FROM DUNITES

	546A	546B
WEIGHT PERCENT OXIDE		
SIO2	-	-
TIO2	0.29	0.21
AL2O3	28.03	12.64
CR2O3	36.65	52.76
FE2O3	4.40	4.41
FEO	21.20	20.26
MNO	0.46	0.55
MGO	9.92	8.52
CAO	-	-
NA2O	-	-
K2O	-	-
NIO	0.02	0.22
TOTAL	101.19	99.57
STRUCTURAL FORMULA ON THE BASIS OF 32 OXYGENS		
SI	0.000	0.000
TI	0.053	0.042
AL	8.041	3.959
CR	7.048	11.076
FE3	0.804	0.881
FE2	4.314	4.500
MN	0.095	0.124
MG	3.598	3.371
CA	0.000	0.000
NA	0.000	0.000
K	0.000	0.000
NI	0.046	0.046

TABLE5-30 SPINELS FROM HARZBURGITES

	325B	324A
WEIGHT PERCENT OXIDE		
SIO2	-	-
TIO2	-	0.20
AL2O3	18.70	25.37
CR2O3	46.15	33.78
FE2O3	7.60	9.32
FEO	12.57	17.84
MNO	0.66	0.42
MGO	14.03	11.21
CAO	-	-
NA2O	-	-
K2O	-	-
NIO	0.18	0.18
TOTAL	99.89	98.33
STRUCTURAL FORMULA ON THE BASIS OF 32 OXYGENS		
SI	0.000	0.000
TI	0.000	0.037
AL	5.491	7.486
CR	9.065	6.682
FE3	1.424	1.755
FE2	2.617	3.732
MN	0.139	0.089
MG	5.206	4.179
CA	0.000	0.000
NA	0.000	0.000
K	0.000	0.000
NI	0.036	0.037

TABLE 5-31 SPINELS FROM WEHRLITES

	319A	318A	532A	532B
WEIGHT PERCENT OXIDE				
SIO2	-	-	-	-
TIO2	0.25	0.20	0.21	0.32
AL2O3	29.40	23.67	26.69	26.98
CR2O3	31.75	36.19	36.24	35.78
FE2O3	6.53	8.71	4.94	6.23
FEO	19.89	19.71	20.72	20.20
MNO	0.40	0.48	0.42	0.43
MGO	10.44	9.93	9.76	10.35
CAO	-	-	-	-
NA2O	-	-	-	-
K2O	-	-	-	-
NIO	0.25	0.20	0.17	0.23
TOTAL	98.90	99.10	99.35	100.51
STRUCTURAL FORMULA ON THE BASIS OF 32 OXYGENS				
SI	0.000	0.000	0.000	0.000
TI	0.046	0.038	0.039	0.058
AL	8.525	7.046	7.879	7.800
CR	6.172	7.221	7.118	6.934
FE3	1.208	1.654	0.923	1.148
FE2	4.090	4.160	4.305	4.142
MN	0.082	0.102	0.087	0.090
MG	3.824	3.735	3.612	3.780
CA	0.000	0.000	0.000	0.000
NA	0.000	0.000	0.000	0.000
K	0.000	0.000	0.000	0.000
NI	0.049	0.041	0.034	0.046

TABLE 5-32 SPINEL FROM PLAGIOCLASE PERIDOTITE

	3158
WEIGHT PERCENT OXIDE	
SIO2	0.56
TIO2	0.14
AL2O3	30.62
CR2O3	34.86
FE2O3	2.02
FEO	17.15
MNO	0.39
MGO	12.78
CAO	0.02
NA2O	0.08
K2O	0.02
NIO	0.24
TOTAL	98.88
STRUCTURAL FORMULA ON THE BASIS OF 32 OXYGENS	
SI	0.135
TI	0.024
AL	8.679
CR	6.624
FE3	0.366
FE2	3.447
MN	0.080
MG	4.576
CA	0.004
NA	0.036
K	0.007
NI	0.046

TABLE 5-33 SPINELS FROM SHEARED TALCOSE SERPENTINITE

	537A	537B	537C
WEIGHT PERCENT OXIDE			
SIO2	0.13	0.09	0.09
TIO2	0.21	0.24	0.20
AL2O3	30.14	27.20	27.87
CR2O3	31.33	32.08	30.94
FE2O3	5.62	9.01	8.09
FEO	20.22	19.64	20.10
MNO	0.42	0.56	0.37
MGO	10.35	10.43	9.91
CAO	-	-	0.05
NA2O	0.11	0.12	0.02
K2O	0.03	0.04	0.02
NIO	0.22	0.28	0.30
TOTAL	98.79	99.68	97.95
STRUCTURAL FORMULA ON THE BASIS OF 32 OXYGENS			
SI	0.033	0.023	0.023
TI	0.040	0.044	0.037
AL	8.723	7.917	8.228
CR	6.080	6.257	6.122
FE3	1.038	1.673	1.524
FE2	4.150	4.052	4.209
MN	0.087	0.116	0.078
MG	3.784	3.835	3.697
CA	0.000	0.000	0.013
NA	0.051	0.056	0.000
K	0.007	0.012	0.007
NI	0.043	0.054	0.061

TABLE 5-34 REPRESENTATIVE SPINEL ANALYSES FROM DUNITES

	300A	300B	304A	305A	528A	531A	531B	517A	517B
WEIGHT PERCENT OXIDE									
SIO2	0.01	0.07	–	–	–	–	0.09	0.05	–
TIO2	0.34	0.36	0.35	0.28	0.19	0.21	0.05	0.25	0.12
AL2O3	13.36	12.33	23.66	14.37	21.39	18.60	18.50	23.60	25.46
CR2O3	47.07	47.24	39.76	47.13	35.68	39.72	42.52	37.77	36.54
FE2O3	8.71	9.93	5.62	9.64	12.80	10.64	8.53	7.44	7.12
FEO	20.62	20.71	18.86	19.01	18.00	20.62	21.48	18.25	18.00
MNO	0.50	0.51	0.43	0.52	0.50	0.54	0.53	0.50	0.46
MGO	8.68	8.27	10.83	9.77	10.80	8.74	8.41	10.90	11.18
CAO	0.02	0.04	–	–	–	–	0.04	–	0.02
NA2O	–	–	–	–	–	–	–	0.07	0.07
K2O	–	–	–	–	–	–	–	–	–
NIO	0.20	0.31	0.20	0.32	0.33	0.33	0.24	0.23	0.24
TOTAL	98.92	99.77	99.93	101.05	99.69	99.41	100.39	99.06	99.22
STRUCTURAL FORMULA ON THE BASIS OF 32 OXYGENS									
SI	0.003	0.018	0.000	0.000	0.000	0.000	0.022	0.012	0.000
TI	0.067	0.072	0.064	0.054	0.037	0.040	0.010	0.046	0.023
AL	4.197	3.675	7.002	4.382	6.370	5.692	5.621	6.981	7.449
CR	9.914	9.952	7.816	9.633	7.122	8.147	8.659	7.468	7.166
FE3	1.746	1.992	1.052	1.876	2.432	2.076	1.654	1.403	1.329
FE2	4.461	4.615	3.923	4.109	3.801	4.475	4.628	3.827	3.735
MN	0.112	0.114	0.089	0.114	0.106	0.119	0.115	0.107	0.096
MG	3.448	3.283	4.012	3.763	4.062	3.377	3.227	4.074	4.134
CA	0.006	0.012	0.000	0.000	0.000	0.000	0.012	0.000	0.004
NA	0.000	0.000	0.000	0.000	0.000	0.000	0.000	0.034	0.033
K	0.000	0.000	0.000	0.000	0.000	0.000	0.000	0.000	0.000
NI	0.043	0.066	0.039	0.067	0.066	0.069	0.049	0.046	0.047

TABLE 5:35 REPRESENTATIVE OLIVINE ANALYSES FROM DUNITES

	300A	300B	304A	305A	528A	531A	531B	517A	517B
WEIGHT PERCENT OXIDE									
SIO2	40.61	40.72	40.37	40.50	40.95	40.24	41.77	40.62	40.84
TIO2	0.02	-	-	0.04	-	-	-	-	-
AL2O3	-	-	-	0.05	0.07	-	-	-	-
CR2O3	-	-	-	-	-	-	-	-	0.03
FEO	9.19	8.96	9.41	8.26	8.72	9.74	9.57	9.35	9.46
MNO	0.02	0.04	0.14	0.12	0.14	0.08	0.05	0.16	0.09
MGO	51.10	51.15	50.31	50.40	50.70	49.54	50.20	50.30	50.98
CAO	0.02	-	-	-	0.01	-	-	0.03	0.01
NA2O	-	-	-	-	-	-	-	0.02	0.02
K2O	-	-	-	-	-	-	-	-	-
NIO	0.22	0.23	0.26	0.27	0.26	0.21	0.21	0.26	0.24
TOTAL	101.18	101.11	100.50	99.64	100.85	99.82	101.79	100.74	101.67
STRUCTURAL FORMULA ON THE BASIS OF 4 OXYGENS									
SI	0.982	0.985	0.985	0.991	0.991	0.989	1.003	0.988	0.984
TI	0.000	0.000	0.000	0.000	0.000	0.000	0.000	0.000	0.000
AL	0.000	0.000	0.000	0.001	0.002	0.000	0.000	0.000	0.000
CR	0.000	0.000	0.000	0.000	0.000	0.000	0.000	0.000	0.000
FE2	0.186	0.181	0.192	0.169	0.176	0.200	0.192	0.190	0.191
MN	0.000	0.000	0.003	0.002	0.003	0.001	0.001	0.003	0.002
MG	1.843	1.843	1.830	1.837	1.829	1.815	1.796	1.823	1.832
CA	0.000	0.000	0.000	0.000	0.000	0.000	0.000	0.000	0.000
NA	0.000	0.000	0.000	0.000	0.000	0.000	0.000	0.001	0.000
K	0.000	0.000	0.000	0.000	0.000	0.000	0.000	0.000	0.000
NI	0.004	0.004	0.005	0.005	0.005	0.004	0.004	0.005	0.004
END MEMBER COMPOSITIONS									
MG	90.83	91.04	90.50	91.57	91.20	90.10	90.33	90.55	90.56
FE	9.16	8.95	9.50	8.42	8.80	9.94	9.66	9.44	9.43

TABLE 5-36 REPRESENTATIVE SPINEL ANALYSES FROM HARZBURGITES

	325A	325C	1037A	1044A
WEIGHT PERCENT OXIDE				
SIO2	-	-	0.02	0.17
TIO2	0.13	0.29	0.04	0.13
AL2O3	21.61	22.40	27.58	22.29
CR2O3	45.27	36.83	39.49	45.78
FE2O3	3.70	10.59	2.70	1.94
FEO	15.60	14.95	16.44	17.67
MNO	0.73	0.64	0.36	0.41
MGO	12.37	12.73	12.59	11.53
CAO	-	-	0.02	-
NA2O	-	-	-	0.19
K2O	-	-	-	0.02
NIO	0.16	0.21	0.19	0.24
TOTAL	99.57	98.63	99.42	100.37
STRUCTURAL FORMULA ON THE BASIS OF 32 OXYGENS				
SI	0.000	0.000	0.003	0.042
TI	0.025	0.054	0.007	0.024
AL	6.345	6.612	7.900	6.513
CR	8.910	7.285	7.582	8.968
FE3	0.694	1.995	0.494	0.360
FE2	3.248	3.129	3.340	3.661
MN	0.153	0.134	0.073	0.086
MG	4.591	4.748	4.558	4.258
CA	0.000	0.000	0.004	0.000
NA	0.000	0.000	0.000	0.091
K	0.000	0.000	0.000	0.007
NI	0.032	0.042	0.037	0.047

TABLE 5.37 REPRESENTATIVE OLIVINE ANALYSES FROM HARZBURGITES

	325A	325C	1037A	1044A
WEIGHT PERCENT OXIDE				
SIO2	41.18	40.96	40.16	41.20
TIO2	-	-	-	0.04
AL2O3	-	-	0.09	-
CR2O3	-	-	-	0.02
FEO	8.14	7.96	9.84	8.54
MNO	-	-	0.14	0.15
MGO	51.61	51.57	49.09	48.44
CAO	-	-	-	-
NA2O	0.01	-	-	-
K2O	0.04	0.03	-	0.01
NIO	0.35	0.32	0.44	0.46
TOTAL	101.53	100.84	100.36	98.87
STRUCTURAL FORMULA ON THE BASIS 4 OXYGENS				
SI	0.988	0.988	0.984	1.015
TI	0.000	0.000	0.000	0.000
AL	0.000	0.000	0.002	0.000
CR	0.000	0.000	0.000	0.000
FE2	0.163	0.161	0.202	0.176
MN	0.000	0.000	0.003	0.003
MG	1.852	1.855	1.814	1.800
CA	0.000	0.000	0.000	0.000
NA	0.000	0.000	0.000	0.000
K	0.001	0.001	0.000	0.000
NI	0.007	0.006	0.008	0.009
END MEMBER COMPOSITIONS				
MG	91.90	92.03	90.00	90.99
FE	8.10	7.97	9.99	9.00

TABLE 5-38 REPRESENTATIVE SPINEL ANALYSIS FROM WEHRLITE

	503A
WEIGHT PERCENT OXIDE	
SIO2	-
TIO2	0.21
AL2O3	27.17
CR2O3	36.01
FE2O3	5.02
FEO	16.58
MNO	0.34
MGO	12.29
CAO	0.04
NA2O	0.04
K2O	0.06
NIO	0.22
TOTAL	98.58
STRUCTURAL FORMULA ON THE BASIS OF 32 OXYGENS	
SI	0.000
TI	0.039
AL	7.676
CR	6.956
FE3	1.039
FE2	3.407
MN	0.071
MG	4.502
CA	0.011
NA	0.019
K	0.018
NI	0.042

TABLE 5-39 REPRESENTATIVE OLIVINE ANALYSIS FROM WEHRLITE

	503A
WEIGHT PERCENT OXIDE	
SIO2	40.17
TIO2	0.01
AL2O3	-
CR2O3	-
FEO	9.76
MNO	0.10
MGO	49.27
CAO	-
NA2O	0.01
K2O	0.03
NIO	0.25
TOTAL	99.60
STRUCTURAL FORMULA ON THE BASIS 4 OXYGENS	
SI	0.990
TI	0.000
AL	0.000
CR	0.000
FE2	0.201
MN	0.002
MG	1.810
CA	0.000
NA	0.000
K	0.001
NI	0.005
END MEMBER COMPOSITIONS	
MG	89.99
FE	10.00

TABLE 5-40 REPRESENTATIVE SPINEL ANALYSIS FROM PLAGIOCLASE PERIDOTITE

	315A
WEIGHT PERCENT OXIDE	
SIO2	0.51
TIO2	0.08
AL2O3	23.35
CR2O3	35.41
FE2O3	11.63
FEO	16.34
MNO	0.40
MGO	12.64
CAO	-
NA2O	-
K2O	0.02
NIO	0.17
TOTAL	100.76
STRUCTURAL FORMULA ON THE BASIS OF 32 OXYGENS	
SI	0.125
TI	0.014
AL	6.735
CR	6.840
FE3	2.139
FE2	3.341
MN	0.083
MG	4.879
CA	0.000
NA	0.000
K	0.006
NI	0.034

TABLE 5-41 REPRESENTATIVE OLIVINE ANALYSIS FROM PLAGIOCLASE PERIDOTITE

	315A
WEIGHT PERCENT OXIDE	
SIO2	41.45
TIO2	0.03
AL2O3	-
CR2O3	0.01
FEO	9.66
MNO	0.13
MGO	47.98
CAO	-
NA2O	-
K2O	0.01
NIO	0.22
TOTAL	99.49
STRUCTURAL FORMULA ON THE BASIS 4 OXYGENS	
SI	1.018
TI	0.000
AL	0.000
CR	0.000
FE2	0.198
MN	0.003
MG	1.756
CA	0.000
NA	0.000
K	0.000
NI	0.004
END MEMBER COMPOSITIONS	
MG	89.85
FE	10.15

TABLE 5-42 REPRESENTATIVE SPINEL ANALYSIS FROM OLIVINE PYROXENITE

	1027A
WEIGHT PERCENT OXIDE	
SIO2	0.15
TIO2	0.20
AL2O3	16.67
CR2O3	45.20
FE2O3	6.86
FEO	20.57
MNO	0.33
MGO	8.66
CAO	0.11
NA2O	0.07
K2O	0.04
NIO	0.22
TOTAL	99.49
STRUCTURAL FORMULA ON THE BASIS OF 32 OXYGENS	
SI	0.038
TI	0.039
AL	5.162
CR	9.305
FE3	1.344
FE2	4.481
MN	0.073
MG	3.439
CA	0.030
NA	0.037
K	0.013
NI	0.046

TABLE 5-43 REPRESENTATIVE OLIVINE ANALYSIS FROM OLIVINE PYROXENITE

	1027A
WEIGHT PERCENT OXIDE	
SIO2	40.99
TIO2	-
AL2O3	-
CR2O3	-
FEO	11.98
MNO	0.10
MGO	47.38
CAO	0.04
NA2O	0.04
K2O	0.02
NIO	0.24
TOTAL	100.78
STRUCTURAL FORMULA ON THE BASIS 4 OXYGENS	
SI	1.006
TI	0.000
AL	0.000
CR	0.000
FE2	0.245
MN	0.002
MG	1.733
CA	0.001
NA	0.001
K	0.000
NI	0.004
END MEMBER COMPOSITIONS	
MG	87.57
FE	12.43

TABLE 5.44 REPRESENTATIVE ORTHOPYROXENE ANALYSES FROM HARZBURGITES

	328A	1031A	1031B	1031C	1044A
WEIGHT PERCENT OXIDE					
SIO2	55.65	56.57	57.34	55.69	56.67
TIO2	-	0.08	0.02	0.05	0.10
AL2O3	2.15	2.65	2.39	2.68	1.65
CR2O3	0.52	0.58	0.64	0.67	0.55
FEO	5.24	6.04	5.93	6.14	5.57
MNO	0.03	0.11	0.13	0.13	0.12
MGO	34.95	33.55	31.44	32.23	33.17
CAO	0.76	1.15	0.61	0.83	0.95
NA2O	0.02	-	0.01	0.01	0.01
K2O	0.03	0.01	0.01	-	0.01
NIO	0.04	0.18	0.10	0.09	0.12
TOTAL	99.40	100.91	98.61	98.52	98.91
STRUCTURAL FORMULA ON THE BASIS OF 6 OXYGENS					
SI	1.929	1.939	1.996	1.951	1.972
TI	0.000	0.002	0.000	0.001	0.002
AL	0.087	0.107	0.098	0.110	0.067
CR	0.014	0.015	0.017	0.018	0.015
FE2	0.152	0.173	0.172	0.180	0.162
MN	0.001	0.003	0.004	0.004	0.003
MG	1.805	1.712	1.631	1.683	1.720
CA	0.028	0.042	0.022	0.031	0.035
NA	0.001	0.000	0.000	0.000	0.000
K	0.001	0.000	0.000	0.000	0.000
NI	0.001	0.005	0.002	0.002	0.003
END MEMBER COMPOSITIONS					
CA	1.42	2.18	1.24	1.64	1.85
MG	90.93	88.84	89.30	88.86	89.70
FE	7.64	8.98	9.45	9.50	8.45

TABLE 5-45 REPRESENTATIVE CLINOPYROXENE ANALYSES FROM HARZBURGITES

	328A	1031A	1031B	1031C	1044A
WEIGHT PERCENT OXIDE					
SIO2	52.97	52.27	53.43	51.67	51.68
TIO2	0.10	0.09	0.08	0.08	0.07
AL2O3	2.64	2.35	2.81	2.82	1.82
CR2O3	1.05	0.76	0.91	0.98	0.88
FEO	2.07	2.33	2.22	3.57	1.81
MNO	0.05	0.08	0.08	0.07	0.10
MGO	16.40	15.67	15.45	17.97	17.55
CAO	24.34	23.98	23.72	24.39	24.83
NA2O	0.09	0.11	0.10	0.06	0.21
K2O	0.01	0.01	0.02	0.01	0.01
NIO	0.10	0.06	0.13	0.05	0.04
TOTAL	99.83	97.66	98.95	101.66	99.00
STRUCTURAL FORMULA ON THE BASIS OF 6 OXYGENS					
SI	1.932	1.949	1.959	1.871	1.910
TI	0.002	0.002	0.002	0.002	0.002
AL	0.114	0.103	0.121	0.120	0.079
CR	0.030	0.020	0.026	0.028	0.025
FE2	0.063	0.072	0.068	0.108	0.056
MN	0.002	0.002	0.002	0.002	0.003
MG	0.892	0.871	0.844	0.969	0.966
CA	0.951	0.958	0.932	0.946	0.983
NA	0.006	0.008	0.007	0.004	0.015
K	0.000	0.000	0.000	0.000	0.000
NI	0.003	0.002	0.004	0.001	0.001
END MEMBER COMPOSITIONS					
CA	49.90	50.40	50.52	46.75	49.02
MG	46.78	45.78	45.76	47.90	48.19
FE	3.31	3.82	3.69	5.34	2.79

TABLE 5-46 REPRESENTATIVE ORTHOPYROXENE ANALYSES FROM OLIVINE PYROXENITES

	1027A	1027B	1030B
WEIGHT PERCENT OXIDE			
SIO2	54.03	54.83	55.67
TIO2	0.07	0.04	0.06
AL2O3	1.76	1.92	1.38
CR2O3	0.58	0.51	0.23
FEO	8.76	8.67	9.99
MNO	0.10	0.04	0.20
MGO	32.16	31.46	32.72
CAO	1.04	1.03	0.58
NA2O	0.01	0.02	–
K2O	0.03	0.02	0.01
NIO	–	0.04	–
TOTAL	98.54	98.58	101.03
STRUCTURAL FORMULA ON THE BASIS OF 6 OXYGENS			
SI	1.924	1.946	1.944
TI	0.002	0.001	0.002
AL	0.074	0.080	0.057
CR	0.016	0.014	0.000
FE2	0.261	0.257	0.290
MN	0.003	0.001	0.006
MG	1.707	1.664	1.696
CA	0.039	0.039	0.021
NA	0.000	0.001	0.000
K	0.001	0.001	0.000
NI	0.000	0.001	0.000
END MEMBER COMPOSITIONS			
CA	1.97	1.99	1.07
MG	85.03	84.88	84.46
FE	12.99	13.13	14.47

TABLE 5.47 REPRESENTATIVE CLINOPYROXENE ANALYSES FROM OLIVINE PYROXENITES

	1027A	1027B	1030B
WEIGHT PERCENT OXIDE			
SIO2	53.02	52.11	51.56
TIO2	0.07	0.09	0.10
AL2O3	2.26	2.08	2.27
CR2O3	0.77	0.86	0.32
FEO	2.90	2.92	3.84
MNO	-	0.03	0.11
MGO	17.07	16.96	16.85
CAO	24.21	23.53	23.52
NA2O	0.13	0.16	0.12
K2O	0.04	0.04	0.01
NIO	-	-	0.08
TOTAL	100.47	98.58	98.78
STRUCTURAL FORMULA ON THE BASIS OF 6 OXYGENS			
SI	1.927	1.930	1.916
TI	0.002	0.002	0.002
AL	0.097	0.090	0.099
CR	0.022	0.025	0.009
FE2	0.088	0.090	0.119
MN	0.000	0.001	0.003
MG	0.924	0.930	0.933
CA	0.943	0.925	0.936
NA	0.009	0.010	0.008
K	0.002	0.001	0.000
NI	0.000	0.000	0.002.
END MEMBER COMPOSITIONS			
CA	48.21	47.41	47.09
MG	47.28	47.95	46.91
FE	4.50	4.63	6.00

TABLE 5.48 REPRESENTATIVE ORTHOPYROXENE ANALYSES FROM CUMULATE OLIVINE GABBROS

	119A	557A	526B(A)
WEIGHT PERCENT OXIDE			
SIO2	55.05	55.76	52.15
TIO2	0.13	0.19	0.28
AL2O3	1.50	1.76	1.42
CR2O3	0.10	0.02	0.03
FEO	12.71	16.80	16.75
MNO	0.26	0.34	0.44
MGO	29.48	26.40	25.92
CAO	1.14	0.97	1.08
NA2O	0.02	0.04	0.06
K2O	0.02	0.01	0.02
NIO	0.08	0.04	0.04
TOTAL	100.49	102.33	98.20
STRUCTURAL FORMULA ON THE BASIS OF 6 OXYGENS			
SI	1.952	1.971	1.936
TI	0.003	0.005	0.008
AL	0.062	0.073	0.062
CR	0.003	0.000	0.000
FE2	0.377	0.496	0.520
MN	0.007	0.010	0.014
MG	1.558	1.391	1.434
CA	0.043	0.036	0.043
NA	0.001	0.002	0.005
K	0.002	0.000	0.000
NI	0.002	0.001	0.001
END MEMBER COMPOSITIONS			
CA	2.19	1.90	2.15
MG	78.75	72.28	71.81
FE	19.05	25.81	26.04

TABLE 5-49 REPRESENTATIVE CLINOPYROXENE ANALYSES FROM CUMULATE OLIVINE GABBROS

	119A	557A	5266(4)
WEIGHT PERCENT OXIDE			
SIO2	53.07	52.89	51.66
TIO2	0.21	0.53	0.55
AL2O3	2.06	3.03	2.30
CR2O3	0.28	0.09	0.07
FEO	6.11	6.70	7.23
MNO	0.17	0.19	0.22
MGO	17.51	14.46	14.10
CAO	22.66	23.09	22.82
NA2O	0.09	0.51	0.38
K2O	0.02	0.01	0.02
NIO	0.01	0.07	0.13
TOTAL	102.20	101.59	99.48
STRUCTURAL FORMULA ON THE BASIS OF 6 OXYGENS			
SI	1.910	1.927	1.931
TI	0.006	0.014	0.015
AL	0.088	0.130	0.101
CR	0.008	0.002	0.002
FE2	0.184	0.204	0.226
MN	0.005	0.006	0.007
MG	0.942	0.786	0.785
CA	0.876	0.901	0.914
NA	0.006	0.036	0.027
K	0.000	0.000	0.001
NI	0.000	0.002	0.004
END MEMBER COMPOSITIONS			
CA	43.75	47.65	47.50
MG	47.03	41.56	40.78
FE	9.21	10.79	11.73

TABLE 5-50 REPRESENTATIVE ORTHOPYROXENE ANALYSIS FROM CUMULATE NORITE

131A

WEIGHT PERCENT OXIDE

SIO2	52.14
TIO2	0.15
AL2O3	1.72
CR2O3	0.05
FEO	18.62
MNO	0.28
MGO	25.16
CAO	1.06
NA2O	0.01
K2O	0.01
NIO	0.04
TOTAL	99.84

STRUCTURAL FORMULA ON THE BASIS OF 6 OXYGENS

SI	1.922
TI	0.004
AL	0.074
CR	0.001
FE2	0.574
MN	0.008
MG	1.382
CA	0.005
NA	0.000
K	0.000
NI	0.001

END MEMBER COMPOSITIONS

CA	3.24
MG	68.37
FE	28.39

TABLE 5-51 REPRESENTATIVE CLINOPYROXENE ANALYSIS FROM CUMULATE NORITE

	131A
WEIGHT PERCENT OXIDE	
SIO2	51.09
TIO2	0.28
AL2O3	2.82
CR2O3	0.20
FEO	9.46
MNO	0.23
MGO	15.88
CAO	20.46
NA2O	0.20
K2O	0.01
NIO	0.07
TOTAL	100.71
STRUCTURAL FORMULA ON THE BASIS OF 6 OXYGENS	
SI	1.894
TI	0.008
AL	0.123
CR	0.006
FE2	0.293
MN	0.007
MG	0.877
CA	0.813
NA	0.014
K	0.000
NI	0.002
END MEMBER COMPOSITIONS	
CA	40.98
MG	44.23
FE	14.79

TABLE 5.52 REPRESENTATIVE ORTHOPYROXENE ANALYSIS FROM NORMAL GABBRO

52oA (A)

WEIGHT PERCENT OXIDE

SIO2	53.09
TIO2	0.18
AL2O3	1.49
CR2O3	0.04
FEO	16.13
MNO	0.38
MGO	26.67
CAO	0.83
NA2O	-
K2O	0.01
NIO	0.05
TOTAL	99.08

STRUCTURAL FORMULA ON THE BASIS OF 6 OXYGENS

SI	1.943
TI	0.005
AL	0.064
CR	0.001
FE2	0.494
MN	0.012
MG	1.455
CA	0.032
NA	0.000
K	0.000
NI	0.001

END MEMBER COMPOSITIONS

CA	1.64
MG	73.57
FE	24.80

TABLE 53 REPRESENTATIVE CLINOPYROXENE ANALYSIS FROM NORMAL GABBRO

52CA(A)

WEIGHT PERCENT OXIDE

SIO2	51.54
TIO2	0.55
AL2O3	2.52
CR2O3	0.07
FEO	7.24
MNO	0.23
MGO	15.32
CAO	21.32
NA2O	0.38
K2O	0.03
NIO	0.06
TOTAL	99.27

STRUCTURAL FORMULA ON THE BASIS OF 6 OXYGENS

SI	1.923
TI	0.015
AL	0.111
CR	0.002
FE2	0.226
MN	0.007
MG	0.852
CA	0.852
NA	0.027
K	0.001
NI	0.001

END MEMBER COMPOSITIONS

CA	44.15
MG	44.14
FE	11.70

TABLE 5.4 REPRESENTATIVE OLIVINE ANALYSES FROM HARZBURGITES

	328A	1031A	1031B	1031C	1044A
WEIGHT PERCENT OXIDE					
SIO2	41.09	40.91	40.91	40.85	41.20
TIO2	-	-	-	-	0.04
AL2O3	-	0.02	0.02	0.02	-
CR2O3	-	-	-	-	0.02
FEO	8.45	8.83	9.35	9.02	8.54
MNO	-	0.06	0.10	0.07	0.15
MGO	51.17	49.17	48.18	48.80	48.44
CAO	0.02	-	-	-	-
NA2O	-	-	-	-	-
K2O	0.03	-	-	-	0.01
NIO	0.38	0.31	0.36	0.33	0.46
TOTAL	101.13	99.30	98.91	99.08	98.87
STRUCTURAL FORMULA ON THE BASIS 4 OXYGENS					
SI	0.991	1.005	1.011	1.006	1.015
TI	0.000	0.000	0.000	0.000	0.000
AL	0.000	0.000	0.000	0.000	0.000
CR	0.000	0.000	0.000	0.000	0.000
FE2	0.170	0.181	0.193	0.186	0.176
MN	0.000	0.001	0.002	0.001	0.003
MG	1.839	1.800	1.774	1.792	1.800
CA	0.000	0.000	0.000	0.000	0.000
NA	0.000	0.000	0.000	0.000	0.000
K	0.000	0.000	0.000	0.000	0.000
NI	0.007	0.006	0.007	0.006	0.009
END MEMBER COMPOSITIONS					
MG	91.52	90.84	90.18	90.60	90.99
FE	8.48	9.15	9.82	9.40	9.00

TABLE 5-5 REPRESENTATIVE CLINOPYROXENE ANALYSES FROM HARZBURGITES

	328A	1031A	1031B	1031C	1044A
WEIGHT PERCENT OXIDE					
SIO2	52.97	52.27	53.43	51.67	51.68
TIO2	0.10	0.09	0.08	0.08	0.07
AL2O3	2.64	2.35	2.81	2.82	1.82
CR2O3	1.05	0.70	0.91	0.98	0.88
FEO	2.07	2.33	2.22	3.57	1.81
MNO	0.05	0.08	0.08	0.07	0.10
MGO	16.40	15.67	15.45	17.97	17.55
CAO	24.54	23.98	25.72	24.39	24.83
NA2O	0.09	0.11	0.10	0.06	0.21
K2O	0.01	0.01	0.02	0.01	0.01
NIO	0.10	0.06	0.13	0.05	0.04
TOTAL	99.83	97.66	98.95	101.66	99.00
STRUCTURAL FORMULA ON THE BASIS OF 6 OXYGENS					
SI	1.932	1.949	1.959	1.871	1.910
TI	0.002	0.002	0.002	0.002	0.002
AL	0.114	0.103	0.121	0.120	0.079
CR	0.030	0.020	0.026	0.028	0.025
FE2	0.063	0.072	0.068	0.108	0.056
MN	0.002	0.002	0.002	0.002	0.003
MG	0.892	0.871	0.844	0.969	0.966
CA	0.951	0.958	0.932	0.946	0.983
NA	0.006	0.008	0.007	0.004	0.015
K	0.000	0.000	0.000	0.000	0.000
NI	0.003	0.002	0.004	0.001	0.001
END MEMBER COMPOSITIONS					
CA	49.90	50.40	50.52	46.75	49.02
MG	46.78	45.78	45.78	47.90	48.19
FE	3.31	3.82	3.69	5.34	2.79

TABLE 5-56 REPRESENTATIVE OLIVINE ANALYSIS FROM PLAGIOCLASE PERIDOTITE

	315A
WEIGHT PERCENT OXIDE	
SIO2	41.45
TIO2	0.03
AL2O3	-
CR2O3	0.01
FEO	9.66
MNO	0.13
MGO	47.98
CAO	-
NA2O	-
K2O	0.01
NIO	0.22
TOTAL	99.49
STRUCTURAL FORMULA ON THE BASIS 4 OXYGENS	
SI	1.018
TI	0.000
AL	0.000
CR	0.000
FE2	0.198
MN	0.003
MG	1.756
CA	0.000
NA	0.000
K	0.000
NI	0.004
END MEMBER COMPOSITIONS	
MG	89.85
FE	10.15

TABLE 5·57 REPRESENTATIVE CLINOPYROXENE ANALYSIS FROM PLAGIOCLASE PERIDOTITE

	315A
WEIGHT PERCENT OXIDE	
SIO2	53.23
TIO2	0.26
AL2O3	3.15
CR2O3	1.37
FEO	2.55
MNO	0.10
MGO	14.87
CAO	22.99
NA2O	0.48
K2O	0.02
NIO	0.09
TOTAL	99.10
STRUCTURAL FORMULA ON THE BASIS OF 6 OXYGENS	
SI	1.952
TI	0.007
AL	0.136
CR	0.040
FE2	0.078
MN	0.003
MG	0.812
CA	0.903
NA	0.034
K	0.001
NI	0.002
END MEMBER COMPOSITIONS	
CA	50.34
MG	45.29
FE	4.36

TABLE 5-58 REPRESENTATIVE OLIVINE ANALYSES FROM WEHRLITES

	503A	503B	603A	604A
WEIGHT PERCENT OXIDE				
SIO2	40.17	39.94	39.90	41.15
TIO2	0.01	0.02	0.01	-
AL2O3	-	-	-	-
CR2O3	-	-	-	-
FEO	9.76	9.83	11.12	10.73
MNO	0.10	0.05	0.05	0.06
MGO	49.27	48.87	47.67	48.58
CAO	-	0.03	0.02	0.05
NA2O	0.01	0.04	-	0.02
K2O	0.03	0.04	-	-
NIO	0.25	0.21	0.28	0.18
TOTAL	99.60	99.02	99.05	100.76
STRUCTURAL FORMULA ON THE BASIS 4 OXYGENS				
SI	0.990	0.990	0.995	1.004
TI	0.000	0.000	0.000	0.000
AL	0.000	0.000	0.000	0.000
CR	0.000	0.000	0.000	0.000
FE2	0.201	0.204	0.232	0.220
MN	0.002	0.001	0.001	0.001
MG	1.810	1.806	1.771	1.766
CA	0.000	0.000	0.000	0.001
NA	0.000	0.002	0.000	0.001
K	0.001	0.001	0.000	0.000
NI	0.005	0.004	0.005	0.004
END MEMBER COMPOSITIONS				
MG	89.99	89.85	88.42	88.97
FE	10.00	10.14	11.60	11.02

TABLE 5-59 REPRESENTATIVE CLINOPYROXENE ANALYSES FROM WEHRLITES

	503A	503B	803A	804A
WEIGHT PERCENT OXIDE				
SIO2	50.94	51.63	49.47	52.69
TIO2	0.20	0.11	0.21	0.19
AL2O3	3.89	3.30	3.68	2.89
CR2O3	1.26	1.14	1.16	1.43
FEO	2.74	2.57	3.15	2.66
MNO	0.04	-	0.04	0.01
MGO	16.90	17.46	19.14	16.81
CAO	22.31	22.08	22.02	23.23
NA2O	0.04	0.26	0.23	0.04
K2O	0.03	0.04	0.03	0.03
NIO	0.09	0.15	-	0.05
TOTAL	98.43	99.35	99.34	100.03
STRUCTURAL FORMULA ON THE BASIS OF 6 OXYGENS				
SI	1.885	1.894	1.826	1.919
TI	0.005	0.003	0.006	0.005
AL	0.169	0.143	0.169	0.124
CR	0.036	0.033	0.033	0.041
FE2	0.084	0.080	0.097	0.081
MN	0.001	0.000	0.001	0.000
MG	0.932	0.955	1.053	0.912
CA	0.885	0.892	0.870	0.906
NA	0.002	0.018	0.016	0.003
K	0.001	0.001	0.001	0.001
NI	0.002	0.004	0.000	0.001
END MEMBER COMPOSITIONS				
CA	46.52	46.30	43.08	47.72
MG	49.02	49.62	52.10	48.02
FE	4.45	4.09	4.81	4.26

TABLE 5·60 REPRESENTATIVE OLIVINE ANALYSES FROM OLIVINE PYROXENITES

	1027A	1027B	1014(3)B	1014(3)C	1030B(A)
WEIGHT PERCENT OXIDE					
SIO2	40.99	40.30	39.66	40.24	39.41
TIO2	–	0.01	0.02	0.04	0.02
AL2O3	–	–	–	–	–
CR2O3	–	0.02	0.05	0.02	–
FEO	11.98	12.04	13.80	13.38	15.48
MNO	0.10	0.10	0.24	0.25	0.20
MGO	47.38	47.10	46.20	45.49	45.59
CAO	0.04	0.04	0.09	0.12	0.01
NA2O	0.04	0.01	–	–	0.05
K2O	0.02	0.03	0.02	0.02	0.02
NIO	0.24	0.21	0.13	0.12	0.18
TOTAL	100.78	99.91	100.41	99.68	100.96
STRUCTURAL FORMULA ON THE BASIS 4 OXYGENS					
SI	1.006	0.999	0.992	1.006	0.984
TI	0.000	0.000	0.000	0.000	0.000
AL	0.000	0.000	0.000	0.000	0.000
CR	0.000	0.000	0.000	0.000	0.000
FE2	0.245	0.249	0.287	0.279	0.323
MN	0.002	0.003	0.005	0.005	0.004
MG	1.733	1.740	1.714	1.700	1.697
CA	0.001	0.001	0.002	0.003	0.000
NA	0.001	0.000	0.000	0.000	0.002
K	0.000	0.001	0.000	0.000	0.000
NI	0.004	0.004	0.002	0.002	0.003
END MEMBER COMPOSITIONS					
MG	87.57	87.45	85.64	85.83	83.99
FE	12.43	12.55	14.36	14.16	16.00

TABLE 5.61 REPRESENTATIVE CLINOPYROXENE ANALYSES FROM OLIVINE ··PYROXENITES

	1027A	1027B	1014(3)B	1014(3)C	1030B (A)
WEIGHT PERCENT OXIDE					
SIO2	53.02	52.11	52.02	52.74	51.56
TIO2	0.07	0.09	0.06	0.09	0.10
AL2O3	2.26	2.08	2.44	2.10	2.27
CR2O3	0.77	0.86	0.47	0.51	0.32
FEO	2.90	2.92	3.39	3.34	3.84
MNO	-	0.03	0.13	0.17	0.11
MGO	17.07	16.96	17.30	17.02	16.85
CAO	24.21	23.35	22.96	23.02	23.52
NA2O	0.13	0.16	0.11	0.14	0.12
K2O	0.04	0.04	0.02	0.02	0.01
NIO	-	-	0.01	0.07	0.08
TOTAL	100.47	98.56	98.91	99.24	98.78
STRUCTURAL FORMULA ON THE BASIS OF 6 OXYGENS					
SI	1.927	1.930	1.921	1.940	1.916
TI	0.002	0.002	0.007	0.002	0.002
AL	0.097	0.090	0.106	0.091	0.099
CR	0.022	0.025	0.013	0.015	0.009
FE2	0.088	0.090	0.104	0.103	0.119
MN	0.000	0.001	0.004	0.005	0.003
MG	0.924	0.930	0.952	0.933	0.933
CA	0.943	0.925	0.908	0.907	0.936
NA	0.009	0.010	0.008	0.010	0.008
K	0.002	0.001	0.001	0.001	0.000
NI	0.000	0.000	0.000	0.002	0.002
END MEMBER COMPOSITIONS					
CA	48.21	47.41	46.23	46.69	47.09
MG	47.28	47.95	48.44	48.01	46.91
FE	4.50	4.63	5.32	5.30	6.00

TABLE 5·62 REPRESENTATIVE OLIVINE ANALYSES FROM OLIVINE GABBROS

	556A	119A	523A	557A	557B	539A	564A	113A	526B (β)
WEIGHT PERCENT OXIDE									
SIO2	38.58	39.19	38.86	38.41	38.21	39.76	37.13	37.20	36.38
TIO2	0.08	0.07	0.05	0.05	0.06	0.02	0.03	0.05	0.04
AL2O3	0.10	-	-	-	0.01	-	-	-	-
CR2O3	0.02	0.01	0.01	0.03	0.04	0.07	0.03	0.01	0.05
FEO	23.07	19.26	25.72	25.53	25.94	13.61	26.35	19.44	28.49
MNO	0.38	0.24	0.36	0.38	0.36	0.16	0.43	0.27	0.47
MGO	36.46	40.08	3.72	34.39	35.08	47.92	36.72	41.02	34.34
CAO	0.27	-	0.07	0.02	0.08	0.01	0.03	-	0.02
NA2O	-	-	-	0.03	0.02	-	-	-	0.04
K2O	0.03	0.01	0.03	0.02	0.01	0.01	0.03	0.01	0.01
NIO	0.14	0.10	0.16	0.16	0.17	0.14	0.15	0.12	0.08
TOTAL	99.14	98.95	100.43	99.03	99.97	101.70	100.89	98.13	99.93
STRUCTURAL FORMULA ON THE BASIS 4 OXYGENS									
SI	1.016	1.010	1.012	1.024	1.011	0.977	0.979	0.977	0.980
TI	0.001	0.001	0.001	0.001	0.001	0.000	0.000	0.001	0.000
AL	0.003	0.000	0.000	0.000	0.000	0.000	0.000	0.000	0.000
CR	0.000	0.000	0.000	0.000	0.000	0.001	0.000	0.000	0.001
FE2	0.508	0.416	0.516	0.569	0.574	0.279	0.581	0.427	0.642
MN	0.008	0.005	0.008	0.008	0.008	0.003	0.009	0.006	0.010
MG	1.431	1.540	1.442	1.366	1.384	1.755	1.443	1.606	1.379
CA	0.007	0.000	0.002	0.000	0.002	0.000	0.000	0.000	0.000
NA	0.000	0.000	0.000	0.001	0.000	0.000	0.000	0.000	0.002
K	0.000	0.000	0.000	0.000	0.000	0.000	0.001	0.000	0.000
NI	0.003	0.002	0.003	0.003	0.003	0.002	0.003	0.002	0.001
END MEMBER COMPOSITIONS									
MG	73.80	78.76	73.36	70.59	70.67	86.25	71.30	78.99	68.23
FE	26.20	21.23	26.36	29.40	29.32	13.75	28.70	21.00	31.77

TABLE 5-63 REPRESENTATIVE CLINOPYROXENE ANALYSES FROM CUMULATE OLIVINE GABBROS

	556A	119A	523A	557A	557B	539A	564A	113A	526B(B)
WEIGHT PERCENT OXIDE									
SIO2	51.10	53.07	51.69	52.89	52.28	52.82	50.79	50.12	50.73
TIO2	0.57	0.21	0.53	0.53	0.53	0.07	0.64	0.13	0.64
AL2O3	3.06	2.06	2.66	3.03	3.05	2.08	2.94	2.31	1.96
CR2O3	0.24	0.28	0.12	0.09	0.14	0.34	0.10	0.30	0.06
FEO	6.87	6.11	7.49	6.70	6.16	3.49	8.85	5.55	7.56
MNO	0.19	0.17	0.19	0.19	0.19	0.12	0.23	-	0.26
MGO	14.77	17.51	15.13	14.48	14.37	17.76	14.95	18.02	15.16
CAO	21.75	22.66	21.28	23.09	23.21	23.79	19.18	20.78	22.58
NA2O	0.41	0.09	0.65	0.51	0.42	0.09	0.39	0.10	0.39
K2O	0.02	0.02	0.02	0.01	0.01	0.01	0.02	0.01	0.02
NIO	0.07	0.01	0.14	0.07	0.07	0.06	0.07	-	0.03
TOTAL	99.05	102.20	99.89	101.59	100.43	100.64	98.18	97.33	99.39
STRUCTURAL FORMULA ON THE BASIS OF 6 OXYGENS									
SI	1.910	1.910	1.920	1.927	1.924	1.921	1.920	1.894	1.906
TI	0.010	0.006	0.014	0.014	0.015	0.002	0.018	0.004	0.018
AL	0.135	0.088	0.116	0.130	0.132	0.089	0.131	0.103	0.086
CR	0.007	0.008	0.003	0.002	0.004	0.010	0.003	0.009	0.002
FE2	0.215	0.184	0.232	0.204	0.200	0.106	0.279	0.175	0.237
MN	0.006	0.005	0.006	0.006	0.006	0.003	0.007	0.000	0.008
MG	0.820	0.942	0.837	0.786	0.786	0.963	0.842	1.015	0.849
CA	0.870	0.876	0.847	0.901	0.915	0.927	0.777	0.841	0.909
NA	0.030	0.006	0.046	0.036	0.030	0.006	0.029	0.007	0.028
K	0.001	0.000	0.001	0.000	0.000	0.000	0.001	0.000	0.000
NI	0.002	0.000	0.004	0.002	0.002	0.001	0.002	0.000	0.000
END MEMBER COMPOSITIONS									
CA	45.63	43.75	44.18	47.65	48.35	46.43	40.92	41.41	45.54
MG	43.11	47.03	43.69	41.56	41.63	48.25	44.35	49.95	42.55
FE	11.24	9.21	12.13	10.79	10.01	5.31	14.73	8.63	11.91

TABLE 5.64 REPRESENTATIVE CLINOPYROXENE ANALYSES FROM HARZBURGITES

	1031C	1044A
WEIGHT PERCENT OXIDE		
SIO2	51.67	51.68
TIO2	0.08	0.07
AL2O3	2.82	1.82
CR2O3	0.98	0.88
FEO	3.57	1.81
MNO	0.07	0.10
MGO	17.97	17.55
CAO	24.39	24.83
NA2O	0.06	0.21
K2O	0.01	0.01
NIO	0.05	0.04
TOTAL	101.66	99.00
STRUCTURAL FORMULA ON THE BASIS OF 6 OXYGENS		
SI	1.871	1.910
TI	0.002	0.002
AL	0.120	0.079
CR	0.028	0.025
FE2	0.108	0.056
MN	0.002	0.003
MG	0.969	0.966
CA	0.946	0.963
NA	0.004	0.015
K	0.000	0.000
NI	0.001	0.001
END MEMBER COMPOSITIONS		
CA	46.75	49.02
MG	47.90	48.19
FE	5.34	2.79

TABLE 5-65 REPRESENTATIVE CLINOPYROXENE ANALYSES FROM WEHRLITES

	503A	804A	804D
WEIGHT PERCENT OXIDE			
SIO2	50.94	52.69	51.61
TIO2	0.20	0.19	0.24
AL2O3	3.89	2.89	3.17
CR2O3	1.26	1.43	1.03
FEO	2.74	2.66	2.59
MNO	0.04	0.01	0.02
MGO	16.90	16.81	16.09
CAO	22.31	23.23	23.61
NA2O	0.04	0.04	0.26
K2O	0.03	0.03	0.04
NIO	0.09	0.05	0.07
TOTAL	98.43	100.03	98.72
STRUCTURAL FORMULA ON THE BASIS OF 6 OXYGENS			
SI	1.885	1.919	1.909
TI	0.005	0.005	0.006
AL	0.169	0.124	0.138
CR	0.036	0.041	0.030
FE2	0.084	0.081	0.080
MN	0.001	0.000	0.000
MG	0.932	0.912	0.886
CA	0.885	0.906	0.936
NA	0.002	0.003	0.018
K	0.001	0.001	0.002
NI	0.002	0.001	0.002
END MEMBER COMPOSITIONS			
CA	46.52	47.72	49.18
MG	49.02	48.02	46.60
FE	4.45	4.26	4.21

TABLE 5·66 REPRESENTATIVE CLINOPYROXENE ANALYSES FROM OLIVINE PYROXENITES

	554D	1027A	1027B
WEIGHT PERCENT OXIDE			
SIO2	53.06	53.02	52.11
TIO2	0.06	0.07	0.09
AL2O3	2.02	2.26	2.08
CR2O3	0.65	0.77	0.86
FEO	3.27	2.90	2.92
MNO	0.02	-	0.03
MGO	17.21	17.07	16.96
CAO	22.76	24.21	23.33
NA2O	0.15	0.13	0.16
K2O	0.03	0.04	0.04
NIO	-	-	-
TOTAL	99.22	100.47	98.58
STRUCTURAL FORMULA ON THE BASIS OF 6 OXYGENS			
SI	1.927	1.927	1.930
TI	0.002	0.002	0.002
AL	0.097	0.097	0.090
CR	0.022	0.022	0.025
FE2	0.088	0.088	0.090
MN	0.000	0.000	0.001
MG	0.924	0.924	0.930
CA	0.943	0.943	0.925
NA	0.009	0.009	0.010
K	0.002	0.002	0.001
NI	0.000	0.000	0.000
END MEMBER COMPOSITIONS			
CA	46.21	48.21	47.41
MG	48.60	47.28	47.95
FE	5.20	4.50	4.63

TABLE 5-67 MAGNETITES IN OLIVINE GABBROS

	106A	526B A	526B B
WEIGHT PERCENT OXIDE			
SIO2	0.99	21.00	0.23
TIO2	2.36	5.92	5.59
AL2O3	3.98	2.29	2.29
CR2O3	0.34	1.25	1.37
FE2O3	58.53	51.32	53.02
FEO	33.43	34.57	34.59
MNO	0.24	0.48	0.49
MGO	0.89	0.62	0.70
CAO	0.27	0.01	0.05
NA2O	0.15	0.15	-
K2O	0.05	0.05	0.05
NIO	0.34	0.29	0.34
TOTAL	101.57	97.16	98.70
STRUCTURAL FORMULA ON THE BASIS OF 32 OXYGENS			
SI	0.291	0.066	0.069
TI	0.520	1.376	1.280
AL	1.376	0.835	0.821
CR	0.079	0.306	0.329
FE3	12.897	11.945	12.146
FE2	8.186	8.941	8.806
MN	0.060	0.125	0.126
MG	0.388	0.287	0.315
CA	0.083	0.004	0.016
NA	0.083	0.089	0.000
K	0.017	0.020	0.018
NI	0.080	0.071	0.082

TABLE 5-68 MAGNETITES ASSOCIATED WITH BASALTIC HORNBLENDE IN NORMAL GABBROS

	859A	526A(A)	526A(B)
WEIGHT PERCENT OXIDE			
SiO_2	0.29	0.27	0.23
TiO_2	1.91	0.17	3.82
Al_2O_3	1.60	2.56	2.48
Cr_2O_3	2.88	1.01	0.05
Fe_2O_3	59.93	63.07	59.74
FeO	32.21	30.26	34.09
MnO	0.34	0.34	0.40
MgO	0.35	0.30	0.64
CaO	0.05	0.09	0.04
Na_2O	0.18	0.09	0.18
K_2O	0.05	0.04	0.05
NiO	0.35	0.35	0.39
TOTAL	100.14	98.54	102.12
STRUCTURAL FORMULA ON THE BASIS OF 32 OXYGENS			
Si	0.088	0.082	0.067
Ti	0.434	0.039	0.847
Al	0.572	0.925	0.863
Cr	0.689	0.244	0.012
Fe3	13.660	14.600	13.265
Fe2	8.160	7.761	8.412
Mn	0.086	0.089	0.099
Mg	0.158	0.138	0.282
Ca	0.015	0.030	0.012
Na	0.107	0.051	0.105
K	0.020	0.017	0.019
Ni	0.086	0.086	0.093

TABLE 5-69 ILMENITES ASSOCIATED WITH BASALTIC HORNBLENDE IN NORMAL GABBROS

	526A(A)	526A(B)
WEIGHT PERCENT OXIDE		
SIO2	0.34	0.27
TIO2	30.02	50.97
AL2O3	2.84	0.12
CR2O3	0.37	0.14
FE2O3	38.98	2.90
FEO	24.97	41.05
MNO	1.30	1.05
MGO	0.45	2.08
CAO	0.04	0.07
NA2O	0.11	0.14
K2O	0.05	0.04
NIO	0.28	0.25
TOTAL	99.76	99.07
STRUCTURAL FORMULA ON THE BASIS OF 6 OXYGENS		
SI	0.017	0.013
TI	1.144	1.923
AL	0.169	0.006
CR	0.015	0.005
FE3	1.487	0.109
FE2	1.058	1.722
MN	0.056	0.044
MG	0.033	0.155
CA	0.002	0.003
NA	0.011	0.014
K	0.003	0.002
NI	0.012	0.010

TABLE 5-70 BASALTIC HORNBLENDE ASSOCIATED WITH MAGNETITES IN OLIVINE GABBROS

	526B A
WEIGHT PERCENT OXIDE	
SIO2	43.03
TIO2	2.40
AL2O3	9.58
CR2O3	0.07
FEO	9.49
MNO	0.15
MGO	15.20
CAO	12.03
NA2O	2.73
K2O	0.05
NIO	0.05
TOTAL	94.77
STRUCTURAL FORMULA ON THE BASIS OF 23 OXYGENS	
SI	6.467
TI	0.270
AL	1.698
CR	0.008
FE2	1.193
MN	0.019
MG	3.406
CA	1.937
NA	0.794
K	0.010
NI	0.006

TABLE 5-71 BASALTIC HORNBLENDE IN NORMAL GABBROS

	859A	859B	526A(A)	526A(B)
WEIGHT PERCENT OXIDE				
SIO2	44.89	46.42	43.73	44.33
TIO2	2.23	2.14	2.38	2.01
AL2O3	9.74	8.65	11.71	12.15
CR2O3	0.04	0.09	0.11	0.07
FEO	11.99	12.77	9.17	9.44
MNO	0.20	0.20	0.13	0.12
MGO	14.08	13.46	14.98	15.45
CAO	11.79	12.02	11.72	11.73
NA2O	1.54	1.25	2.30	2.59
K2O	0.08	0.07	0.06	0.05
NIO	0.08	0.11	0.12	0.02
TOTAL	96.66	97.18	96.40	97.95
STRUCTURAL FORMULA ON THE BASIS OF 23 OXYGENS				
SI	6.625	6.817	6.411	6.396
TI	0.248	0.236	0.262	0.217
AL	1.696	1.498	2.024	2.067
CR	0.005	0.010	0.013	0.008
FE2	1.500	1.568	1.123	1.138
MN	0.024	0.024	0.016	0.014
MG	3.100	2.946	3.272	3.322
CA	1.863	1.892	1.840	1.813
NA	0.440	0.356	0.653	0.723
K	0.015	0.013	0.011	0.009
NI	0.009	0.012	0.013	0.003

TABLE 5-72 ACTINOLITE FROM LEUCOCRATIC GABBRO

	541A
WEIGHT PERCENT OXIDE	
SIO2	55.23
TIO2	0.04
AL2O3	3.25
CR2O3	-
FEO	5.38
MNO	0.04
MGO	20.04
CAO	12.12
NA2O	0.06
K2O	0.02
NIO	0.06
TOTAL	96.24
STRUCTURAL FORMULA ON THE BASIS OF 23 OXYGENS	
SI	7.756
TI	0.003
AL	0.540
CR	0.000
FE2	0.632
MN	0.005
MG	4.194
CA	1.825
NA	0.016
K	0.003
NI	0.007

TABLE 5-73 CHLORITE FROM LEUCOCRATIC GABBRO

	541B
WEIGHT PERCENT OXIDE	
SIO2	31.00
TIO2	0.02
AL203	17.07
CR203	0.02
FEO	8.44
MNO	0.02
MGO	27.99
CAO	0.09
NA20	-
K20	0.01
NIO	0.12
TOTAL	84.79
STRUCTURAL FORMULA ON THE BASIS OF 28 OXYGENS	
SI	6.145
TI	0.003
AL	3.990
CR	0.002
FE2	1.399
MN	0.004
MG	8.300
CA	0.019
NA	0.000
K	0.003
NI	0.019

TABLE 5.7 ANALYSES OF LOBATE AREAS FROM A SERPENTINISED DUNITE

	515A	515B
WEIGHT PERCENT OXIDE		
SIO2	6.86	23.19
TIO2	0.01	0.04
AL2O3	23.58	14.80
CR2O3	-	0.01
FEO	2.61	6.41
MNO	0.02	0.33
MGO	42.15	22.08
CAO	0.82	9.71
NA2O	-	-
K2O	-	0.19
NIO	-	-
TOTAL	76.04	76.75
STRUCTURAL FORMULA ON THE BASIS OF 28 OXYGENS		
SI	1.582	5.334
TI	0.000	0.007
AL	6.419	4.016
CR	0.000	0.000
FE2	0.503	1.232
MN	0.000	0.064
MG	14.495	7.569
CA	0.203	2.393
NA	0.000	0.000
K	0.000	0.056
NI	0.000	0.000

TABLE 5-75 AMPHIBOLES

	818A	818B	818C
WEIGHT PERCENT OXIDE			
SIO2	52.02	51.77	52.29
TIO2	0.56	0.62	0.67
AL2O3	4.96	5.23	5.03
CR2O3	0.31	0.13	0.14
FEO	7.44	7.76	7.73
MNO	0.21	0.18	0.18
MGO	17.51	18.03	18.29
CAO	12.30	12.45	12.39
NA2O	0.63	0.70	0.66
K2O	0.31	0.30	0.38
NIO	0.09	0.03	0.05
TOTAL	96.34	97.21	97.81
STRUCTURAL FORMULA ON THE BASIS OF 23 OXYGENS			
SI	7.450	7.360	7.390
TI	0.060	0.066	0.070
AL	0.837	0.870	0.839
CR	0.034	0.014	0.016
FE2	0.891	0.920	0.910
MN	0.025	0.020	0.020
MG	3.740	3.820	3.850
CA	1.880	1.898	1.870
NA	0.175	0.193	0.180
K	0.060	0.050	0.068
NI	0.010	0.003	0.006

REFERENCES

ALLEMANN, F. and PETERS, T. (1972). The Ophiolite-Radiolarite belt of the North Oman Mountains, Ecologae Geol. Helvetiae, v.65, No.3, p.657-697.

ALLEN, C.R. (1975). The petrology of a portion of the Troodos Plutonic Complex, Cyprus. Unpub. Ph.D. thesis, Cambridge University.

BARNES, I., LA MARCHE, V.C. and HIMMELBERG, G.R. (1967). Geochemical evidence of present-day serpentinization. Science, v.156, p.830-832.

BELL, J.M., CLARKE, E. de C. and MARSHALL, P. (1911). The geology of the Dun Mountain subdivision, Nelson. New Zealand Geol. Survey Bull. 12, p.1-71.

BLANFORD, W.T. (1872). Notes on the geological formations seen along the coasts of Baluchistan and Persia, from Karachi to the head of the Persian Gulf, and some of the Gulf Islands. India Geol. Survey Recs., v.5, p.41-45.

BOUDIER, F. (1972). Relations Lherzolite-Gabbro-Dunite dans Le Massif de Lanzo (Alpes pie montaises): Exemple de fusion pantielle. Ph.D. Thesis Nantes 1-106.

BOUDIER, F. (1978). Structure and petrology of the Lanzo Peridotite Massif (Piedmont Alps). Bull. Geol. Soc. Amer. v.89, p.1574-1591.

BOYD, F.R. Jr. (1970). Garnet peridotites and the system $CaSiO_3$-$MgSiO_3$-Al_2O_3. Mineral. Soc. Amer. Spec. Paper, 3, p.63-75.

BOYD, F.R. Jr. and SCHAIRER, J.F. (1964). The system $MgSiO_3$-$CaMgSi_2O_6$. Jour. Petrol. v.5, p.275-309.

BROWN, G.M. (1957). Pyroxenes from the early and middle stages of fractionation of the Skaergaard intrusion, East Greenland. Mineral. Mag., v.31, p.511-543.

BROWN, G.M., EMELEUS, C.H., HOLLAND, J.G. and PHILLIPS, R. (1970). Petrographic, mineralogic and X-ray fluorescence analysis of lunar igneous-type rocks and spherules. Science v.167, p.559-601.

BUDDINGTON, A.F. and LINDSLEY, D.H. (1964). Iron-titanium oxide minerals and synthetic equivalents. Jour. Petrol. v.5, p.310-357.

BURNS, R.G. (1970). Mineralogical applications of crystal field theory. Cambridge University Press.

CARNEY, J.N. and WELLAND, M.J.P. (1974). Geology and Mineral Resources of the Oman Mountains. Inst. Geol. Sci. Overseas Div. Rept. 27, 49p.

CHALLIS, G.A. (1965). The origin of New Zealand ultramafic intrusions. Jour. Petrol., v.6, p.322-364.

COLEMAN, R.G. (1977). Ophiolites. In: Wyllie, P.J., Ed. Minerals and Rocks: New York, Springer-Verlag.

DAVIS, B.T.C. and BOYD, F.R. Jr. (1966). The join $Mg_2Si_2O_6$-$CaMgSi_2O_4$ at 30 kilobars pressure and its application to pyroxenes from kimberlites. Jour. Geophys. Res. v.71, p.3567-3576.

DEWEY, J.F. (1974). Continental margins and ophiolite obduction. Appalachian Caledonian System; In: Burk, C.A. and Drake, C.L., eds. The geology of continental margins: New York, Springer-Verlag, p.933-950.

DEWEY, J.F. (1976). Ophiolite obduction. Tectonophysics. v.31, p.93-120.

DICKEY, J.S. Jr. (1970). Partial fusion products in alpine-type peridotites. Serrannia de Rondo and other examples. Mineralog. Soc. Am. Spec. Pub. v.3, p.33-49.

DUNCUMB, P. and REED, S.J.B. (1968). The calculation of stopping power and back scatter effects in electron-probe microanalysis. In Quantitative electron probe microanalysis. Nat. Bur. Standards, Special Publ. 298, p.133-154.

ENGIN, T. and HIRST, D.M. (1970). The Alpine chrome ores of the Andizlik-Zimparalik area, Fethiye (southwest Turkey). Trans. Inst. Mining Met., Sect.B, 79: B.16-27.

ENGLAND, R.N. and DAVIES, H.L. (1973). Mineralogy of ultramafic cumulates and tectonites from eastern Papua. Earth Planet. Sci. Letters, v.17, p.416-425.

FLANAGAN, F.J. (1969). U.S. Geological Survey Standards - II. First compilation of data for the new U.S.G.S. rocks. Geochim. et Cosmochim. Acta, v.33, p.81-120.

FLANAGAN, F.J. (1973). 1972 values for international reference samples. Geochim. et Cosmochim. Acta, v.37, p.1189-1200.

GLENNIE, K.W., BOEUF, M.G.A., HUGHES CLARK, M.W., MOODY-STUART, M., PILAAR, W.F.H. and REINHARDT, B.M. (1973). Late Cretaceous Nappes in Oman Mountains and their geologic evolution, A.A.P.G. Bull., v.57, No.1, p.5-27.

GLENNIE, K.W., BOEUF, M.G.A., HUGHES-CLARK, M.W., MOODY-STUART, M., PILAAR, W.F.H. and REINHARDT, B.M. (1974). Geology of the Oman Mountains. Kon. Nederlands Geol. Mijb. Gen. Ver. Verh. 31, 423p.

GREENWOOD, J.E.G.W. and LONEY, P.E. (1968). Geology and mineral resources of the Trucial Oman Range. Institute of Geol. Sciences, Overseas Div., London S.W.7, p.1-108.

HAKLI, T.A. and WRIGHT, T.L. (1967). The fractionation of nickel between olivine and augite as a geothermometer. Geochimica et Cosmochimica Acta, v.31, p.877-884.

HAKLI, T.A. (1968). An attempt to apply the Makaopuhi nickel fractionation data to the temperature determination of a basic intrusive. Geochim. et Cosmochim. Acta, v.32, p.449-460.

HARRIS, P.G., REAY, A. and WHITE, I.G. (1967). Chemical composition of the upper mantle. Jour. Geophys. Res., v.72, p.6359-6369.

HEINRICH, K.F.J. (1966). The absorbtion correction model for microprobe analysis. Trans. 2nd. Nat. Conf. Electron Microprobe Analysis, Boston, Paper 7, 2p.

HIMMELBERG, G.R. and COLEMAN, R.G. (1968). Chemistry of primary minerals and rocks from the Red Mountain - Del Puerto ultramafic mass, California. U.S. Geol. Survey Prof. Paper 600-C, p.C18-C26.

HIMMELBERG, G.R. and LONEY, R.A. (1973). Petrology of the Vulcan Peak Alpine-type Peridotite, Southwestern Oregon. Bull. Geol. Soc. Am., v.84, p.1585-1600.

HOLLAND, J.G. and BRINDLE, D.W. (1966). A self consistent mass absorbtion correction for silicate analysis by X-ray fluorescence. Spectrochim. Acta, v.22, p.2083-2093.

HUDSON, R.G.S. (1960). The Permian and Triassic of the Oman Peninsula, Arabia, Geol. Mag., v.97, No.4, p.299-308.

HUDSON, R.G.S., BROWN, R.V. and CHATTON, M. (1954a). The structure and stratigraphy of the Jabal Qamar area, Oman. Proc. Geol. Soc., London, No.1513, p.xcix-civ.

HUDSON, G.R.S. and CHATTON, M. (1959). The Musandam Limestone (Jurassic to Lower Cretaceous) of Oman, Arabia. Notes et Memoires sur le Moyen-Orient, v.7, p.69-94, Paris: Museum National d'Histoire Naturelle.

HUDSON, R.G.S., McGUGAN, A. and MORTON, D.M. (1954b). The structure of the Jabel Haṭab area, Trucial Oman. Quart. Jour. Geol. Soc., London, v.110, part 2, No. 438, p.121-152.

IRVINE, T.N. (1965). Chromium spinel as a petrogenetic indicator. Part 1. Theory. Canadian Jour. Earth Sci., v.2, p.648-672.

IRVINE, T.N. (1967). Chromium spinel as a petrogenetic indicator. Part 2. Petrologic applications. Canadian Jour. Earth Sci., v.4, p.71-103.

IRVINE, T.N. and FINDLAY, T.C. (1972). Alpine-type peridotite with particular reference to the Bay of Islands igneous complex. In: The ancient ocean lithosphere (ed. E. Irving), V.42, No.3, p.97-128. Ottawa: Earth Physics Branch, E.M.R.

ITO, K. and KENNEDY, G.C. (1967). Melting and phase relations in a natural peridotite to 40 kilobars. Am. J. Sci., v.265, p.519-539.

JACKSON, E.D. (1961a). Primary textures and mineral associations in the ultramafic zone of the Stillwater Complex, Montana, U.S.G.S. Prof. Paper 358, 106p.

JACKSON, E.D. (1969). Chemical variation in coexisting chromite and olivine in chromitite zones of the Stillwater Complex. Econ. Geol. Monograph, v.4, p.41-71.

JACKSON, E.D. and THAYER, T.P. (1972). Some criteria for distinguishing between stratiform, concentric, and alpine peridotite-gabbro complexes. Internat. Geol. Cong., 24th Montreal, Sec.2, p.289-296.

KUNO, H. (1968). Differentiation of basaltic magma. In "Basalts", v.2., p.623-688. Ed. H.H. Hess and A. Poldervaart. Interscience, London.

LE BAS, M.J. (1962). The role of aluminium in igneous clinopyroxenes with relation to their parentage. Am. J. Sci., v.260, p.267-288.

LEES, G.M. (1928). The geology and tectonics of Oman and parts of south-eastern Arabia. Quart. Jour. Geol. Soc., London, v.84, part 4, No.336, p.585-670.

LONEY, R.A., HIMMELBERG, G.R. and COLEMAN, R.G. (1971). Structure and petrology of the Alpine-type peridotite at Burro Mountain, California, U.S.A. Jour. Petrology, v.12, p.245-309.

MACDONALD, G.A. (1968). Composition and origin of Hawaiian lavas. Geol. Soc. Amer. Mem. 116, p.477-522.

MALPAS, J. (1978). Magma generation in the upper mantle, field evidence from ophiolite suites, and application to the generation of oceanic lithosphere. Phil. Trans. R. Soc. London, v.288A, p.527-546.

MEDARIS, L.G. (1972). High pressure peridotites in southwest Oregon. Bull. Geol. Soc. Amer., v.83, p.41-57.

MENZIES, M. (1973). Mineralogy and partial melt textures within an ultramafic-mafic body, Greece. Contr. Mineral. Petrol., v.42, p.273-285.

MENZIES, M.A. (1974). Petrogenesis of the Makrirraki Ultramafic Complex. Unpubl. Ph.D. Thesis, University of Cambridge.

MONTIGNY, R., BOUGAULT, H., BOTTINGA, Y. and ALLEGRE, C.J. (1973). Trace element geochemistry and genesis of the Pindos ophiolite suite. Geochim. et Cosmochim. Acta, v.37, p.2135-2147.

MORTON, D.M. (1959). The geology of Oman, Proc. 5th World Petrol. Congress. Sect.1, paper No.14, p.277-294.

MOSSMAN, D.J. (1973). Geology of the Greenhills Ultramafic Complex, Bluff Peninsula, Southland, New Zealand. Geol. Soc. America Bull., v.84, p.39-62.

MYSEN, B. and BOETTCHER, A.L. (1975b). Melting of a hydrous mantle. II. Geochemistry of crystals and liquids formed by anatexis of mantle peridotite at high pressures and temperatures of water, hydrogen and carbon dioxide. Jour. Petrol. v.16, p.549-593.

NEUMANN, E.R. (1974). The distribution of Mn^{2+} and Fe^{2+} between ilmenites and magnetites in igneous rocks. Am. Jour. Sci. v.274, p.1074-1088.

NORMAN, R.E. and STRONG, D.F. (1975). The geology and geochemistry of ophiolitic rocks exposed at Ming's Eight, Newfoundland. Canadian Jour. Earth Sci., v.12, p.777-797.

O'HARA, M.J.(1967). Mineral paragenesis in ultrabasic rocks. In Wyllie, P.J. ed., Ultramafic and related rocks: New York, John Wiley and Sons, p.393-403.

O'HARA, M.J. (1968). The bearing of phase equilibria studies in synthetic and natural systems on the origin and evolution of basic and ultrabasic rocks. Earth Sci. Rev. v.4, p.69-133.

PAGE, N.J. (1967b). Serpentinization at Burro Mountain, California, U.S.A. Contr. Mineral. Petrol., v.14, p.321-342.

PEARCE, J.A. (1975). Basalt geochemistry used to investigate past tectonic environments on Cyprus. Tectonophysics, v.25, p.41-67.

PEARCE, J.A. and CANN, J.R. (1973). Tectonic setting of basic volcanic rocks determined using trace element analyses. Earth and Planetary Science Letters, v.19, p.290-300.

PILGRIM, G.E. (1908). The geology of the Persian Gulf and the adjoining portions of Persia and Arabia. Mem. Geol. Surv. India, v.34, part 4, 177p.

PINSENT, R.H. (1974). The emplacement and metamorphism of the Blue River ultramafic body, Cassiar district, British Columbia, Canada. Unpubl. Ph.D. thesis, University of Durham.

POWELL, M. and POWELL, R. (1974). An olivine-clinopyroxene geothermometer. Contr. Mineral. Petrol., v.48, p.249-263.

REED, S.J.B. (1965). Characteristic fluorescence corrections in electron-microprobe microanalysis. British Jour. Appl. Phys., v.16, p.913-926.

REEVES, M.J. (1971). Geochemistry and mineralogy of British Carboniferous seatearths from northern coalfields. Unpubl. Ph.D. thesis, University of Durham.

REINHARDT, B.M. (1969). On the genesis and emplacement of Ophiolites in the Oman Mountains Geosyncline. Schweiz. Mineralogische und petrographische Mitteil, v.49/1, p.1-30.

REINHARDT, B.M. (1974) The relationship between spilites and other members of the Oman Mountains Ophiolite Suite. In: Spilites and spilitic rocks (Ed. G.C. Amstutz). p.207-227. Springer Verlag, Heidelberg.

RINGWOOD, A.E. (1966). Chemical evolution of the terrestrial planets. Geochim. et Cosmochim. Acta, v.30, p.41-104.

RODGERS, K.A. (1973). Chrome-spinels from the Massif du Sud, southern New Caledonia. Mineralog. Mag., v.39, p.326-339.

RODGERS, K.A. (1975). A comparison of the geology of the Papuan and New Caledonian Ultramafic Belts. Jour. Geology, v.83, p.47-60.

SINTON, J.M. (1977). Equilibration history of the basal Alpine-type Peridotite, Red Mountain, New Zealand. Jour. Petrol., v.18, p.216-246.

STEVENS, R.E. (1944). Composition of some chromites of the western hemisphere. Am. Miner. v.29, p.1-34.

STROH, J.M. (1976). Solubility of alumina in orthopyroxene plus spinel as a geobarometer in complex systems. Applications to spinel-bearing alpine-type peridotites. Contr. Mineral. Petrol., v.54, p.173-188.

SWEATMAN, T.R. and LONG, J.V.P. (1969). Quantitative electron-probe microanalysis of rock forming minerals. Jour. Petrology, v.10, p.332-379.

TAYLOR, S.R. (1965). The application of trace element data to problems in petrology. Phys. Chem. Earth, v.6, p.133-213.

THAYER, T.P. (1967). Chemical and structural relationships of ultramafic and feldspathic rocks in alpine instrusive complexes. In Wyllie, P.J., ed. Ultramafic and related rocks. New York, Wiley, p.222-239.

TSCHOPP, R.H. (1967). The general geology of Oman, 7th World Petroleum Congress Proc., Mexico, v.2, p.231-242.

UPADHYAY, H.D. (1973). The Betts Cove ophiolite and related rocks of the Snooks Arm Group. Unpubl. Ph.D. thesis, Memorial Univ. of Newfoundland, St. John's Newfoundland.

VINCENT, E.A. (1960). Ulvöspinel in the Skaergaard intrusion, Greenland. Neues Jb. Miner. Abh. 94, p.993-1016.

WAGER, L.R. and BROWN, G.M. (1967). Layered igneous rocks. Oliver and Boyd, Edinburgh.

WAGER, L.R., BROWN, G.M. and WADSWROTH, W.J. (1960). Types of igneous cumulates. Jour. Petrology, v.1, part 1, p.73-85.

WARNER, R.D. and LUTH, W.C. (1974). The diopside-orthoenstatite two-phase region in the system $CaMgSi_2O_6$-$Mg_2Si_2O_6$. Amer. Min., v.59, p.98-109.

WELLAND, M.J. and MITCHELL, A.H.G. (1977). Emplacement of the Oman Ophiolites: A mechanism related to subduction and collision. Bull. Geol. Soc. Am., v.88, p. 1081-1088.

WILSON, H.H. (1969). Late Cretaceous Eugeosynclinal Sedimentation, Gravity Tectonics, and Ophiolite Emplacement in Oman Mountains, Southeast Arabia, A.A.P.G. Bull, v.53, No.3, p.626-671.

WOOD, B.J. and BANNO, S. (1973). Garnet-orthopyroxene and orthopyroxene-clinopyroxene relationships in simple and complex systems. Contrib. Mineral. Petrol. v.42, p.109-124.

WOOD, B.J. (1976). An olivine-clinopyroxene geothermometer. A discussion. Contr. Mineral. Petrol., v.56, p. 297-303.

APPENDIX I

METHODS USED FOR CALCULATIONS OF TEMPERATURES AND PRESSURES OF EQUILIBRATION

1. Jackson (1969)

The Mg-Fe^{2+} exchange reaction between coexisting olivine and chromian spinel can be written:

$$Fe^{2+}Si_{0.5}O_2 + Mg(Cr\alpha, Al\beta, Fe^{3+}\gamma)_2O_4 = MgSi_{0.5}O_2 + Fe^{2+}(Cr\alpha, Al\beta, Fe^{3+}\gamma)_2O_4$$

The values α, β and γ are the respective fractions of Cr, Al and Fe^{3+} in chromian spinel. The thermodynamic equilibration coefficient (K_D) may be defined by the following equation, assuming ideal solid solution behaviour (Irvine, 1965; Jackson, 1969):

$$K_D = \frac{\left(X^{ol}_{Mg}\right)\left(X^{sp}_{Fe^{2+}}\right)}{\left(X^{ol}_{Fe^{2+}}\right)\left(X^{sp}_{Mg}\right)}$$

where X^{ol}_{Mg} and $X^{ol}_{Fe^{2+}}$ are mole fractions of the end members $MgSi_{0.5}O_2$ and $FeSi_{0.5}O_2$ respectively, and X^{sp}_{Mg} and $X^{sp}_{Fe^{2+}}$ are the fractions of divalent cations in the spinels.

Using Jackson's formula (1969), it is possible to calculate the equilibation temperature for olivine-spinel pairs, using Gibbs free-energy data, and substituting different values for α, β and γ in the following equation:

$$T(^{o}K) = \frac{5580\alpha + 1018\beta - 1720\gamma + 2400}{0.90\alpha + 2.56\beta - 3.08\gamma - 1.47 + 1.987\ \ln K}$$

Sample No.	α	β	υ	X^{ol}_{Mg}	X^{ol}_{Fe}	X^{sp}_{Mg}	$X^{sp}_{Fe^{2+}}$	T(°K)	T(°C)
300A Dunite	0.6196	0.2623	0.1091	0.9083	0.0916	0.4310	0.5576	1321	1048
300B Dunite	0.6220	0.2422	0.1245	0.9104	0.0895	0.4103	0.5768	1279	1006
304A Dunite	0.4885	0.4376	0.0657	0.9050	0.0950	0.5015	0.4903	1263	990
305A Dunite	0.6020	0.2738	0.1172	0.9157	0.0842	0.4704	0.5136	1348	1075
528A Dunite	0.4451	0.3981	0.1520	0.9120	0.0880	0.5077	0.4751	1258	985
531A Dunite	0.5092	0.3557	0.1298	0.9010	0.0994	0.4221	0.5593	1212	939
531B Dunite	0.5412	0.3513	0.1033	0.9033	0.0966	0.4033	0.5785	1177	904
517A Dunite	0.4680	0.4363	0.0877	0.9055	0.0944	0.5092	0.4784	1200	927
517B Dunite	0.4478	0.4655	0.0830	0.9056	0.0943	0.5167	0.4669	1145	872
325A Hzb.	0.5568	0.3965	0.0434	0.9190	0.0810	0.5738	0.4060	1440	1167
325C Hzb.	0.4553	0.4132	0.1247	0.9203	0.0797	0.5935	0.3911	1411	1138
1037A Hzb.	0.4739	0.4937	0.0309	0.9000	0.0999	0.5697	0.4175	1418	1145
1044A Hzb.	0.5605	0.4070	0.0225	0.9099	0.0900	0.5322	0.4576	1372	1099
503A Wehrl.	0.43725	0.4922	0.0649	0.8999	0.1000	0.5627	0.4260	1377	1104
315A Plg.Peri.	0.4275	0.4209	0.1337	0.8985	0.1015	0.5850	0.4176	1536	1263
1027A Ol.Py.	0.5815	0.3240	0.0840	0.8757	0.1243	0.4298	0.5601	1152	879

Mineral data are shown in Table 5.34 - 5.43.

A typical calculation, worked out to give a temperature

Sample 300A

$R_8^{2+}R_{16}^{3+}O_{32}$

$\alpha = \frac{Cr}{16} = 0.619625$

$\beta = \frac{Al}{16} = 0.2623125$

$\delta = \frac{Fe^{3+}}{16} = 0.109125$

$X_{Mg}^{ol} = 0.9083$

$X_{Fe^{2+}}^{ol} = 0.0916$

$X_{Mg}^{sp} = \frac{3.448}{8} = 0.431$

$X_{Fe^{2+}}^{sp} = \frac{4.461}{8} = 0.557625$

$$T(^{o}K) = \frac{5580\alpha + 1018\beta - 1720\delta + 2400}{0.90\alpha + 2.56\beta - 3.08\delta - 1.47 + 1.987 \ln K}$$

$$K_D = \frac{\left(X_{Mg}^{ol}\right)\left(X_{Fe^{2+}}^{sp}\right)}{\left(X_{Fe^{2+}}^{ol}\right)\left(X_{Mg}^{sp}\right)}$$

$$K_D = \frac{(0.9083)\ (0.557625)}{(0.0916)\ (0.431)}$$

$$= 12.82917727$$

$$\ln K = 2.5517221$$

$$(2.5517221)(1.987) = 5.070271812$$

$$T(^{o}K) = \frac{3457.5075 + 267.034125 - 187.695 + 2400}{0.5576625 + 0.67152 - 0.336105 - 1.47 + 5.070271812}$$

$$T(^{o}K) = \frac{5936.846625}{4.493349312}$$

$$T(^{o}K) = 1321$$

$$T(^{o}C) = 1048$$

2. Wood and Banno (1973)

$$\underset{\text{opx}}{Mg_2Si_2O_6} \rightleftharpoons \underset{\text{cpx}}{Mg_2Si_2O_6}$$

Taking account of X_{Fe}^{opx} (relative to the data of Davis and Boyd (1966) on Di-En at 30Kb):

$$T\ (^{o}K) = \frac{-10202}{\ln\left(\frac{a_{Mg_2Si_2O_6}^{cpx}}{a_{Mg_2Si_2O_6}^{opx}}\right) - 7.65X_{Fe}^{opx} + 3.88\left(X_{Fe}^{opx}\right)^2 - 4.6}$$

where; $$\ln\left(\frac{a_{Mg_2Si_2O_6}^{cpx}}{a_{Mg_2Si_2O_6}^{opx}}\right) = \ln\left[\frac{\left(X_{Mg}^{M_2}\right)^{cpx} \cdot \left(X_{Mg}^{M_1}\right)^{cpx}}{\left(X_{Mg}^{M_2}\right)^{opx} \cdot \left(X_{Mg}^{M_1}\right)^{opx}}\right]$$

Sample No	$\left(X_{Mg}^{M1}\right)^{cpx}$	$\left(X_{Mg}^{M2}\right)^{cpx}$	$\left(X_{Mg}^{M1}\right)^{opx}$	$\left(X_{Mg}^{M2}\right)^{opx}$	$\left(X_{Fe}\right)^{opx}$	T (^{o}K)	T (^{o}C)
328A Hzb.	0.8509	0.0383	0.8693	0.8946	0.0776	1223	950
1031A Hzb.	0.8557	0.0295	0.8441	0.8673	0.0912	1182	909
1031B Hzb.	0.8435	0.0546	0.8467	0.8810	0.0954	1262	989
1031C Hzb.	0.8187	0.0432	0.8365	0.87176	0.0966	1224	951
1027A Ol.Px	0.8468	0.0438	0.8196	0.8309	0.1326	1206	933
1027B Ol.Px	0.8461	0.0583	0.8185	0.8307	0.1337	1247	974
1030B Ol.Px	0.8332	0.0470	0.8279	0.8309	0.1460	1200	927
119A Ol.Gb.	0.7880	0.0945	0.7753	0.7841	0.1948	1272	999
557A Ol.Gb.	0.7296	0.0452	0.7065	0.7017	0.2628	1127	854
526B A Ol.Gb.	0.7240	0.0403	0.7052	0.6883	0.2661	1112	839
131 A Norite	0.6929	0.1244	0.6768	0.6549	0.2934	1248	975
526A (A) Gabbro	0.7330	0.0901	0.7194	0.7149	0.2521	1224	951

Mineral data are shown in Tables 5.44 - 5.53.

Typical calculation, worked out to give a temperature.

Sample 328A

$$T(^{o}K) = \frac{-10202}{\ln\left(\frac{0.03258}{0.77767}\right) - 7.65(0.0776) + 3.8(0.0776)^2 - 4.6}$$

$$T(^{o}K) = \frac{-10202}{-3.1726 - 0.5936 - 4.5771}$$

$$T(^{o}K) = \frac{-10202}{-8.3428}$$

$$T(^{o}K) = 1223$$

$$T(^{o}C) = 950$$

3 . Mysen and Boettcher (1975)

$$\underset{\text{cpx}}{CaAl_2SiO_6} + \underset{\text{opx}}{MgCrAlSiO_6} \rightleftharpoons \underset{\text{cpx}}{CaCrAlSiO_6} + \underset{\text{opx}}{MgAl_2SiO_6}$$

Assuming ideal mixing:

$$K = \frac{\left(X_{Cr}^{Ml}\right)^{cpx} \cdot \left(X_{Al}^{Ml}\right)^{opx}}{\left(X_{Cr}^{Ml}\right)^{opx} \cdot \left(X_{Al}^{Ml}\right)^{cpx}}$$

$$\ln K = \frac{1000}{T} (4.0910 \pm 0.2603) - (2.7898 \pm 0.2713)$$

$$\therefore T\,(^{o}K) = \frac{4091}{\ln K + 2.7898}$$

Sample No.	$\left(X^{Ml}_{Cr}\right)^{cpx}$	$\left(X^{Ml}_{Al^{VI}}\right)^{opx}$	$\left(X^{Ml}_{Cr}\right)^{opx}$	$\left(X^{Ml}_{Al^{VI}}\right)^{cpx}$	T (^{o}K)	T (^{o}C)
328A Hzb.	0.030	0.043	0.014	0.057	1251	978
1031A Hzb.	0.020	0.053	0.015	0.051	1329	1056
1031B Hzb.	0.026	0.049	0.017	0.060	1361	1088
1031C Hzb.	0.028	0.055	0.0180	0.060	1300	1027
1044A Hzb.	0.025	0.033	0.015	0.039	1304	1031
1027A Ol.Px	0.022	0.037	0.016	0.048	1441	1168
1027B Ol.Px	0.025	0.040	0.014	0.045	1258	985
1030B Ol.Px	0.009	0.028	0.000	0.049	-	-
119A Ol.Gb	0.008	0.031	0.003	0.044	1196	923
557A Ol.Gb	0.002	0.036	0.000	0.065	-	-
526B (A) Ol.Gb	0.002	0.031	0.000	0.050	-	-
131A Norite	0.006	0.037	0.001	0.061	1002	729
526A (A) Gabbro	0.002	0.032	0.001	0.055	1391	1118

Mineral data are shown in Tables 5.44 - 5.53.

Typical calculation, worked out to give a temperature

Sample 328A

$$T(^{o}K) = \frac{4091}{\ln K + 2.7897}$$

$$T(^{o}K) = \frac{4091}{0.4803 + 2.7898}$$

$$T(^{o}K) = \frac{4091}{3.2701}$$

$$T(^{o}K) = 1251$$

$$T(^{o}C) = 978$$

4. Hakli and Wright (1967); Hakli (1968)

Temperature varies with the distribution coefficient $K = Ol^{Ni}/Cpx^{Ni}$ values in ppm, according to the equation:

$$\ln k = \frac{-A}{T} + B$$

where the numerical values of the A and B parameters of the mineral pairs olivine - clinopyroxene are A = 8647, B = 7.838

Sample No.	ppm Ni in olivine	ppm Ni in clinopyrox.	K	T(°K)	T(°C)
328A Hzb.	2987	786	3.800	1330	1057
1031A Hzb.	2437	472	5.163	1395	1122
1031B Hzb.	2830	1022	2.769	1267	994
1031C Hzb.	2594	393	6.600	1453	1180
1044A Hzb.	3616	314	11.519	1603	1330
315A Plag. Peridotite	1730	707	2.445	1245	972
503A Wehrlite	1965	707	2.779	1268	995
503B Wehrlite	1650	1179	1.399	1152	879
803A Wehrlite	2201	-	-	-	-
804A Wehrlite	1415	393	3.600	1318	1045
1027A Ol. Pyrox.	1886	-	-	-	-
1027B Ol. Pyrox.	1650	-	-	-	-
1014(3)B Ol. Pyrox.	1022	78	13.102	1642	1369
1014(3)C Ol. Pyrox.	943	550	0.539	1184	911
1030B(A) Ol. Pyrox.	1415	628	2.253	1230	957
556A Ol. Gabbro	1100	550	2.000	1210	937
119A Ol. Gabbro	786	78	10.076	1564	1291
523A Ol. Gabbro	1258	1100	1.143	1122	849
557A Ol. Gabbro	1257	550	2.285	1233	960
557B Ol. Gabbro	1336	550	2.429	1244	971
539A Ol. Gabbro	1100	471	2.335	1237	964
564A Ol. Gabbro	1179	550	2.143	1222	949
113A Ol. Gabbro	943	-	-	-	-
526B(B) Ol. Gabbro	628	235	2.666	1261	988

Mineral data are shown in Tables 5.54 - 5.63.

Typical calculation, worked out to give a temperature.

Sample 328A

$$K = Ol^{Ni}/Cpx^{Ni}$$

$$\ln K = \frac{-A}{T} + B$$

where A = 8647, B = 7.838

$$\ln 3.800 = \frac{-8647}{T} + 7.838$$

$$1.335 - 7.838 = \frac{-8647}{T}$$

$$-6.503 = \frac{-8647}{T}$$

$$T(^{o}K) = 1330$$

$$T(^{o}C) = 1057$$

5. O'Hara (1967)

The two parameters suggested by O'Hara (1967) to provide the necessary pressure/temperature data for clinopyroxene are:

$$\alpha_c = \frac{\text{wt\% } CaSiO_3 \times 100}{\text{wt\%}(CaSiO_3+MgSiO_3)}$$

$$\beta_c = \frac{\text{wt\% } Al_2O_3 \times 100}{\text{wt\%}(CaSiO_3+MgSiO_3+Al_2O_3)}$$

where $CaSiO_3$ = wt% $CaSiO_3$ equivalent to all CaO; $MgSiO_3$ = wt% $MgSiO_3$ equivalent to all MgO, MnO, NiO and FeO; and Al_2O_3 = wt% Al_2O_3 equivalent to all Al_2O_3, Cr_2O_3 and Fe_2O_3.

Sample No.	α_c	β_c
1031C Harzburgite	50.30	3.34
1044A Harzburgite	52.57	2.38
503A Wehrlite	50.09	4.86
804A Wehrlite	51.11	3.91
804D Wehrlite	52.79	3.97
554D Olivine Pyroxenite	49.73	2.51
1027A Olivine Pyroxenite	51.88	2.79
1027B Olivine Pyroxenite	51.88	2.71

Mineral data are shown in Tables 5.64 - 5.66

Typical calculation, worked out to give values for α_c and β_c.

Sample 1031C

$Mg + Fe + Mn + Ni \quad (MgSiO_3)$

$= (0.969 + 0.108 + 0.002 + 0.001)(100.4)$

$= (1.08)(100.4)$

$= 108.432$

$(Ca)\,(CaSiO_3)$

$= (0.946)(116.19)$

$= 109.9157$

$\frac{Al}{2} + \frac{Cr}{2} \quad (Al_2O_3)$

$= (0.06 + 0.014)(101.96)$

$= 7.545$

$MgSiO_3 = 108.432 = 48\%$

$Al_2O_3 = 7.545 = 3.34\%$

$CaSiO_3 = \frac{109.9157}{225.8927} = 48.658\%$

$\alpha_c = \frac{4865.8}{96.658} = 50.34$

$\beta_c = \frac{334}{100} = 3.34$

6. Powell and Powell (1974)

$$2CaMgSi_2O_6 + Fe_2SiO_4 = 2CaFeSi_2O_6 + Mg_2SiO_4$$

cpx ol cpx ol

The clinopyroxene M1 site is non-ideal, and it is expressed as a regular solution. The pressure dependence of the geothermometer has been calculated as 5°C per kilobar. The following equation may be used to determine temperature (T) in degrees Kilvin, at a given pressure (P) in bars.

$$T(^{o}K) = \frac{-2X_{Al}(920000+3.6P)-0.0435(P-1)+10100}{8+2R\ln K\left(\frac{X_{Mg}^{ol}}{X_{Fe}^{ol}}\right)\left(\frac{X_{Fe}^{M1}}{X_{Mg}^{M1}}\right) - 714.3\ (2X_{Al})}$$

The symbols X_{Mg}, X_{Fe} and X_{Al} denote the mole fractions of these elements in olivine, and in the clinopyroxene M1 site. The value for Al includes other trivalent cations in octahedral coordination. The value for R is the gas constant (1.987 cals/mole °K). A pressure of 5 kilobars is assumed for P.

Sample No.	$\left(X_{Al}^{Ml}\right)^{cpx}$	$\left(X_{Mg}\right)^{ol}$	$\left(X_{Fe}^{Ml}\right)^{cpx}$	$\left(X_{Fe}\right)^{ol}$	$\left(X_{Mg}^{Ml}\right)^{cpx}$	T(^{o}K)	T(^{o}C)
328A Harzburgite	0.0900	0.9152	0.0600	0.0848	0.8500	1306	1033
1031A Harzburgite	0.0745	0.9084	0.0706	0.0915	0.8548	1309	1036
1031B Harzburgite	0.0895	0.9018	0.0700	0.0982	0.8405	1306	1033
1031C Harzburgite	0.0910	0.9060	0.0911	0.0940	0.8178	1321	1048
1044A Harzburgite	0.0675	0.9099	0.0511	0.0900	0.8814	1291	1018
315A Plag.Perid.	0.1185	0.8985	0.0772	0.1015	0.8042	1311	1038
503A Wehrlite	0.128	0.8999	0.0721	0.1000	0.7999	1310	1037
503B Wehrlite	0.109	0.8985	0.0700	0.1014	0.821	1307	1034
803A Wehrlite	0.1265	0.8842	0.0736	0.1160	0.7998	1306	1033
804A Wehrlite	0.1105	0.8897	0.0723	0.1102	0.8172	1305	1032
1027A Ol. Pyrox.	0.0735	0.8757	0.0810	0.1243	0.8455	1298	1025
1027B Ol. Pyrox.	0.0730	0.8745	0.0820	0.1255	0.8450	1298	1025
1014(3)B Ol.Pyrox.	0.0765	0.8564	0.0909	0.1436	0.8320	1297	1024
1014(3)C Ol.Pyrox.	0.0635	0.8583	0.0930	0.1416	0.8435	1295	1022
1030B(A) Ol.Pyrox.	0.0615	0.8399	0.1060	0.1600	0.8325	1294	1021
556A Ol.gabbro	0.0895	0.7380	0.1890	0.2620	0.7215	1305	1032
119A Ol.gabbro	0.0610	0.7860	0.1530	0.2123	0.7860	1299	1026
523A Ol.gabbro	0.0820	0.7336	0.1990	0.2636	0.7190	1306	1033
557A Ol.gabbro	0.0880	0.7059	0.1879	0.2940	0.7241	1297	1024
557B Ol.gabbro	0.0925	0.7067	0.1837	0.2932	0.7238	1297	1024
539A Ol.gabbro	0.0575	0.8625	0.0942	0.1375	0.8477	1296	1023
564A Ol.gabbro	0.0955	0.7130	0.2251	0.2870	0.6794	1310	1037
113A Ol.gabbro	0.0665	0.7899	0.1373	0.2100	0.7962	1294	1021
526B(B) Ol.gabbro	0.072	0.6823	0.2026	0.3177	0.7253	1292	1019

Mineral data are shown in Tables 5.54 - 5.63

GENERALISED LITHOLOGICAL MAP OF THE NORTHERN OMAN RANGE *(after Greenwood and Loney, 1968. Modified by A.H. Al-Khamees)*

0 miles 50

0 kilometres 50

LOCATION MAP

I R A N

ARABIAN GULF

Sharjah

GULF of OMAN

OMAN

55°00' 55°30' 56°00' 56°30'

26°00' 25°30' 25°00' 25°45'

IRANIAN GULF OF OMAN

Ras Shalkh Masud

RUUS AL JIBAL

Ras Limah

RAS AL KHAIMAH

JABAL HAQAB

JABAL QAMAR

UMM AL QAWAIN

DAYD

Ras Dibba

AJMAN

SHARJAH

DUBAI

FIELD AREA

MASAFI GHADF

KHAWR FAKKAN

SIJI

FUJAIRAH

Kalba

Khawr Kalba

FAIYAH

LEGEND

QUATERNARY

- SABKHAH
- AEOLIAN SAND

MAESTRICHTIAN LIMESTONE, MARL, CONGLOMERATE and BOULDERS

SEMAIL OPHIOLITES

- GABBROS

UPPER CRETACEOUS

- SERPENTINITES and SERPENTINIZED ULTRAMAFIC ROCKS

HAWASINA SERIES

- RADIOLARIAN CHERT, LIMESTONE, SHALE and MARL

JURASSIC to LOWER CRETACEOUS

- MUSANDAM LIMESTONE, including CHALKY LIMESTONE and DOLOMITE

PERMIAN to TRIASSIC

- MAINLY LIMESTONE and DOLOMITE

FIGURE 1·1

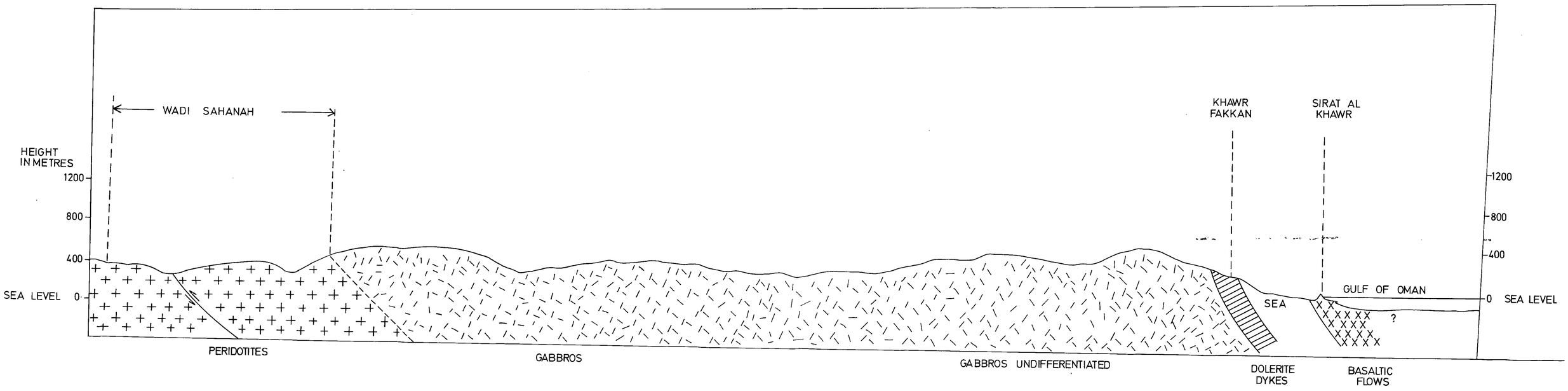

SCALE 1: 20 000

FIGURE 2·2

FIGURE 2-2. GEOLOGICAL MAP OF THE KHAWR FAKKAN REGION, UNITED ARAB EMIRATES

LEGEND

QUATERNARY

RECENT
- Wadi Alluvium
- Alluvial Fan

PLEISTOCENE TO RECENT
- Sabhkhah
- Beach Sand
- Fluviatile Terrace Deposits
- Boulders, gravel, sand and silt

SEMAIL OPHIOLITES

UPPER CRETACEOUS
- Basalt Flows
- Dolerite Dykes with Subordinate Intermediate Members
- Gabbro
- Peridotite, more or less Serpentinized

SYMBOLS

- D Dunite
- H Harzburgite
- W Wehrlite
- P Pyroxenite
- Strike and dip of Dolerite Dykes
- Dip of Layering in Gabbros
- Bands of Dunite and Wehrlite
- ▲ Mountain Peaks (heights in metres)
- SC Scattered Cultivation
- Vegetation
- Villages
- Motorable Tracks
- Wadi
- Fault
- Inferred Fault
- Pass
- Geological Boundary

LOCATION MAP

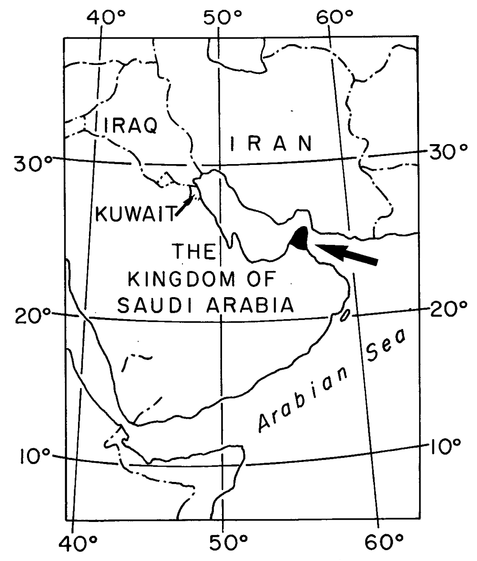

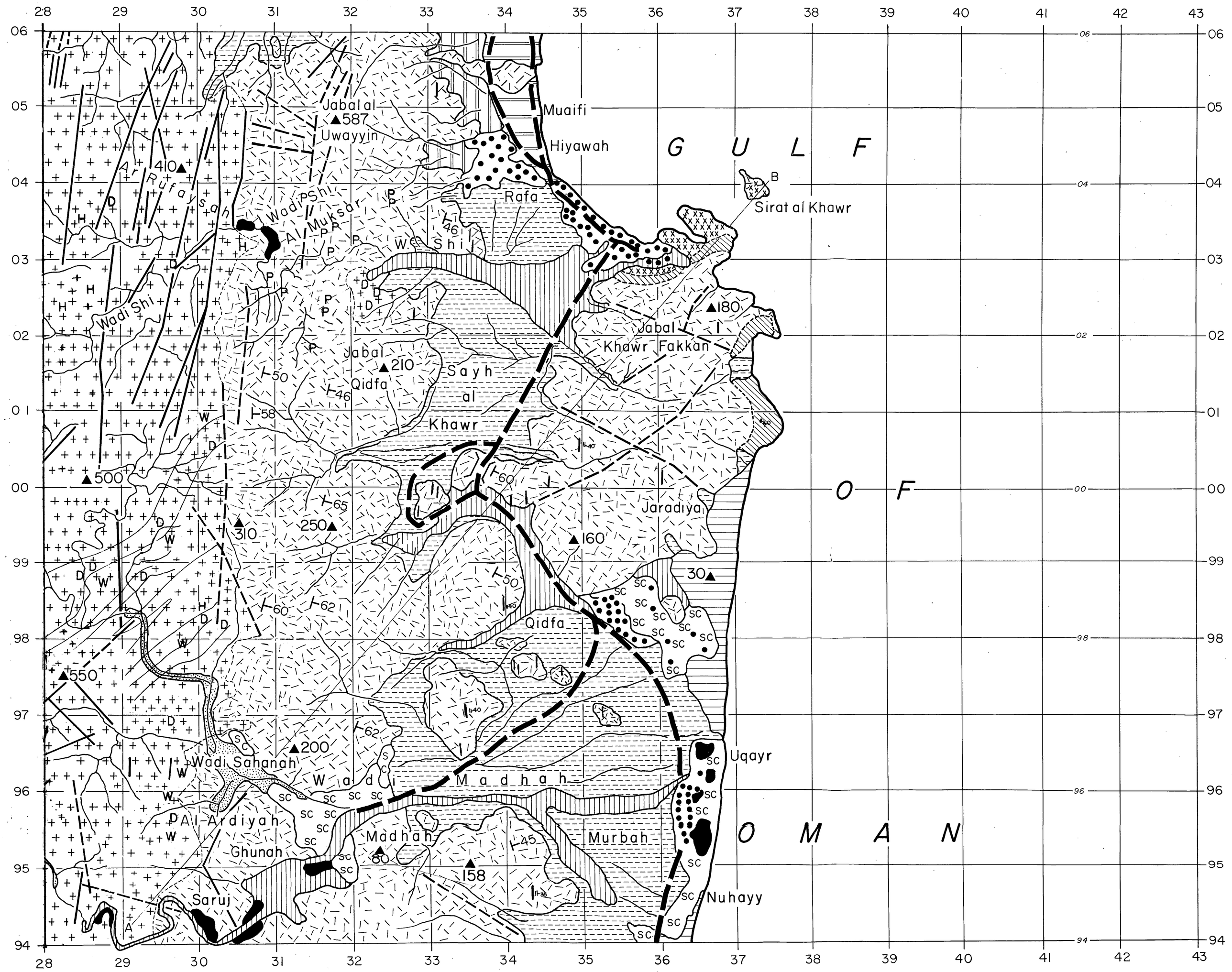

Scale 1:20,000

Miles: 0, ½, 1, 2, 3, 4

Kilometres: 0, 1, 2, 3, 4, 5

TN
GN MN
0° 25'
1° 50'

SAMPLE LOCATION MAP

·100 Sample Number

▲ Mountain Peaks (heights in metres)

FIGURE 2·1

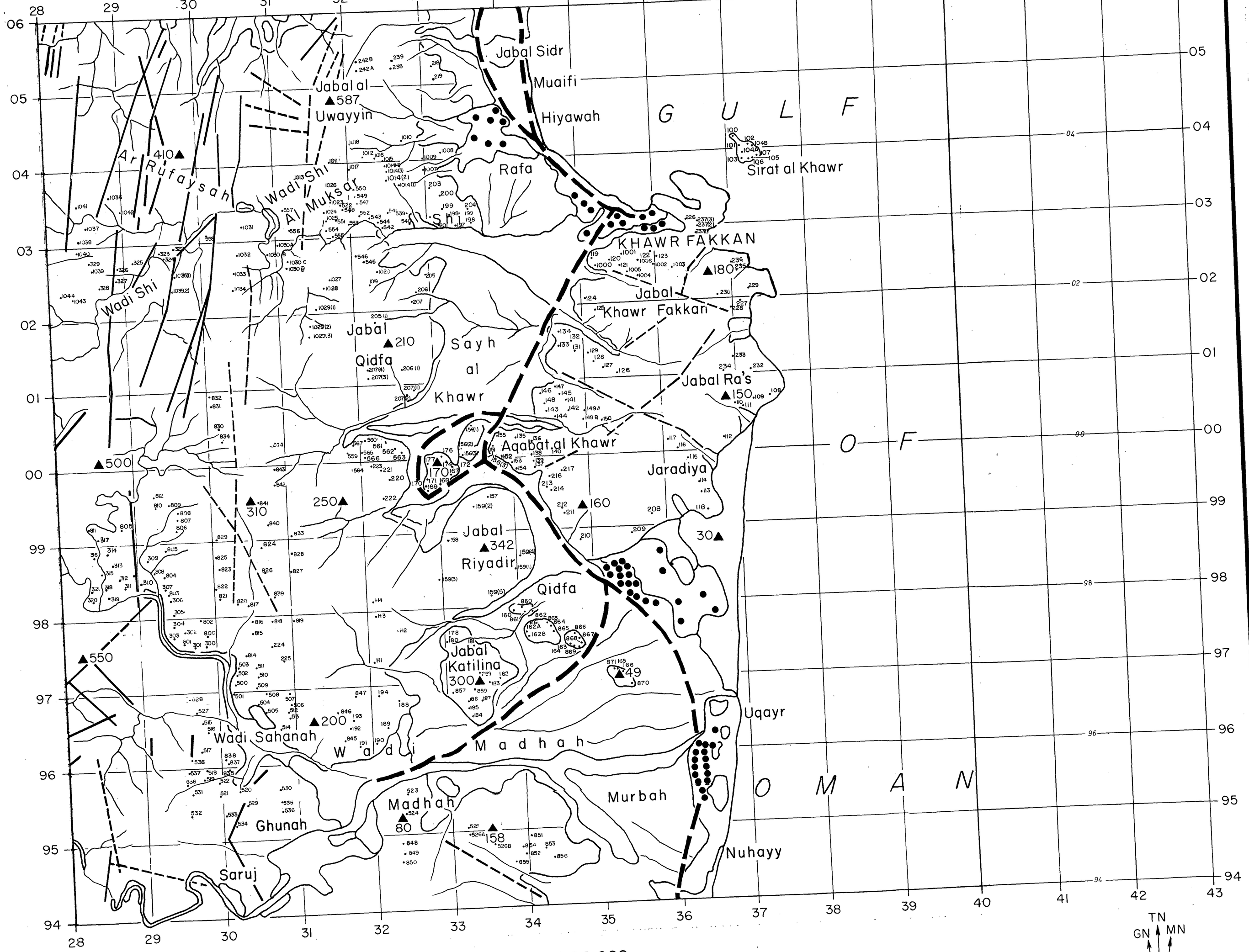

LOCATION MAP

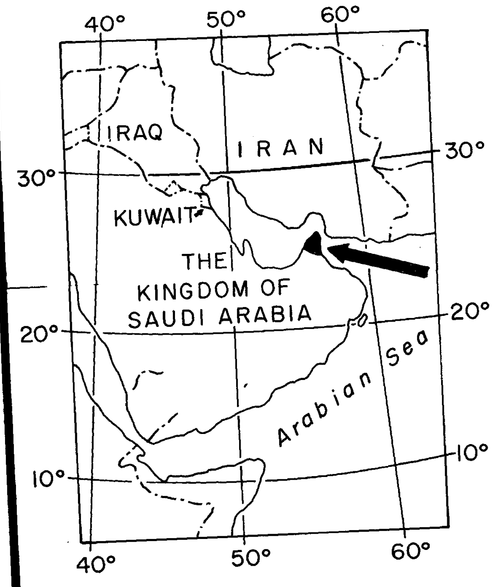

Scale 1:20,000

Miles 0 ½ 1 2 3 4

Kilometres 0 1 2 3 4 5

TN GN MN

0° 25' 1° 50'